THE M$_W$ 6.2 AMATRICE, ITALY EARTHQUAKE

OF 24th AUGUST 2016

A FIELD REPORT BY EEFIT

THE M~W~ 6.2 AMATRICE, ITALY EARHQUAKE OF 24th AUGUST 2016

Prof Dina D'Ayala, *University College London – CEGE EPICentre*

Dr Joanna Faure-Walker, *University College London – IRDR*

Zoe Mildon, *University College London – IRDR*

Dr Domenico Lombardi, *University of Manchester*

Dr Carmine Galasso, *University College London – CEGE EPICentre*

Dr Davide Pedicone, *WME*

Valentina Putrino, *University College London – CEGE EPICentre*

Paolo Perugini, *ARUP*

Dr Flavia De Luca, *University of Bristol*

Giuseppe Del Gobbo, *University of Oxford*

Dr Tristan Lloyd, *AIR Worldwide*

Elisabeth C. Morgan, *Sellafield Ltd*

Dr Andrea Totaro, *Mott Mac Donald*

Prof David Alexander, *University College London - IRDR*

Serena Tagliacozzo, *University College London – IRDR*

Executive Summary

At 3.36 am on 24th August 2016 a M_w 6.2 earthquake struck the central region of Italy, with epicentre in the Apennines range, near the village of Accumoli and with a fault surface rupture of approximately 25 km. Earthquake shaking was felt as far as Rome (120 km SW), Florence (220 km NW) and Urbino (200 km N). The worst affected region had a radius of approximately 20 km around the epicentre, including a number of towns and small villages across the regions of Umbria, Lazio and Marche. The epicentre of the M_w 6.0 of 24th August 2016 earthquake is located in the municipality of Accumoli (Lat 42.70, Lon 13.25, depth 8.1km). The event strongly damaged the villages of Amatrice, Accumoli, Arquata and Pescara del Tronto. The shaking led to a death toll of 295, injured 388 and left more than 2000 people homeless. This was the second deadliest earthquake in Italy since 1980. The event has been attributed an epicentral MCS intensity of IX (INGV, 2016). Peak ground acceleration (PGA) larger than 0.3g has been recorded at the near source stations of AMT (PGA= 0.87g, R_{jb} = 1.38km, type B ground according to EC8) (CEN, 2004), NRC (PGA= 0.37g, R_{jb} = 2.01km, type B ground according to EC8), (INGV, 2016).

An Earthquake Engineering Field Investigation Team (EEFIT) undertook the mission fieldwork during a period of thirteen days between the 4th and 16th of October 2016. The team was composed of 15 members covering a broad range of expertise from seismology to social recovery, with the objective of surveying and recording observations and measurements that would help the scientific and professional communities understand the event and its consequences. The team, organised in 4 sub-teams conducted accurate measurements around the surface rupture of the fault and studied the co-seismic effects and ground failures; analysed the strong ground motion data; collected vulnerability and damage data within the historic centres and the 'red zones' using ominidirectional camera technology; conducted damage survey of critical infrastructure such as schools, hospitals, bridges, etc; studied the emergency response and social consequences to the population. The most salient observations and findings, discussed in detail in this report, are summarised below.

Seismological and Geotechnical Observations:

- The 24 August 2016 earthquake ruptured the southern end of the Mt Vettore Fault and northern section of the Laga Fault. Surface offsets have been observed semi-continuously along the Mt Vettore Fault, but not the Laga Fault. During the EEFIT mission in October 2016, where surface offsets were identified, detailed measurements were taken every 2m or 5m along approximately 1,200m of the Mt Vettore Fault. The slip at the surface along the measured parts varied between 3cm and 30cm with and mean slip vector azimuth of 223° and mean slip vector plunge of 50°, consistent with the regional extension direction.
- The event of 24th August 2016 was followed up by two other events of similar magnitude in October 2016. From the analysis of historical seismicity and past recent events, several researchers indicate that this sequence is part of a complex system of faulting that extends from Gubbio to L'Aquila and ruptures at regular and frequent intervals.
- Peak ground accelerations (PGAs) larger than 0.3g have been recorded at a number of near source stations. In particular, the station in Amatrice, AMT, recorded a PGA= 0.87g, (R_{jb} = 1.38km, type B ground according to EC8) and the station in Norcia, NRC, recorded a PGA = 0.37g, (R_{jb} = 2.01km, type B ground according to EC8). In particular, the E-W PGA of the AMT station is the highest horizontal PGA ever recorded in Italy,
- Comparison between available recordings and accelerations provided by the reference seismic hazard model (MPS04) for Italy show that the elastic response spectra recorded are in some case in exceedance of the design code spectra at both 475 and 2475 years, particularly in the epicentral area and short-to-medium vibration periods. By developing hazard curves using the same earthquake rate model of MPS04 but a more recent GMPE than those originally adopted, results show a strong increase of

expected values for both PGA and other spectral ordinates, making the probabilistic seismic hazard estimates more consistent with the observations.

- One objective of the mission was to compare the intensity determined using the ESI scale and the intensity determined using the EMS '98. This earthquake provides a unique opportunity for a concurrent comparison. The ESI scale does not include the potential effects of the soil type or slope angle when observing environmental effects. However, these effects may be important when assessing the epicentral intensity. For example, in slopes characterised by steep angles and/or low frictional strengths, relatively low intensity shaking may result in landslides. A revision of the ESI scale taking into account these considerations warrants further research.

Structural observations:

- Notwithstanding early prescription for repair and reconstruction post-earthquakes date back to 1860 locally, and to 1909 at national level, the national seismic service was only established in Italy in 1976 with the main goal of providing the seismic zonation for the whole Italian territory. The first national seismic hazard map was produced in 1984. The town of Norcia was not classified as seismic until the late 70's and Amatrice was classified as seismic zone 2 in 1984. and upgraded to seismic zone 1 in 2003. Following each reclassification, the existing building stock underwent periods of retrofitting to comply with the new increase in seismic demand. Of particular relevance to the retrofitting of the towns visited by the EEFIT mission are: the Ministerial Decree D.M. 24th January 1986 (Ministro dei Lavori Pubblici, 1986), "Norme tecniche relative alle costruzioni antisismiche" and the Ministerial Decree D.M. 20th November, 1987, "Norme tecniche per la progettazione, esecuzione e collaudo degli edifici in muratura e per il loro consolidamento" (Technical code for the design, execution and testing of masonry buildings and for their strengthening) who sanctioned the concept of improvement of the performance for masonry structure in historic centres, without reaching full compliance with the current code. These documents also prescribed detailed type of intervention as discussed in Chapter 5.
- The mission conducted observation in the five more severely hit towns and villages in the epicentral area with the scope of determining the effectiveness of such interventions. Overall the quality of the masonry fabric is rather poor, largely made of rubble with mud and lime mortar. Extensive interventions on walls and floor structures have been observed, ranging from strengthened plaster, to grouting, from steel girder floors to concrete slabs and ring beams. Metal ties and anchors were also common, but their effectiveness was very variable, with many without proper anchoring plates, pulling out of the masonry. Norcia was the least affected of the towns visited during the mission, while Pescara del Tronto was the worst. The damage assessment to masonry buildings was carried out by means of RVS and interpretation from OD imagery, then compared to satellite imagery. The different nature and capabilities of capturing the damage to building components of the three methods used is discussed in light of the results obtained.
- The distribution of damage within the historic centres visited during the mission was very diverse. The towns more affected were Amatrice, with a collapse rate in the historic centre nearing 50% and Pescara del Tronto were the collapse rate was even greater (up to 70%) however collapses were cause not just by shaking, but by extensive soil failure and landslide of the hollow in which it was seated. Arquata del Tronto had two very different level of performance the "citta' alta" suffered topographical effect and one portion collapse with the hill ridge, while the rest of the houses had structural damage to partial collapse. Buildings in Arquata Bassa, a mixture of modern unreinforced masonry and reinforced concrete frame structures, in general had suffered little damage. Finally, buildings in Accumoli, although closest to the epicentre, seemed to have suffered modest to serious structural damage with a minority of collapses. The team also visited Norcia, less than 50 km north of the epicentre, to find only 3 partial collapses within the walled city.
- In comparison to ordinary URM buildings in Amatrice, churches here had performed relatively well with severe damage and some atrial collapses, but still substantially standing. In contrast churches surveyed

in Norcia and its vicinity show damage greater than what experienced by the surrounding residential buildings. Most of those churches had had some form of retrofitting. Some of the church damage observed matched the collapse mechanisms tabulated in the Protezione Civile's Scheda per il rilievo del danno ai beni culturali – Chiese.these are detailed in the report.

- In terms of critical infrastructure, the EEFIT team assessed the performance of a number of schools and hospitals. A school in Amatrice was emblematic for its collapse. Two reinforced concrete columns wrapped in FRP sheets were left standing next to a totally collapsed unreinforced masonry structure. Next to it an apparently heavily retrofitted Carabinieri station, a regular 3-storeys URM had experienced severe damage and had been evacuated. A large primary and secondary URM school building in Arquata del Tronto Bassa had also experienced very severe damage, although no collapses. A preliminary comparison of the damage evaluation carried out for three of the schools surveyed during the mission with respect to empirical fragility curves derived on the basis of damage data collected after the 2009 L'Aquila earthquake shows a reasonable agreement between the damage state attributed and the damage level with the largest expected probability of occurrence given the PGA assumed at the site from USGS shakemaps.

- Bridges represent a critical element of the transport infrastructure within a region and their functionality can be vital for the rescue operations in the aftermath of an earthquake or other exceptional events. When only one or few access roads are available to reach a given urban settlement, the bridges' category (i.e. importance) becomes higher, as their failure would isolate the population. The road network into the town of Amatrice was particularly hit by the earthquake and the EEFIT team carried out a detailed survey of the bridges constituting the critical access to the hill top town. Masonry arch bridges suffered local severe deformation and partial collapse, causing the road closure. An old reinforced concrete bridge also suffered severe damage and was partially closed. The viaducts of the Salaria Road and other neighbouring highways did not appear to have suffered noticeable damage during the earthquake, except minor damage, however their state of maintenance was rather poor.

Social observations:

- Despite the limited size of the affected area and small number of affected settlements, we noted considerable diversity in the situation encountered at each town. Common elements included a strong desire to map out a clear strategy to guide the recovery over the coming months and years. The overwhelming reliance on face-to-face communication had its inefficiencies, but it may have helped social cohesion, which local protagonists were struggling to maintain. Small, close-knit mountain communities were having to cope with seismic devastation on a scale that had not been witnessed in Italy for more than 35 years. The practical problems were legion.

- The August 2016 earthquakes elicited a strong response from the Italian Government and the national emergency management community. There was no shortage of emergency resources and there prevailed a fairly liberal attitude to the recovery demands. Emergency procedures had been consolidated and used in previous disasters and they functioned well in this one. On the other hand, there was little sense of a shared common operating picture. Indeed, it was not adequately shared with the civil protection operatives or the local population.

- The picture that emerged of the social situation in the four towns was one of great strain caused by exceptional loss and damage. The local area is characterised by mass 'emigration' to other parts of Italy and beyond. Indeed, it is estimated that Amatrice hosts about 5,000 second homes often belonging to people residing elsewhere in the Lazio region (mostly in Rome).[1] No doubt this diaspora will rally around its home town. However, considerable isolation and dislocation are being experienced by the survivors. If the social fabric is not unravelling, it is certainly under strain. One saving grace is strong, articulate

---

[1] See https://www.comune.amatrice.rieti.it/amatrice-solidale/

local leadership, and another is the work of young people to provide on-line points of contact. Hence, the problems faced by the affected towns are probably not unsolvable (with the possible exception of Pescara del Tronto), but they are an exceptionally hard test of mettle for small mountain communities with relatively few resources

EEFIT

ACKNOWLEDGMENTS

TABLE OF CONTENTS

LIST OF FIGURES

LIST OF TABLES

1   INTRODUCTION

1.1   Preamble

At 3.36 am on 24th August 2016 a M$_w$ 6.2 earthquake struck the central region of Italy, with epicentre in the Apennines range, near the village of Accumoli and with a fault surface rupture of 25 km. Earthquake shaking was felt as far as Rome (120 km SW), Florence (220 km NW) and Urbino (200 km N). The worst affected region had a radius of approximately 20 km around the epicentre, including a number of towns and small villages across the regions of Umbria, Lazio and Marche. The building stock of these urban centres mainly consists of historic rubble masonry structures, with a modest proportion of reinforced concrete (RC) construction. The performance of the former was very poor and collapses were widespread. In particular, the historic building stock of Amatrice suffered widespread destruction. Although the area is sparsely populated, the time of occurrence of the main shock, during the night, and the fact that much of the tourist accommodation was nearly at full capacity, led the death toll to be 295, injured 388 and left more than 2000 people homeless. This was the second deadliest earthquake in Italy since 1980.

This event was the first of a sequence which lasted until January 2017 with two other major events, one of Mw 5.9 on 26th October 2016 and one of M$_w$ 6.5 on 30th October 2016. No casualties were associated with these two shocks, although especially the second one caused substantial destruction in Norcia and its surrounding region. The map in Figure 1-1shows the epicentral location and magnitude of the 3 events, as computed by INGV (http://cnt.rm.ingv.it/)
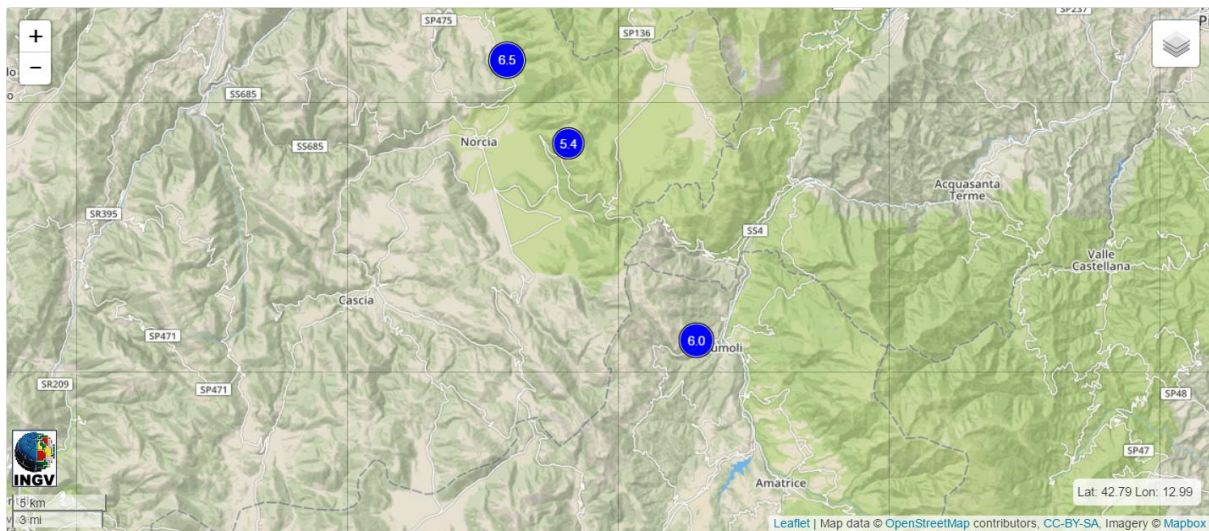
Figure 1-1 Magnitude and location of the Central Italy sequence August-October 2016 (INGV)

1.2   The EEFIT Mission

The high death toll compared to the comparatively modest magnitude of the first shock and the modest population density of this mountainous region of Italy, was a shock to the media and the public and renewed the debate about the extreme fragility of the masonry buildings which constitutes the majority of the building stock of the towns in the region. Because many of these masonry buildings had been retrofitted in previous years, their damage and collapse have important structural and judicial implications. From a legal point of view, the issue is whether the interventions have been implemented according to the provisions of the seismic codes and following appropriate construction practice, while from a structural point of view, the effectiveness of such strengthening strategies and procedures, implemented since the late 1980s, is called into question. Given the high death toll and the possible penal consequences, the historic centres were designated as "red zones" and largely cordoned off.

The EEFIT team was able to gain access to these restricted "red zones", thanks to the support of the Protezione Civile and the Fire Services, an undertook the mission fieldwork during a period of ten days

between the 4th and 16th of October 2016. The team was composed of 15 members covering a broad range of expertise from seismology to social recovery, as shown in Table 1-1.

The EEFIT mission was organised in 4 sub-teams so as to maximise the effectiveness of the deployment by fulfilling different objectives:

- a seismological and geotechnical team deployed mainly around the surface rupture of the faults;
- a team tasked with collecting vulnerability and damage data at urban level, including observation on road failures were deployed mainly in the historic city centres;
- a team tasked with the damage survey of critical infrastructure such as schools and hospitals targeted the locations of these buildings, often in the new part of the towns;
- a team focusing around the emergency response and social consequences to the population deployed mainly around the temporary administration sites and housing.

A common base camp in Rieti and daily debriefing ensured that observations carried out by the different groups were communicated and shared promptly allowing cross over where needed and relevant.

Table 1-1 Team membership and roles

Name	Initial	Affiliations	Research Interest
Prof Dina D'Ayala	DDA	University College London - CEGE	Seismic vulnerability and resilience of historic centres and critical infrastructure
Prof David Alexander	DA	University College London - IRDR	Social vulnerability and resilience
Dr Flavia De Luca	FDL	University of Bristol	Seismic response of concrete structures and critical infrastructure
Giuseppe Del Gobbo	GDG	University of Oxford	Seismic response of concrete structures
Dr Joanna Faure-Walker	JFW	University College London - IRDR	Earthquake Geology of the central Apennines and post-disaster recovery
Dr Carmine Galasso	CG	University College London – CEGE - IRDR	Engineering seismology and earthquake risk
Dr Domenico Lombardi	DL	University of Manchester	Geotechnical engineering and Structural Dynamics
Dr Tristan Lloyd	TL	AIR Woldwide	Catastrophe modelling, Insurance, structural engineering
Zoe Mildon	ZM	University College London - IRDR	Earthquake mechanics of faults in the central Italian Apennines.
Elisabeth C. Morgan	ECM	Sellafield Ltd	Safety Assessment of nuclear power plants
Dr Davide Pedicone	DP	WME	Seismic Design and Strengthening
Paolo Perugini	PP	ARUP	Seismic Response of bridges and historic buildings

Valentina Putrino	VP	University College London - CEGE	Seismic Vulnerability Assessment of Masonry Structures and clusters
Serena Tagliacozzo	ST	University College London - IRDR	Post-disaster communication and use of social media
Dr Andrea Totaro	AT	Mott Mac Donald	Seismic response of bridges and buildings

The initial objectives of the mission were determined in relation to the aftermaths of the first event and they can be summarised as follows:

- To carry out observations of primary rupture surfaces, including the azimuth and plunge of the slip vector, the strike and dip of fault geometry, and the magnitude of the surface slip.
- To carry out similar measurements of selected secondary cracks and offsets relating to the earthquake that are not part of the main fault rupture, for example, in roads and paths.
- To collect and analyse ground motion data and to study effects of local soil conditions on ground motion, particularly at sites characterized by high IM values.
- To investigate failure of slopes and foundations and damage to geotechnical structures.
- To collect geo-referenced data for the validation of remote sensing techniques designed to augment damage surveys, such as drone-mounted video cameras and omnidirectional cameras and to correlate results with satellite and aerial imagery and environmental damage.
- To collect information on details of construction techniques and damage in retrofitted and improved masonry buildings on a street by street basis using rapid survey datasheets and seismic damage expert systems.
- To survey the response of bridges and other critical road infrastructures, documenting and analysing failures.
- To collect data on the transitional period after the event and to observe the process of decision making by various levels of stakeholders, to limit further damage, house and assist the affected population, and provide a basis for eventual reconstruction and recovery.
- To collect information and document the emergency response and recovery strategy speaking to residents, community leaders, emergency responders, disaster managers and public administrators.

The official mission was completed by 16th October and there were no further EEFIT deployments following the two shocks of 26th and 30th October 2016, which affected an area north west of the immediate region around Amatrice. This notwithstanding, although the main findings presented in the report relate to the event of the 24th August 2016, where appropriate and relevant, information on the characteristics and effects of the two latter events are also included. The locations visited during the mission are listed in Table 1-2 and Figure 1-2.
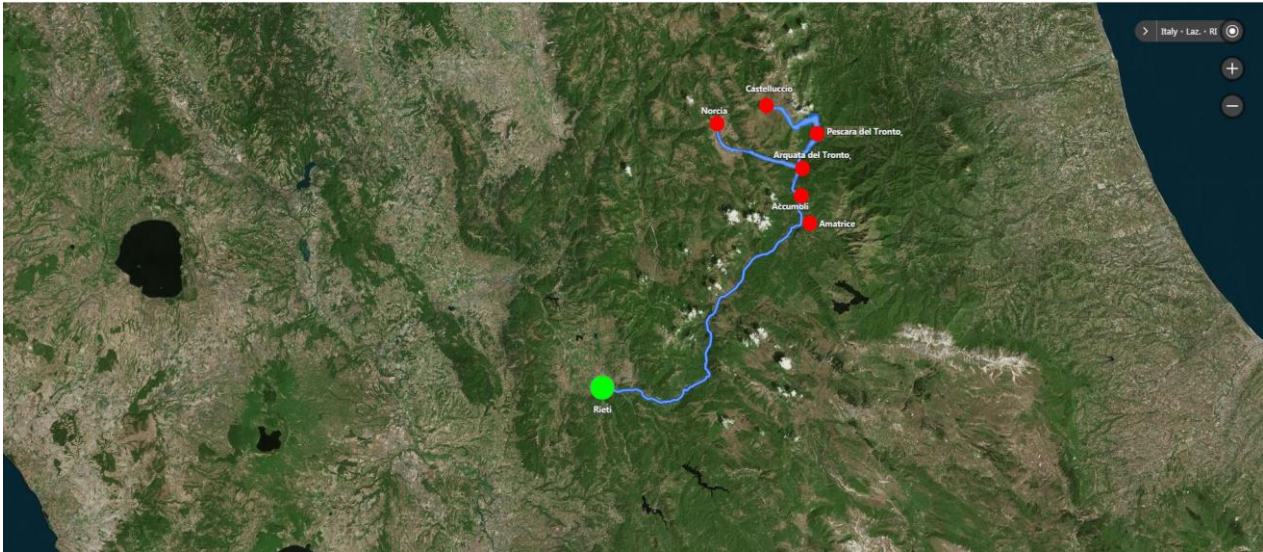
Figure 1-3 Sites visited by the EEFIT teams

Table 1-2 Sub-teams' mission itinerary and support

Date	Locations visited	EEFIT team	Accompanied by
Day 1: 05/10/2016	Arquata del Tronto, Castelluccio di Norcia, Monte Vettore, Norcia	Team 1: JFW, CG, DL, ZM	
Day 2: 06/10/2016	Monte Vettore	Team 1: JFW, CG, DL, ZM	
Day 3: 07/10/2016	Monte Vettore, Rieti DICOMAC Briefing, Amatrice red zone	Team 1: JFW, DL, ZM, Team 2: DDA, PP, VP, AT, CG, Team 4: DA, ST	Meeting Prof Mauro Dolce, Dr Elena Speranza, Italian Civil Protection, Site visit: Dr Alessandra Marini, University of Brescia, Capt.R. Marchioni, VVFF
Day 4: 08/10/2016	Monte Vettore, Arquata del Tronto Bassa, rapid street survey, Arquata del Tronto Alta, Pescara Red zones, Masonry bridges on road access to Amatrice, Interviews with Protezione civile and Vigili del Fuoco and Croce Rossa in Arquata	Team 1: JFW, ZM, Team 2: DDA, VP, CG, DL, Team 3: PP, AT, Team 4: DA, ST	Site visit: Dr A. Marini, Site visit: Dr Luigi di Sarno, University of Benevento and Dr R. Paolacci, University La Sapienza, Rome, VVFF: Piero Paoletti, Rino Furloni and Loris Diamantini
Day 5: 09/10/2016	Amatrice, Campotosto, Environmental damage survey, Survey of churches in Campi, Preci, Norcia	Team 1: JFW, DL, ZM, Team 2: DDA, PP, VP, AT	Prof Andrea Giannantoni, University of Ferrara

		Team 3: FDL, GDG, TL, ECM, DP	Dr Giulio Castori, University of Perugia
	Norcia Industrial district Visit to L'Aquila	Team 4: DA, ST	
Day 6: 10/10/2016	Survey red zone in Arquata del Tronto Alta, Log-HIDEA Survey of masonry bridge in Tufo and concrete viaducts on Survey of reinforced concrete school in Amatrice	Team 1: DL, ZM Team 2: DDA, PP, VP, AT Team 3: FDL, GDG, TL, ECM, DP Team 4 : DA, ST	Dr L. Di Sarno, Dr Luigi Sorrentino, University La Sapienza, Rome
Day 7: 11/10/2016	Environmental damage survey Accumoli and Pescara del Tronto Rapid Street survey Accumoli, Log-IDEAH Amatrice, detailed inspection of "Ponte Tre Occhi",	Team 1: DL, ZM Team 2: DDA, PP, VP, AT Team 3: FDL, GDG, TL, ECM, DP	Claudio Ortoni, SAF Vigili Del Fuoco Campania
Day 8: 12/10/2016	Rapid Street Survey and Log-IDEAH In Amatrice and Castelluccio Detailed survey of schools in Arquata del Tronto Survey of Concrete structures in Pescara del Tronto	Team 2: DDA, PP, PV, AT Team 3: FDL, GDG, TL, ECM, DP	VV FF Nucleo Interventi Speciali VV FF
Day 9: 13/10/2016	Debriefing, DICOMAC Rieti	Team 2: DDA, PP, PV, AT Team 3: FDL, GDG, TL, ECM, DP	Dr Mario Nicoletti, Protezione Civile, Seimsic Monitoring David Fabi, Protezione Civile, Emergency Coordination
Day 10: 14/10/2016	Norcia hospital and concrete structures Amatrice hospital	Team 3a: GDG, ECM, DP Team 3b: FDL, TL	

1.3 Cooperation and support by Italian Institutions

The success of the EEFIT mission in Central Italy is largely due to the strong support and collaboration received by several Italian institutions and researchers. The team is particularly indebted to the Protezione Civile and the Vigili del Fuoco Service. Prof Mauro Dolce (Civil Protection) and Dr Elena Speranza (Civil Protection) provided the EEFIT members with the necessary credentials to access the red zones in Amatrice, Arquata del Tronto, Pescara del Tronto, Accumoli and Castelluccio. The in situ survey and data gathering could have not been possible were not for the logistical support and escorting organised by Ing. Mariano Tusa (Dirigente - Comando Provinciale VV.F. di Lucca).

In the aftermath of the earthquake, many Italian academics and professionals lent their support to the Protezione Civile, to carry out the screening of residential buildings, but also heritage and critical infrastructure, for the purpose of determining access or need for repairs or demolition. The EEFIT teams took advantage of the insight gained in this way by some of the Italian colleagues, who shared their knowledge of specific buildings or bridges or other structures warranting specific attention. Dr Alessandra Marini of university of Brescia, provided information on the state of damage of churches in Amatrice; Dr

Luigi di Sarno, University of Benevento, and Dr Roberto Paolacci, University la Sapienza Rome, carried out joint inspections with EEFIT team members of a number of masonry arch bridges and viaducts that had experienced damage. Of great value was the visit, organised by Prof Andrea Giannantoni, to a series of churches in the Norcia Region, Campi Alto di Norcia, Preci. A full acknowledgements list is presented at the beginning of this report.

Figure 1-4 EEFIT team at the DICOMAC of Rieti. From left to right: (front) Prof D.D'Ayala, Eng Mario Nicoletti (Civil Protection Rieti), Valentina Putrino, Paolo Perugini, Dr Flavia De Luca; (back) Dr Tristan Lloyd, Dr Andrea Totaro, Giuseppe del Gobbo, Dr Serena Tagliacozzo, Elizabeth Morgan

1.4 Report structure

The reminder of the report is organised in eight thematic chapters. Chapter 2 presents an introduction to the seismic sequence, reference shake maps and an analysis of the historic records to provide the seismological setting of these events. The chapter also reports on direct measurements of surface fault rupture undertaken by members of the mission. Chapter 3 provides the ground motion characterisation and presents the comparison between ground motion prediction equations, derived for this region and the measured peak ground acceleration. Chapter 4 introduces the Environmental Seismic Intensity Scale to evaluate the geotechnical observations and the seismic site response. Chapter 5 focuses on the analysis of damage in urban centres, while Chapter 6 reports on damage to monumental structures and religious buildings, Chapter 7 reports on the performance of reinforced concrete structures and schools and Chapter 8 reports the performance of the transport infrastructure. Chapter 9 reviews the effects on society of the earthquake and a set of Appendix conclude the report.

2 THE EARTHQUAKE SEQUENCE OF 24TH AUGUST TO 30TH OCTOBER 2016

2.1 Seismotectonic of the region

The 24th August and 30th October earthquakes occurred on the Mt Vettore and Laga faults which are situated in the central Italy near the borders of the Lazio, Abruzzo, Umbria and Marche regions. The Italian Apennines axis runs northwest-southeast and is characterised by normal faults that strike southeast and dip towards the southwest with typical lengths between 20km and 40km (Figure 2-1, e.g. Roberts and Michetti, 2004, Papanikolaou et al., 2005, Faure Walker et al., 2010, 2012). Active northeast-southwest extension has been confirmed through focal mechanisms of recent earthquakes, borehole break-out data, geodesy, and studies of striated normal fault scarps exposed at the surface (e.g. Anderson and Jackson, 1987, Pondrelli et al., 1995, Amato and Montone, 1997, Michetti et al., 2000, Hunstad et al., 2003, Montone et al., 2004, Roberts and Michetti, 2004, Anzidei et al., 2005, Serpelloni et al., 2005, Faure Walker et al., 2010, 2012). This extension is thought to have started about 2.5 Myrs ago, as evidenced by extensional basin infill sediments (Cavinato et al., 2002). There is debate regarding the precise cause of the present-day extension in the region, in particular whether the driving forces for the extension is related to edge forces, such as rotation of microplates, or forces from beneath the crust relating to mantle upwelling (see Faure Walker et al., 2012). Before the change to an extensional setting, this region was characterised by thrust-faulting accommodating convergence between the Eurasian and African plates (Dewey et al., 1973), this thrusting continues on the Adriatic side of the Apennines to the present-day (Patacca et al., 1990). Present-day extension rates across this area have been measured as up to a few mm/yr (e.g. Serpelloni et al., 2005, D'Agostino et al., 2009, Faure Walker et al., 2010). It is the present-day northeast-southwest extension that causes the damaging earthquakes in the region.
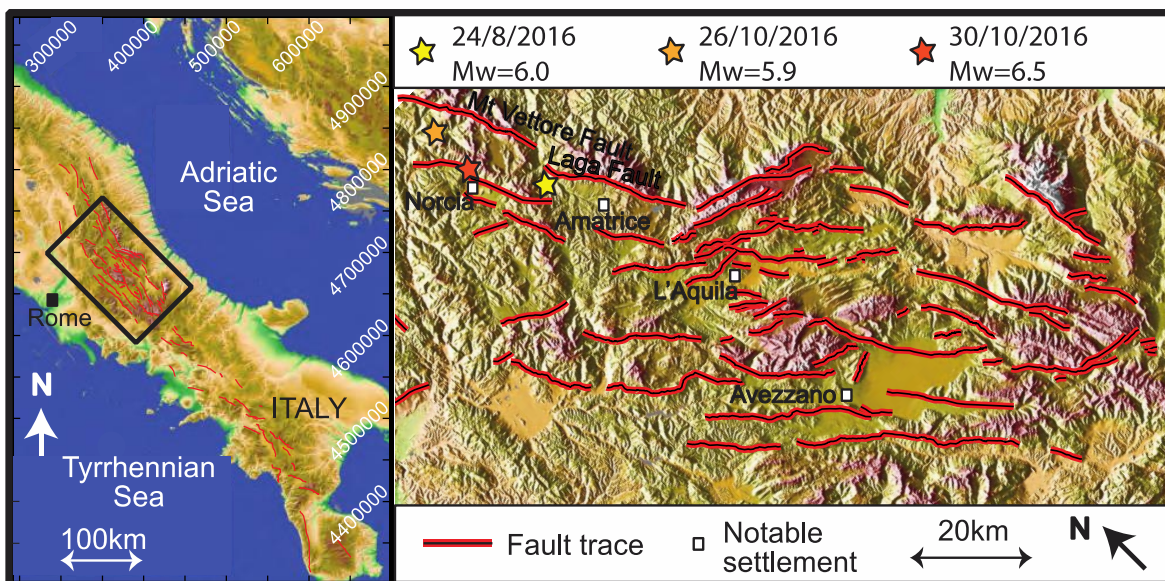
Figure 2-1 Fault map of the central Apennines (adapted from Faure Walker et al., 2018), showing general region (left) and more detailed fault map (right) with the locations of the three main events of the 24th August to 30th October 2016 earthquake sequence.

2.2 Shake maps

At 03.36 (ECT) on 24th August 2016 a M_w 6.2 earthquake struck the central region of Italy, with epicentre in the Apennines range, near the village of Accumoli and with a fault surface rupture length of approximately 25km. Figure 2-2 shows the instrumental peak ground acceleration contour map obtained by interpolation of 109 instruments on a distance range from 3.7km to 120km. The macroseismic intensity shakemap, produced by INGV and expressed in MCS intensity scale, is based on ground motions parameters recorded

at these stations and determined using the Faenza and Michelini (2010, 2011) conversion relations. The event has been attributed an epicentral MCS intensity of IX.

PERCEIVED SHAKING	Not felt	Weak	Light	Moderate	Strong	Very strong	Severe	Violent	Extreme
POTENTIAL DAMAGE	none	none	none	Very light	Light	Moderate	Mod./Heavy	Heavy	Very Heavy
PEAK ACC.(%g)	<0.06	0.2	0.8	2.0	4.8	12	29	70	>171
PEAK VEL.(cm/s)	<0.02	0.08	0.3	0.9	2.4	6.4	17	45	>120
INSTRUMENTAL INTENSITY	I	II–III	IV	V	VI	VII	VIII	IX	X+

Scale based upon Faenza and Michelini, 2010, 2011
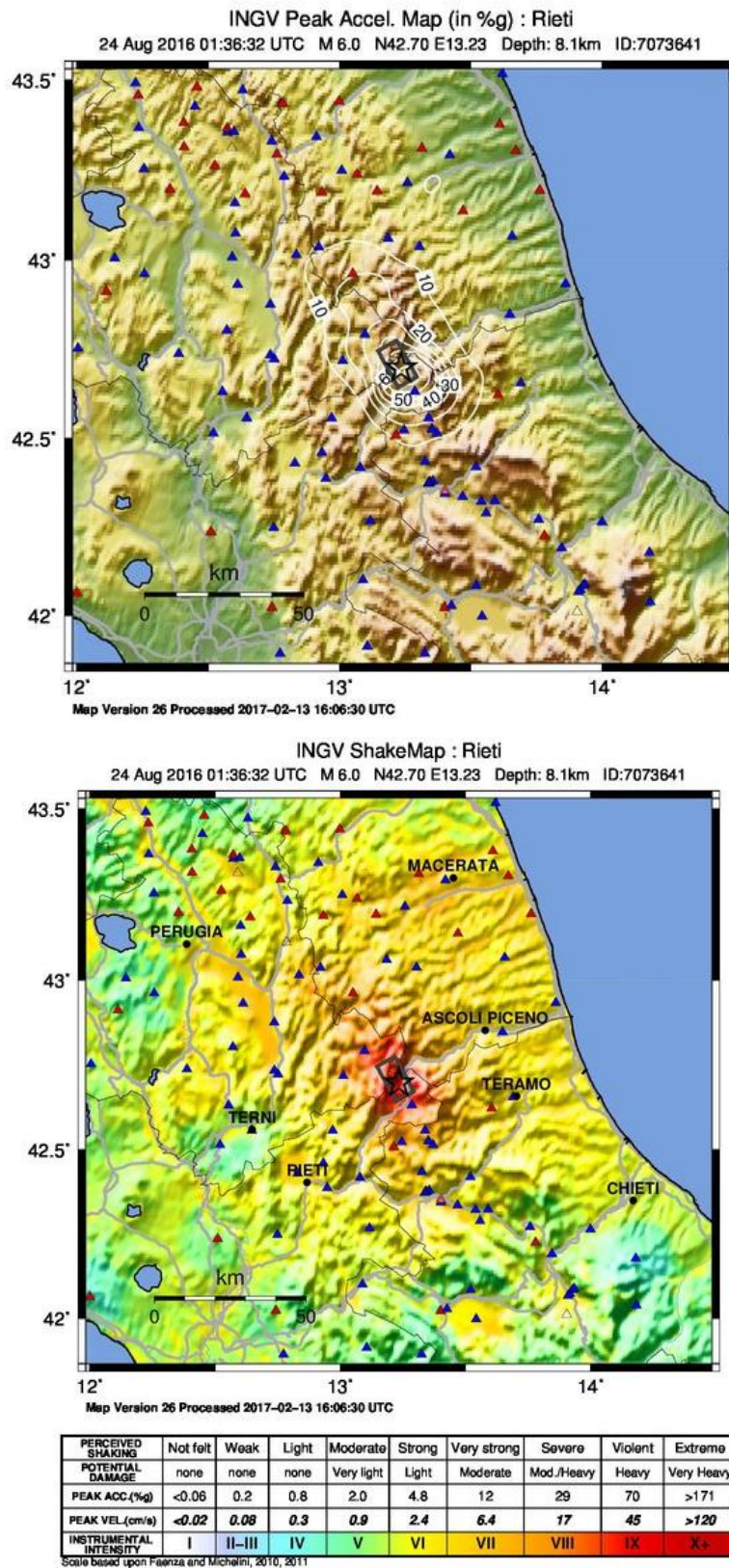
Figure 2-2: a) Instrumental peak ground acceleration contour map and b) macroseismic Intensity shakemap for the event of 24th August 2016 at 01:36:32 UTC (INGV, 2016)

2.3   Analysis of historic records

The historic record for earthquakes $M_w>5.5$ in this region of the Appennines straddling the Lazio, Umbria, Marche and Abruzzo regions, is considered complete since 1349 (Michetti et al., 1996). The CPTI15, Parametric Catalogue of Italian Earthquakes, from year 1000 to 2015 (Rovida et al. 2016), contains 38 events $M_w>5.5$ in a region bounded northwest by the epicentre of the 1984 Gubbio earthquake and southeast by the epicentre of the 1915 Avezzano earthquake, the strongest ever recorded in this region. (see Figure 2-3a). In particular, the historic records show a strong correlation between events generated in the Valnerina, the Sibillini range including Monte Vettore, and the range of Monti della Laga, east of Amatrice.

Of particular relevance to this correlation is the sequence of events of the year 1703, which saw first an intensity MCS 11 event on January 14th, with epicentre in Val Nerina south of Norcia, then an intensity MCS 8 event on January 16th in the Mountain range between Abruzzo and Lazio, finally and intensity MCS 10 earthquake on February 2nd in the L'Aquila valley. The first caused devastation in Norcia and Amatrice and extensive damage in L'Aquila, the second one, for which the epicentre has not been located precisely, caused further damage in Amatrice, Accumoli and Norcia and minor damage in L'Aquila. For the third, with epicentre northwest of L'Aquila, there are no records of damage in Norcia or Amatrice, possibly because of the extent of destruction of the previous two, but it caused damage in towns north and west of Amatrice and Norcia. This correlation is further proven by many other events as summarised in Figure 2-4 showing the epicentral and local intensity for earthquakes with MCS>=6 recorded in the towns affected by the 24 August 2016 event. The time sequence shows that several event with epicentres in the Norcia region have destructive effects in Amatrice and Accumoli and vice versa.
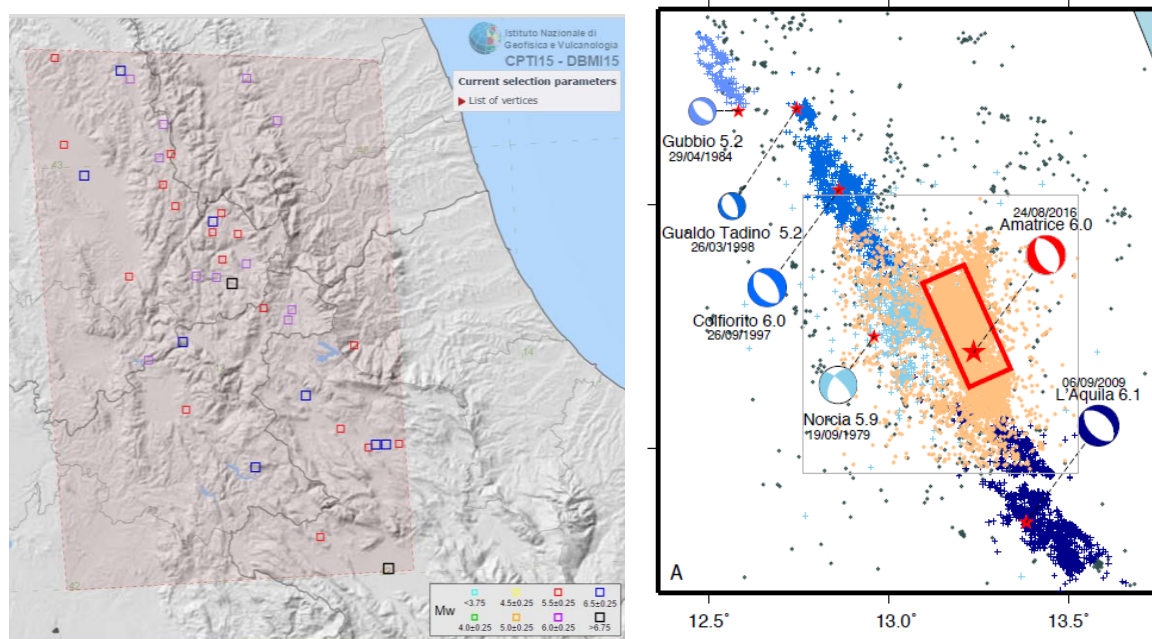
Figure 2-3 a) Historic earthquakes of Mw > 5.5 in the region of interest; b) Mapping of the moment tensors for the recent historic earthquake sequences since 1979 and the 24th August event rupturing, overall activating a 150km long sector of the Appennine chain (image credit: Micheli et al, 2016, DOI:10.4401/ag-7227)

Indeed the recent seismic history, for which not just the main shock's epicentre, but also the source of the aftershock can be accurately located (see Figure 2-3b) shows that the fault ruptures of these events are substantially aligned and adjacent. The globes in Figure 2-3b represent the focal mechanisms and depict the type of faulting that occurred. For the central Apennines, the dominant faulting style is normal faulting along north-west to south-east aligned faults. The events of the 26th and 30th October (M_w 5.9 and 6.5 respectively) also follow this faulting style. The most recent event prior to 2016 in this part of the Apennines was the 2009 L'Aquila M_w 6.3 earthquake, which occurred along the Paganica Fault approximately 45km

southeast of Amatrice. Prior to this, in 1997-1998 there was a prolonged sequence of earthquakes on the Umbria-Marche border approximately 40 km northwest of Amatrice, and prior to that two more sequences, one centred in the vicinity of Gubbio in 1984 and close to Norcia in 1979. These events are particularly significant as they triggered changes in the Italian seismic code, both in terms of seismic zoning and in terms of provision for post-earthquake repair and strengthening of masonry buildings, which have affected the building stock of the region hit by the events of 2016 and determined their response. (see section 5.4).
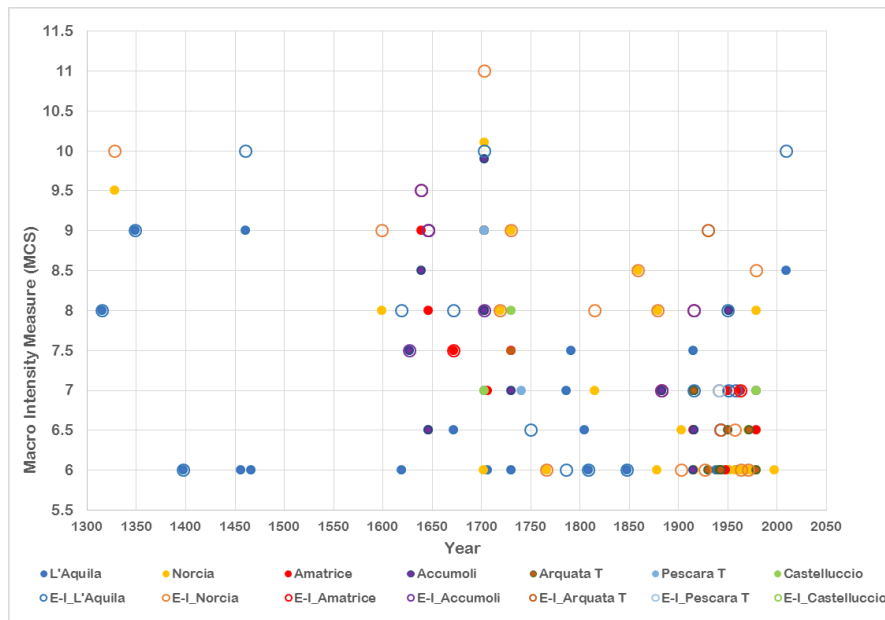
Figure 2-4 : Local and Epicentral Macroseimsic intensity for historic earthquakes with MCS >= 6

2.4   Fault rupture

2.4.1   *Summary of the earthquake surface ruptures*

The 24 August 2016 earthquake ruptured the southern end of the Mt Vettore Fault and northern section of the Laga Fault (Livio et al., 2016). Surface offsets have been observed semi-continuously along the Mt Vettore Fault, but not the Laga Fault (Livio et al., 2016). During the EEFIT mission in October 2016, where surface offsets were identified, detailed measurements were taken every 2m or 5m along approximately 1,200m of the Mt Vettore Fault. The slip at the surface along the measured parts varied between 3cm and 30cm with and mean slip vector azimuth of 223° and mean slip vector plunge of 50°, consistent with the regional extension direction (e.g. Faure Walker et al., 2010). The Mt Vettore Fault had not previously been reported to have ruptured during the historical record. Palaeoseismic trenching suggests the last earthquake to rupture this fault occurred sometime between the 7th century AD and 4155yrs BP (Galadini and Galli, 2003). However, the Laga Fault is thought to have last ruptured in 1639 (DISS, 2015).

2.4.2   *Surface ruptures along faults in Italy*

There continues to be some debate whether observed surface ruptures for this earthquake and certain previous events are coseismic, aseismic fault creep displacements, or related to land sliding or gravitational compaction (see Mildon et al. (2016a) for a summary). The debate regarding whether slip during earthquakes reaches the surface along visible fault scarps is important because coseismic slip provides evidence for the observed surface scarps associated with active faults and hence contributing to the understanding of related earthquakes' magnitude and seismic hazard. Several years after the 1997

earthquake along the Mt Scalette Fault, Mildon et al. (2016a) measured and analysed relationships between surface observations along the fault (strike, dip and coseismic throw (interpreted as a white un-weathered strip at the base of the fault plane)). They used the relationships between these observations and the dip direction of the upper and lower slopes to show the offsets were of tectonic rather than gravitational origin. Observations of the slip direction of the measured surface offsets along the Mt Vettore Fault following the August 2016 earthquake during the EEFIT mission have also shown that the offsets were not parallel to the down-sip direction of the slopes that were offset along long sections of the rupture (Mildon et al., 2016b). This supports a tectonic origin for the observed surface offsets. These measurements were made six weeks after the event and so fresh offsets were still present before being degraded over time, thus allowing a detailed analysis of the magnitude and directions of coseismic throw. Some surface offsets had been observed and made public within a week of the event confirming they were fresh (Pace et al., 2016). The surface offsets are also in agreement with preliminary InSAR interpretations in that the InSAR shows that slip did propagate to the surface (e.g. GSI, 2016, INGV, 2016) supporting exposed fault scarps being of tectonic origin. However, some of the offsets may have increased in size by creep during the weeks following the event (Livio et al., 2016), therefore measurements of offset within this report may include a small component of post-seismic slip.

The minimum magnitude earthquake for producing surface offsets in the Apennines is thought to be c. M_w 5.6. This follows from the M_w 5.6 Lauria earthquake (1998) in the southern Apennines that produced centimetre surface ruptures on a bedrock scarp along the Mercure Fault (Michetti et al., 2000). Therefore, such studies of surface offsets are restricted to larger events with M_w greater than approximately 5.6.

2.4.3 *Methods – how observations were made*

Where the surface offsets could be identified along the section of the rupture studied, measurements were taken every 2m or 5m (Figure 2-4). This allowed a continuous record of the rupture along this part of the fault that could be joined with observations from other groups in order to obtain a detailed dataset of the surface ruptures (e.g. Livio et al., 2016). At each site, when possible, the vertical offset (throw), horizontal offset (heave) and total offset (slip) were measured (see Figure 2-5 for an explanation of these terms). The slip vector azimuth (direction of slip) and slip vector plunge (angle below horizontal of the slip vector) were also measured. These measurements were taken by finding identifiers on either side of the rupture that were previously connected.
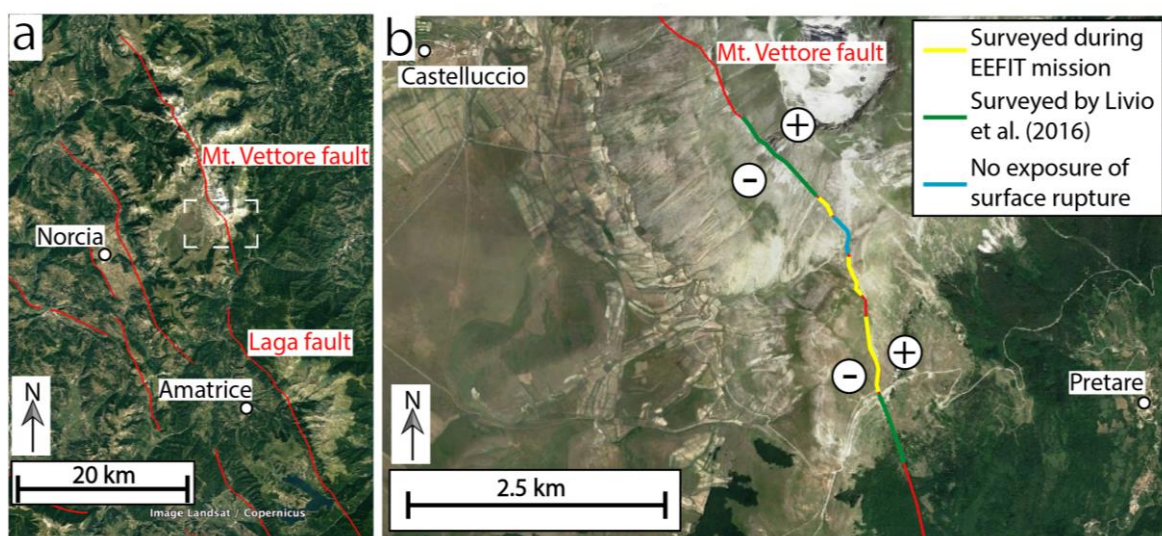
Figure 2-5 Location map of earthquake surface rupture observations (adapted from Mildon et al., 2016a, Faure Walker et al., 2012).

In Figure 2-5a red lines show mapped faults in the region and key towns are marked. Figure 2-5a is a map of the region, showing the Mt. Vettore Fault and Laga Fault. The dashed box in Figure 2-5a shows the extent of the enlargement of Figure 2-5b. showing the section of the Mt. Vettore Fault that had surface ruptures interpreted to be due to the 24 August 2016 earthquake. In Figure 2-5b yellow lines show the section of the fault surveyed during the EEFIT mission, green lines are sections published in Livio et al. (2016), blue lines is an absence of surface rupture. The + and – signs indicate the uplift and subsidence of the ground either side of the fault. Figures 2-6 – 2-8 show some examples of offsets seen along the fault rupture.
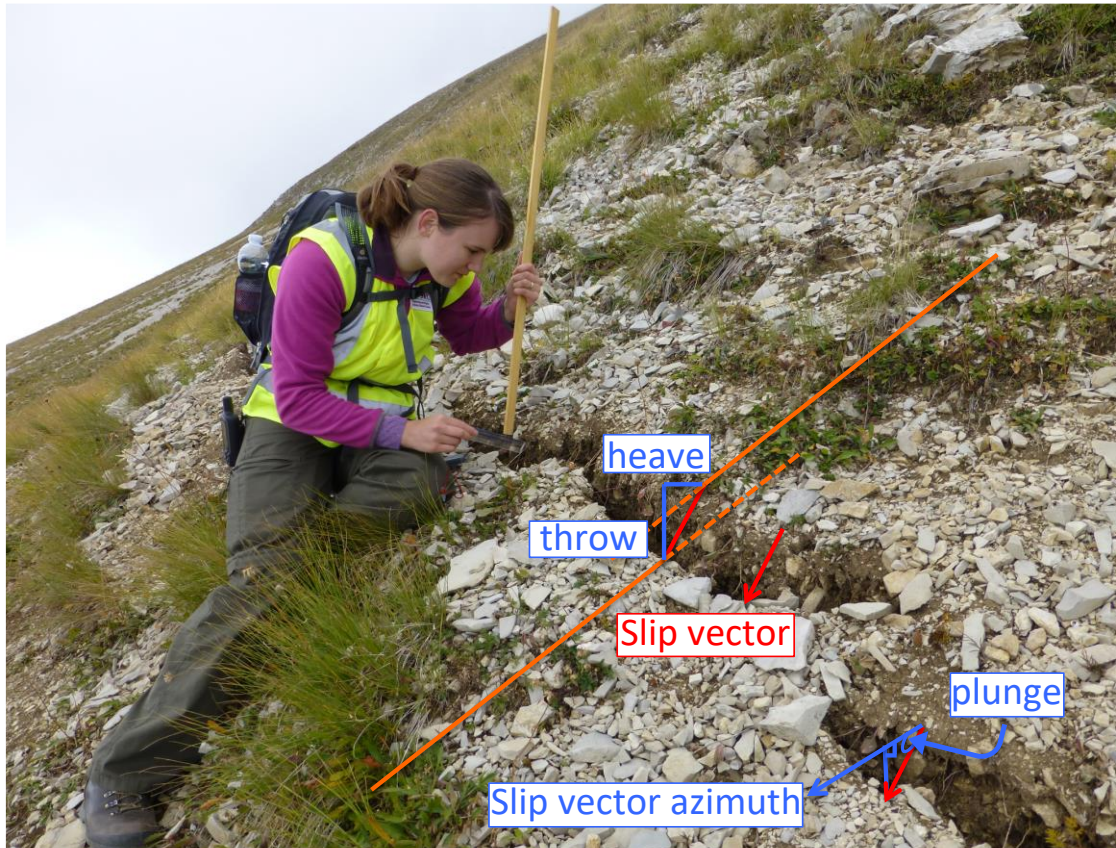
Figure 2-6 Explanation of measurements taken in the field, photograph taken looking north-west along the fault rupture.

Figure 2-7: 12cm long rock split in two along rupture, the red arrow indicates the slip vector, deduced because the sides of the rock were joined together prior to the earthquake rupturing. UTM: 33T 357958,4741996.

Figure 2-8 Example of a colluvium offset seen continuously along the rupture. Throw (vertical offset) is approximately 11cm, slip is approximately 14cm. At this site, slip vector azimuth is 2400, the slip vector plunge is 600. UTM: 33T 357961 4740995.

Figure 2-9 Example of rupture offset. Observed total offset in some locations was up to 30cm, with a throw (vertical offset) up to 28cm.

2.5   Conclusions and future work

The observations along the Mt Vettore Fault surface ruptures following the August 2016 earthquake provided an opportunity to study detailed measurements and how they change along the surface rupture. Surface offsets were observed both along fault scarps in limestone rock and along sections with colluvium cover where limestone rock was not present at the surface. Vertical and horizontal offsets within the 1.2km fault section studied varied up to 28cm and 16cm respectively, with the maximum calculated displacement

being 30.5cm. The interquartile range of slip vector trend and plunge were 211°-236° and 42°-58°, which are typical for normal earthquakes within this region. Further analyses of the data will be performed for this earthquake by combining the data with other datasets along the remaining parts of the fault with surface ruptures.

References

DISS Working Group (2015). Database of Individual Seismogenic Sources (DISS), Version 3.2.0: A compilation of potential sources for earthquakes larger than M 5.5 in Italy and surrounding areas. http://diss.rm.ingv.it/diss/, Istituto Nazionale di Geofisica e Vulcanologia; DOI:10.6092/INGV.IT-DISS3.2.0

Faure Walker, J. P., G. P. Roberts, P. R. Sammonds, and P. A. Cowie (2010), Comparison of earthquake strains over 10 2 and 10 4 year timescales: Insights into variability in the seismic cycle in the central Apennines, Italy, J.ournal of Geophysical Research, 115, (B10), B10418, doi:10.1029/2009JB006462.

Faure Walker, J. P., G. P. Roberts, P. A. Cowie, I. D. Papanikolaou, A. M. Michetti, P. R. Sammonds, M. Wilkinson, K. J. W. McCaffrey, and R. J. Phillips (2012), Relationship between topography, rates of extension and mantle dynamics in the actively-extending Italian Apennines, Earth Planet. Sci. Lett., 325–326, 76–84, doi:10.1016/j.epsl.2012.01.028.

Galadini, F., and P. Galli (2003), Paleoseismology of silent faults in the Central Apennines (Italy): the Mt . Vettore and Laga Mts . faults, Ann. Geophyics 46 (5), 815 - 836.

GSI (2016), http://www.gsi.go.jp/cais/topic160826-index-e.html

INGV (2016), https://ingvterremoti.wordpress.com/2016/08/30/la-sequenza-sismica-in-italia-centrale-un-primo-quadro-interpretativo-dellingv

Livio F., Michetti A.M., Vittori E., Gregory L., Wedmore L., Piccardi L., Tondi E., Roberts G. and CENTRAL ITALY EARTHQUAKE WORKING GROUP: Blumetti A.M., Bonadeo L., Brunamonte F., Comerci V., Di Manna P., Ferrario M.F., Faure Walker J., Frigerio C., Fumanti F., Guerrieri L., Iezzi F., Leoni G., McCaffrey K., Mildon Z., Phillips R., Rhodes E., Walters R.J., Wilkinson M. (2016), Surface faulting during the August 24, 2016, Central Italy earthquake (Mw 6.0): preliminary results

Michele M., Di Stefano R., Chiaraluce L., Cattaneo M. et al.,2016, The Amatrice 2016 seismic sequence: a preliminary look at the mainshock and aftershocks distribution. Annals of Geophyscics, 59, Fast Track 5, 2016; DOI: 10.4401/ag-7197

Michetti A.M., Brunamonte F., Serva L., Vittori E., (1996), Trench investigations of the 1915 Fucino earthquake fault scarps (Abruzzo, Central Italy): geological, evidence of large historical events, Journal of Geophysical Research, 101 (B3), 5921-5936

Michetti A.M., Ferreli L., Esposito E., Porfido S., Blumetti A.M., Vittori

E., Serva L., and Roberts G.P., (2000) Ground Effects during the 9 September 1998, Mw = 5.6, Lauria Earthquake and the seismic potential of the aseismic Pollino Region in Southern Italy, Seismological Research Letters, 71, 31-46

Mildon Z.K., Roberts G.P., Faure Walker J.P., Wedmore L.N.J., McCaffrey K.J.W, Active normal faulting during the 1997 seismic sequence in Colfiorito, Umbria: Did slip propagate to the surface? (2016a) Journal of structural geology, http://dx.doi.org/10.1016/j.jsg.2016.08.011, 2016, http://www.sciencedirect.com/science/article/pii/S0191814116301134

Z.K. Mildon, F. Iezzi, L. Wedmore, L. Gregory, K.McCaffrey, M. Wilkinson, J.P. Faure Walker, G.P. Roberts, F. Livio, E. Vittori, A.M. Michetti, C. Frigerio, A.M. Blumetti, L. Guerrieri, P. Di Manna, V. Comerci (2016b). Detailed surface rupture geometry from the 2016 Amatrice earthquake (24th August and 30th October). AGU abstract, poster Dec 2016 #S43F-3212

Pace B., Visini F., and Valentini A., (2016), 24 August 2016, Amatrice Earthquake: Field Observations, Preliminary Photo Album, vers. 31/08/2016, https://www.researchgate.net/publication/307478094_24_AUGUST_2016_AMATRICE_EARTHQUAKE _FIELD_OBSERVATIONS_PRELIMINARY

Rovida A., Locati M., Camassi R., Lolli B., Gasperini P. (eds), 2016. CPTI15, the 2015 version of the Parametric Catalogue of Italian Earthquakes. Istituto Nazionale di Geofisica e Vulcanologia. doi:http://doi.org/10.6092/INGV.IT-CPTI15

3   GROUND MOTION CHARACTERIZATION

3.1   Introduction

Several national and regional ground motion recording networks have been installed in Italy during the last decades, with the aim of monitoring and recording the ground shaking generated by moderate to strong events occurring in the Italian territory. Those networks make available, rapidly after each seismic event, some hundreds ground motion records.

In particular, the Rete Accelerometrica Nazionale (RAN http://ran.protezionecivile.it), owned and operated by the Dipartimento della Protezione Civile (DPC), and the Rete Sismica Nazionale (RSN; http://www.ingv.it/it), owned and operated by the Istituto Nazionale di Geofisica e Vulcanologia (INGV), contribute to most of the ground motion data for 2016 Central Italy seismic sequence. RAN comprises stations located inside the former Italian National Electric Company (Ente Nazionale per l'Energia ELettrica, ENEL) transformer cabins, generally equipped with Syscom MS2007 instruments and free-field stations mostly equipped with Kinemetrics sensors (Etna, K2, Makalu, FBA23 or Episensor). General characteristics of the instruments are: 3-channel accelerometers, a full-scale range of 1g/2g, and 18-24 bit resolution. RSN instruments are generally Kinemetrics Episensor FBA-ES-T; the unit consists of three Episensor force balance accelerometer modules mounted orthogonally, with full-scale recording ranges of ± 1g to ± 2g (Luzi, Puglia, Russo, & ORFEUS, 2016). Both unprocessed data and corrected data and processing details are available on the Engineering Strong-Motion database (ESM; http://esm.mi.ingv.it; last accessed March 2017). The accelerometric records are manually processed using the procedure described by Paolucci *et al.*, (2011), which prescribes the application of a second-order time-domain Butterworth filter to the zero-padded acceleration time series and zero-pad removal to make acceleration and displacement consistent after double integration. The typical band-pass frequency range is between 0.08 and 40 Hz because the entire set is composed of digital records. The spectral ordinates used for the analysis are selected only within the usable frequency band, defined by the band-pass frequencies.

Specifically, in this chapter, a strong-motion data set, consisting of nearly 1,000 waveforms, has been analysed to gather insights about the main features of the ground motion shaking intensity. The considered ground motions refer to the three largest earthquakes of the 2016 Central Italy seismic sequence, i.e., the M_w 6.0 of 24th August 2016 01:36:32 GMT, the M_w 5.9 of 26th October 2016 19:18:06 GMT, and the M_w 6.5 of 30th October 2016 06:40:18 GMT. These three main events with magnitude larger than 5.5 struck an area approximately more than 50 km long and 30 km wide. The causative fault mechanism of the three mainshocks herein considered, obtained from Time Domain Moment Tensor technique and implemented at INGV National Earthquake Centre (Luzi et al., 2017), features pure normal faulting, in agreement with the prevailing extensional regime of the central Apennines and with the mechanisms, for instance, of the 1997 M_w 6.0 Colfiorito and 2009 M_w 6.1 L'Aquila earthquakes. The three considered events have NW-SE or NNW-SSE strike and dip towards SW. Nearly 10,000 waveforms were recorded from the 24 August to December 2016, considering mainshocks and the 48 aftershocks with moment magnitude larger than or equal to M_w 4. (Luzi et al., 2017). They are of major relevance not only for a complex regional context such as Italy, but also at the worldwide scale, because they increase the set of normal fault and near-source recordings that are usually poorly represented in global strong-motion databases (e.g., the Next Generation Attenuation [NGA]-West2, Ancheta *et al.*, 2014; or the Reference database for Seismic grOund-motion pRediction in Europe [RESORCE], Akkar *et al.*, 2014).

The epicentre of the M_w 6.0 of 24th August 2016 earthquake is located in the municipality of Accumoli (Lat 42.70, Lon 13.25, depth 8.1km). The event strongly damaged the villages of Amatrice and Accumoli, causing about 300 fatalities due to the collapse of several buildings in the towns and villages in the epicentral area. The fault geometry was calculated by Tinti *et al.* (2016) and has the following characteristics: strike 156°, dip 50°, rake -85°, length 26km and width 16km. According to the ESM database, this event has been recorded by 260 (of which 20 are classified as 'bad quality record') digital strong-motion instruments. It is worth noting

that after the Amatrice event, INGV and DPC installed about 35 temporary stations to monitor the earthquake aftershock sequence at higher resolution to obtain more accurate values of the source parameters and of the ground shaking in the near-source region (Luzi et al., 2017).

The epicentre of the M_w 5.9 of 26th October 2016 earthquake is located below the municipality of Ussita (Lat 42.91, Lon 13.13, depth 7.5km). The event resulted in additional damage to the buildings and infrastructure previously hit by the 24 August event. The fault geometry was calculated by Chiaraluce et al. (2017) and has the following characteristics: strike 159°, dip 47°, rake -93°, length 18km and width 10km. According to the ESM database, this event has been recorded by 267 (of which 19 are classified as 'bad quality record' and one as 'automatically processed/restricted') digital strong-motion instruments.

The epicentre of the M_w 6.5 of 30th October 2016 earthquake is located south of the municipality of Norcia (Lat 42.85, Lon 13.11, depth 9.4km). The event caused the total collapse of several structures damaged by the previous events and the complete destruction of the village of Amatrice. No fatalities were reported as most of the population had already been evacuated. The fault plane solution indicates again normal faulting. The fault geometry was calculated by Chiaraluce et al. (2017) has the following characteristics: strike 151°, dip 47°, rake -89°, length 26km and width 14km. According to the ESM database, this event has been recorded by 268 (of which 28 are classified as 'bad quality record') digital strong-motion instruments. The location of the epicentres and the surface projection of the causative faults of the three considered events are shown in Figure 3-1.

The ground motion records of the M_w 6.0 of 24th August 2016 earthquake were first downloaded in the third week of September 2016, in order to provide timely input to the field reconnaissance team regarding ground motions. For all the tree vents, the records classified as 'bad quality' or 'restricted' in the database are not considered here.
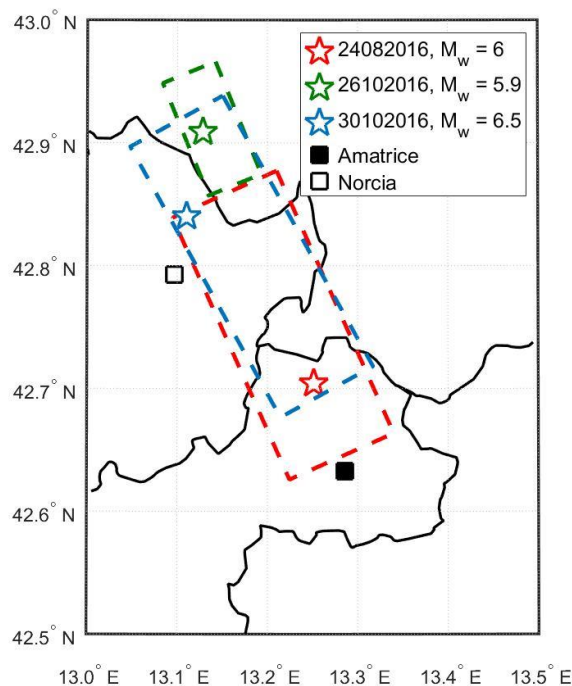
Figure 3-1 Epicentres and surface projection of the causative faults of the three considered events. (Tinti et al., 2016; Chiaraluce et al., 2017)

The EEFIT team inspected a number of stations. In particular, the AMT and NRC stations which recorded the highest accelerations values during the M_w 6.0 of 24th August 2016 earthquake. At the inspected stations no

---

ground failure features or earthquake-induced damage has been observed, to be considered in the evaluation of the records.

3.2 Ground motion intensity measures

Peak and integral ground motion intensity measures (IMs) and spectral forms are available from the ESM database. The analysis in this chapter only considers recording stations within 100km from the source, with 10 stations within 30km, and 37 within 50km from the epicentre for the M_w 6.0 of 24th August 2016 earthquake; 27 stations within 30km, and 55 within 50km from the epicentre for the M_w 5.9 of 26th October 2016 earthquake, and 26 stations within 30km, and 52 within 50km from the epicentre for the M_w 6.5 of 30th October 2016 earthquake.
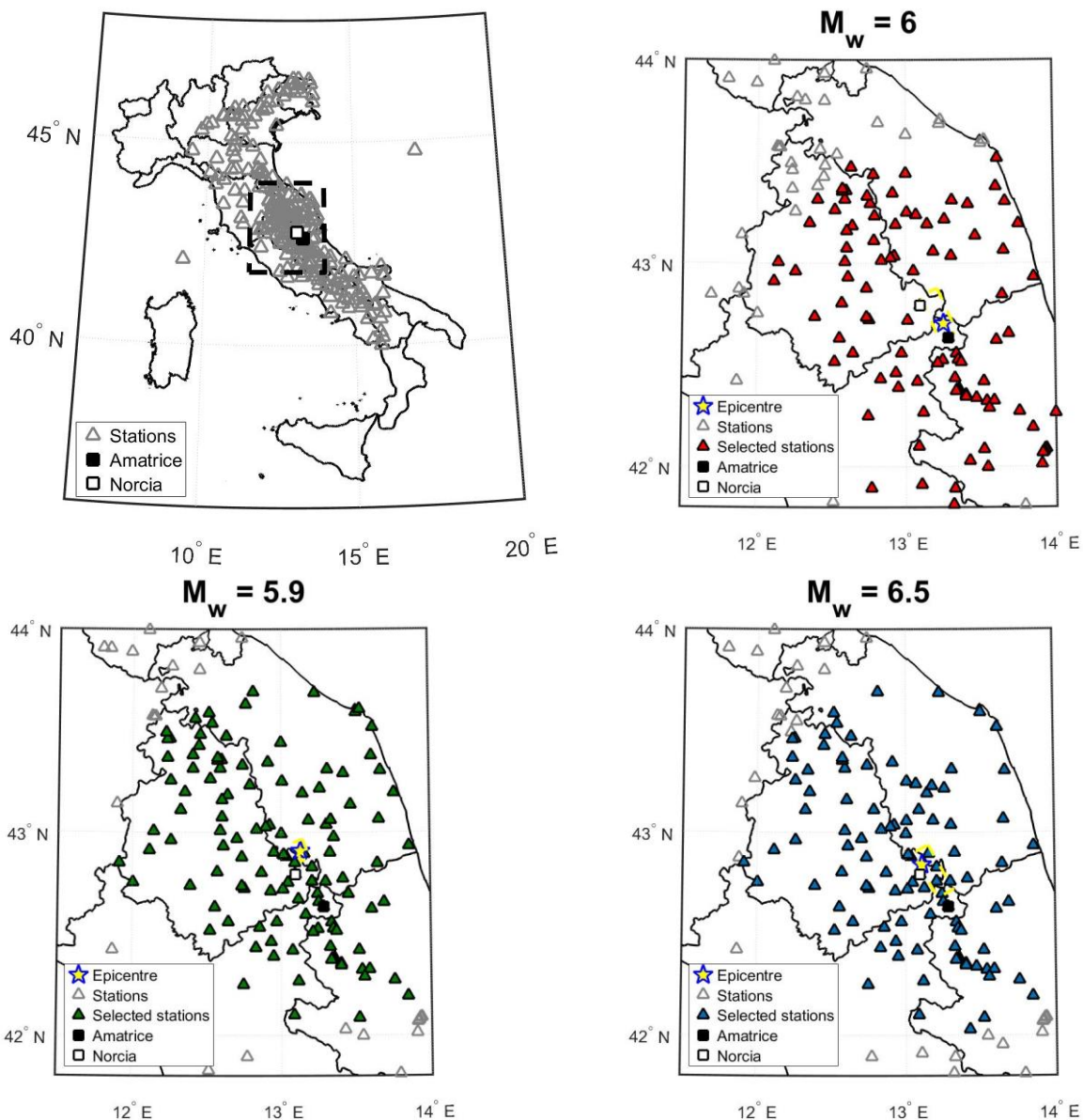
Figure 3-2 (a) Map of Italy and recording stations for three considered events. Location of the epicentre, the surface projection of the causative fault (see Figure 3-1 for a larger view) and the spatial distribution of the recording stations for (b) M_w 6.0 of 24th August 2016 earthquake, (c) M_w 5.9 of 26th October 2016 earthquake, and (d) M_w 6.5 of 30th October 2016 earthquake. Coloured triangles represent the recording stations considered in this study (i.e., within 100km from the source). The same colour code for each event is used across the report.

Figure 3-2a shows the location of the recording stations of the three considered seismic events. Figure 3-2b-2d show a close-up view of the location of the epicentre, the surface projection of the causative fault and the spatial distribution of the considered stations (i.e., those within 100km from the epicentre) for each event.

The recording sites are classified according to Eurocode 8 (2003; hereafter, EC8), based on the shear-wave velocity averaged over the top 30 m of the soil profile, V_{S30} (in which EC8 class A>800 m/s, B=360–800 m/s, C=180–360 m/s, and D<180 m/s), available for a limited number of sites (approximately 30 out of a total of 230). In cases where the geological/geophysical information is not available, the class has been inferred from the surface geology (Di Capua, Lanzo, Pessina, Peppoloni, & Scasserra, 2011). Descriptions of the surface geology based on small-scale maps (1:100000) are available from station monographies available on the ESM website. The majority of stations belong to class A or B, whereas a few stations are classified as C.

Contour maps of several ground shaking characteristics are available from the US Geological Survey (USGS) website for the three main shocks. Figure 3-3 shows the PGA and Sa (T=0.3s) of the 24/August/2016 event and Figure 3-4 shows the same features for the event of 30/October/2016. The two shake maps are generated with the software package ShakeMap® developed by the USGS Earthquake Hazards Program (Wald, Worden, Quitoriano, & Pankow, 2005). Similar maps using the same software are also produced by INGV. However, these include revisited data, including the identification of the fault plan projection, and hence might provide a more accurate description of the shaking accounting for more detailed data that became available some weeks after the earthquake. These maps can be accessed at http://shakemap.rm.ingv.it/shake/index.html.
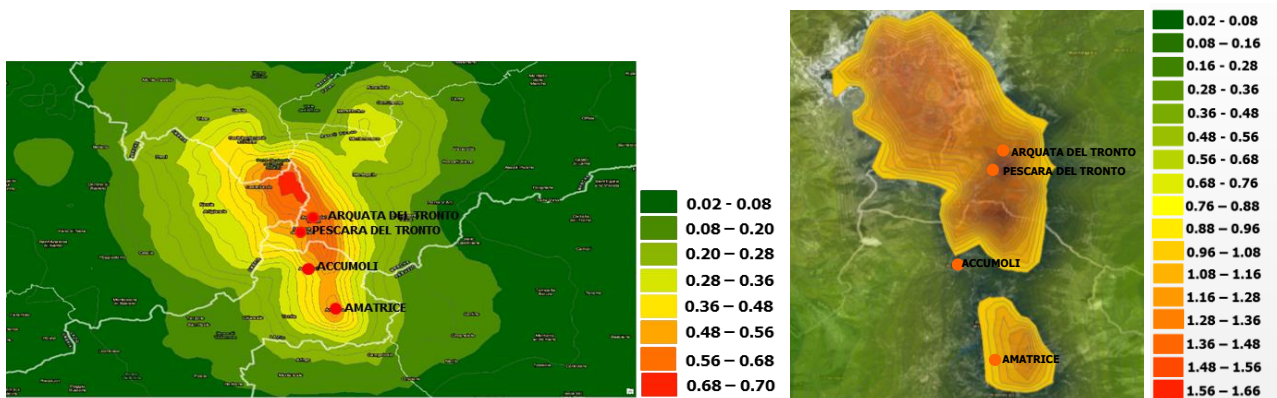
Figure 3-3 : Shake map according to USGS (Mw 6.2) for (a) PGA and (b) Sa(0.3 s) for the Mw 6.2 of 24/08/2016
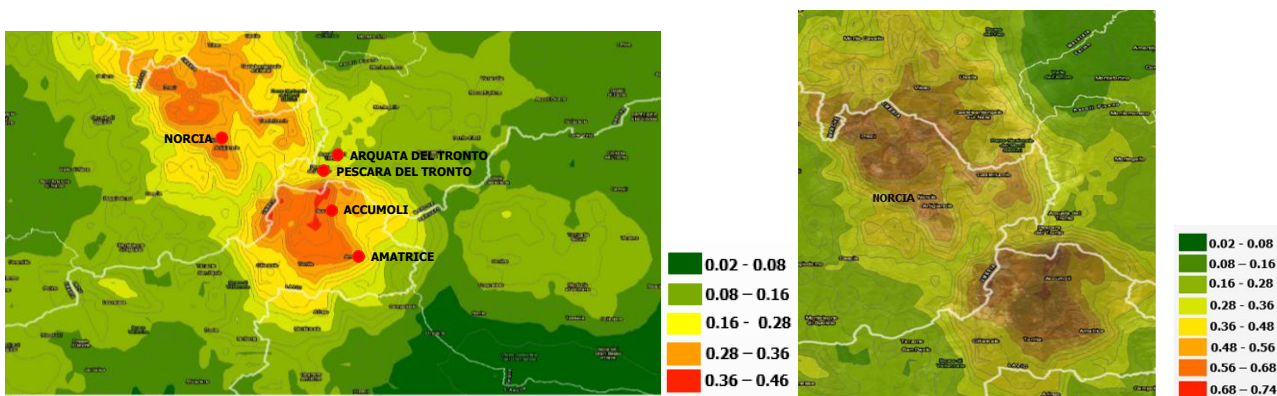
Figure 3-4: Shake map according to USGS (Mw 6.2) for (a) PGA and (b) Sa(0.3 s) for the Mw 6.5 of 30/10/2016

For the M6.0 24th August 2016 earthquake, peak ground accelerations (PGAs) larger than 0.3g have been recorded at the near source stations, in terms of Joyner-Boore distance (R_{jb}). i.e., the shortest distance from

a site to the surface projection of the rupture surface: AMT (PGA= 0.87g, R_{jb} = 1.38km, type B ground according to EC8) (CEN, 2004), NRC (PGA= 0.37g, R_{jb} = 2.01km, type B ground according to EC8), FOC (name, R_{jb} = 26.3km, type C ground according to EC8), and PCB (name, R_{jb} = 10.66km, type B ground according to EC8).

Data shows that the maximum PGAs recorded by NRC and AMT stations are significantly higher than those recorded by all other stations. In particular, the E-W PGA of the AMT station is the highest horizontal PGA ever recorded in Italy. The spectral shapes of these records are presented and discussed in Section 3.4.

3.3 Comparison with ground motion prediction equations (GMPEs)

The recorded intensity measures (IMs) have also been compared to ground motion prediction equations (GMPEs). The aim is to assess the main features of the recorded data (e.g., attenuation with distance), rather than validate predictive models against data. To this aim the geometric mean of the horizontal ground motion components at the selected stations is compared with the GMPEs median and their logarithmic standard deviation. Note that the median (i.e., 50% percentile) is the natural 'central value' and the 84% and 16% percentiles correspond to the median times $e^{\pm dispersion}$, where 'dispersion' is the standard deviation of the logarithm of the values. Residual analysis is finally performed in this section with the aim of interpreting the strong-motion parameters as functions of source-to-site distance and local site conditions.

Specifically, the PGA and (acceleration) spectral ordinates $(S_a)^2$ at 0.3s, 1s, and 2s are compared to the recent GMPEs by Bindi *et al.* (2011) for Italy, and Bindi *et al.* (2014) for Europe and the Middle East. The selected GMPEs have similar functional form and use moment magnitude and the Joyner-Boore distance as source-to-station distance metric. The EC8 soil classification (four ground types from A to D) discriminates recording sites and four classes (normal, reverse, strike-slip, and unspecified) describe the style of faulting. A similar comparison including NGA-West 2 GMPEs is provided by Zimmaro *et al.* (2018). The latter study also found that stations at close distance, including near the hanging wall, exhibit fling step in some cases but no obvious rupture directivity; however, these aspects are not discussed here.

Specifically, the Bindi *et al.* (2011) model is derived for the magnitude range M_w 4 to 6.9 and considering distanced up to 200km. The equations are derived for PGA, peak ground velocity (PGV) and 5%-damped spectral accelerations at 20 periods between 0.04s and 2s for the geometric mean of the horizontal components and the vertical one. The reference database is the ITalian ACcelerometric Archive (or ITACA, http://itaca.mi.ingv.it/).

Similarly, the Bindi *et al.* (2014) model is derived for the magnitude range M_w 4 to 7.6 and considering distanced up to 300km. The equations are derived for PGA, peak ground velocity (PGV) and 5%-damped spectral accelerations at 23 periods between 0.04s and 3s for the geometric mean of the horizontal components and the vertical one. The reference database is RESORCE (Akkar *et al.*, 2014).

Figure 3-5, Figure 3-6 and Figure 3-7 show the comparison between the GMPEs and the observed IMs (geometrical mean of the horizontal components) for the three considered events and for three EC8 ground types. Note: solid line is for median, dashed lines are for 16th and 84th percentile predictions.

---

[2] S_a values, provided by the ESM database, are used in this chapter as a proxy for pseudospectral acceleration.
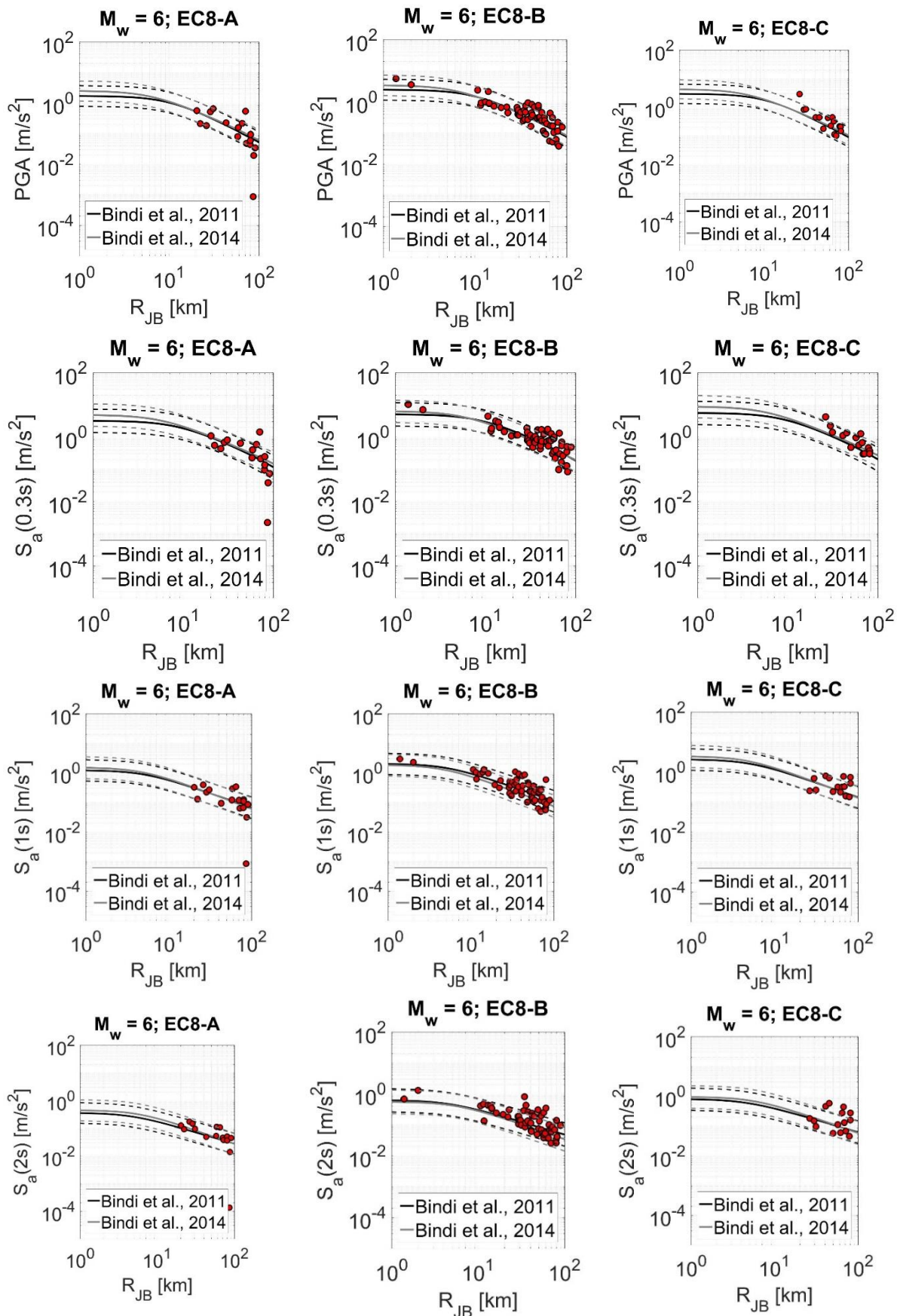
Figure 3-5 Observed IMs vs GMPEs for the geometric mean of the horizontal components for the M6.0 of 24th August 2016 earthquake.
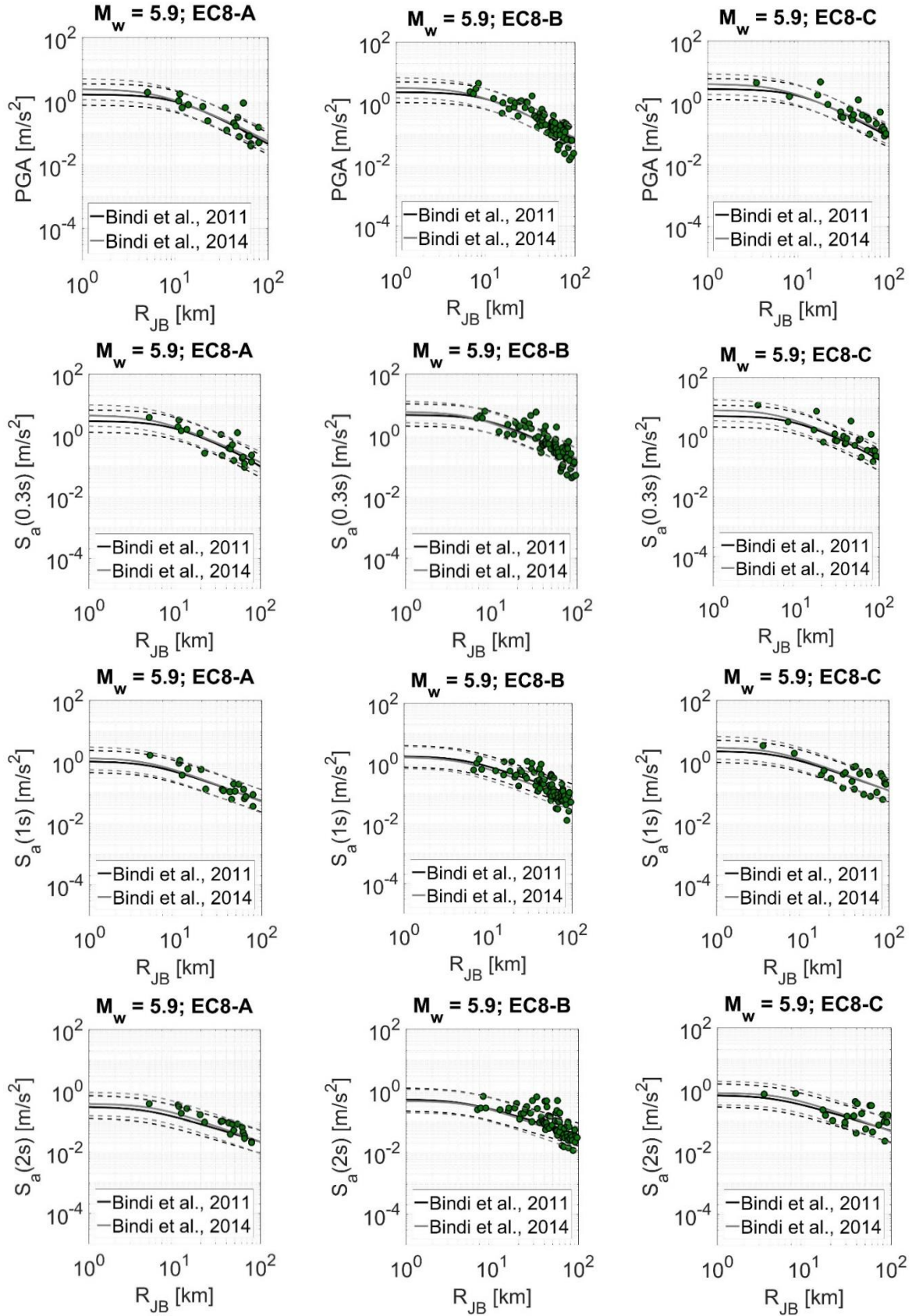
Figure 3-6 Observed IMs vs GMPEs for the geometric mean of the horizontal components for the M5.9 of 26th October 2016 earthquake.
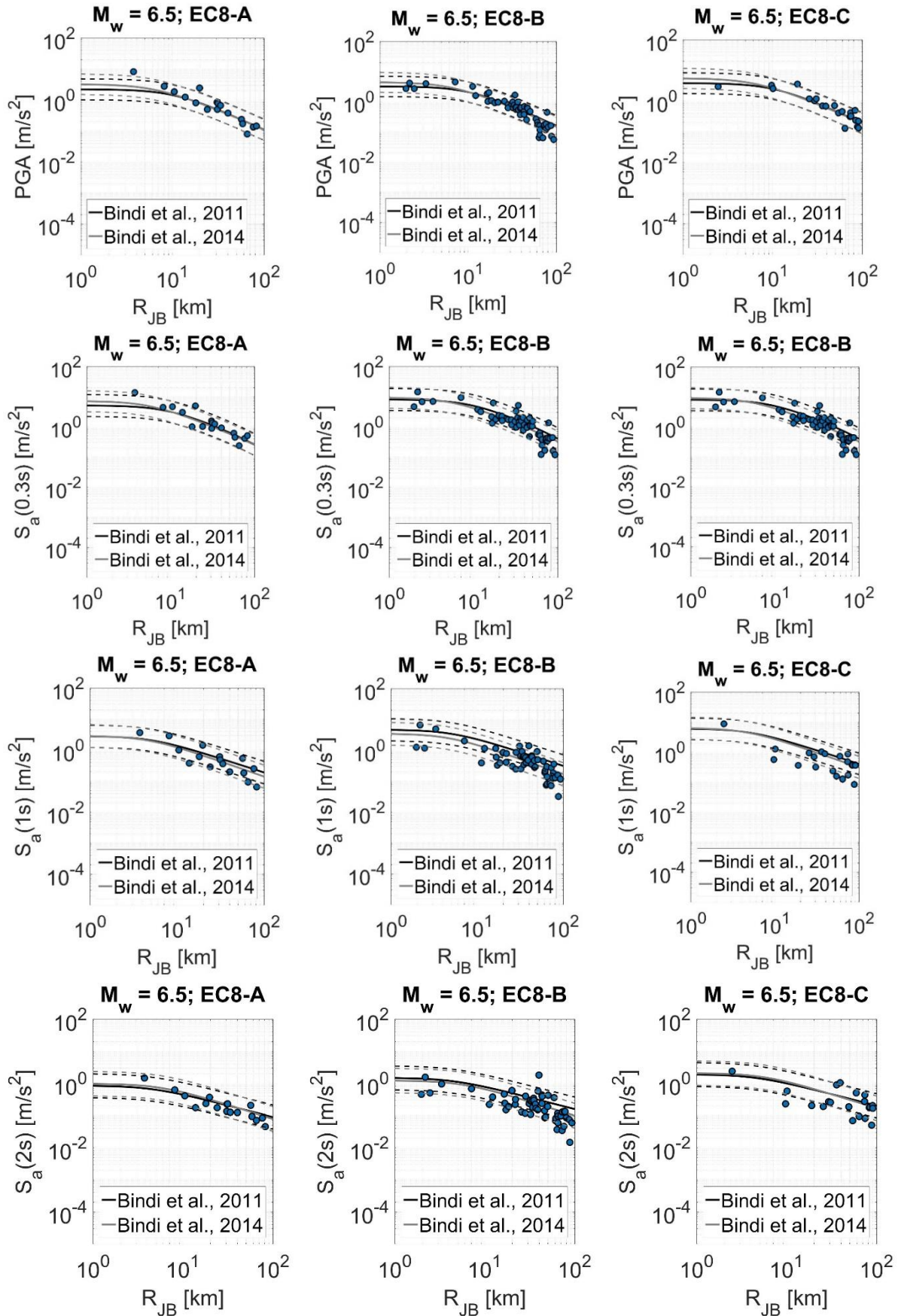
Figure 3-7 Observed IMs vs GMPEs for the geometric mean of the horizontal components for the M6.5 of 30th October 2016 earthquake.

The observations generally match well the GMPEs for low spectral period and short source-to-site distances, where the observed IMs fall in the standard deviation range of the two GMPEs considered. The observed IMs are generally under predicted, on average, in the distance range 20km to 50km and over predicted, on average, at distances larger than 80km (i.e., the observed ground motion attenuation with distance is faster than that of the GMPEs).

The residuals are also calculated as logarithmic difference between observations and predictions:

$$R_i = ln(IM_i)_{rec} - ln(IM_i)_{GMPE}$$

$(IM_i)_{rec}$ and $(IM_i)_{GMPE}$ are the recorded and GMPE-based estimate of the IMs (i.e., PGA and S_a at 0.3s, 1s, and 2s) at the recording station i-th. The residual analysis of strong-motion data is essential to identify the role of source and site in the variability of ground motion values, and to highlight path effects or other features that are not accounted for by GMPEs.

Figure 3-8 to Figure 3-10 show the residuals for four IMs as a function of the source-to-site distance. All data are compared in each plot with binned averages of the residuals using 10 intervals of R_{JB} values. Positive residuals indicate under-prediction while negative residuals indicate over-prediction. The data exhibit fast anelastic attenuation at large distances (>80 km), as predicted by recent Italy-adjusted global models, but not by Italy- or Europe-specific models, e.g., Zimmaro *et al.* (2018).
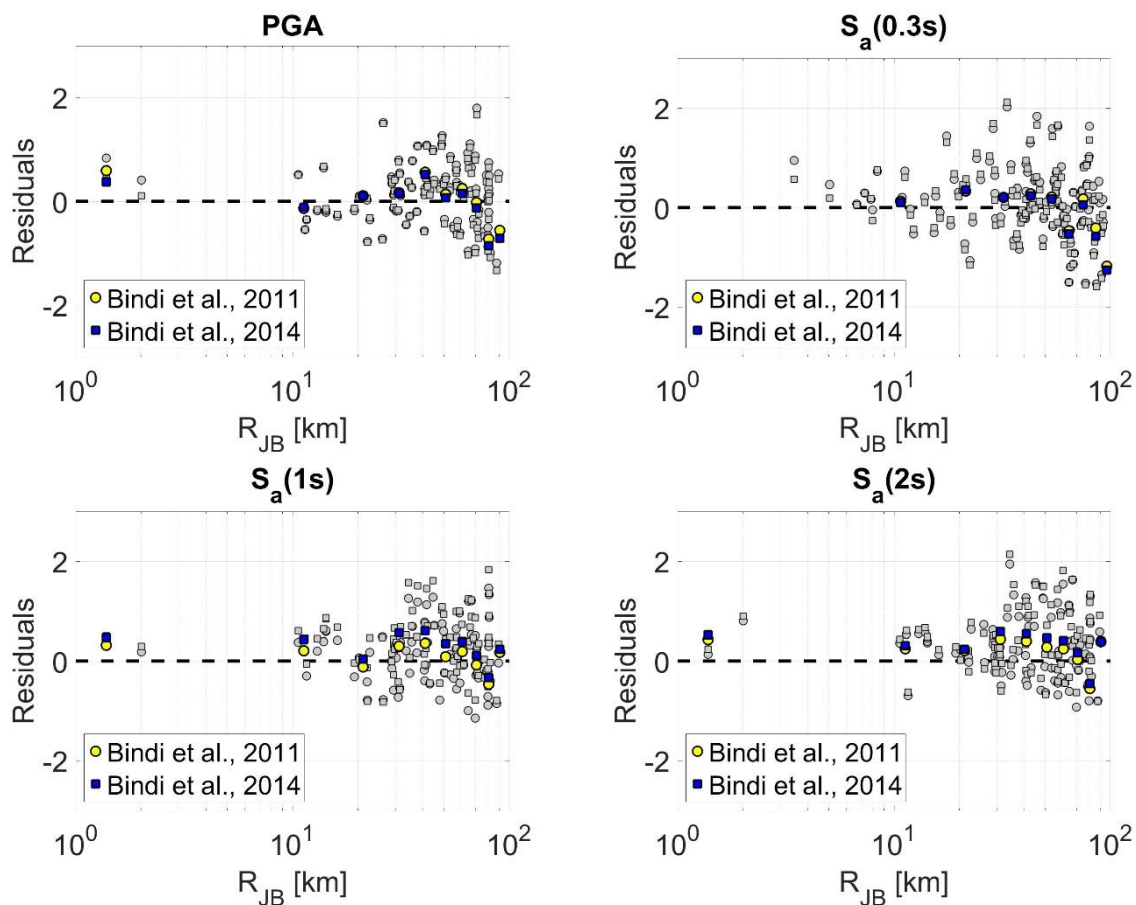
Figure 3-8 Residuals of the considered IMs for the geometric mean of the horizontal components for the M_w 6.0 of 24th August 2016 earthquake.
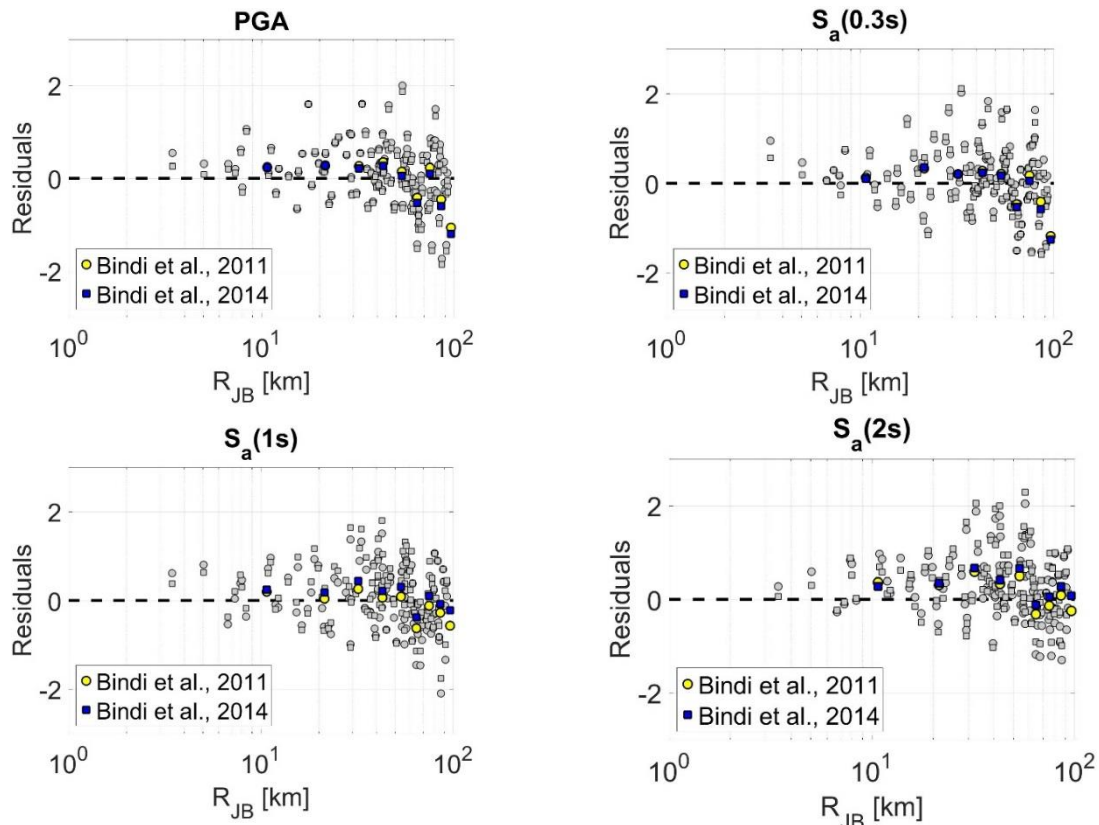
Figure 3-9 Residuals of the considered IMs for the geometric mean of the horizontal components for the M_w 5.9 of 26th October 2016 earthquake.
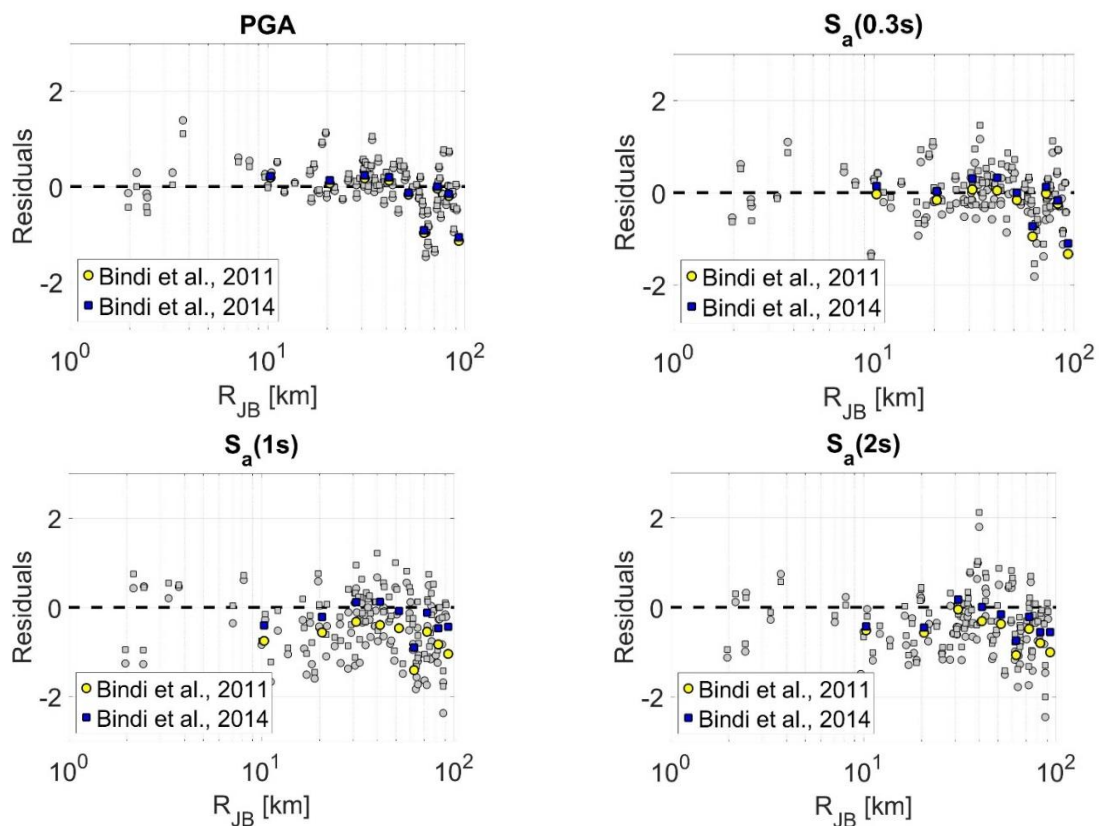
Figure 3-10. Residuals of the considered IMs for the geometric mean of the horizontal components for the M_w 6.5 of 30th October 2016 earthquake.

The between-event term, defined as the average of the residuals for each event, measures the overall misfit of recordings with respect to an attenuation model. In particular, it seems that the ground motion level generated by the M_w 6.5 event is, on average, lower than the predictions by the Bindi *et al.* (2011). The standard deviation of the between-event residual is in the 0.35 to 0.55 range in natural log scale. These values are comparable to the Italian and European GMPEs (Bindi *et al.*, 2011; 2014).

3.4 Comparison with the Italian seismic code

The three considered events struck a large area, characterized by the highest seismic hazard in Italy (Figure 3-11) in terms of horizontal PGA with 10% probability of exceedance in 50 years (PGA 10% in 50 yrs), according to the national reference seismic hazard model (Mappa di Pericolosità Seismica 2004; or MPS04: http://zonesismiche.mi.ingv.it; Stucchi *et al.*, 2011). In particular, this area is characterized by PGA 10% in 50 yrs larger than 0.25g. The three considered events occurred in the large area source ZS923 of the ZS9 seismic source model (Meletti et al., 2008) i.e., an area source characterized by prevalent normal faulting focal mechanism and a maximum magnitude of 7.2. A number of strong earthquakes have occurred in the same area source over the last 700 years (http://emidius.mi.ingv.it/CPTI15-DBMI15), as shown in Figure 2-3. including the 2009 M_w 6.3 L'Aquila event.
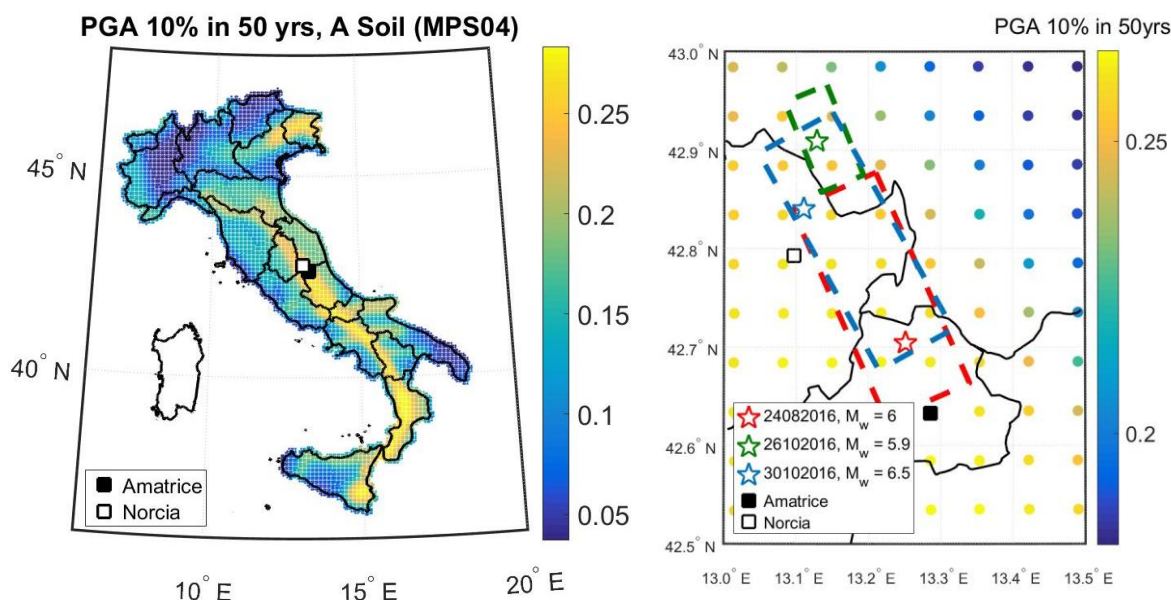
Figure 3-11. Seismic hazard map (MPS04) for Italy (a); and (b) for Central Italy, in terms of horizontal PGA on rock with 10% probability of exceedance in 50 years. The fault plane projections and the epicentres of three considered events are also shown together with the two recording stations (AMT and NRC) considered in the rest of this section.

In particular, the MPS04 provides, on a 5 km-spaced grid covering the whole Italian territory with over 10^3 nodes, PGA and spectral accelerations computed for 10 periods (from 0.1s to 2s), for nine probabilities of exceedance in 50 years (from 2% to 81%, corresponding to mean return periods from 2475 to 30 years), for type A ground (i.e., rock) and flat topography. All the data of MPS04 are accessible at http://esse1.mi.ingv.it.

The MPS04 is the basis for the current Italian Building Code (NTC08; CS. LL. PP, 2008), in defining the elastic response spectra to be used as input in the seismic design of structures. NTC08 defines design spectra given with standard functional forms, which practically coincide with uniform hazard spectra (UHS) on rock for the site location in question (Iervolino, Galasso, & Cosenza, 2010). The reference exceedance probability for the UHS depends on the limit state of interest, the type and the

nominal life of the structure. In case the soil is not rock/stiff (the site classification is the same as in EC8) coefficients apply to amplify the spectrum accordingly.

The 5%-damped pseudo-acceleration elastic response spectra at two selected stations (i.e., those nearest to the fault during the M_w 6.0 of 24th August 2016) are investigated and compared to code-based elastic response spectra for different reference return periods of the seismic action).

In Figure 3-12 the horizontal elastic response spectra recorded by the two stations are compared with the elastic response spectra provided by NTC18 (Ministero delle Infrastrutture e dei Trasporti, 2018) at the corresponding sites, for three different reference return periods of the seismic action. These spectra are a direct approximation of the uniform hazard spectra (UHSs) computed through probabilistic seismic hazard analysis (PSHA), also reported in Figure 3-12. It is worth noting that probabilistic models cannot be validated (or rejected) on the basis of a single event. However, a comparison between the expected shaking with observed data allows to evaluate the relative 'position' of a given seismic event with respect to the expected seismic shaking in a given region as discussed in Meletti, Visini, & D'Amico, (2016).
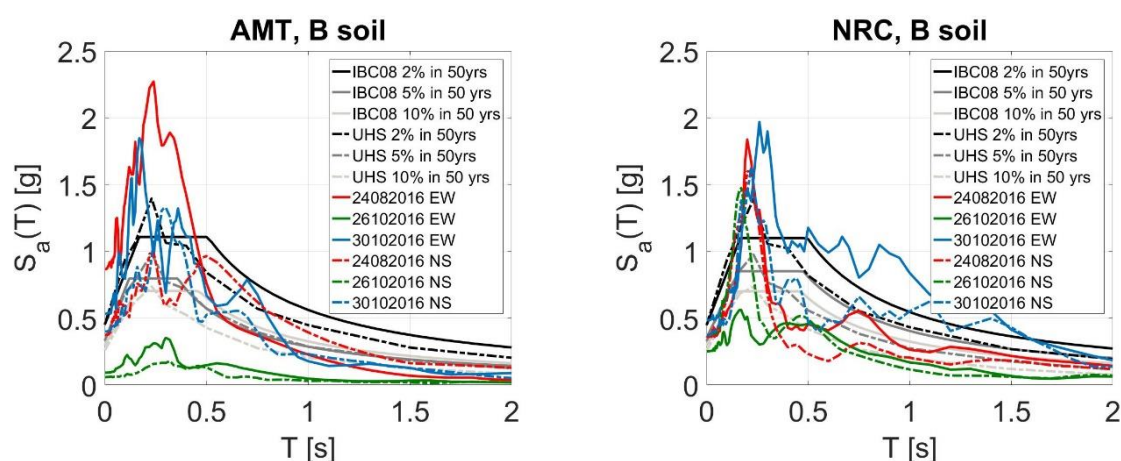
Figure 3-12 Comparison in terms of elastic response spectra between the observed ground motion data and the elastic response spectra provided by NTC08 for (a) AMT; and (b) NRC.

Figure 3-12 shows that the E-W component of AMT exceeds the 2475 years spectrum in the 0s to 0.4s range of periods; while at least one component of the same station exceeds the 475 years spectra for spectral periods up to 2.1s. NRC exceeds the 475 years spectra in the range of periods 0s-0.3s, 0.35s to 0.5s, and 0.67s to 0.88s. This applies to at least one of the two horizontal components. The NRC record also exceeds the 2475 years spectrum for periods between 0.13s and 0.28s. However, at all the stations for longer oscillation periods spectral ordinates become comparable with code-spectra corresponding to return periods of a few tens of years. The shape and the amplitude of these spectra appear compatible with extensive damage in some villages, where the building stock suffered significant damage or total collapse.

It is worth noting that exceedance of code spectra close to the source of a strong earthquake does not directly imply inadequacy of PSHA at the basis of the code spectra (Iervolino, 2013). This is also because spectra from PSHA, are the results of an 'average' of a series of scenarios considered possible (e.g., small and large source-to-site distances). Such an average may be exceeded close to the source of an earthquake, even if the corresponding scenario is included in the PSHA.

3.5 Comparison with the Italian seismic hazard model

As discussed, the maximum horizontal PGA recorded by the AMT station, the nearest to the epicentre (at about 9km), was 0.87g during the M_w 6.0 of 24th August 2016 earthquake, 0.09g during the M_w 5.9 of 26th October 2016 earthquake (at about 33km from the epicentre), and 0.53g during the M_w 6.5 of 30th October 2016 earthquake (at about 27km from the epicentre). Similarly, the maximum horizontal PGA recorded by the NRC station, the second nearest to the epicentre (at about 16km), was 0.37g during the M_w 6.0 of 24th August 2016 earthquake, 0.37g during the M_w 5.9 of 26th October 2016 earthquake (at about 13km from the epicentre), and 0.49g during the M_w 6.5 of 30th October 2016 earthquake (at about 5km from the epicentre).

Such values are compared with the hazard curves, typically representing the annual frequency of exceedance (λ) or the mean return period (the inverse of λ) of different levels of a ground motion IM.

The hazard curves in Figure 3-14 and Figure 3-15 refer to the closest nodes of the MPS04 grid to the AMT and NRC stations. To make the comparison meaningful, the MPS04 hazard curves computed for type A ground (i.e., rock or very stiff soil with $V_{S,30}$ > 800 m/s) by applying the coefficient for type B ground – the soil class of both AMT and NRC station – prescribed by NTC08.

To investigate the impact of the GMPE on seismic hazard estimates, the MPS04 hazard curves are re-computed here retaining the same earthquake rate model but using the GMPE of Bindi *et al.* (2011) instead of the originally adopted GMPEs. In particular, a site-specific PHSA accounting for uncertainty in the factors affecting ground motions is carried out by using a Monte Carlo simulation-based approach (Assatourians & Atkinson, 2013). To this aim, a synthetically generated set of potential earthquakes, with their temporal and geographical distribution, is developed by drawing random samples from the assumed PSHA model components (and related probability distributions), i.e., source-zone geometries and magnitude-recurrence parameters and maximum magnitude. The official Italian seismogenetic zonation, named ZS9 (Meletti et al., 2008), is used in this study; the calculation is limited to events with source-to-site distance up to 125 km (Figure 3-13). Gutenberg-Richter parameters implemented for generating each record are adapted from Barani *et al.* (2009, 2010).
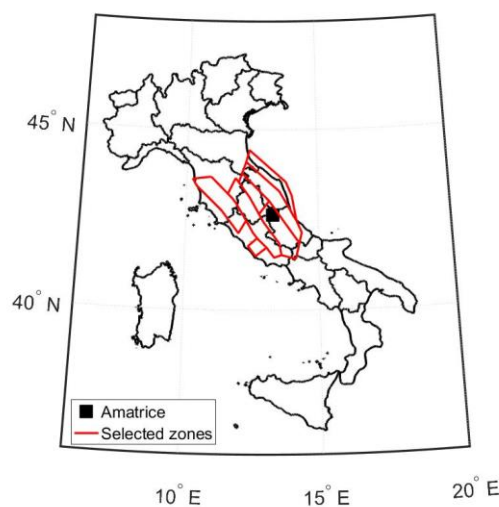
Figure 3-13. ZS9 seismic sources considered in this study.

The resulting synthetic catalogue has a duration of 5,000 years; each record of the synthetic catalogue contains the following fields: time (in decimal years), coordinates (latitude and longitude) and magnitude of earthquake, source zone number and corresponding fault-style. In fact, ZS9 assigns a prevalent mechanism of faulting – interpreted as the mechanism with the highest probability of generating future earthquakes – to all its source zones for use in the GMPEs. The considered IMs are evaluated for each seismic event contained in the catalogue by using the Bindi *et al.* (2011) GMPE assuming type B ground. 500 realizations of random numbers drawn from the standard normal distribution is multiplied by the given sigma value (variability of the GMPE model) and added to the median log-ground motions (from the GMPE) to model the aleatory variability in ground motions. The resulting site-specific hazard curves for each realization as well as the median, 16th and 84th hazard curves are shown in Figure 3-14 for AMT and Figure 3-15 for NRC.

For the AMT station, the resulting hazard curve returns the highest estimates of PGA, that is ~0.9g at a mean return period of 2475 yrs. It is clear that the MPS04 curve, even modified for soil class B, does not reach the PGA recorded at AMT. However, adopting a more recent GMPE shifts the hazard curve toward higher values, making the ground shaking recorded at AMT consistent with the expected PGA for a mean return period of 2475 years. Moreover, we are considering the PGA recorded at a site very close to the epicentre. A strong decrease of the recorded PGA is observed at the other ground motion stations.

Recent GMPEs produce higher hazard estimates due to the larger values of uncertainty (standard deviation) with respect to older GMPEs. Moreover, the considered GMPE was derived from an Italian strong-motion dataset that includes also recordings in the near field, that were lacking in previous GMPEs used for the MPS04 model (e.g., Sabetta and Pugliese, 1996).
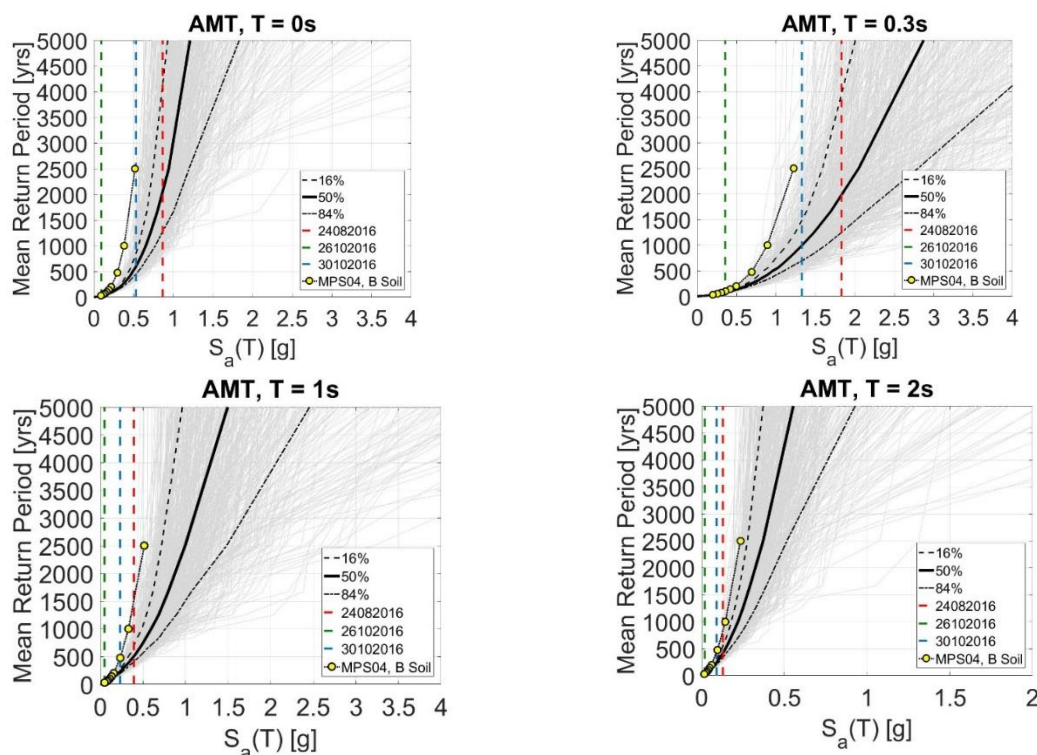
Figure 3-14 (a) Comparison of the maximum horizontal PGA recorded at the AMT station with the hazard curve of MPS04 (at the node of the computational grid closest to the AMT site) and a newly computed hazard curve using the GMPE of Bindi et al., 2011.
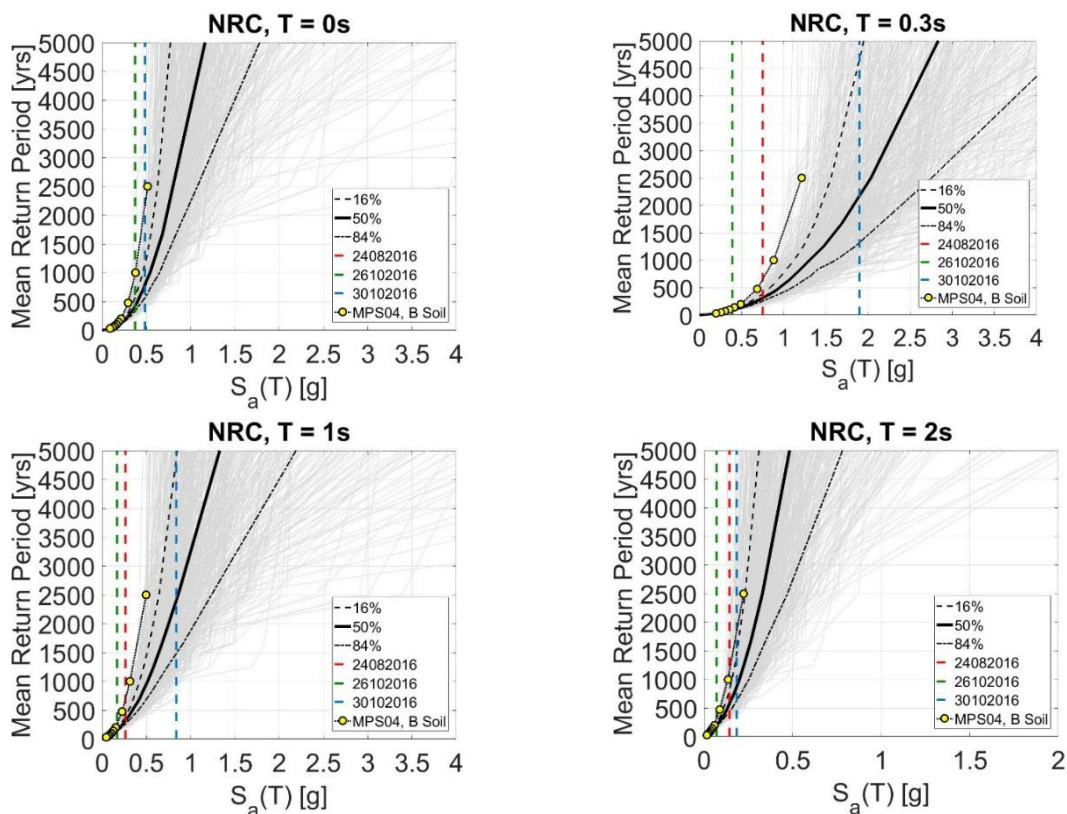
Figure 3-15 (a) Comparison of the maximum horizontal PGA recorded at the NRC station with the hazard curve of MPS04 (at the node of the computational grid closest to the NRC site) and a newly computed hazard curve using the GMPE of Bindi et al., 2011.

3.6   Conclusions

This chapter presented an engineering analysis of the ground shaking recorded during the three largest earthquakes of the 2016 Central Italy seismic sequence. These events, along with aftershocks, were well recorded by Italian networks, and are among the normal fault earthquakes with the highest number of recordings globally. The strong-motion dataset, consisting of nearly 10,000 waveforms available at the ESM database, allowed the analysis of the main features of the ground motion, in terms of distribution of shaking, ground-motion variability, comparison with both the Italian seismic code and the Italian seismic hazard model.

Specifically, an overview of the ground motion IMs has been first provided. A comparison with GMPEs has also been presented, showing that GMPEs generally fit well the observation in the near-fault for low-period spectral ordinates.

Finally, a comparison between available recordings and accelerations provided by the reference seismic hazard model (MPS04) for Italy has been presented. As expected, the comparison of some of the elastic response spectra with the code spectra showed cases of exceedance of the latter at both 475 and 2475 years, particularly in the epicentral area and short-to-medium vibration periods. By developing hazard curves using the same earthquake rate model of MPS04 but a more recent GMPE than those originally adopted, results show a strong increase of expected values for both PGA and other spectral ordinates, making the probabilistic seismic hazard estimates more consistent with the observations.

Akkar, S., Sandıkkaya, M. A., Şenyurt, M., Azari Sisi, A., Ay, B. Ö., Traversa, P., … Godey, S. (2014). Reference database for seismic ground-motion in Europe (RESORCE). *Bulletin of Earthquake Engineering*, *12*(1), 311–339.

Ancheta, T. D., Darragh, R. B., Stewart, J. P., Seyhan, E., Silva, W. J., Chiou, B. S.-J., … Donahue, J. L. (2014). NGA-West2 Database. *Earthquake Spectra*, *30*(3), 989–1005.

Assatourians, K., & Atkinson, G. (2013). EqHaz: An open-source probabilistic seismic-hazard code based on the Monte Carlo simulation approach. *Seismological Research Letters*, *84*(3), 516–524.

Barani, S., Spallarossa, D., & Bazzurro, P. (2009). Disaggregation of probabilistic ground-motion hazard in Italy. *Bulletin of the Seismological Society of America*, *99*(5), 2638–2661.

Barani, S., Spallarossa, D., & Bazzurro, P. (2010). Erratum to Disaggregation of Probabilistic Ground-Motion Hazard in Italy. *Bulletin of the Seismological Society of America*, *100*(6), 3335–3336.

Bindi, D., Massa, M., Luzi, L., Ameri, G., Pacor, F., Puglia, R., & Augliera, P. (2014). Pan-European ground-motion prediction equations for the average horizontal component of PGA, PGV, and 5%-damped PSA at spectral periods up to 3.0 s using the RESORCE dataset. *Bulletin of Earthquake Engineering*, *12*(1), 391–430.

Bindi, D., Pacor, F., Luzi, L., Puglia, R., Massa, M., Ameri, G., & Paolucci, R. (2011). Ground motion prediction equations derived from the Italian strong motion database. *Bulletin of Earthquake Engineering*, *9*(6), 1899–1920.

Bosi, A., Marazzi, F., Pinto, A., & Tsionis, G. (2011). *The L'Aquila (Italy) earthquake of 6 April 2009: report and analysis from a field mission*. https://doi.org/10.2788/188

CEN. Eurocode 8: Design of structures for earthquake resistance - Part 1 : General rules, seismic actions and rules for buildings, 1 European Committee for Standardization § (2004). https://doi.org/[Authority: The European Union per Regulation 305/2011, Directive 98/34/EC, Directive 2004/18/EC]

Chiaraluce, L., Di Stefano, R., Tinti, E., Scognamiglio, L., Michele, M., Casarotti, E., … Marzorati, S. (2017). The 2016 Central Italy Seismic Sequence: A First Look at the Mainshocks, Aftershocks, and Source Models. *Seismological Research Letters*, *88*(3), 757–771.

Consiglio Regionale Umbria. Aggiornamento della classificazione simisca del territorio regionale dell'Umbria (2012).

Copernicus EMS. (n.d.). Retrieved May 20, 2018, from http://emergency.copernicus.eu/

CS. LL. PP. (2008). DM 14 Gennaio 2008: Norme tecniche per le costruzioni. *Gazzetta Ufficiale Della Repubblica Italiana*.

D'Ayala, D., & Speranza, E. (2003). Definition of Collapse Mechanisms and Seismic Vulnerability of Historic Masonry Buildings. *Earthquake Spectra*, *19*(3), 479–509. https://doi.org/10.1193/1.1599896

De Luca, F., Verderame, G. M., & Manfredi, G. (2015). Analytical versus observational fragilities: the case of Pettino (L'Aquila) damage data database. *Bulletin of Earthquake Engineering*, *13*(4), 1161–1181. https://doi.org/10.1007/s10518-014-9658-1

Del Gaudio, C., Ricci, P., & Verderame, G. M. (2017). First remarks about the expected damage scenario following the 24th August 2016 earthquake in Central Italy. In *Proceedings of the 16th World Conference on Earthquake Engineering*.

Di Capua, G., Lanzo, G., Pessina, V., Peppoloni, S., & Scasserra, G. (2011). The recording stations of the Italian strong motion network: geological information and site classification. *Bulletin of Earthquake Engineering*, *9*(6), 1779–1796.

DPCM. Norme Tecniche per il Progetto, la Valutazione e L'Adeguamento Sismico degli Edifici (2005). Italia.

Franco, G., Stone, H., Ahmed, B., Chian, S. C., Hughes, F., Jirouskova, N., … Lopez, J. (2017). The April 16 2016 M w 7 . 8 Muisne Earthquake in Ecuador – Preliminary Observations from the EEFIT

Reconnaissance Mission of May 24 - June 7. In *16th World Conference on Earthquake Engineering, 16WCEE 2017* (pp. 1–12).

Grünthal, G. (1998). *European Macroseismic Scale 1998. European Center of Geodynamics and …* (Vol. 15). Retrieved from http://scholar.google.com/scholar?hl=en&btnG=Search&q=intitle:European+Macroseismic+Scale+1998#0

Guidoboni, E., Ferrari, G., & Tarabusi, G. (2010). Terremoti e monumenti : storie di restauri e perdite. In *Viaggio nelle aree del terremoto del 16 dicembre 1857* (pp. 69–102).

Iervolino, I. (2013). Probabilities and Fallacies: Why Hazard Maps Cannot Be Validated by Individual Earthquakes. *Earthquake Spectra*, *29*(3), 1125–1136.

Iervolino, I., Galasso, C., & Cosenza, E. (2010). REXEL: Computer aided record selection for code-based seismic structural analysis. *Bulletin of Earthquake Engineering*, *8*(2), 339–362.

Liel, A. B., & Lynch, K. P. (2012). Vulnerability of Reinforced-Concrete-Frame Buildings and Their Occupants in the 2009 L'Aquila, Italy, Earthquake. *Natural Hazards Review*, *13*(1), 11–23. https://doi.org/10.1061/(ASCE)NH.1527-6996.0000047

Luzi, L., Pacor, F., Puglia, R., Lanzano, G., Felicetta, C., D'Amico, M., … Chioccarelli, E. (2017). The Central Italy Seismic Sequence between August and December 2016: Analysis of Strong-Motion Observations. *Seismological Research Letters*, *88*(5), 1219–1231.

Luzi, L., Puglia, R., Russo, E., & ORFEUS, W. (2016). *Engineering Strong Motion Database*.

Masi, A., Chiauzzi, L., Santarsiero, G., Manfredi, V., Biondi, S., Spacone, E., … Verderame, G. M. (2017). Seismic response of RC buildings during the M$_w$6.0 August 24, 2016 Central Italy earthquake: the Amatrice case study. *Bulletin of Earthquake Engineering*. https://doi.org/10.1007/s10518-017-0277-5

Masi, A., Santarsiero, G., Chiauzzi, L., Gallipoli, M. R., Piscitelli, S., Vignola, L., … Grimaz, S. (2016). Different damage observed in the villages of Pescara del Tronto and Vezzano after the M6.0 august 24, 2016 central Italy earthquake and site effects analysis. *Annals of Geophysics*, *59*(5), 1–12. https://doi.org/10.4401/AG-7271

Meletti, C., Galadini, F., Valensise, G., Stucchi, M., Tectonophysics, R. B.-, & 2008, U. (2008). A seismic source zone model for the seismic hazard assessment of the Italian territory. *Tectonophysics*, *450*(1–4), 85–108.

Meletti, C., Visini, F., & D'Amico, V. (2016). Seismic hazard in Central Italy and the 2016 Amatrice earthquake. *Annals of Geophysics*, *59*.

Ministero delle Infrastrutture e dei Trasporti. Aggiornamento delle "Norme Tecniche per le Costruzioni" - NTC 2018 - In Italian (2018).

Ministro dei Lavori Pubblici. Decreto Ministro dei Lavori Pubblici 24 Gennaio 1986 - In Italian (1986).

Novelli, V. I., & D'Ayala, D. (2014). LOG-IDEAH: LOGic trees for identification of damage due to earthquakes for architectural heritage. *Bulletin of Earthquake Engineering*, 153–176. https://doi.org/10.1007/s10518-014-9622-0

Paolucci, R., Pacor, F., Puglia, R., Ameri, G., Cauzzi, C., & Massa, M. (2011). Record Processing in ITACA, the New Italian Strong-Motion Database (pp. 99–113). Springer, Dordrecht.

Paz, M. (2012). *International handbook of earthquake engineering: codes, programs, and examples*. (S. S. & B. Media, Ed.).

Presidente del Consiglio dei Ministri. Modificazioni alle norme tecniche igieniche di edilizia obbligatoria per e localita' colpite dai terremoti - Regio Decreto n. 705 (1926).

Presidente del Consiglio dei Ministri. D.M. N.6: Ulteriori interventi urgenti a favore delle zone terremotate delle regioni Marche e Umbria e di altre zone dcopite da eventi calamitosi - In Italian (1998).

Regione Lazio. (2007). Retrieved from http://www.regione.lazio.it/prl_ambiente/?vw=contenutidettaglio&id=221

Regione Marche. (2018). Retrieved from http://www.regione.marche.it/

Romeo, R. ., & Pugliese, A. (1997). *"La pericolosità sismica in Italia. Parte 1: analisi della scuotibilità*.

Sabetta, F., & Pugliese, A. (1996). Estimation of Response Spectra and Simulation of Nonstationary Earthquake Ground Motions. *Bulletin of the Seismological Society of America*, *86*(2), 337–352.

SISTEMA STATISTICO NAZIONALE. ISTITUTO NAZIONALE DI STATISTICA (ISTAT). 15° Censimento generale della popolazione e delle abitazioni. Struttura demografica della popolazione. Dati definitivi. (2011). Retrieved from http://www.istat.it/it/files/2012/12/volume_popolazione-legale_XV_censimento_popolazione.pdf

Spence, R. ., & D'Ayala, D. (1999). Damage assessment and analysis of the 1997 Umbria-Marche earthquakes. *Structural Engineering International*, *9*(3), 229–233.

Stone, H., Putrino, V., & D'Ayala, D. (2018). Earthquake damage data collection using omnidirectional imagery - Under Revision. *Frontiers*.

Tinti, E., Scognamiglio, L., Michelini, A., & Cocco, M. (2016). Slip heterogeneity and directivity of the ML 6.0, 2016, Amatrice earthquake estimated with rapid finite-fault inversion. *Geophysical Research Letters*, *43*(20), 10,745-10,752. https://doi.org/10.1002/2016GL071263

Tosone, A., & Bellicoso, A. (2017). Anti-seismic presidia in the historical building of l'aquila: The role of the wooden elements. *International Journal of Heritage Architecture: Studies, Repairs and Maintence*, *2*(1), 48–59. https://doi.org/10.2495/HA-V2-N1-48-59

Wald, D. J., Worden, B. C., Quitoriano, V., & Pankow, K. L. (2005). ShakeMap manual: technical manual, user's guide, and software guide. *Geological Survey (U.S.), Techniques and Methods*, *12-A1*, 132 pp.

Zimmaro, P., Scasserra, G., Stewart, J., & Kishida, T. (2018). Strong ground motion characteristics from 2016 Central Italy earthquake sequence. *Earthquake Spectra*.

4 SEISMIC SITE RESPONSE AND GEOTECHNICAL OBSERVATIONS

4.1 Introduction

This chapter presents the main observations and findings drawn from a geotechnical survey carried out during the EEFIT mission in the epicentral area struck by the Mw 6.0 24 August 2016 earthquake, (Figure 1-1). The effects caused by the subsequent seismic events occurred in late October 2016 are not discussed. The objective of the EEFIT geotechnical survey was twofold. First, it aimed to locate and characterise secondary co-seismic effects (e.g., ground cracks, landslides, hydrological anomalies and water effects) and geotechnical failures (e.g., collapse of retaining walls, settlement, etc.). The collected data was subsequently used to determine the epicentral intensity according to the Environmental Seismic Intensity 2007 (ESI 2007) scale, introduced by Michetti et al. (2007). Differently from macroseismic scales, such as the Modified Mercalli Intensity (MMI) scale and European Macroseismic Scale, EMS '98 (Grünthal, 1998), which are based on damage to the built environment, the ESI 2007 scale is based on observation of co-seismic effects on the natural environment. This therefore provides a complimentary measure of the earthquake intensity. It is noted that this chapter reports only the most severe environmental effects observed in the epicentral area, and these are subsequently used for the definition of the epicentral intensity following the ESI-2007 scale.

4.2 Geological settings

The study area is located in the Umbro-Marchean Apennines in central Italy (see Figure 4-2). The geological formations in the northen part consist of Meso-Cenozoic calcareous and marly-calcareous sequences, and pelithic-arenaceous flysch formations, known as "Laga flysch". In the southern part of the surveyed area, the geomorphological setting consists of Miocene sedimentary deposits of clayey-arenaceous flysch and marls formations. The topographic surface is irregular and includes many cliffs, ridges and gulley made of alluvium and fluvial deposits resulting from the weathering and erosion of the parent material. The geological setting and topographic features played an important role in the distribution and extent of damage as discussed in the following sections, which include higher scale geological maps of the sites visited.

4.3 Environmental Seismic Intensity 2007 (ESI 2007) scale

Macro-seismic intensity scales (e.g., Mercalli-Cancani-Sieberg Scale, Modified Mercalli Scale and the Medvedev Sponheuer-Karnik Scale), are based on a qualitative description of the effects caused by the earthquake at a particular location as evidenced by observed damage to both built and natural environments, including human reactions. The effects of the earthquakes on the natural environment, however, are often disregarded for the assessment of the earthquake intensity, arguably due to lack of a systematic classification and quantification of geological, hydrological and geomorphic features for different intensity degrees. Yet, co-seismic environmental effects are less sensitive to the quality of the construction, thus they can provide a complementary measure of the epicentral intensity, especially in areas where the effects on man-made structures are scarce, and/or quickly default to collapse due to poor structural quality of the building stock. As collapse and damage to the built environment was widespread in the epicentral area of the 24 August 2016 earthquake, the use of the ESI 2007 scale provides an alternative epicentral intensity measure, which can be compared to that determined from more conventional macro-seismic intensity scales. It is noted that, when observations of damage to both built and natural environments are available the final epicentral intensity is provided by the observation that leads to the greatest level of intensity.

The Environmental Seismic Intensity 2007 (ESI 2007) Scale (Michetti et al., 2007) was first introduced at the XVII INQUA Congress (Cairns, 28 July – 3 August 2007), substituting the former INQUA EEE

2004 intensity scale (Michetti et al., 2004). The revised version of the scale is named Environmental Seismic Intensity Scale, hereafter referred to as ESI 2007. The scale is divided in twelve degrees I-XII, to broadly correlate to the built environment scales. These are defined on the basis of effects induced by the earthquake on the natural environment. The accuracy of the ESI 2007 description effects is greater for the higher degrees of the scale, starting from intensity VIII –when primary effects start to become evident, and with growing resolution for intensity IX-XII, whereby XII denotes a "completely devastating" event. It is worth noting that for degree I to III, there are no observable environmental effects that can be used for the definition of the earthquake intensity, with first apparent effects starting from intensity IV. A qualitative description of each intensity degree of the ESI 2007 is given in Table 4.1 and Figure 4-1.

Table 4-1: Environmental Seismic Intensity scale ESI 2007 (after Michetti et al., 2007)

Degree	Environmental effect	Total area affected[*]
I	*NO ENVIRONMENTAL EFFECTS*	-
II	*NO ENVIRONMENTAL EFFECTS*	-
III	*NO ENVIRONMENTAL EFFECTS*	-
IV	*LARGELY OBSERVED:* First unequivocal effects in the environment	-
V	*STRONG:* Marginal effects in the environment	-
VI	*SLIGHTLY DAMAGING:* Modest effects in the environment	-
VII	*DAMAGING:* Appreciable effects in the environment	10 km²
VIII	*HEAVILY DAMAGING:* Extensive effects in the environment	100km²
IX	*DESTRUCTIVE:* Effects in the environment are a widespread source of considerable hazard and become important for intensity assessment	1000km²
X	*VERY DESTRUCTIVE:* Effects in the environment become a leading source of hazards and are critical for intensity assessment	5000km²
XI	*DEVASTATING:* Effects in the environment become decisive for intensity assessment, due to saturation of structural damage	10000km²
XII	*COMPLETELY DEVASTATING:* Effects in the environment are the only tool for intensity assessment	>50000km²

[*]area affected by secondary co-seismic effects

Most of the environmental secondary co-seismic effects observed in the surveyed area were ground cracks and landslides. Two hydrological anomalies and water effects were observed close to the municipality of Amatrice. A detailed account on the reported co-seismic effects is provided in the following sections.
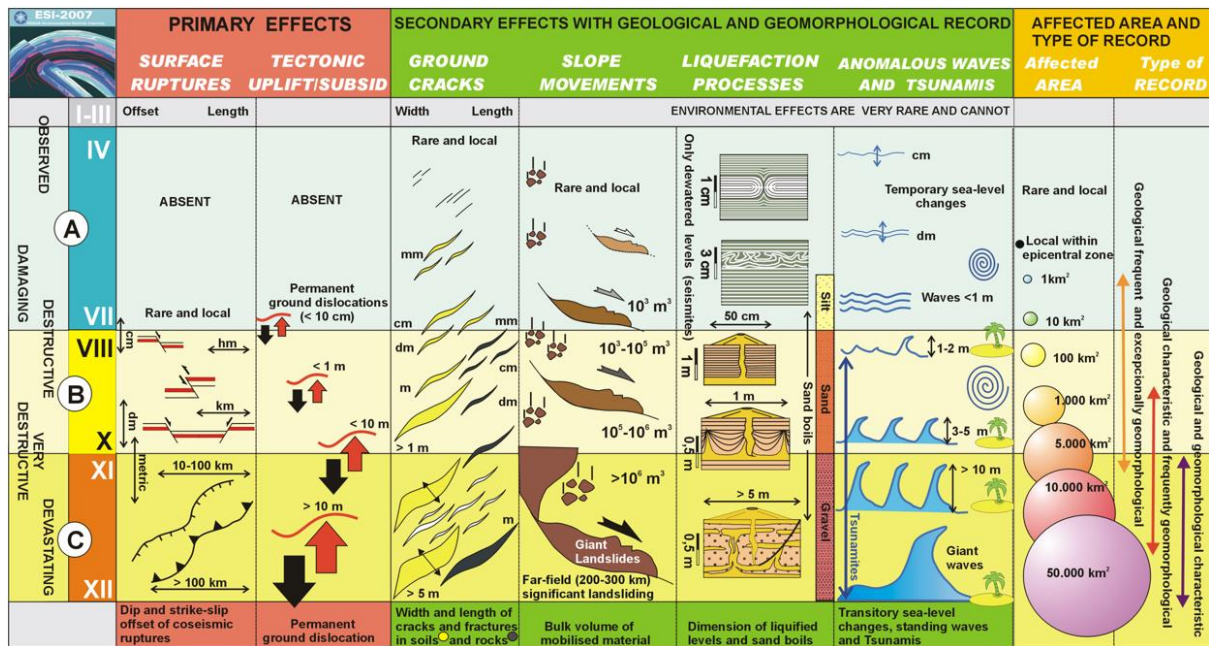
Figure 4-1: Main features of primary and secondary effects of each intensity degree in the Environmental Seismic Intensity (ESI 2007) scale (modified after Silva et al., 2008; Reicherter et al., 2009).

4.4 Environmental effects

It is customary to classify environmental effects into two categories:

- *Primary effects*, these consist of coseismal effects directly related to the fault rupture, and expression of the seismogenic source (e.g., fault ruptures and tectonic uplift/ subsidence). The size of primary effects is typically quantified in terms of surface rupture, maximum displacement and amount of tectonic surface deformation.
- **Secondary effects**, these are coseismal effects caused by the ground response to the seismic shaking (e.g., landslides, rock falls, ground cracks, etc.). Differently from primary effects, these include effects due to potential amplification of ground motion, such as site and topographic effects.

The environmental effects provide important information for the definition of the geographical area affected by the earthquake and its intensity. As the primary coseismic effects have already been discussed in section 2.4.1, this section presents the secondary coseismic effects and geotechnical failures observed by the EEFIT team. It is worth noting that the definition of each degree in the ESI 2007 scale considers primary and secondary effects, and the extent of the affected area, whereby larger affected areas correspond to higher seismic degrees as shown in Figure 4-1 and Table 4-1: Environmental Seismic Intensity scale ESI 2007 (after Michetti et al., 2007).

The EEFIT team surveyed an area of about 490 km², reported 50 observations. The spatial distribution, of the observations together with the location of the epicentre of the 24 August 2016 earthquake, are shown in Figure 4-2a. It is worth noting that due to the large extent of the area affected by the earthquake, the area surveyed by the EEFIT mission focused on the epicentral area where most of the damage to the built and natural environment occurred. According to the definition of the ESI 2007 scale, the extent of the epicentral region corresponds to an intensity degree in the range of VIII-IX, which is consistent with the environmental observations discussed hereafter.

4.5 Methods for recording ESI observations

The locations of the environmental effects were recorded using a handheld Garmin GPS. The type of environmental effect was recorded, whether it was a landslide, rockfall, ground crack or hydrological effect. The size or volume of the effect was also recorded by measuring its dimensions or estimating its size qualitatively.

Where landslides were observed and where it was possible, in-situ tests were conducted to ascertain the strength of the soil; the slope angle was measured to help gauge slope stability, and soil samples were taken for further analysis. For rockfalls, where it was possible to access the rockfall directly, the lithology was noted.

Where there were ground cracks present, measurements were taken of the width, orientation and opening direction of the cracks. If the cracks were >1m long, several measurements were taken along the length. The presence of cut clasts was also noted.

Observations were made around the towns of Amatrice, Accumoli, Arquata and Pescara del Tronto. These areas were selected because the team recording the damage to building stock were using this evidence to estimate the macroseismic intensity in these towns. Therefore, a comparison of intensity assessments using the environmental seismic intensity scale and calculated intensities based on damage to the built environment can be obtained, see Table 4-2.

The different types of observed environmental secondary coseismic effect are shown in the pie chart given in Figure 4-2b. 62% of the observations consisted of landslides The term landslide is hereafter used to refer to movements of a mass of rock, earth or debris down a slope. Furthermore in this report landslides are classified based on the type of movement (e.g., falls, topples, slides spreads, flows) and material displaced, following the modified Varnes classification system (Varnes, 1978; Cruden & Varnes, 1996; Hungr et al., 2014). The observed landslides included: (*i*) rock falls, concentrated particularly in the northern part of the surveyed area where the geomorphologic setting consisted of Meso-Cenozoic calcareous ridges and flysch formations; (*ii*) rotational and translational slides along hillsides of road cuts and embankments, which displaced colluvial and eluvial deposits covering the bedrock. A number of retaining wall failures were observed adjacent to the major landslides in the municipalities of Amatrice, Accumoli and Arquata del Tronto (in the locality of Pescara del Tonto). Several researchers have shown positive correlation between area affected by landslides and earthquake magnitude. One of such correlations is given by equation (1), which was derived by Keefer (2002) using data from Keefer and Wilson (1989).

$$log_{10} A = M - 3.46(\pm 0.47) \qquad \text{for 5.5<M<9.2} \qquad (4.1)$$

where *A* is the area affected by landslides in square kilometres, and *M* is the moment magnitude. According to eq. (4.1), the area affected by landslides following the 24 August 2016 earthquake is consistent with the area investigated by the EEFIT team, which is approximately 500km^2.

Other environmental observations included ground cracks with substantial vertical and horizontal displacements; these corresponded to 34% of the observed coseismic effects. Effects associated to hydrological anomalies and water effects were also observed in the area, corresponding to 4% of the observed co-seismic effects. (see Figure 4-2b). Specifically, the hydrological anomalies and water included:
- significant variation of the flow-rate of springs, i.e. spring along SS577 road, between Arquata del Tronto and Pescara del Tronto shown in Figure 4-3a;
- anomalous waves up to 1m height in a small artificial pond (see Figure 4-3b), 5km south of Amatrice. The latter was observed immediately after the 24 August 2016 mainshock by a local eyewitness interviewed by the EEFIT team. No liquefaction phenomena were recorded in the surveyed area

The evaluation of the epicentral intensity is based on the most severe secondary coseismic effects observed in the municipalities of Amatrice, Accumoli and Arquata del Tronto (locality of Pescara del Tronto), which in all cases consisted of landslides. Table 4-2 lists, for each locality, the distance from the epicentre R_{ep}, significant volume of material displaced, intensities levels according to both ESI 2007 and EMS scales, and revised version of the Mercalli-Cancani-Sieberg scale. The latter reported by Galli et al. (2016). From Table 4-2, it can be concluded that the different scales provide consistent epicentral intensities for the three main epicentral locations.

Table 4-2: Epicentral intensities for different localities surveyed

Locality	R_{ep} [km]	Type of event	Volume [m³]	Intensity $I_{ISO-2007}$	Intensity$_{EMS-98}$	Intensity[3] I_{MCS}
Amatrice	~8	Disrupted slide	~6,000	8	9	9
Accumoli	~1	Rotational slide	~10,000	8-9	8	8-9
Pescara del Tronto	~9	Disrupted slide	~15,000	9	10	10-11
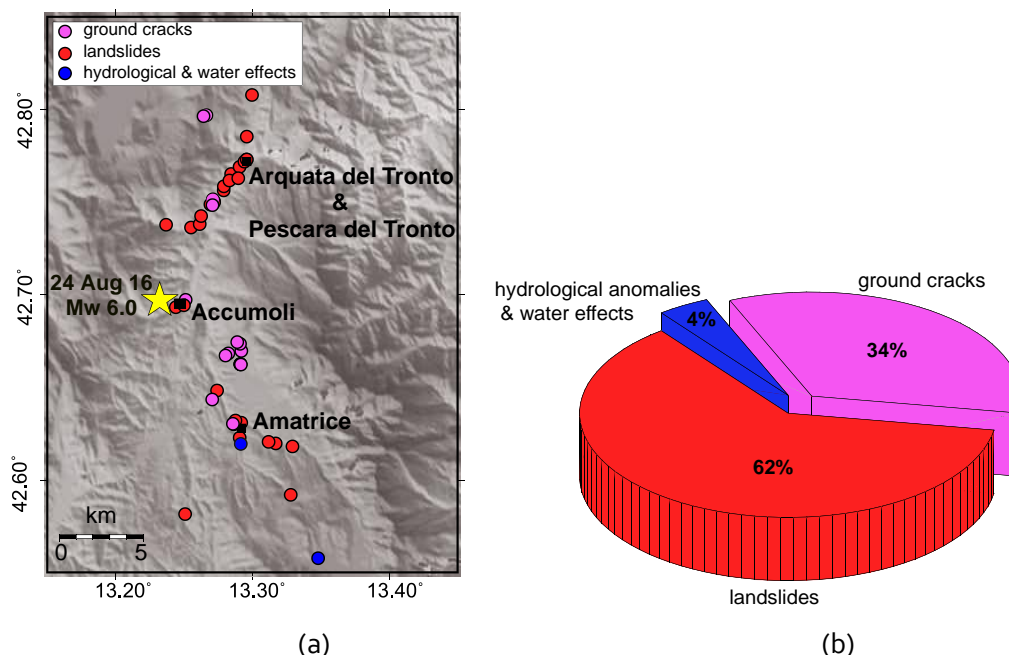
Figure 4-2 Surveyed area and observed secondary coseismic effects. Most of these observations were made along roads and all had easy access to the vicinity of the effects. Sites were chosen to allow comparisons with damage to the built environment planned by the EEFIT mission: (a) spatial distribution of secondary coseismic effects and location of the epicentre of the 24 August 2016 earthquake; (b) types of secondary coseismic effects.

In summary landslides and rockfalls in the range of <10m³ to approximately 1000m³ and ground cracks up to 40mm wide were observed. The observations described in detail in the next sections

---

[3] Galli et al. (2016)

were made six weeks after the earthquake occurred, but it was possible to compare them to those made by Michetti (pers. comm.) made immediately after the earthquake, showing that many of the observations remained consistent, six weeks later. Moreover, some additional effects could also be observed along roads that had been shut immediately after the earthquake, but accessible during the EEFIT mission, showing the value of conducting environmental surveys weeks after an event as the access improves in the epicentral region. Nonetheless some difficulties were encountered observing environmental effects that had affected built structures, specifically roads, because reconstruction work had already begun in some areas to re-open vital road links. These "partial" observations were integrated with information gleamed by querying local people and site workers.

(a)   (b)
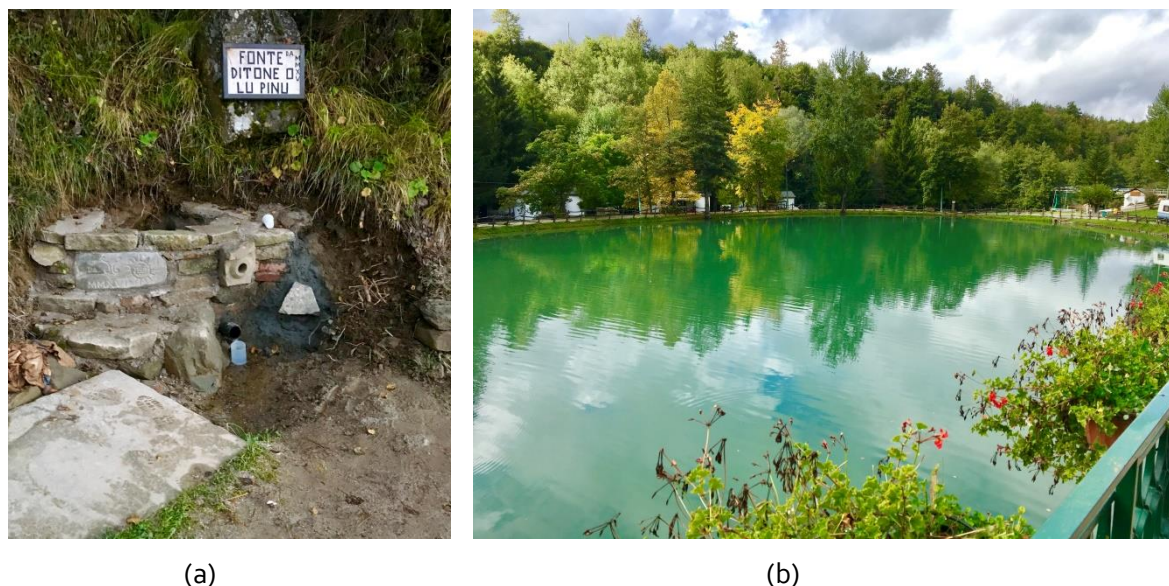
Figure 4-3 Examples of hydrological anomalies and water effects: (a) Spring along SS577 road near Campotosto Lake (see Figure 4-1 for location), which exhibited drop in water flow-rate following the 24 August 2016 earthquake; (b) artificial pond located 5 km south of Amatrice where a local eyewitness reported anomalous waves up to 1m high, lasting for about 3 minutes after the mainshock.

4.5.1   *Amatrice*

The historic town of Amatrice is located on a hilltop at an elevation of 900 to 1000m above sea level (asl), and approximately 8km from the epicentre of the 24 August 2016 mainshock. The bedrock consisted of flysch formation made of sandstone with some marls and carbonate units (see Figure 4-4). In the historic town the bedrock was covered by 3 to 40m thick colluvial deposits, comprising poorly graded gravel sand and silt mixtures. The northern and western parts of the old town consisted of highly fractured flysch outcrops, whereas the gulley in the northern and western parts of Amatrice consisted of alluvium and fluvial deposits, with thicknesses in the range 3 to 10m. Microtremor surveys carried out by Pagliaroli (2016) showed peaks of horizontal and vertical spectra at frequencies of 2 and 3Hz respectively, thus confirming the presence of shallow soft deposits.

Figure 4-5 shows two satellite images of Amatrice taken before (Figure 4-5a) and after (Figure 4-5b) the 24 August 2016 earthquake. The extent of damage is clearly seen from the damage proxy map (DMP) shown in Figure 4-6. The DPM was derived by comparing Interferometer Synthetic Aperture Radar (InSAR) data from the Italian Space Agency's COSMO SkyMed Spotlight before and after mainshock. The DPMs for the entire epicentral region are available from the Advanced Rapid Imaging and Analysis (ARIA) Center for Natural Hazards (http://aria.jpl.nasa.gov/). The colour grading from yellow to red indicates increasing ground deformation. From the figure, it can be seen that most of

the damage was concentrated in the central part of the historic town, where the presence of thick soft deposits, together with the steep topography of the area, were partially responsible for local site effects resulting in the higher concentration of damage.
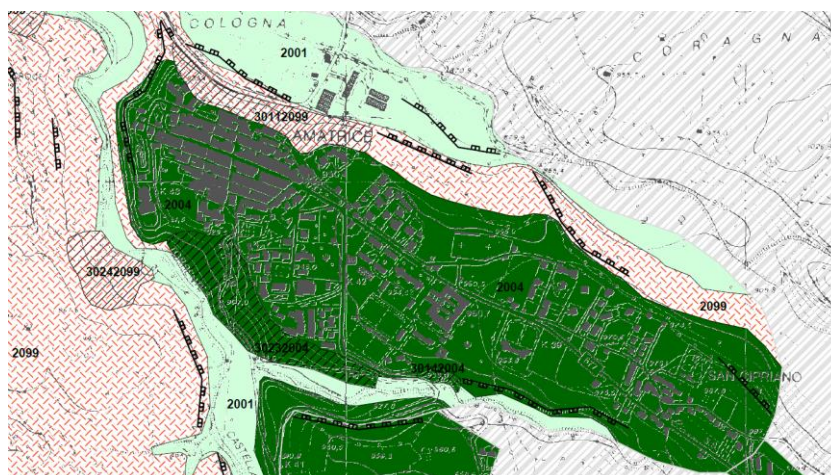
Figure 4-4: Geological map of Amatrice from Microzonazione Sismica Livello 1
(http://www.regione.lazio.it/binary/prl_ambiente/tbl_sismicita/AMB_UAS_RI_Amatrice_MOPS_TAV01.pdf)

The most severe environmental effect was observed along the road adjacent to the hillside located on the northwest extremity of the town (see Figure 4-7). This consisted of disrupted soil slide whose crest (point 1 in Figure 4-6) and toe (point 2 in Figure 4-6) were confined by the SS260 road. The segment of the road running along the crest of the slope was supported by a masonry gravity retaining wall that partially collapsed. At the base of the failed slope, a new retaining wall was being constructed at the time of EEFIT mission (see Figure 4-7b). The failure plane of the slide was relatively shallow, possibly located at the interface between the soft colluvial deposit and the underlying flysch formation. The exposed scarp at the head of the slide (see Figure 4-7a) was almost vertical and exhibited little backward rotation. The displaced material consisted of lightly cemented gravel, sand and silt blocks, which disintegrated during the downward movement. The material displaced was estimated to be approximately of the order of 6,000m[3].

(a)   (b)

Figure 4-5 : Google Earth satellite image of Amatrice: (a) before first mainshock on 24th August 2016; (b) after first mainshock on 24th August 2016.
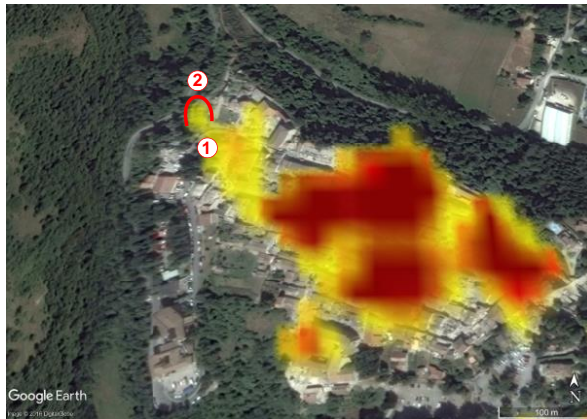
Figure 4-6: Damage Proxy Map (DPM) of Amatrice available from the Advanced Rapid Imaging and Analysis (ARIA) Center for Natural HazardsMD (https://aria-share.jpl.nasa.gov//events/20160824-Italy_EQ/DPM/. The colour grading from yellow to red indicates increasingly higher ground deformation

(a)   (b)

Figure 4-7 : Slide and retaining wall failure observed along SS260 road on the northern-western part of Amatrice: (a) view from the crest and collapsed retaining wall whose debris are visible in the background; (b) view from the base. The displaced material had already been removed and a new retaining wall was being constructed at the time of the EEFIT mission (October 2016). An existing undamaged retaining wall is visible in the background.

Figure 4-8 : Retaining wall failure located in the locality "Ponte Sommati": (a) Google street view before 24th August 2016 event; (b) collapsed retaining wall.

Figure 4-8 shows the collapse of a cantilever retaining wall, located in the locality "Ponte Sommati". This was a small retaining structure, with dimensions of 2.5m high and 50m long, which supported a relatively shallow slope. The cause of the collapse was attributed to a poor engineering design and insufficient reinforcement at the connection between masonry filling and the surrounding reinforced concrete frames.

One of the largest rock falls observed in the epicentral area was observed along the SS260 road, approximately 4km north of Amatrice. At the time of the EEFIT mission, a protective embankment and new road had been constructed adjacent to the failed slope (see Figure 4-9). The slope was protected by a 1.8m high retaining wall supporting a catchment fence, made of hexagonal wire mesh draped over the slope. Boulders –with dimensions up to 0.6m across, detached from the highly fractured flysch formation, and descended by bounding and rolling along the hillslope. Several larger boulders punched through the catchment fence and were still visible on the main road. It was difficult to estimate the total volume of material displaced as this had been partially removed at the time of the EEFIT survey.

Figure 4-9: Rock fall along the SR260. The detached boulders punched through the wire mesh and catchment fence located above the retaining wall. A protective embankment and new road had been already constructed on the side of the old road at the time of the EEFIT mission.

4.5.2 *Accumoli*

The municipality of Accumoli develops along the hillside and crest of a WNW-ESE ridge at a maximum elevation of 890m asl. The geology of the area shown in Figure 4-10, consists of pelithic-arenaceous flysch formations, commonly referred to as "Laga flysch formation", covered by 3 to 5m thick deposits of weathered parent rock and man-made fills. The southern and western sides of Accumoli rest on 10 to 15m thick fluvial soft sediments. Owing to the topography and stratigraphy of the area, local site effect, particularly topographic effect, may have contributed to the large extent of damage caused by the 24th August 2016 shock.

Figure 4-11 shows two aerial satellite images of Accumoli taken before and after the 24 August 2016 earthquake. Although the extent of damage is not clearly visible, the damage proxy map shown in Figure 4-12 shows that most of the damage occurred on the eastern extremity of the old town, where multiple instability phenomena were observed by the EEFIT team. As shown in Figure 4-13 these multiple slides resulted in significant horizontal and vertical ground displacements, and cracks on the road pavement. Furthermore, a reinforced-concrete gravity retaining wall exhibited substantial rotation and outward displacement of up to 60cm (Figure 4-13b). The largest slide was observed on the western extremity of the town, which displaced over 10,000m³ of material.
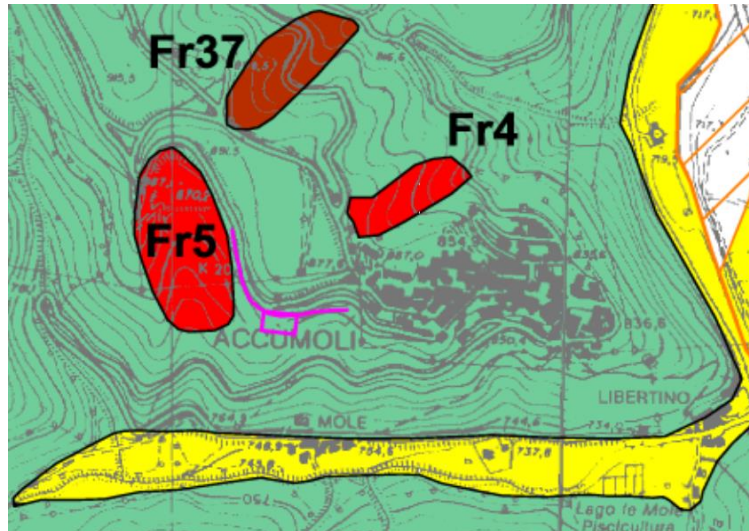
Figure 4-10: Geological map of Accumoli from Microzonazione Sismica Livello 1 (http://www.regione.lazio.it/binary/prl_ambiente/tbl_sismicita/AMB_UAS_RI_Accumoli_MOPS_TAV02.pdf)

(a)

(b)

Figure 4-11: Google Earth satellite image of Accumoli: (a) before first mainshock; (b) after first mainshock.
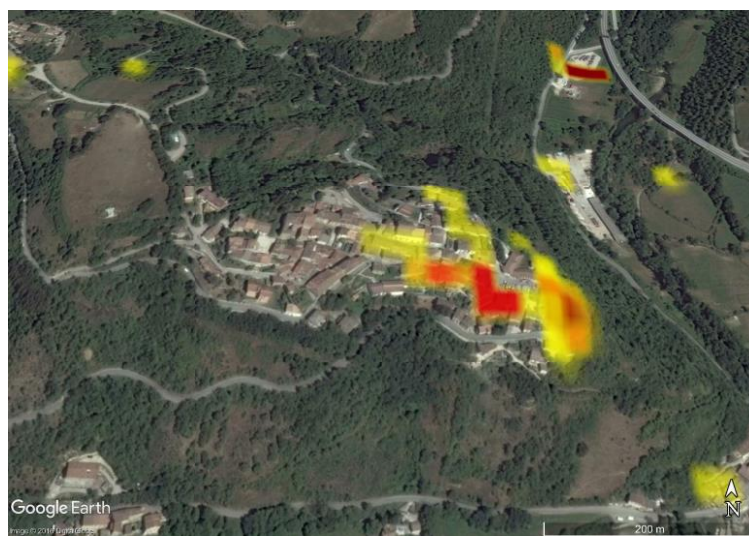
Figure 4-12: Damage Proxy Map (DPM) of Accumoli available from the Advanced Rapid Imaging and Analysis (ARIA) Center for Natural HazardsMD (https://aria-share.jpl.nasa.gov//events/20160824-Italy_EQ/DPM/. The colour grading from yellow to red indicates increasingly higher ground deformation.

Because of the presence of highly fractured flysch formations, rock falls and slides were common in the area. Figure 4-14 shows an example of rock slide observed along the main access road to Accumoli, whereby boulders up to 1.2m diameter, which detached from the bedrock and slid along an almost planar sliding surface and punched through the protective wire mesh.

| (a) | (b) | (c) |
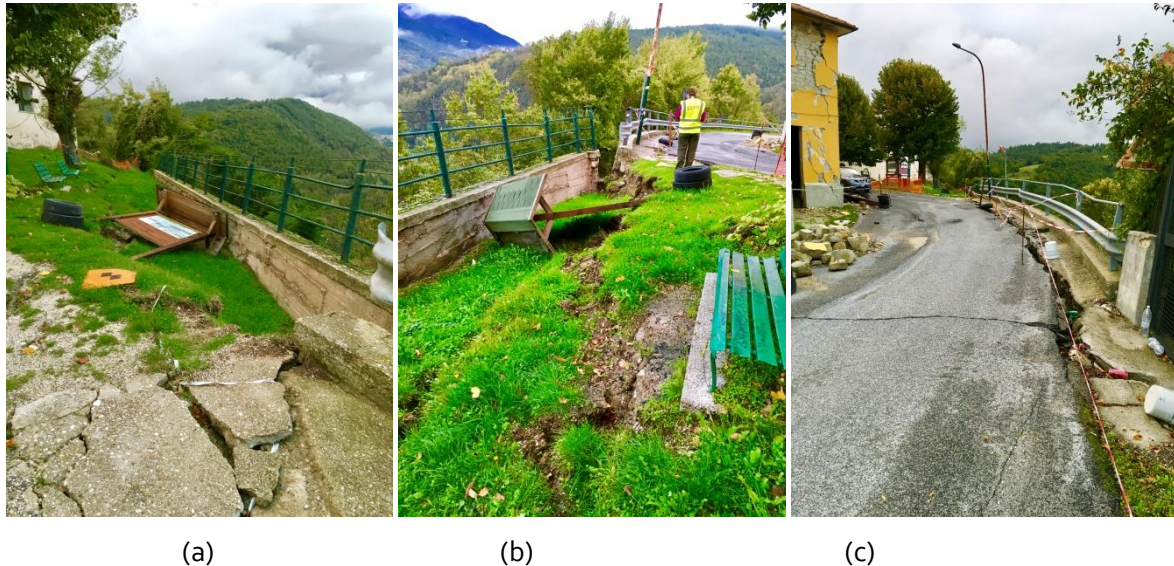
Figure 4-13: Slope instability phenomenon that occurred on the eastern side of Accumoli in the locality of "Fonte del Campo": (a) lateral ground displacement and settlement occurring on the rear at the retaining wall; (b) rotation and outwards displacement of the reinforced concrete retaining wall; longitudinal and transverse cracks on adjacent to pavement road.

Figure 4-14: Rock slide along the main access road to Accumoli, where boulders detached from the bedrock and punched through the wire mesh.

4.5.3   *Pescara del Tronto*

Pescara del Tronto is a locality in the municipality of Arquata del Tronto. This develops along the hillside and crest of a NNE-SSW oriented ridge, at a maximum elevation of 1150m ASL. Figure 4-15 shows the geology of the area. The bedrock consists of so-called Laga flysch formation (see Figure 4-16a), covered by colluvial and eluvial deposits made of coarse-grained material with little fine

content. A typical particle size distribution curve of the material is given in Figure 4-16(b). Single station noise measurements by Masi et al. (2017) showed amplifications in the frequency range 3-7 Hz Data from seismic array tests showed two impedance contrasts at different depths. The first discontinuity was located at about 10m depth –with shear wave velocities increasing from 300 to 600m/s, probably due to the interface between the superficial deposits and the underlying bedrock. The second discontinuity was located at about 30m depth –with shear wave velocity increasing from 600 to 1000 m/s, arguably owing to the change from pelitic to arenaceous Laga flysch formations. Figure 4-17 shows two aerial satellite images of Pescara del Tronto taken before and after the 24 August 2016 earthquake. The extent of damage to the built and natural environment is clearly visible across the entire old town. This is partially confirmed by the damage proxy map shown in Figure 4-18 although a number of slides on the southern-eastern part of the town are not captured in their full extent in the DPM due to the presence of dense vegetation.
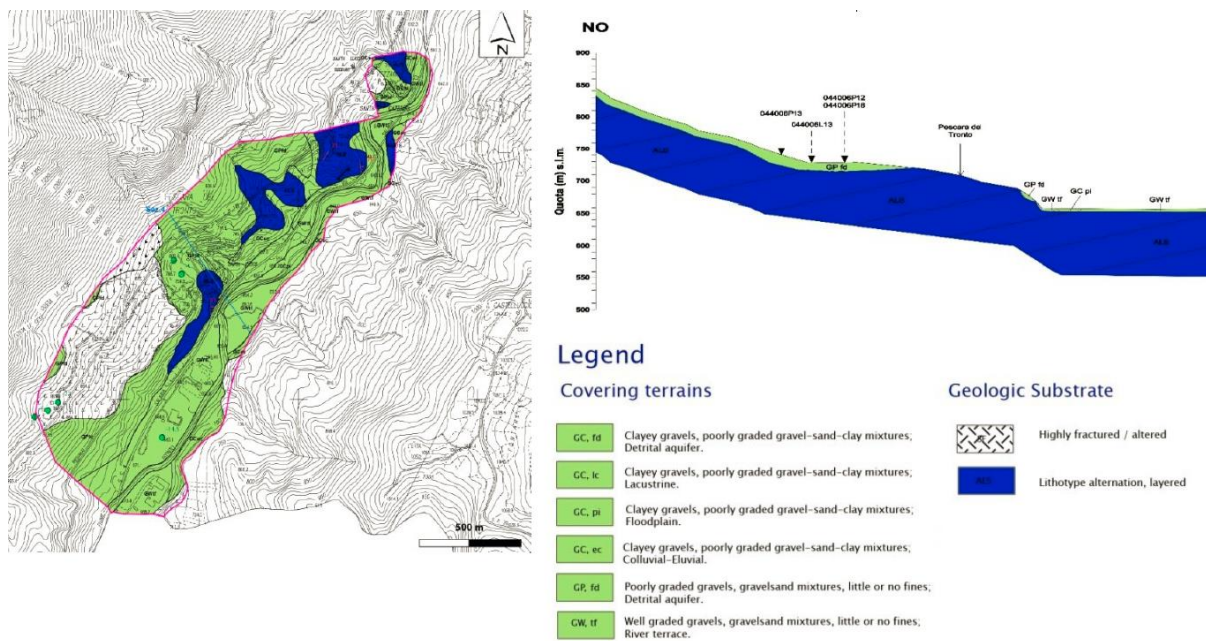
Figure 4-15: Geological map and cross-section of Pescara del Tronto (Zimmaro and Stewart, 2016).

(a)   (b)
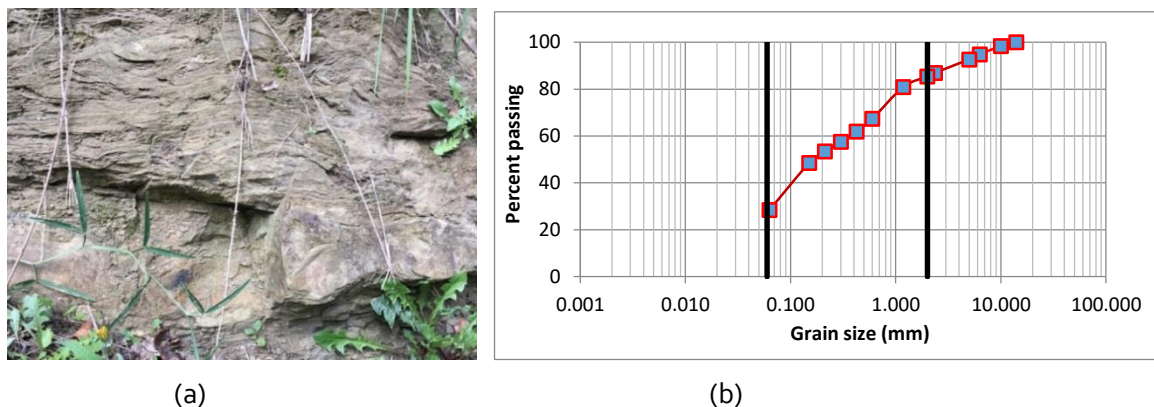
Figure 4-16: Geology in Pescara del Tronto: layered Laga flysch formation; (b) particle size distribution of the shallow formations.

| (a) | (b) |

Figure 4-17: Google Earth satellite image of Pescara del Tronto: (a) before first mainshock; (b) after first mainshock.
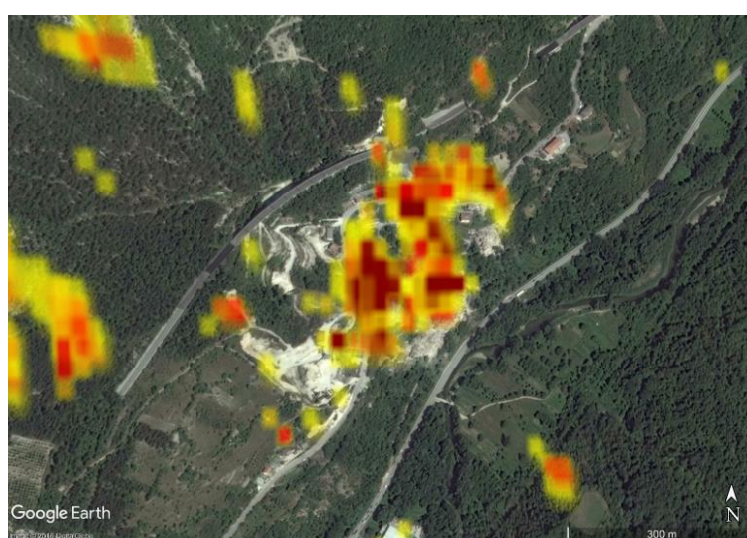
Figure 4-18: Damage Proxy Map (DPM) of Pescara del Tronto available from the Advanced Rapid Imaging and Analysis (ARIA) Center for Natural HazardsMD (https://aria-share.jpl.nasa.gov//events/20160824-Italy_EQ/DPM/. The colour grading from yellow to red indicates increasingly higher ground deformation.

Figure 4-19 shows a disrupted slide that occurred along the SP129 road on the easternmost side of Pescara del Tronto. The site was a gravel pit and relatively large blocks up to 2m across detached and descended downslope. A 0.4m diameter pipeline was visible on the failure plane on the slide although no evident damage to the pipeline and adjacent road was observed by the EEFIT team.

The largest environmental effect in Pescara del Tronto consisted of multiple disrupted slides on the southern slopes adjacent to the SS4 highway (Via Salaria), an important artery connecting Rome to the Adriatic coast. The largest of these slides displaced about 15,000 m^3 of material, which included relatively large blocks of travertine, and caused severe damage to the retaining wall located on the crest of the slope (see Figure 4-20b and Figure 4-20d). A second translational slide occurred along the same slope at about 70m south-east from the earlier slide. This was smaller in terms of volume of material displaced, just about 5,000m^3.

(a)

(b)

(c)

(d)
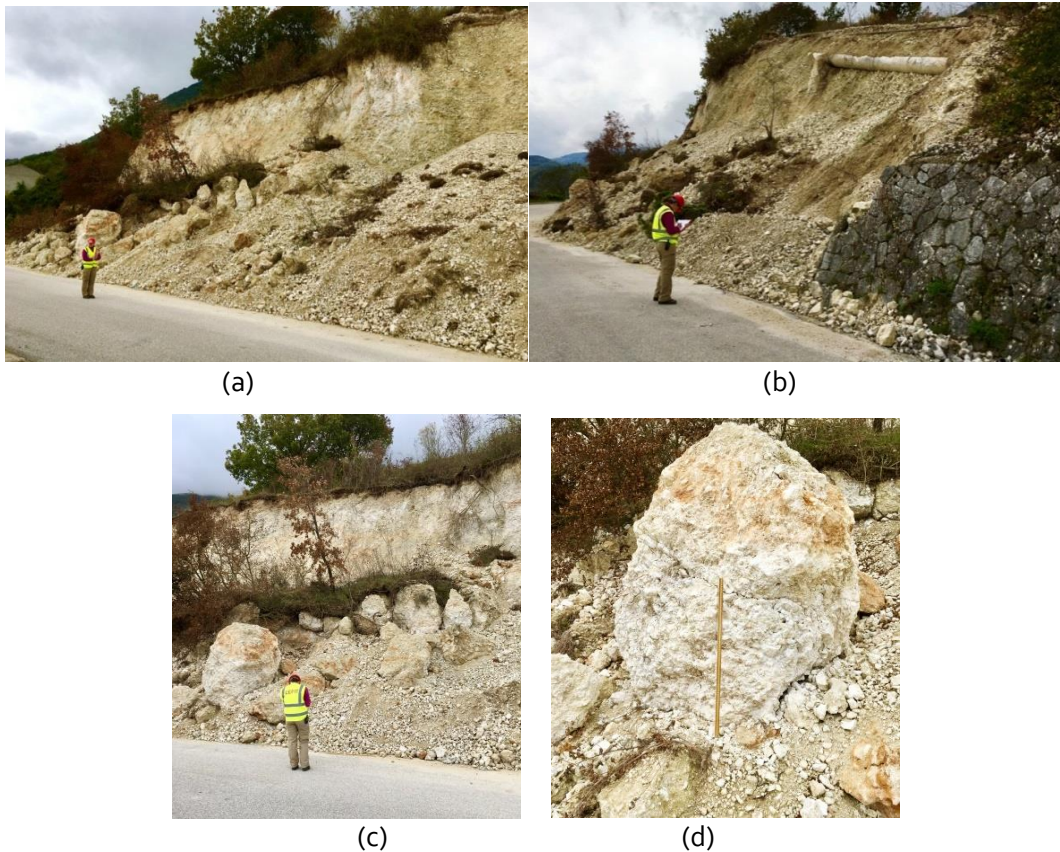
Figure 4-19: Disrupted soil slide observed at the gravel pit in Pescara del Tronto: (a) view of the slide from SP129 road; (b) pipeline exposed on the failure plane; (c) blocks of displaced material; (d) largest block with dimensions up to 1.2m across.

(a)

(b)

(c)

(d)
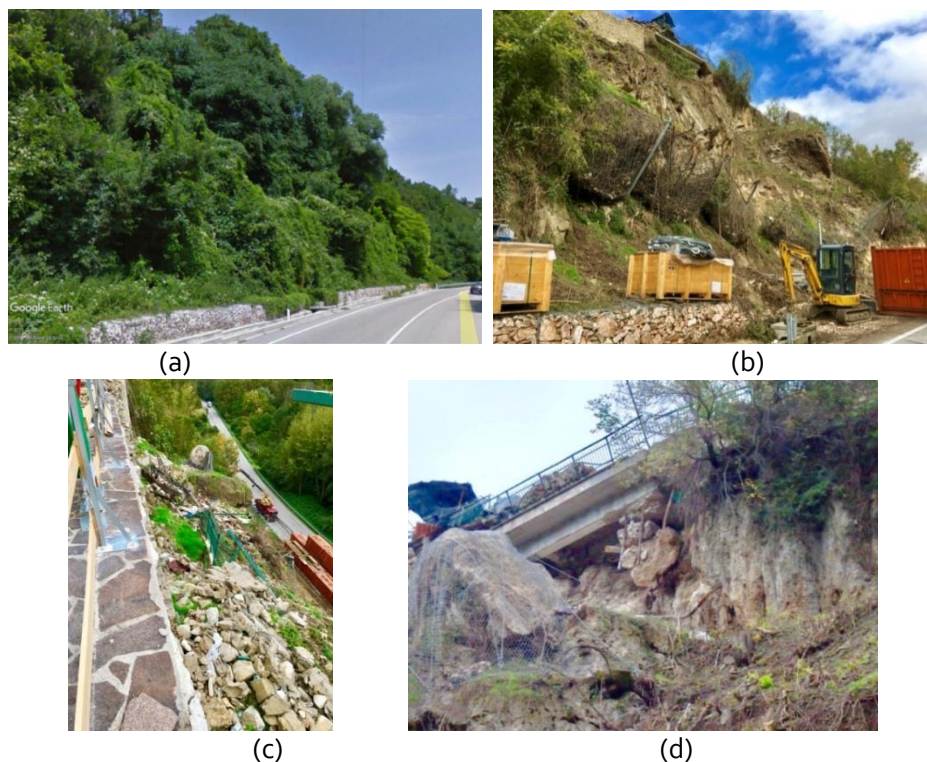
Figure 4-20: Largest slide observed in Pescara del Tronto: (a) Google street view from SS4 highway before the 24 August 2016 earthquake; (b) view from SS4 highway of slide and damaged retaining wall; (c) view from the crest of the slide; (d) large block of travertine captured by the steel wire mesh.

Figure 4-21 Observed slides in the locality of Pescara del Tronto and related induced-damage.

Figure 4-22: Ground cracks on paved roads along SP129 road.

Figure 4-22 shows ground cracks observed on the pavement of the SP129 road. The width of the cracks measured by the EEFIT team showed maximum horizontal and vertical displacement up to 10cm and 5cm, respectively.

4.6   Behaviour of Dams

The EEFIT team performed a rapid survey of dams located within the epicentral area. This section summarises the observation made in four dams impounding the reservoirs of Campotosto and Scanderello.

4.6.1   *Campotosto reservoir*

With 300,000m^3 of water, Campotosto Lake is the third largest artificial reservoir in Europe. This has been used for electrical production by ENEL since the 1970s. The reservoir (Figure 4-23), is impounded by a system of three dams, ie, an earth fill dam in Poggio Cancelli (Figure 4-24a), concrete gravity and earthfill dam in Sella di Pedicate (Figure 4-24b) and concrete gravity dam in Rio Fucino. A walk over survey was carried out to inspect the three dams. Although no damage was observed by the EEFIT team, at the time of the survey, there were major concerns for the stability of the Rio Fucino dam because of its proximity to the Laga Mountains Fault, which was partly reactivated in the seismic events of late October 2016.

Figure 4-23: Google Earth satellite view of Campotosto artificial reservoir and locations of Laga Mts Fault and main dams.

Figure 4-24: Dams in Campotosto reservoir: (a) upstream view of Poggio cancelli dam; (b) upstream view of Sella di Pedicate dam.

4.6.2 *Scanderello lake*

Scanderello lake is located 2km North-East of Amatrice and is impounded by a single concrete gravity dam shown in (Figure 4-25). The dam was not damaged by the seismic event, but personnel from Enel,the owner of the dam, interviewed by the EEFIT team confirmed that, following the main shock, the water level in the reservoir was lowered by 4 to 6m, as a mean f precaution. The decrease in water level can also be appreciated from the change in colour along the shoreline shown in Figure 4-25.

Figure 4-25: Scanderello reservoir and dam: (a) upstream view of Scandarello; (b) view of Scandarello lake.

4.7 Arquata del Tronto: topografic effects

Topographic effects are interpreted to have played a major role in the concentration of damage in several towns due to their peculiar topography and geomorphological settings. Topographic effects are responsible for the amplification of seismic wave due to topographic irregularities, such as steep and narrow mountains range and hills. The concentration of damage in Arquata del Tronto, which is presented and discussed in detail in chapter 5, suggested that topographic effects may have played a significant role in the extent of the damage. Arquata del Tronto is located on the crest of a relatively high and steep ridge, which is schematically depicted in Figure 4-26. Because of its topographical features, the municipality of Arquata del Tronto falls into Category 4 of both the Italian Building Code NTC Norme Tecniche per le Costruzioni (2008) and Eurocode 8: Part 5 (CEN, 2004). Thus, it is expected an amplification of the peak ground acceleration by a factor of 1.4.
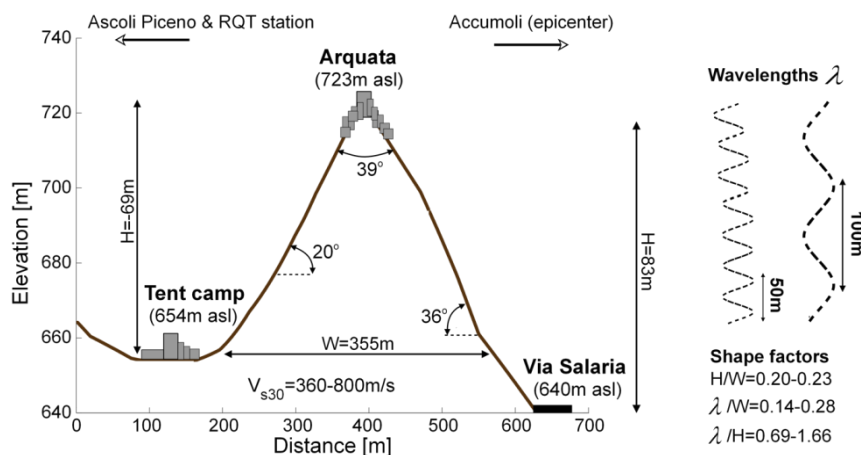
Figure 4-26: Topographical features of Arquata del Tronto: (a) schematic topography of Arquata del Tronto and main geometrical feature. (b) computed wave length of seismic waves induced by 24 August 2016 earthquake.

4.8 Conclusions

The primary objective of this work was to perform a comparison between the intensity determined using the ESI scale and the intensity determined using more traditional approaches using damage of

the built environment. Such comparisons have been previously carried out for historical earthquakes, but this earthquake provides an opportunity for a concurrent comparison. In addition, a full comparison between the effects observed immediately after the earthquake (from Michetti personal communication) and observations conducted by the EEFIT team six weeks later, proved the advantage of carrying out surveys several weeks post-disaster and the value of repeated surveys of the epicentral region. In addition, the ESI scale does not include the potential effects of the soil type or slope angle when observing environmental effects. However, these effects may be important when assessing the epicentral intensity based on the ESI scale. For example, in marginally stable slopes, eg, slopes characterised by steep angles and/or low frictional strengths, relatively low intensity shaking may result in landslides. A revision of the ESI scale taking into account these considerations would be out of the scope of the present work, however, it is highlighted herein that this aspect warrants further research.

References

CEN (Comité Européen de Normalisation) (2004). EN 1998-5: Eurocode 8: Design of structures for earthquake resistance part 5: Foundations, retaining structures and geotechnical aspects. Brussels, Belgium: CEN.

Cruden, DM & Varnes, DJ. 1996. Landslide types and processes. In Special Report 247: Landslides: Investigation and Mitigation, Transportation Research Board, Washington D.C.

Galli, P., Peronace, E., Bramerini, F., Castenetto, S., Naso, G., Cassone, F. and Pallone, F., 2016. The MCS intensity distribution of the devastating 24 August 2016 earthquake in central Italy (MW 6.2). Annals of Geophysics, 59.

Grünthal, G., 1998. European Macroseismic Scale 1998. European Seismological Commission.

Hungr, O, Leroueil, S and Picarelli, L. 2014. The Varnes classification of landslide types, an update, Landslides, Volume 11, Issue 2, pp 167–194.

Masi, A., Santarsiero, G., Chiauzzi, L., Gallipoli, M.R., Piscitelli, S., Vignola, L., Bellanova, J., Calamita, G., Perrone, A., Lizza, C. and Grimaz, S., 2017. Different damage observed in the villages of Pescara del Tronto and Vezzano after the M6. o August 24, 2016 Central Italy earthquake and site effects analysis. Annals of Geophysics, 59.

Michetti A.M., Esposito E., Guerrieri L., Porfido S., Serva L., Tatevossian R., Vittori E., Audemard F., Azuma T., Clague J., Comerci V., Gurpinar A., Mc Calpin J., Mohammadioun B., Mörner N.A., Ota Y. & Roghozin E. (2007) – Intensity Scale ESI 2007. In. GUERRIERI L. & VITTORI E. (Eds.): Mem. Descr. Carta Geol. d'Italia., vol. 74, Servizio Geologico d'Italia – Dipartimento Difesa del Suolo, APAT, Rome, Italy.

Michetti A.M., Esposito E., Gurpinar A., Mohammadioun B., Mohammadioun J., Porfido S., Roghozin E., Serva L., Tatevossian R., Vittori E., Audemard F., Comerci V.,.Marco S., Mc Calpin J. & Mörner N.A. (2004) – The INQUA scale: an innovative approach for assessing earthquake intensities based on seismically-induced ground effects in natural environment. In VITTORI E. & COMERCI V. (Eds.): Mem. Descr. Carta Geol. d'Italia, vol. 67, Servizio Geologico d'Italia - Dipartimento Difesa del Suolo, APAT, Rome, Italy.

NTC (2008). Norme Tecniche per le Costruzioni, D.M. 14 Gennaio 2008.

Reicherter, K., Michetti, A.M. and Barroso, P.S., 2009. Palaeoseismology: historical and prehistorical records of earthquake ground effects for seismic hazard assessment. Geological Society, London, Special Publications, 316(1), pp.1-10.

Silva, P.G., Rodríguez-Pascua, M.A., Pérez-López, R., Bardají, T., Lario, J., Alfaro, P., Martínez-Díaz, J.J., Reichert, K., Giménez, J., Giner, J. and Azañón, J.M., 2008. Catalogación de los efectos geológicos y ambientales de los terremotos en España en la Escala ESI-2007 y su aplicación a los estudios paleosismológicos. Geotemas, 6, pp.1063-1066

Varnes, DJ. 1978. Slope movement types and processes. In Special report 176: Landslides: Analysis and Control, Transportation Research Board, Washington, D.C.

5   DAMAGE OBSERVATIONS AND ANALYSIS IN THE URBAN CENTRES

5.1   Introduction

It has been noted that the worst affected region has a surface area of approximately 500 km², including a number of towns and small villages across the regions of Umbria, Marche, Abruzzo and Lazio. The main cities and towns that were visited by the EEFIT Team included Amatrice, Accumoli, Arquata and Pescara del Tronto, Norcia and its surroundings and Castelluccio di Norcia. Figure 5-1a shows the map released by INGV of the PGA contours and overlaid intensity values at each of the locality visited during the mission. Figure 5-1b shows the contour map for PSA (T=0.3s), considered the most significant local amplification in relation to low-rise masonry structures, which are the most common building type of the area.
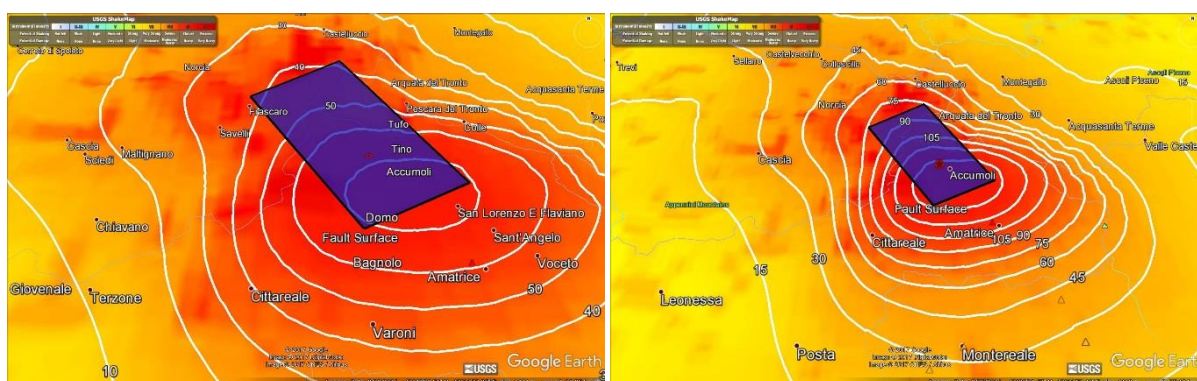
Figure 5-1: a) PGA contour map and b) PSA (T=0.3s) contourmap, with overlaid intensity map of the 24th August 2016 event according to INGV shakemap (http://shakemap.rm.ingv.it/shake/7073641/products.html, accessed 25/06/2017)

Due to their geographical location adjacent to the Apennines chain, almost all the cities struck by the earthquake are built with the same building stone (turbiditic sandstone) coming directly from the Tronto River's quarries.

The large majority of the building stock is made of unreinforced masonry in the historic centres, and reinforced concrete frame in the outer more recently built neighbours. Masonry buildings show a high degree of variation, in relation to building's height, footprint, materials used for the horizontal structures and for the walls structures through time, producing clusters of buildings with severe irregularity in plan and elevation, although the single units might appear to be relatively regular. The layout and connections of the buildings in clusters has a critical influence on the response of the single buildings and the resulting observed damage. (Vicente et al. 2013)

The extent of damage observed at territorial scale shows an overall poor performance of the masonry structures, especially within the residential sector. The quality of materials and construction techniques were interpreted to have had a significant impact on the overall seismic response of the residential buildings in the town centres visited. The majority of these buildings were constructed between the end of the 19th Century and the first half of the 20th Century, as it can be seen by comparing the two photographs of the main street of Amatrice, taken 60 years apart (see Figure 5-2).

Notwithstanding the fact that seismic regulations in Italy were developed progressively since the aftermath of the destructive 1907 Messina earthquake (Guidoboni et al., 2010), the majority of the buildings in these centres were originally built with no explicit reference to lateral load bearing capacity beyond the traditional detailing of good construction practice of the time. However, in the intervening years, and particularly after the earthquakes in the late 1970s and 1980s, following the

seismic reclassification of these territories in 1984, most buildings were retrofitted to improve their seismic response (Romeo & Pugliese, 1997). These interventions, regulated by the technical guidelines in existence at the time, were not isolated occurrences, with buildings undergoing retrofits with a cyclic cadence after each earthquake.

Figure 5-2: (a) Amatrice 1951, (b) Amatrice 2011

To understand better the extent and relevance of the retrofitting in this region, and its effect on the response of buildings at territorial level, Section 5.2 presents a brief overview of the evolution of seismic codes in Italy. Particular attention is paid to provisions for masonry buildings and their applicability to the region of interest, given its seismic classification at the time. A summary of the NTC08 prescription for strengthening of masonry structures is presented and compared with the Ministerial Decree on Masonry Structures, issued in 1986 and 1987. Section 5.3 reports on the damage observation in the six towns visited and section 4 shows the results of the Rapid Visual Screening survey and discusses the use of virtual surveys technology for rapid damage assessment, used during the field mission.

5.2   Development of seismic and retrofitting building codes in Italy

In Italy, prescriptions relating to safer construction in seismic prone areas have typically followed destructive events. Because of the division in a multitude of small states until the second half of the 19th Century, many of these provisions had limited geographical jurisdiction across the Italian peninsula, although they contributed to create a common culture, which eventually build up to a shared body of technical knowledge distilled in the decrees of the early 20th century. A list of documents relevant to masonry structures is collated in Table 5-1. (Bellicoso, 2011)

The first Royal Decree that included some sort of seismic provision was enacted in 1627 following a catastrophic earthquake that stroke the Campania region, in southern Italy. This document included very basic recommendations and introduced a new lightweight timber construction technique, called "sistema baraccato". Following the 1627 RD, there was modest implementation and technical evolution. Three decrees only were published in the following two centuries, in 1784, 1860 and 1884 respectively. The 1860 Decree included some significant prescription to masonry buildings especially for the city of Norcia, specifically the requirement for regular vertical alignment of windows and openings, to create a system of masonry piers going from foundation all the way up to the roof level and spandrels connecting them together. It also required the insertion of tie-rods, buttresses and limited the building height to 2 storeys. The buildings observed during the EEFIT mission are generally compliant with the above prescription as shown in Figure 5-3.

Table 5-1 Seismic events and consequent regulation documents issued by the government of the time.

Year	Seismic Event	Ordinance, Decree, Code
1627	1627 Campania Earthquake	1st Royal Decree with some preliminary seismic prescriptions
1784	1783 Messina and Calabria Earthquake	Instructions for the Reconstruction of Reggio
1860	1857 Napoli Earthquake and 1859 Norcia Earthquake	Pontifical Decree
1884	1883 Ischia Earthquake	Law n. 1985, 5th March 1884
1909	1908 Messina Earthquake	Royal decree n.193, 18th April 1909
1926	1915 Avezzano earthquake	Royal Decree n.705, 3rd April 1926
1962	1962 Irpinia Earthquake	Law n.1684, 25th November 1962
1976	1971-1975 Seismic Activity in Umbria	Law, n. 64 02/02/1974 Provvedimenti per le costruzioni con particolari prescrizioni per le zone sismiche Law n. 176, 26 Aprile 1976
1981	1981 Irpinia Earthquake	Ministerial Decree 2nd July 1981
1984		Ministerial Decree 29th February 1984
1986		Ministerial Decree 24th January 1986
1987		Ministerial Decree 20th November 1987
1996		Ministerial Decree 9th January 1996
1999	1997 Marche and Umbria Earthquake	DM n.6 of 30/01/1998. "Ulteriori interventi urgenti in favore delle zone terremotate delle regioni Marche e Umbria e di altre zone colpite da eventi calamitosi"
2003	Molise Earthquake	Prime Minister Decree OPCM 3274
2008		Italian Seismic Code NTC08

Figure 5-3 Alignment of vertical openings in the main square in Accumoli. The building also has buttresses to the first two storeys of the façade

In 1908, after the devastating earthquake that destroyed the city of Messina and caused more than 100,000 casualties, the first national seismic code was published in Italy, the Royal decree n.193, 18th April 1909 (Paz, 2012). The decree introduced for the first time in the world the idea of designing a structure against the horizontal forces induced by an earthquake. A specific section dealt with repairs of ordinary buildings, including criteria intended to upgrade existing buildings to the requirements of new constructions. Among the provisions, it was required that buildings with cracks, which had not been built using the baraccata system of timber frames with lightweight infills above the ground storey, should be reduced in height, and then reinforced using vertical supports in timber, iron, or

reinforced concrete, firmly slotted and fixed into the foundations. These vertical elements should be extended to the top floor and connected by bands at the level of the foundation and at the roof eaves to form a strengthening cage. The vertical supports should be present at all corners of the building, and spaced at no more than 5m. The floor structures should also be connected to this cage by cross beams or by ties spaced at no more than 3 m.

Following the 1909 decree, the Italian seismic codes have been increasingly comprehensive in terms of seismic recommendations. The idea of a seismic zonation, with design forces associated to the seismicity of the locality, was firstly introduced in Italy in 1926. In fact, the royal decree n.705 published on the 3rd of April 1926 (Presidente del Consiglio dei Ministri, 1926) distinguished between 2 seismic zones. However, the Italian territory was not fully mapped and only those towns and villages known to have been previously hit by an earthquake were associated with a seismic category. In decrees issued between 1924 and 1930 (Tosone & Bellicoso, 2017), the materials used for framing buildings changed from wood, steel or reinforced concrete to steel alone. Masonry wall could only be built up to 8m height in zone 1 and with a minimum wall thickness of 300mm at the top story increasing by 150 mm at each lower storey.

The Law n.1684, 1962 (Presidente del Consiglio dei Ministri, 1926), which appears to be quite comprehensive, included:
- Reduction of seismic action for foundations on competent soil;
- New limits for maximum heights and maximum number of storey;
- Inclusion in urban master plans of state of the art construction rules;
- Update of the seismic coefficient, distribution of the action and reduction of the overloads;
- Inclusion of structures of all materials in seismic zones;
- Exclusion of thrusting structures;
- Introduction of cement mortar instead of mud mortar.

However, it should be borne in mind that these clauses and regulations were only applicable to zones considered seismic, and these were usually the sites of recent earthquake events, while historic seismicity was not considered as an indicator of seismic hazard and need for specific construction restrictions in regions that had not witness recent shaking. These laws did not cover Amatrice and the neighbouring towns, therefore only the prescriptions related to constructions in non-seismic areas were applicable.

The national seismic service was established in 1976 with the main goal of providing the seismic zonation for the whole Italian territory. The first national seismic hazard map was produced in 1984. (Slejko et al. 1998).

For example, the town of Norcia, which has been damaged during the M_w 6.5 30th of October 2016 earthquake, was not classified as seismic until the late 70's. Amatrice was only classified as seismic zone 2 in 1984. In 2003, (DPCM, 2005), Amatrice was upgraded to seismic zone 1 (Masi et al., 2017).

Following each reclassification, the existing building stock underwent periods of retrofitting to comply with the new increase in seismic demand. Of particular relevance to the retrofitting of the towns visited by the EEFIT mission are:
- the Ministerial Decree D.M. 24th January 1986 (Ministro dei Lavori Pubblici, 1986), "Norme tecniche relative alle costruzioni antisismiche" (Seismic Design code); and
- the Ministerial Decree D.M. 20th November, 1987, "Norme tecniche per la progettazione, esecuzione e collaudo degli edifici in muratura e per il loro consolidamento" (Technical code for the design, execution and testing of masonry buildings and for their strengthening).

Figure 5-3: Italian Seismic Hazard Map (a) 1984, (b) 1998, (c) 2004

These two decrees sanctioned the use of concrete slabs to introduce the concept of a rigid diaphragm in masonry structures and the use of ring beams to enforce the box behaviour. The DM87 introduced the concept of improvement, rather than full compliance with the requirements for new structures, giving the designer the responsibility for proving that the capacity of the structure had been increased without changing the overall original structural concept. It prescribed various means of improving the capacity of masonry structures. Among these: injections of mortar to fill the gaps within the wall; concrete encasement of the wall; formation of concrete columns within cuts made into the masonry; use of steel ties/ rods; local patching of the masonry corresponding to points of weakness of the wall (chimneys, cracks, very wide or irregular openings); concrete or steel frame to stiffen irregular opening. Indications were provided on the minimum cross section of ring beams, to have depth at least equal to the slab and width of at least 2/3 of the wall thickness.

Retrofitting measures, designed to take the building to a level of full compliance to the DM86, were compulsory only if the building underwent modifications to extend its footprint or increase its number of storeys or applied gravity loads. Despite the fact that DM86 prescribed the reduction of the masses as one of the main strategies for the improvement of the seismic capacity of a building, DM87 recommended that traditional timber floors and roof be replaced by concrete slabs (or steel, although far less established in the Italian market at the time) to implement the rigid diaphragm model (see examples of these in Figure 5-4. These measures were extensively implemented in the towns visited as testified by the EEFIT team observations. For instance, the use of precast concrete joists had been rather common since the 60's and especially the 70's, as a very effective way of quickly replacing old and degraded timber floors, and they were visible in several buildings inspected (see Figure 5-9c, for instance).

Following the Umbria Marche earthquake, 1997, there was substantial evidence of the detrimental effects of concrete slabs and ring beams on the seismic response of masonry structures (Spence & D'Ayala, 1999, EEFIT, 1998). As a result, the provisions for repair and strengthening of DM n.6 of 30/01/1998 (Presidente del Consiglio dei Ministri, 1998), shifted the emphasis on establishing connections between horizontal structures and vertical structures, while avoiding the increase in mass due to the insertion of concrete slabs and ring beams. The DM n.6 of 30/01/1998 recommended the use of tie rods to connect walls, and the stiffening of timber floors and roofs by anchoring the beams, joists and rafter to the walls and creating thin mortarcrete slabs overlaying the floor planks. Reinforced plaster, or shotcreting or jacketing, was also recommended, while concrete columns were ruled out in favour of brick and masonry encasements. These interventions were also implemented beyond the reconstruction of the towns hit by the Umbria- Marche earthquakes, in many of the

mountainous towns of Central Italy, when buildings were renovated and expanded in the last 20 years, to develop a building stock to support the development of environmental tourism in this region (Bosi et al, 2011).

Figure 5-4: Examples of (a) traditional wooden roof structure; (b) concrete roof with lightweight brick tiles; (c) steel beam profile roof on mixed masonry -concrete ring beam.

Figure 5-5 shows a typical case of an upper storey built in modern brickwork added over a roughly dressed stone masonry older structure. The stone masonry had been extensively repointed and ring beams and roof slabs are visible. The difference in stiffness between the two storeys and weight of the roof can be the reason for the observed shear crack pattern, denouncing the expulsion of the corner.

Figure 5-5: a) Shear crack of corner in building with second floor addition in concrete blocks and ring beams; b) out of plane failure of façade wall of 3 storey high building with traditional vaulted structures at ground storey, intermediate timber floors and RC roof slab. No evidence of ties.

With the increasing appreciation of the historic, cultural and environmental value of these constructions, both owners and professionals became more supportive of intervention with traditional materials. For instance, grouting was preferred to shotcreting, to leave the stone fabric exposed. Figure 5-6a shows a building with a typical 3 leaf masonry wall, which had lost part of the external leaf, due to poor quality of the grouting and its execution. The building also shows ties anchors underneath the roof, which seem to have worked well in preventing a roof collapse. The instigation of damage is possibly caused by pounding with the adjacent building, as the vertical cracks at the interface suggest.

Figure 5-6: Consolidation of local masonry fabric: a) poor grouting in Arquata del Tronto; b) adequate quality grouting and rc frames around opening, delivered a better seismic performance (Amatrice)

Figure 5-7: a) stone masonry building with ties and grouting of the rubble stone masonry in Pescara del Tronto; b) ONMI Institute in Amatrice, where seven people died. The concrete beams can be seen punching through the façade.

Anchors together with proper grouting and repointing seemed to have in general performed better than other solutions. The example in Figure 5-7a is one of the few buildings that survived in Pescara del Tronto, where earthquake intensity was classified as X-XI of the CMS scale, by the Italian Civil Protection. The building is equipped with ties and had the mortar reinstated, and despite the collapse of a small portion of the corner, due to the presence of water pipes, it survived the earthquake. Figure 5.7b shows a large masonry building in Amatrice, in which traditional floors had been substituted with reinforced concrete beams, which can be seen punching the façade.

5.3 Residential Building Stock and Damage Overview

5.3.1 *Amatrice*

Amatrice is a municipality of 2500 residents, in the province of Rieti, in the Lazio region. Given its strategic position on the River Tronto and along the Salaria, the roman road connecting Rome to the Adriatic coast, Amatrice was a thriving centre since mediaeval times, with a history of independent government as well as control over the Laga territory. The city was severely damaged by an

earthquake in 1639 which killed 500 people. (Tiberi,1639). Another earthquake with epicentre in Norcia affected Amatrice in 1703, also causing widespread destruction and damage. Both earthquakes are considered to have had local intensity MCS 9. Amatrice is classified in seismic zone 1 since 2003, (DPCM, 2005), corresponding to an expected acceleration a_g>0.25g, and a reference peak ground acceleration value ag_{orif}= 0.26 g, as maximum expected acceleration for the municipality with probability of exceedance <= 10% in 50 years, based on uniform hazard spectra. Before 2003 it was classified in zone 2. The maximum PGA recorded at the AMT instrument according to the ESM Database was 0.867 g, i.e three times higher than the code value.

Amatrice urban grid probably dates back to the medieval period and it is fairly regular with arrays of buildings aligned in a NW-SE direction due to the elongated shape of the hill top on which it is built. Although many buildings show medieval elements and details, especially the characteristic Norman Romanic churches, much of the building stock is probably dating back to the late 17th and 18th century reconstructed after the destructive earthquakes of 1639 and 1703. Buildings are constructed in adjacency without gaps, indeed in many cases sharing party walls.

From the observation of masonry walls still standing a multi-layered wall system has been generally identified (see Figure 5-8a) often made of rounded fluvial cobbles and boulders, with poor or almost no inner connection, and cast in a sandy or mud based mortar. Building's height is mostly two to three storeys, with a minority of buildings with 4 storeys. The older buildings have vaulted structures at the ground level and timber floor structures at the upper storey (Figure 5-8). Although the façades show generally a regular distribution of openings vertically aligned, in buildings that had lost their façade it was common to see different floor structures at different levels, with more modern and stiffer concrete slabs with prefabricated concrete joists at the upper storey and solid cast slabs. Traditionally roofs were also made of simple timber rafters and purlin systems or, for wider spans, trusses. However, in the late twentieth century many of these were replaced with solid concrete slabs supported on the masonry walls by means of ring beams.

Chimneys have been spotted among the wall fabric of almost all the residential buildings, very often located at the corners, substantially reducing the integrity of the connections among orthogonal wall and hence the capacity of the system to withstand lateral loading.

Figure 5-8: Amatrice. a) Typical 2 leaves with cavity masonry wall system. b) Vaulted structures at the ground level of a three storey building. c) Inner chimney, located at the corner of a residential unit.

Figure 5-9: Out-of-plane failures and total collapse caused by concrete roof slabs.

Given the large number of collapses and highly damaged buildings, the historic city centre of Amatrice was declared as red zone and cordoned off the day after the earthquake. As a result, the EEFIT team only managed to gain access to the site in two successive visits each about one hour long, during the mission. The visit itineraries are shown in Section 5.4, whereby the team was allowed to walk down the main street and one of the largest transversal roads. Out of plane collapse mechanisms were the major cause of collapse, which could be identified on buildings still standing, while relatively few in plane failures were recorded. These out-of-plane failures are of type F according to the nomenclature provided by D'Ayala & Speranza (2003), whereby the walls form a vertical arch restrained at the bottom by the foundation and at the top by the concrete ring beam and roof, but free to move out of plane at the intermediate floor level, as the wall is not restrained by ties or floor structures. In the cases in which the walls had proper restraints at floor level, partial mechanisms occurred, of type G (D'Ayala & Speranza, 2003)

On top of the stone rubble that were the walls of collapsed buildings, is possible to identify some smooth ties, which might have connected transversal walls, and many pitched roof whole slabs which remained virtually solid.

Given the restricted and time limited access to the urban centre of Amatrice, the Rapid Visual Survey (RVS) that the team performed was limited to very few buildings. Of the buildings surveyed and recorded with the omnidirectional camera (see Section 5.4) only a minority show the presence of ties or corner quoins to prevent out-of-plane collapse. The damage observed is consistent with the PGA recorded by the AMT instrument located 8.5 km from the city centre with major component in EW direction. According to the extent and distribution of damage level surveyed in the city centre and taking into account that only few of the concrete frame buildings present show structural damage, the macro seismic intensity level attributed by the EEFIT team is IX of the EMS' 98 scale (see Grünthal,

1998). This correlate well with environmental damage scale level attributed to the locality, as discussed in Section 4.4.

5.3.2   *Amatrice, following the October 2016 events*

There were no many buildings left to be affected by the subsequent earthquake swarm that occurred during October 2016. The most emblematic cases were the so called 'red building' (Figure 5-10) and the civic tower of Amatrice shown in Figure 5-11. The residential brick building, which had withstood the seismic event of the 24th of August, collapsed during the earthquake on October 26th 2016, together with what was left of the Municipality Building. The top part of the civic tower collapsed during the 30th October event, together with the partially still-standing bell tower of the Saint Agustin Church, located at the entrance of the 'red zone'.

Figure 5-10: 'Red Building' and Civic tower, Corso Umberto I, Amatrice from http://i.dailymail.co.uk/i/pix/2016/08/24/16/378C961500000578-3755722-image-a-6_1472052123020.jpg

Figure 5-11: Civic Tower Amatrice, after the 26th of October even retrieved from http://newsok.com/gallery/6035374/pictures/4501462

5.3.3   *Accumoli*

Accumoli is a municipality of 650 people, some 18km north of Amatrice on the SS4 Salaria road, situated on a hill at 855 m asl. Accumoli is part of the Rieti province in the Lazio region, contained in a valley bounded on the north by Monti Sibillini and on the east by Monti della Laga. Accumoli was founded as a municipality in the XII century by the Normans. The civic tower, of unique architectural value, was built during this period. Accumoli, like Amatrice, was seriously affected by the 1639 earthquake with epicentre in the Monti della Laga and the 1703 earthquake of Valnerina. This last had the worst effect with estimated local I_{MCS} 10 (see Figure 2-4). In modern times Accumoli was hit by an earthquake in 1950, with epicentre in Gran Sasso with local intensity 8. Accumoli is classified as seismic zone 1 since 2003 (DPCM, 2005), having previously been classified as zone 2. The Lazio Region provides a reference PGA value for Accumoli ag_{orif}= 0.2593 g, as maximum expected acceleration for the municipality with probability of exceedance <= of 10% in 50 years, based on uniform hazard spectra. ("Regione Lazio," 2017).

Accumoli's urban layout follows the contour lines of the mountain slope on which it is located. Buildings are 2 to 3 storey high, with a minority of 4 storey buildings, built adjacent to each other without gaps clustered along the slops. This implies that floor structures of adjacent buildings are on different levels and potentially generate hammering and pounding forces during shaking. Several buildings had vaulted structures at ground floors and a variation of floor structures at the upper storeys depending on the year of refurbishment. Several buildings appear to have had their traditional timber roof structures replaced by concrete slabs anchored to the masonry with reinforced

concrete ring beams. Many of the older buildings show quoins at the corners among walls and in some cases ties. Other buildings show heterogeneity of load bearing wall structures at different storey level, highlighting addition of storeys on original structures at different times.

Figure 5-12: Accumoli a) Main street; b) view of the relationship between the building stock and the natural environment.

Although the village of Accumoli is the closest village to the epicentre of the August 24th earthquake, the level of damage recorded was not as intense as Amatrice or Pescara del Tronto. It was notable that many buildings had not been properly maintained in years and the damage observed after the 24th August was clearly concentrated on such buildings. No complete collapse was observed, while structural damage ranged from roof failure to some disconnections among walls, denouncing incipient out-of-plane mechanisms and shear cracks in buildings along the main street that had been refurbished and possibly retrofitted.

According to the extent and distribution of damage level surveyed, taking into account that no collapse had been observed, while many buildings had structural damage and partial collapse and some buildings had light damage the macro seismic intensity level attributed by the EEFIT team is VII-VIII of the EMS' 98 scale (see Grünthal, 1998).

Figure 5-13 a) Corner expulsion in a building retrofitted with ring beam; b)Roof failures and vertical cracks in several poorly maintained buildings.

While the team was collecting data in Accumoli, the Fire Department shoring specialist squad were on site conducting a shoring and propping intervention of the XII century Civic Tower and to remove the bell tower. The work in progress is shown in Figure 5-14.

Figure 5-14 : Civic Tower in Accumoli: live intervention by Vigili fdel Fuoco to secure the tower with temporary shoring and hoops

5.3.4   *Accumoli Following the October 2016 Events*

The condition of the town after the 26th and 30th of October events was irreversibly worsened. Although Accumoli was relatively closer to the epicentre of the August event, the majority of the buildings collapsed after the latter events, although located at greater epicentral distance. This increase in damage is attributed to the increased fragility of the buildings following damage in the August earthquake.

5.3.5   *Arquata Del Tronto Bassa and Arquata Del Tronto Alta*

Arquata Del Tronto is a municipality of about 1300 people, located within the Ascoli Piceno Province, which rises up in strategic position on a hilltop, dominating the whole Tronto River Valley. Its territory extends partly within the Gran Sasso and Monti della Laga National Park. The town is clearly divided into two different sections: the lower and more recent one, which extends towards the valley, and the upper and older historical centre is located on the rocky hill shown in Figure 5-15.

Figure 5-15: Arquata del Tronto old town

Due to its strategic position in between 4 different regions, Arquata and its territory has been considered a battle field for two main contenders, the cities of Ascoli Piceno and Norcia. That was the main reason for the construction of the symbolic military tower defined as 'Rocca di Arquata del Tronto', which started between the XI and XII century. Historically, Arquata del Tronto was severely damaged as a result of the 1703 Valnerina earthquake, the 1917 Monti Sibillini earthquake and the 1950 Gran Sasso event. The 1703 Valnerina event had local intensity MCS IX, while both the 1917 Sibillini and the 1950 Gran Sasso events had intensity MCS VIII. Arquata del Tronto has been classified in seismic zone 2 since 2003 (DPCM, 2005). The Marche Region provides a reference PGA value for Arquata del Tronto ag_{orif}= 0.2559 g, as maximum expected acceleration for the municipality with probability of exceedance <= of 10% in 50 years, based on uniform hazard spectra. (Marche Region, 2018)

The two parts of Arquata del Tronto have different characteristics and different building typologies, thus resulting in different levels of damage experienced. The lower and newer part of the town is mainly characterized by the presence of reinforced concrete frame buildings with reinforced concrete slabs and roofs of 2-3 storeys (Figure 5-16a), which cohabit with traditional masonry buildings characterized by masonry primary structural elements and timber roofs (Figure 5-16b).

Figure 5-16 : Typical buildings in Arquata del Tronto Bassa.

On the contrary, the old historical city centre located on the top of the hill is predominantly characterised by masonry buildings clustered around the main Piazza (Fig 5.17). Most buildings have masonry walls and timber horizontal structures. However, many of these old buildings have been retrofitted with ringbeams and concrete slabs.

Figure 5-17: Masonry Buildings around the main Piazza in Arquata del Tronto Alta

The overall quality of the stone masonry walls was generally observed as relatively poor. Stones are river round pebbles and cobblers bonded with poor mud and lime mortar. In some cases, grouting had been implemented but the quality of the work was poor. The level of connection among wall's leaves is poor (refer to Figure 5-18) with few through stones. Some buildings had corner stones and quoins. Some of the buildings also had ties, the effectiveness of those strengthening interventions was very low, due to the poor quality of the masonry walls they were restraining. A minority of well executed and effective strengthening interventions were observed.

EEFIT conducted a fairly detailed rapid street survey of most of the buildings of both the lower and upper parts of the town (see Section 5.4). The different topology and divers structural typologies of both parts of the town resulted in very different level and extent of damage. Accordingly, on the upper town, taking into account that some collapses had been observed, while most buildings had structural damage and partial collapse and some buildings had light damage, the macro seismic intensity level attributed by the team is VIII-XI of the EMS' 98 scale (see Grünthal, 1998).

Figure 5-18: a) Detail of masonry wall and ties in Arquata del Tronto Alta; b) details of anchor and ring beam above.

The damage recorded in Arquata Bassa was relatively modest when compared to the upper and older part of the town. No collapse was recorded, but there were a few RC buildings with high structural damage, namely the local school. Representative of the level of damage in this part of the town is the 'Casa Forestale' building, where most of the damage is superficial and not structural, and is mainly located around the openings in the form of shear cracks (Figure 5-19). The macro seismic intensity level attributed by the EEFIT team is VII-VIII of the EMS' 98 scale (see Grünthal, 1998).

Figure 5-19: Casa Forestale in Arquata del Tronto Bassa

Figure 5-20 a) and b) Collapsed buildings in the main Piazza of Arquata del Tronto Alta

Figure 5-21 a) and b) Collapsed corner building and its ring beam

There was not much left to survey from the buildings shown in Figure 5-20a) and b), except from the clear presence of the heavy concrete roof which had a detrimental effect on the overall behaviour of the building. The building in Figure 5-21a shows all the subsequent forms of strengthening interventions which have weakened the overall structure leading to full collapse. The 600 mm ring beam shown in Figure 5-20b) which was sat on the fourth floor masonry wall to support the roof above, had a very detrimental effect on the stability of the wall under seismic excitation. The overall seismic performance is interpreted to have been worsened by the corner position of the building unit within the building stock as well as the steep slope upon which the building is constructed.

5.3.6   *Arquata Del Tronto Bassa and Alta after the October events*
Following the two seismic events of October 2016, Arquata Del Tronto Alta has been nearly completely destroyed as shown in Figure 5-22, while Arquata Del Tronto Bassa, was evacuated. It can be argued that in the case of Arquata del Tronto, no shoring or propping intervention was in place, as the Team had observed in other towns visited, such as Castelluccio, Accumoli or Norcia, and as a result the weakened buildings were more susceptible to further damage and collapse by the later events.

Figure 5-22 Arquata del Tronto Alta after the October 2016 seismic events
https://www.youtube.com/watch?v=q56R3j3BhlQ

5.3.7   *Pescara Del Tronto*

Pescara del Tronto was the hardest-hit site among the ones visited on the EEFIT mission. The small town belongs to the municipality of Arquata del Tronto and is located 36 km far from the main province of Ascoli Piceno, at 743 m asl. The village is located in the Tronto Valley, on the banks of the Tronto river.

The building stock of Pescara Del Tronto was mostly made up of low-rise masonry structures. The majority of buildings were 2-3 storeys, characterised by an unreinforced masonry structure. The quality of masonry was generally very poor, with highly inhomogeneous stone elements. Limestone block walls were usually characterized by the presence of brick elements or travertine stones. The quality of mortar, as well as the bond it provides, was also very poor, being made of sand and hydraulic lime (Masi et al., 2016). The high level of destruction observed was interpreted to be partially due to landslides and failure of the geological structure upon which the town was built, affecting the foundation of many of these buildings.

The level of maintenance of buildings was observed to be very poor. In addition, strengthening devices, such as tie rods, were absent, although their absence could not be completely verified as rods would be difficult to detect in the case of totally collapsed buildings. Regarding the horizontal structures, clearly visible through the collapsed facades, wood and steel were predominantly used, as well as shallow arch vaults mainly at ground floor.

Figure 5-23: Heavy concrete roofs in Pescara del Tronto, causing partial and total collapse

In addition to the extremely poor quality of load bearing structures and the lack of connection between orthogonal walls, the presence of heavy reinforced concrete roofs has represented the worst additional element leading most of the buildings of the village to partial or total collapse as shown in Figure 5-23.

In terms of structural damage, it is worth noting that, while the building located along the Salaria Road were heavily damaged but still standing (Figure 5-24), the ones located within the valley experienced complete collapse. The structural damage observed on the buildings that were still standing shows that the combined effect of in-plane action and out-of-plane actions was further exacerbated by the thrusting wooden roofs, in some cases, as shown in Figure 5-25.

Figure 5-24: Buildings along Via Salaria and buildings in the valley

Figure 5-25: Typical structural damage recorded in Pescara del Tronto along the Salaria Road.

According to the Marche Region, Pescara del Tronto, whose main municipality is Arquata del Tronto, is classified as seismic zone 2, since 2003. The Marche Region provides a reference PGA value for Arquata del Tronto 0.15 g < ag< 0.25 g, as maximum expected acceleration for the municipality with probability of exceedance <= of 10% in 50 years, based on uniform hazard spectra. (Regione Marche, 2018). According to the damage observed, taking into account that most buildings had collapsed, while some buildings had structural damage and partial collapse, the macro seismic intensity level attributed by the EEFIT team is X of the EMS' 98 scale (see Grünthal, 1998).

5.3.8 *Pescara Del Tronto Following the October 2016 Events*

What was left standing in Pescara del Tronto after the 24th of August event experienced further damage leading to collapse as a result of the late October events. The few buildings still standing on the Salaria Road partially or totally collapsed.

5.3.9 *Norcia*

Historically known as Nursia, the town of Norcia is one of the cities within the Province of Perugia, in the southern east of Umbria and has a population of 4.900. Unlike other historic towns in this region, it is located in a wide plain abutting the Monti Sibillini, a subrange of the Apennines. The town is popularly associated with the Valnerina Valley.

The historic town of Norcia is bounded by the ancient walls built around the XIII century characterized by eight access gates and several towers. The core of the town is the main Piazza, around which the Cathedral and St Benedict Basilica stand together with the Town Hall building, the civic tower adjacent to it and the Castellina fortress. The convent on one side, the portico and the bell tower on the other side, flank the St Benedict church, creating a structural complex.

Due to its historical importance, Norcia's urban fabric has been continuously improved and strengthened over time, especially after the Valnerina earthquake in 1703, the earthquake in 1730, the 1859 earthquake with epicentre in Norcia and the Valnerina earthquake in 1979. (see Figure 2-4)

According to the Delibera Giunta Regionale of 18/09/2012 n.1111 (Consiglio Regionale Umbria, 2012) of Perugia Province, Norcia has been classified as seismic zone 1. Figure 5-26 a) and b) show the seismic zonation before and after the Delibera in 2003 (Consiglio Regionale Umbria, 2012). Figure 5-27 shows in greater detail the seismic risk map of Umbria Region, expressed in terms of ground acceleration (a_g) with probability of exceedance of 10% in 50 years return period.
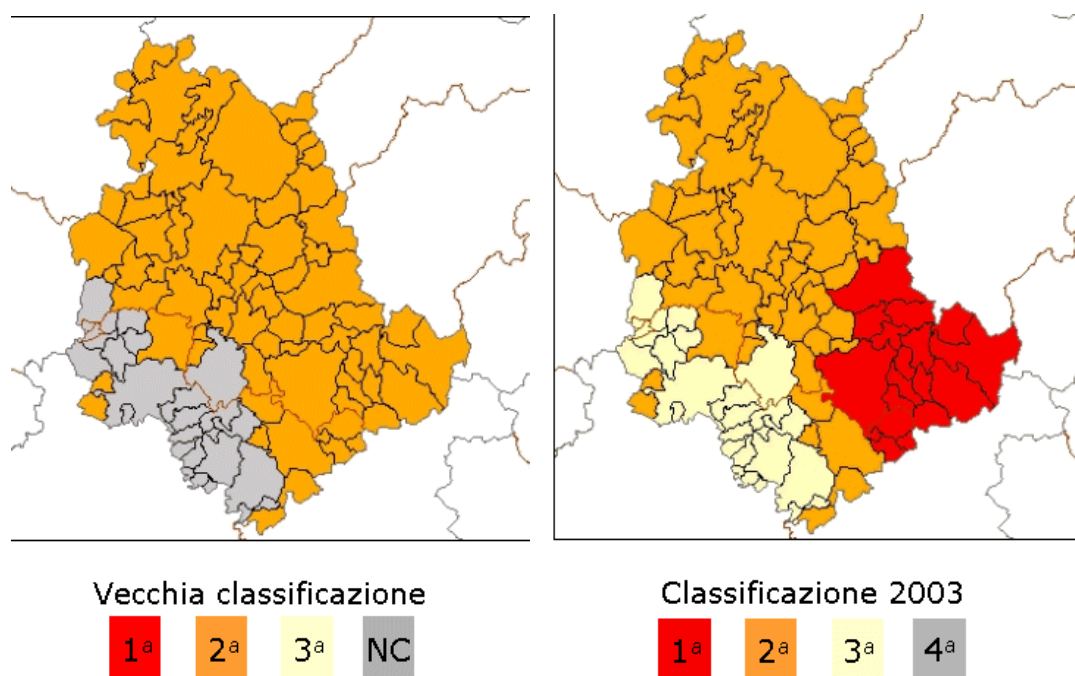
Figure 5-26 a) Seismic zonation before 2003, b) seismic zonation after 2003

The EEFIT team managed to have a short visit to the town. From Porta Romana, one of the 8 gates that access the inner town, the team walked towards the main Piazza, passing through Via Roma, to

visit both the Cathedral and the Basilica. Buildings were overall in very good conditions compared to other towns visited. The level of damage was comparatively modest. Figure 5-28 shows the typical level of damage observed in a building strengthened with metal ties and buttresses (located at ground floor).
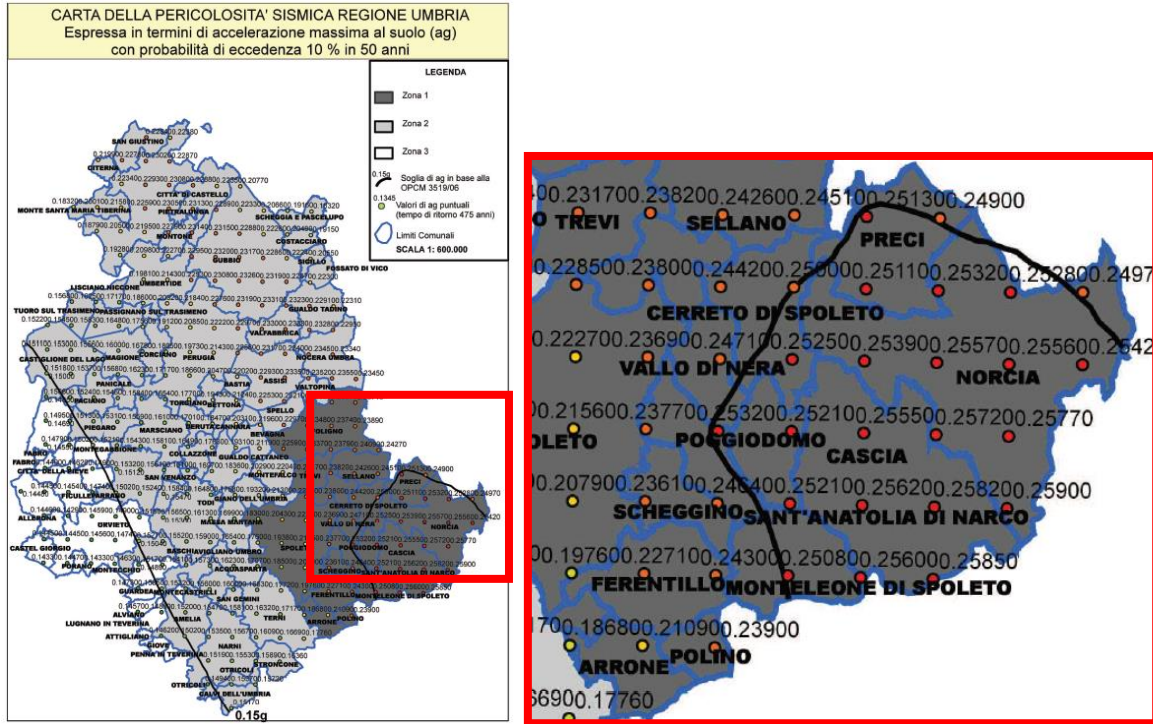
Figure 5-27 Detailed map of the seismic zonation of Umbria Region, from the Delibera Regionale n.1111 of 18/09/2012, available at http://www.provincia.perugia.it/guidetematiche/sicurezzaprevenzione/controllocostruzioni/classificazionesismica. The values are the expected acceleration for 475 return period or 10% in 50 year on a grid of 10x10km.

Figure 5-28 Residential building in Norcia, nearby Porta Romana. Note the buttresses, ties, and quoins, as prescribed in the 1859 decree. A diagonal airline crack is visible in the return wall.

Figure 5-29 Residential building in Norcia, nearby St Benedict Basilica. Ties and quoins are visible

The EEFIT mission team carried out a more detailed survey of a number of churches and this is reported in Chapter 6. According to the damage observed, taking into account that most buildings were undamaged, with only a minority of buildings showing light to moderate damage, and also taking into account that buildings were strengthened, seismic intensity level attributed by the EEFIT team is VII of the EMS' 98 scale (see Grünthal, 1998).

5.3.10   *Norcia after the October events*

The epicentre's proximity to the October 2016 sequence of seismic events caused severe damage to Norcia and its surrounding area. Further details related to the damage undergone by the Churches of St Benedetto and Santa Maria Argentea, as well as the ones in the vicinity of the town are given in Chapter 6. At the time the team was deployed on site, no activity of propping/shoring was in place. Even though the level of damage was not as widespread as other towns, no preventive action was taken in case of possible aftershocks.

5.3.11   *Castelluccio di Norcia*

Castelluccio di Norcia is a village located 28 km from Norcia, with a population of about 130 people. The village lies at 1452 m from sea level, making it the highest settlements in the Apennines, right above the 'Great Plane' (Piano Grande – 1270 m), next to the Monti Sibillini National Park.

The first documents referring to Castelluccio date back to 1276. Historically Castelluccio was reported to be damaged after both the 1703 Valnerina earthquake and the 1730 seismic event.

The village developed along the levels of a small mound as shown in Figure 5-30 resulting in narrow lanes which spiral up the hill with the civic tower at the centre. The buildings are predominantly oriented towards the south side of the hill, while the north side remains empty, due to the very harsh climatic and orographic conditions. The main part of the village develops around the 'Cassero' the highest and oldest part of the town, while, in the lower part there are some modern concrete frame housing. Most buildings in the upper part have been built around the XVI century.

According to the Ordinanza del Consiglio dei Ministri n.3274/2003 Castelluccio di Norcia has been declared seismic zone 2, namely a medium/high risk zone, where heavy shakings can happen. The map has been later updated though Ordinanza del PCM n 3519/2006, whereby a value of a_g is assigned on a 10 km grid, for a 10% probability of exceedance in 50 years. Typical values for zone 2 are 0.15 g < a_g < 0.25 g.

Figure 5-30 View of Castelluccio di Norcia village

While on site, the EEFIT team collected damage data of most of the houses located in the lower part of the village. Traditional masonry buildings have from 2 to 4 storeys made of traditional stonework with wooden roofs and timber horizontal structures as shown in Figure 5-31. However, many roof structures have been replaced with concrete slabs and ringbeams, where buildings have been refurbished for touristic purposes. The quality of stonework used and the level of inner connection between masonry leaves is relatively poor. Strenghtening or restraining elements (ties, buttresses, ring beams) that could help preventing out of plane mechanisms and enhance the box-behaviour were relatively sparse and many buildings were in a state of disrepair and neglect. The complete detachment between opposite facades is shown in Figure 5-32 a) and b)

Figure 5-31 Traditional stonework and horizontal structural elements in Castelluccio

The few RC buildings with infill frames located in the lower part of the town are 4 to 5 storeys. However, due to the steep ground slope which characterise the village orography, the common three-storey-level house would present a ground floor (used as basement) with entrance at lower street-level, a middle storey functional to connect to the upper floor (used as living space), with main entrance at upper street-level, as shown in Figure 5-33. The damage level recorded in RC buildings

surveyed was relatively low and manly ascribable to in plane actions and detachment between infills and main concrete frame, as shown in Figure 5-34.

Figure 5-32 a) and b) Failure Mechanisms: partial overturning of the façade and collapse of the corner

Figure 5-33 Typical residential building on steep slope. The building on the right is a concrete frame. The damage observed in this structure is shown in Figure 5-34

5.3.12   *Castelluccio di Norcia after the October events*

Castelluccio di Norcia was severely destroyed by the earthquakes in October 2016 with most buildings at the top of the hill and on the south side undergoing partial or total collapse.

Figure 5-34 Cracks surveyed in RC buildings in Castelluccio di Norcia

5.4 Systematic Damage Assessment at Territorial Scale

Three main investigation methods were used on site during the EEFIT mission to collect damage data in a more systematic fashion:

- Rapid visual survey forms (RVS)
- Omnidirectional camera (OD)
- The web based knowledge expert system for the damage investigation and failure mechanism identification, Log-IDEAH (Novelli, D'Ayala 2015).

The RVS form shown in Figure 5-35 has been specifically tailored to accommodate the survey of the building stocks in this region, made up of masonry and RC buildings. The form is made of approximately thirty entries, requiring no more than ten minutes to fill them in, and it is structured in three sections:

- Building location
- Structural information and data related to the main feature of the building investigated;
- Building tagging for safety of access; and
- Damage section, based on the five damage levels underpinning the twelve- degrees Intensity European Macroseismic Scale (EMS-98) (Grünthal, 1998).

Figure 5-35 Rapid Visual Survey Form Italy Mission 2016

Omnidirectional imagery captures were essential in the 'red zones', where time to be spent on- site was very limited. If collected in sequence, 360-degree images can be uploaded on web platforms (i.e. Mapillary ©) giving the user the chance to virtually 'walk through' the damaged streets. This can extensively improve the quality of data collected on site, since it makes extensive surveying more viable and faster. As documented in literature, omnidirectional cameras were first introduced as tools to collect data during reconnaissance missions in the 2011, Mw 7.2 Van earthquake in Turkey. Since then, imaging technology is being increasingly employed as data gathering or data enriching tool as it enhances mission capabilities and ensures the safer deployment of engineers to affected regions (Stone et al., 2018). Particularly successful use was made during the EEFIT mission in Ecuador (Franco et al., 2017).

The field damage assessment was then compared to the damage maps provided by the European Copernicus Emergency Management Service (Copernicus EMS), a service that provides timely geospatial information derived from remote satellite sensing and completed by in situ open data sources. The maps show the assessment of both buildings and transportation routes, which are assessed on a scale of four damage grades, from negligible to collapse.

In terms of on-site damage collection, the extent of improvement achieved by integrating Rapid Visual Survey Form data with ODC imagery, was considerable. The map shown in Figure 5-36 for the town of Amatrice, shows the data collection using the RVS Forms and ODC imagery.
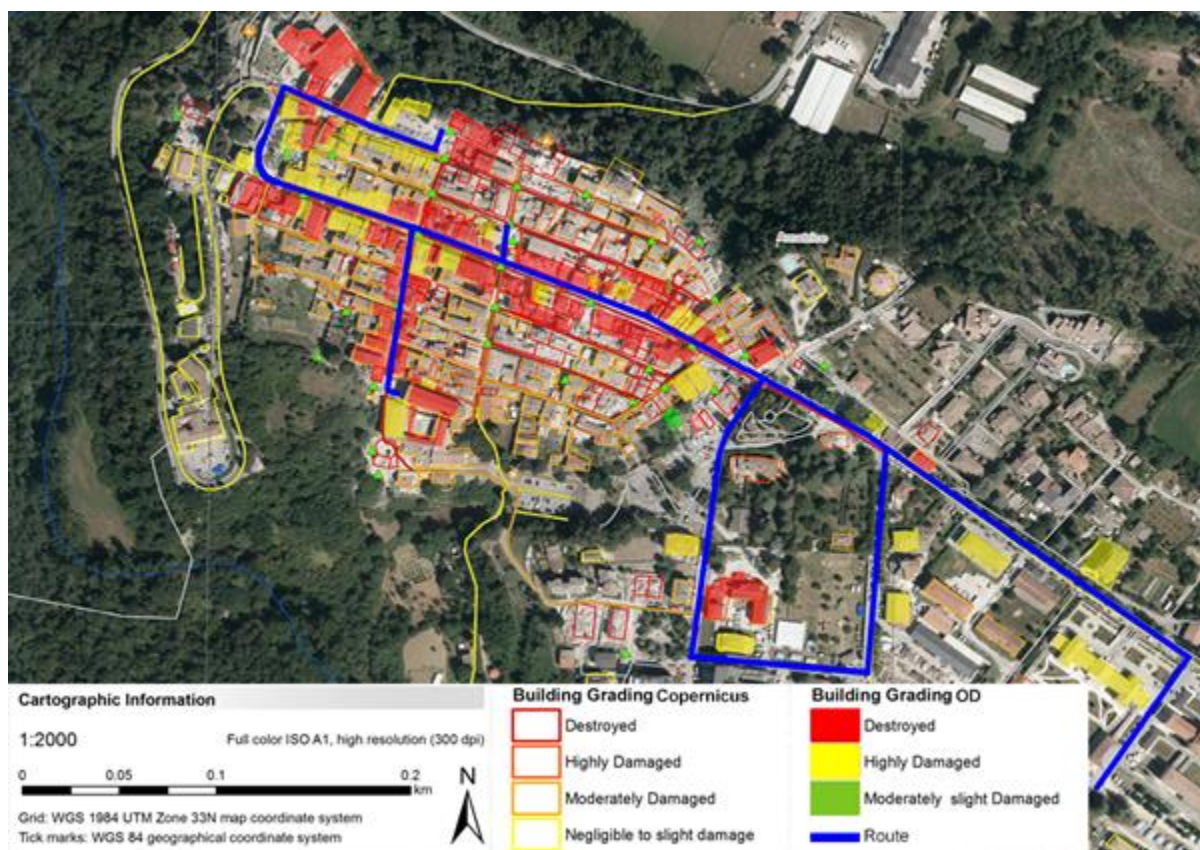
Figure 5-36 Amatrice: mapping of damage collected through RVS Forms and OD imagery categorised in three classes overlaid on the Copernicus map with mapping of damaged buildings after the 24ᵗʰ August 2016. The route followed by the team is shown in blue.

The third method used was the Log-IDEAH knowledge expert system for damage collection and failure mode investigation. Developed within the PERPETUATE Project by Novelli & D'Ayala (2015), the web-based tool uses logic trees for the interpretation of the seismic damage to historic masonry buildings. The method has been applied to the case studies of the historic centre of L'Aquila in Italy, the Casbah of Algiers in Algeria and the historic centre of Ljubljana, Slovenia. The app can be accessed on a tablet or mobile phone and works both on Apple or Android platforms connected either by Wi-Fi or data connection enabled phone line. The data collection requires situating the building using geo reference coordinates, then providing its position and connections with other adjacent buildings, the topology of the façades to be surveyed, the layout of cracks, their extent and corresponding severity in terms of damage levels. This data collection requires about 20 minutes per façade. The application then provides in seconds an output outlining possible mechanisms, their likelihood and their severity and extension. During the mission, given the limited time that was allowed to be spent within the 'red zones', and the poor telephone signal in these areas, the Log-IDEAH tool was used to collect data only for very few buildings in each town and therefore these results are not discussed further.

5.5   Results and Discussion of the Field Survey

A substantial spatial variation in building damage distribution and effects on the built environment was observed even within the same locality or between towns at few kilometres apart. The damage data collected on site with the RVS has been used to assign a EMS '98 grade to each locality on the basis of the distribution of damage states to both masonry and reinforced concrete structures as

summarised in Table 4-2. As shown in Figure 5-37a, Arquata Del Tronto Bassa has been assigned Grade VII, (defined as "Many buildings of vulnerability class A suffer damage DG3; a few of DG4. Many buildings of vulnerability class B suffer damage of DG2; a few of DG3"). Arquata del Tronto Alta has been graded between VIII and IX and Accumoli was graded VIII (defined as "Many buildings of vulnerability class A suffer damage of DG4; a few DG5. Many buildings of vulnerability class B suffer damage DG 3; a few DG 4"). Pescara Del Tronto and Amatrice have been graded IX –X, as not many building in class C suffered DG3 with few DG4 (according to grade IX definition) but many buildings in class B suffered DG5 (according to grade X definition). Castelluccio represents the case with the most heterogeneous range of damage, scoring from no damage to complete collapse; it was assigned intensity grade VIII.
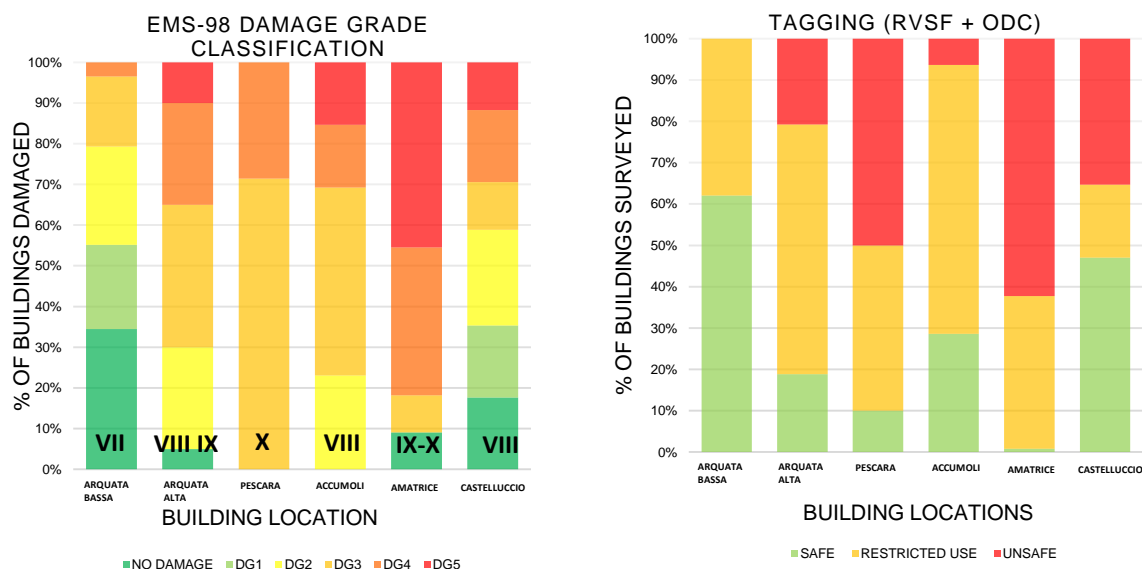
Figure 5-37: a) EMS-98 Damage grade classification; b) tagging classification after the 24/08/2016 event

The tagging classification results are obtained on the basis of the integration of the results of the RVS maps and the ODC photos and are shown in Figure 5-37b. According to this survey in Arquata Del Tronto Bassa, more than 60% of the buildings were considered safe to be used, even though on the date of the survey, all buildings had been evacuated and inhabitants relocated to tents. In the case of Arquata Del Tronto Alta, located 1.5 km uphill from the lower part of the town, 80% of the buildings were tagged as 'restricted use' or unsafe, with only 20% safe for use. In Pescara Del Tronto, our survey extended only to the roads that were walkable on the north east side of the settlement, the more recent extension of the village. Here 50% of the buildings were classified as unsafe and 40% as restricted use. However, of the older houses in the hollow below the main roads none was usable, and the large majority had collapsed. A similar situation could be observed in the historic city centre of Amatrice. Here only 1% of the building was considered safe, 36% restricted use and 63% unsafe. Finally, in Castelluccio around 45% of the buildings were rated as safe, 20% shored and with restricted use and 35 % unsafe.

The EMS 98 damage rating and the tagging classification showed substantial agreement. The data used for the tagging classification was also mapped for each of the towns visited, to integrate the RVS forms data and OD imagery. The mapped distribution are overlapped on the damage maps provided by the European Emergency Management Service Copernicus (Copernicus EMS, n.d.) based on satellite remote sensing and mapped on aerial images. The comparison between the on-site damage collection and the aerial views shows good agreement in the case of Amatrice (Figure 5-36)

and Pescara Del Tronto (Figure 5-38), where the extent of damage was such that the two layers corresponded almost completely.
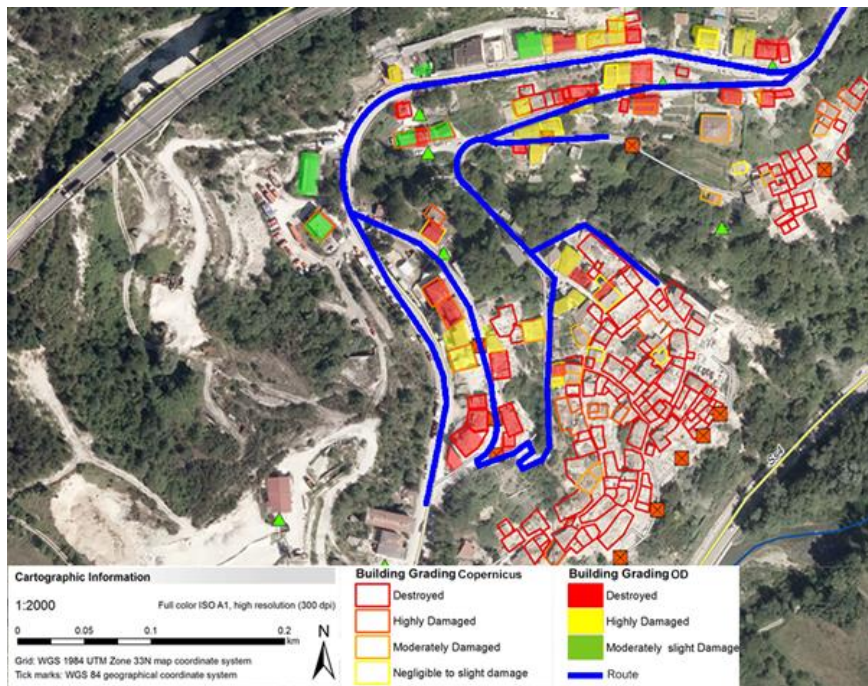
Figure 5-38 Pescara del Tronto map: Copernicus layer and EEFIT team survey results
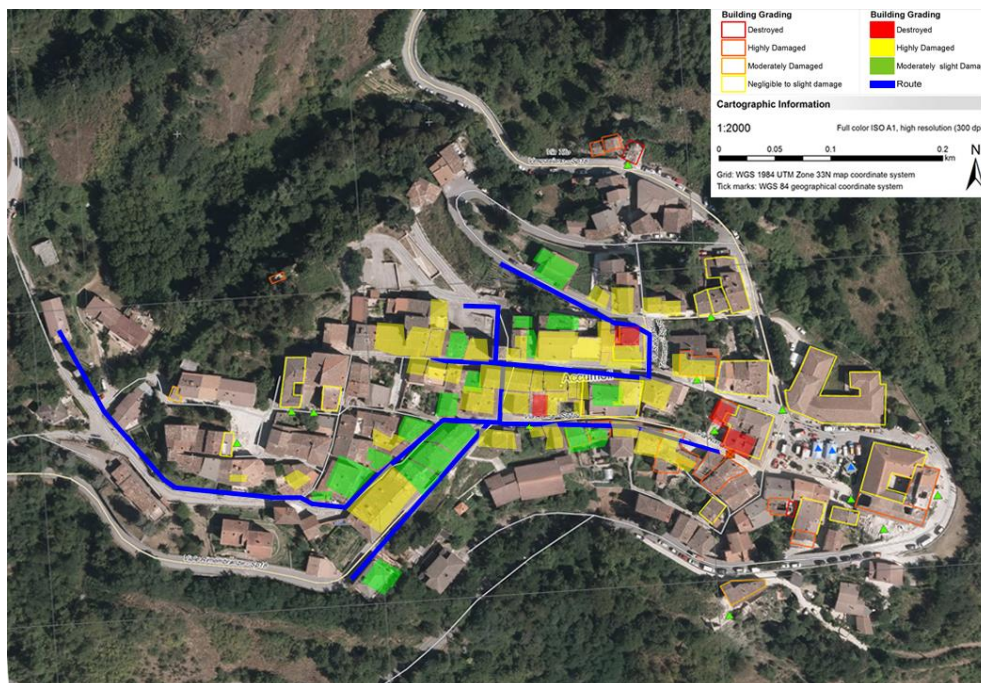
Figure 5-39 Accumoli map: Copernicus layer and EEFIT team survey results

In the case of Accumoli (Figure 5-39), where the level and extent of damage was more limited, the comparison between the Copernicus and EEFIT mapping shows evident mismatch, owing to the inability of the horizontal satellite picture to capture structural damage when there is no major failure

visible at roof level. The case of Arquata del Tronto is a representative example of the extent of this mismatch. The lower part of the town was not even mapped, thus indicating that the buildings were considered as not damaged (see Figure 5-40). The major differences between aerial and ground views were fully understood after the site deployment.
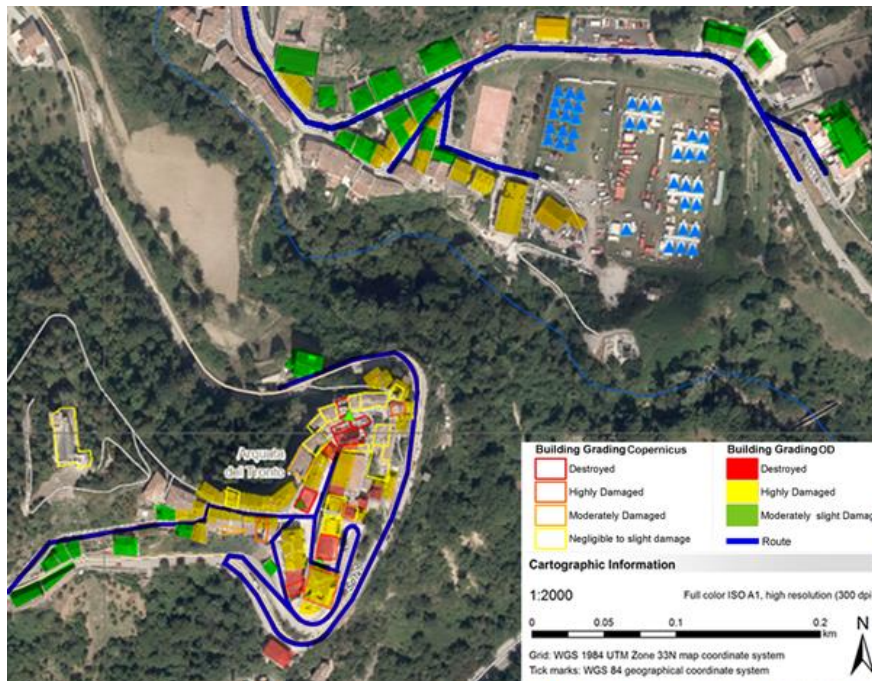
Figure 5-40 Arquata del Tronto map: Copernicus layer and EEFIT team survey results

The building marked in blue in Figure 5-41a was classified as no damaged by the Copernicus map. The field survey and the pictures taken via OD camera demonstrate the real condition of the building which, although was not damaged at roof level, was however extremely damaged in its walls (see Figure 5-41b). Other similar cases are discussed in Stone et al.(2018).

Figure 5-41 Arquata del Tronto (a) aerial view of the City Hall Building from Copernicus; (b) photographic record © Valentina Putrino

5.6   Conclusion

The scope of the investigation was to evaluate the extent of damage caused by the 24th of August 2016 event to the historic urban fabric of the towns hit by the earthquake shaking, including summary information relating to the effects of the late October 2016 events, which were not directly surveyed by the team. The mission conducted observation in the five more severely hit towns and villages in the epicentral area. Overall the quality of the masonry fabric is rather poor, largely made of rubble with mud and lime mortar. Extensive interventions on walls and floor structures have been observed, ranging from strengthened plaster, to grouting, from steel girder floors to concrete slabs and ring beams. Metal ties and anchors were also common, but their effectiveness was very variable, with many without proper anchoring plates, pulling out of the masonry. Norcia was the least affected of the towns visited during the mission, while Pescara del Tronto was the worst. The damage assessment to masonry buildings was carried out by means of RVS and interpretation from OD imagery, then compared to satellite imagery. The different nature and capabilities of capturing the damage to building components of the three methods used is discussed in light of the results obtained.

References

Bellicoso, A., (2011), Italian Anti-Seismic legislation and building restoration, International Journal for Housing Science and its Applications,

Akkar, S., Sandıkkaya, M. A., Şenyurt, M., Azari Sisi, A., Ay, B. Ö., Traversa, P., … Godey, S. (2014). Reference database for seismic ground-motion in Europe (RESORCE). *Bulletin of Earthquake Engineering*, *12*(1), 311–339.

Ancheta, T. D., Darragh, R. B., Stewart, J. P., Seyhan, E., Silva, W. J., Chiou, B. S.-J., … Donahue, J. L. (2014). NGA-West2 Database. *Earthquake Spectra*, *30*(3), 989–1005.

Assatourians, K., & Atkinson, G. (2013). EqHaz: An open-source probabilistic seismic-hazard code based on the Monte Carlo simulation approach. *Seismological Research Letters*, *84*(3), 516–524.

Barani, S., Spallarossa, D., & Bazzurro, P. (2009). Disaggregation of probabilistic ground-motion hazard in Italy. *Bulletin of the Seismological Society of America*, *99*(5), 2638–2661.

Barani, S., Spallarossa, D., & Bazzurro, P. (2010). Erratum to Disaggregation of Probabilistic Ground-Motion Hazard in Italy. *Bulletin of the Seismological Society of America*, *100*(6), 3335–3336.

Bindi, D., Massa, M., Luzi, L., Ameri, G., Pacor, F., Puglia, R., & Augliera, P. (2014). Pan-European ground-motion prediction equations for the average horizontal component of PGA, PGV, and 5%-damped PSA at spectral periods up to 3.0 s using the RESORCE dataset. *Bulletin of Earthquake Engineering*, *12*(1), 391–430.

Bindi, D., Pacor, F., Luzi, L., Puglia, R., Massa, M., Ameri, G., & Paolucci, R. (2011). Ground motion prediction equations derived from the Italian strong motion database. *Bulletin of Earthquake Engineering*, *9*(6), 1899–1920.

Bosi, A., Marazzi, F., Pinto, A., & Tsionis, G. (2011). *The L'Aquila (Italy) earthquake of 6 April 2009: report and analysis from a field mission*. https://doi.org/10.2788/188

CEN. Eurocode 8: Design of structures for earthquake resistance - Part 1 : General rules, seismic actions and rules for buildings, 1 European Committee for Standardization § (2004). https://doi.org/[Authority: The European Union per Regulation 305/2011, Directive 98/34/EC, Directive 2004/18/EC]

Chiaraluce, L., Di Stefano, R., Tinti, E., Scognamiglio, L., Michele, M., Casarotti, E., … Marzorati, S.

(2017). The 2016 Central Italy Seismic Sequence: A First Look at the Mainshocks, Aftershocks, and Source Models. *Seismological Research Letters*, *88*(3), 757–771.

Consiglio Regionale Umbria. Aggiornamento della classificazione simisca del territorio regionale dell'Umbria (2012).

Copernicus EMS. (n.d.). Retrieved May 20, 2018, from http://emergency.copernicus.eu/

CS. LL. PP. (2008). DM 14 Gennaio 2008: Norme tecniche per le costruzioni. *Gazzetta Ufficiale Della Repubblica Italiana*.

D'Ayala, D., & Speranza, E. (2003). Definition of Collapse Mechanisms and Seismic Vulnerability of Historic Masonry Buildings. *Earthquake Spectra*, *19*(3), 479–509. https://doi.org/10.1193/1.1599896

De Luca, F., Verderame, G. M., & Manfredi, G. (2015). Analytical versus observational fragilities: the case of Pettino (L'Aquila) damage data database. *Bulletin of Earthquake Engineering*, *13*(4), 1161–1181. https://doi.org/10.1007/s10518-014-9658-1

Del Gaudio, C., Ricci, P., & Verderame, G. M. (2017). First remarks about the expected damage scenario following the 24th August 2016 earthquake in Central Italy. In *Proceedings of the 16th World Conference on Earthquake Engineering*.

Di Capua, G., Lanzo, G., Pessina, V., Peppoloni, S., & Scasserra, G. (2011). The recording stations of the Italian strong motion network: geological information and site classification. *Bulletin of Earthquake Engineering*, *9*(6), 1779–1796.

DPCM. Norme Tecniche per il Progetto, la Valutazione e L'Adeguamento Sismico degli Edifici (2005). Italia.

Franco, G., Stone, H., Ahmed, B., Chian, S. C., Hughes, F., Jirouskova, N., … Lopez, J. (2017). The April 16 2016 M w 7 . 8 Muisne Earthquake in Ecuador – Preliminary Observations from the EEFIT Reconnaissance Mission of May 24 - June 7. In *16th World Conference on Earthquake Engineering, 16WCEE 2017* (pp. 1–12).

Grünthal, G. (1998). *European Macroseismic Scale 1998*. *European Center of Geodynamics and …* (Vol. 15). Retrieved from http://scholar.google.com/scholar?hl=en&btnG=Search&q=intitle:European+Macroseismic+Scale+1998#0

Guidoboni, E., Ferrari, G., & Tarabusi, G. (2010). Terremoti e monumenti : storie di restauri e perdite. In *Viaggio nelle aree del terremoto del 16 dicembre 1857* (pp. 69–102).

Iervolino, I. (2013). Probabilities and Fallacies: Why Hazard Maps Cannot Be Validated by Individual Earthquakes. *Earthquake Spectra*, *29*(3), 1125–1136.

Iervolino, I., Galasso, C., & Cosenza, E. (2010). REXEL: Computer aided record selection for code-based seismic structural analysis. *Bulletin of Earthquake Engineering*, *8*(2), 339–362.

Liel, A. B., & Lynch, K. P. (2012). Vulnerability of Reinforced-Concrete-Frame Buildings and Their Occupants in the 2009 L'Aquila, Italy, Earthquake. *Natural Hazards Review*, *13*(1), 11–23. https://doi.org/10.1061/(ASCE)NH.1527-6996.0000047

Luzi, L., Pacor, F., Puglia, R., Lanzano, G., Felicetta, C., D'Amico, M., … Chioccarelli, E. (2017). The Central Italy Seismic Sequence between August and December 2016: Analysis of Strong-Motion Observations. *Seismological Research Letters*, *88*(5), 1219–1231.

Luzi, L., Puglia, R., Russo, E., & ORFEUS, W. (2016). *Engineering Strong Motion Database*.

Masi, A., Chiauzzi, L., Santarsiero, G., Manfredi, V., Biondi, S., Spacone, E., … Verderame, G. M.

(2017). Seismic response of RC buildings during the M<inf>w</inf>6.0 August 24, 2016 Central Italy earthquake: the Amatrice case study. *Bulletin of Earthquake Engineering*. https://doi.org/10.1007/s10518-017-0277-5

Masi, A., Santarsiero, G., Chiauzzi, L., Gallipoli, M. R., Piscitelli, S., Vignola, L., ... Grimaz, S. (2016). Different damage observed in the villages of Pescara del Tronto and Vezzano after the M6.0 august 24, 2016 central Italy earthquake and site effects analysis. *Annals of Geophysics*, *59*(5), 1–12. https://doi.org/10.4401/AG-7271

Meletti, C., Galadini, F., Valensise, G., Stucchi, M., Tectonophysics, R. B.-, & 2008, U. (2008). A seismic source zone model for the seismic hazard assessment of the Italian territory. *Tectonophysics*, *450*(1–4), 85–108.

Meletti, C., Visini, F., & D'Amico, V. (2016). Seismic hazard in Central Italy and the 2016 Amatrice earthquake. *Annals of Geophysics*, *59*.

Ministero delle Infrastrutture e dei Trasporti. Aggiornamento delle "Norme Tecniche per le Costruzioni" - NTC 2018 - In Italian (2018).

Ministro dei Lavori Pubblici. Decreto Ministro dei Lavori Pubblici 24 Gennaio 1986 - In Italian (1986).

Novelli, V. I., & D'Ayala, D. (2014). LOG-IDEAH: LOGic trees for identification of damage due to earthquakes for architectural heritage. *Bulletin of Earthquake Engineering*, 153–176. https://doi.org/10.1007/s10518-014-9622-0

Paolucci, R., Pacor, F., Puglia, R., Ameri, G., Cauzzi, C., & Massa, M. (2011). Record Processing in ITACA, the New Italian Strong-Motion Database (pp. 99–113). Springer, Dordrecht.

Paz, M. (2012). *International handbook of earthquake engineering: codes, programs, and examples*. (S. S. & B. Media, Ed.).

Presidente del Consiglio dei Ministri. Modificazioni alle norme tecniche igieniche di edilizia obbligatoria per e localita' colpite dai terremoti - Regio Decreto n. 705 (1926).

Presidente del Consiglio dei Ministri. D.M. N.6: Ulteriori interventi urgenti a favore delle zone terremotate delle regioni Marche e Umbria e di altre zone dcopite da eventi calamitosi - In Italian (1998).

Regione Lazio. (2017). Retrieved from http://www.regione.lazio.it/prl_ambiente/?vw=contenutidettaglio&id=221

Regione Marche. (2018). Retrieved from http://www.regione.marche.it/Regione-Utile/Protezione-Civile/Emergenza/Rischio-sismico#205_Normativa

Romeo, R. ., & Pugliese, A. (1997). *"La pericolosità sismica in Italia. Parte 1: analisi della scuotibilità*.

Sabetta, F., & Pugliese, A. (1996). Estimation of Response Spectra and Simulation of Nonstationary Earthquake Ground Motions. *Bulletin of the Seismological Society of America*, *86*(2), 337–352.

SISTEMA STATISTICO NAZIONALE. ISTITUTO NAZIONALE DI STATISTICA (ISTAT). 15° Censimento generale della popolazione e delle abitazioni. Struttura demografica della popolazione. Dati definitivi. (2011). Retrieved from http://www.istat.it/it/files/2012/12/volume_popolazione-legale_XV_censimento_popolazione.pdf

Slejko, D., Peruzza, L., Rebez A. (1998). Seismic hazard maps of Italy, *Annal of Gephysics Vol 41, No 2, 1998*.

Spence, R. ., & D'Ayala, D. (1999). Damage assessment and analysis of the 1997 Umbria-Marche earthquakes. *Structural Engineering International*, *9*(3), 229–233.

Stone, H., Putrino, V., & D'Ayala, D. (2018). Earthquake damage data collection using omnidirectional imagery. *Frontiers of the Built Environment. vol.4. pp.51*. doi.org/10.3389/fbuil.2018.00051

Tinti, E., Scognamiglio, L., Michelini, A., & Cocco, M. (2016). Slip heterogeneity and directivity of the ML 6.0, 2016, Amatrice earthquake estimated with rapid finite-fault inversion. *Geophysical Research Letters*, *43*(20), 10,745-10,752. https://doi.org/10.1002/2016GL071263

Tosone, A., & Bellicoso, A. (2017). Anti-seismic presidia in the historical building of l'aquila: The role of the wooden elements. *International Journal of Heritage Architecture: Studies, Repairs and Maintence*, *2*(1), 48–59. https://doi.org/10.2495/HA-V2-N1-48-59

Vicente, R., D'Ayala, D., Ferreira, T.M., Varum, H., Costa, A., da Silva, J.A.R.M., Lagomarsino, S. (2013). Seismic Vulnerability and Risk Assessment of Historic Masonry Buildings. In: Structural Rehabilitation of Old Buildings. Springer-Verlag, Berlin, Heidelberg, Germany, pp. 307 – 348, DOI: 10.1007/978-3-642-39686-1_11.

Wald, D. J., Worden, B. C., Quitoriano, V., & Pankow, K. L. (2005). ShakeMap manual: technical manual, user's guide, and software guide. *Geological Survey (U.S.), Techniques and Methods*, *12-A1*, 132 pp.

Zimmaro, P., Scasserra, G., Stewart, J., & Kishida, T. (2018). Strong ground motion characteristics from 2016 Central Italy earthquake sequence. *Earthquake Spectra*.

6 PERFORMANCE OF RELIGIOUS AND HERITAGE BUILDINGS

6.1 Introduction

On October 9th, 2016 the team visited Norcia and surrounding villages inspecting a number of churches that had been affected by the 24th August earthquake. Reports were that the town of Norcia did not suffer the extensive damage (particularly total collapses) witnessed in Amatrice and other towns so the team took the opportunity to verify this in the field. Almost all the buildings visited were closed to the public in the aftermath of the earthquake. A team of local engineers and representatives of the University of Perugia arranged access[4]. The local team provided the EEFIT team with a great deal of information, on the history of the buildings and previous strengthening works, as well as insights on the assessment methodology applied for the post-earthquake churches assessment (Scheda per il Rilievo del Danno ai Beni Culturali – Chiese) produced by the Ministry for Culture and the Protezione Civile, (MiBAC, 2006). Their input is gratefully acknowledged and some of their observations are reported in the following sections describing each church building in detail. The Scheda per il Rilievo del Danno ai Beni Culturali – Chiese (MiBAC, 2006) was initially developed after the 1997 Umbria-Marche earthquake (Lagomarsino, Podesta', 2004) and extensively used during the L'Aquila 2009 earthquake (da Porto et al.,2012) and the 2012 Emilia earthquake. This form was used by engineers and architects in the post-earthquake reconnaissance visits to standardise the surveying and damage assessment activities as well as to aide making temporary shoring recommendations.

Table 6-1 Name and coordinates of visited churches and relative location to epicentre of event causing damage

Church Name	Building GIS coordinates	Date and Mw of mainshock	Epicentral Coordinates	Distance from epicentre	Station name (ESM database) and PGA values	Macroseismic Intensity USGS (MMI)
S. Andrea in Campi Alto	(42°51'12.2"N 13°06'04.5"E)	2016/08/24 Mw 6.0	(42°42'36.0"N 13°13'12.0"E)	18.7 km	NRC 0.378(g)	VIII
S. Salvatore in Campi	42°51'09.8"N 13°05'26.8"E)	2016/10/26 Mw 5.4	(42°52'48.0"N 13°07'48.0"E)	4.4 km	NRC 0.378(g)	VIII
Madonna Bianca in Forca d'Ancarano	42°50'13.7"N 13°06'16.3"E	2016/10/26 Mw 5.9	(42°54'36.0"N 13°07'48.0"E)	8.4 km	USGS shakemap 0.247 (g)	VII
Sant'Eutizio Abbey	42°52'13.8"N 13°03'51.2"E	2016/10/30 Mw 6.5	(42°49'48.0"N 13°06'36.0"E)	5.9 km	USGS shakemap 0.247 (g)	VII
S. Benedetto Cathedral in Norcia	42°47'32.5"N 13°05'35.4"E	2016/10/30 Mw 6.5	(42°49'48.0"N 13°06'36.0"E)	4.4 km	NOR 0.249 (g)	VIII
S. Maria Argentea in Norcia	42°47'30.9"N 13°05'33.4"E	2016/10/30 Mw 6.5	(42°49'48.0"N 13°06'36.0"E)	4.5 km	NOR 0.249 (g)	VIII

It should be noted that, at the time of writing the EEFIT report, the situation in the field had changed greatly from what was observed during the mission. This is due to the seismic events that took place

---

[4] Ing. Andrea Giannantoni, Ing. Giuseppe Paci, Ing. Romina Sisti and Ing. Giulio Castori.

on October 26th and 30th. Some information reported later in this chapter also covers the effects of these later events. These follow-on observations are based on images found in the general press as well as on a follow up field visit by a member of the team on the 22nd of December 2016. The additional information acquired is limited if compared with what was acquired during the EEFIT mission, but nevertheless is reported for completeness.

The church buildings visited by the EEFIT mission are listed in Table 6-1and located with green pins in the map of Figure 6-1, alongside the epicentres of the earthquakes with $M_w>5.0$ that took place in August and October 2016 (INGV, 2016) posted with red pins in Figure 6-1. Table 6-1 also lists the distance between the churches and the closest epicentre and date of the event causing the major damage.
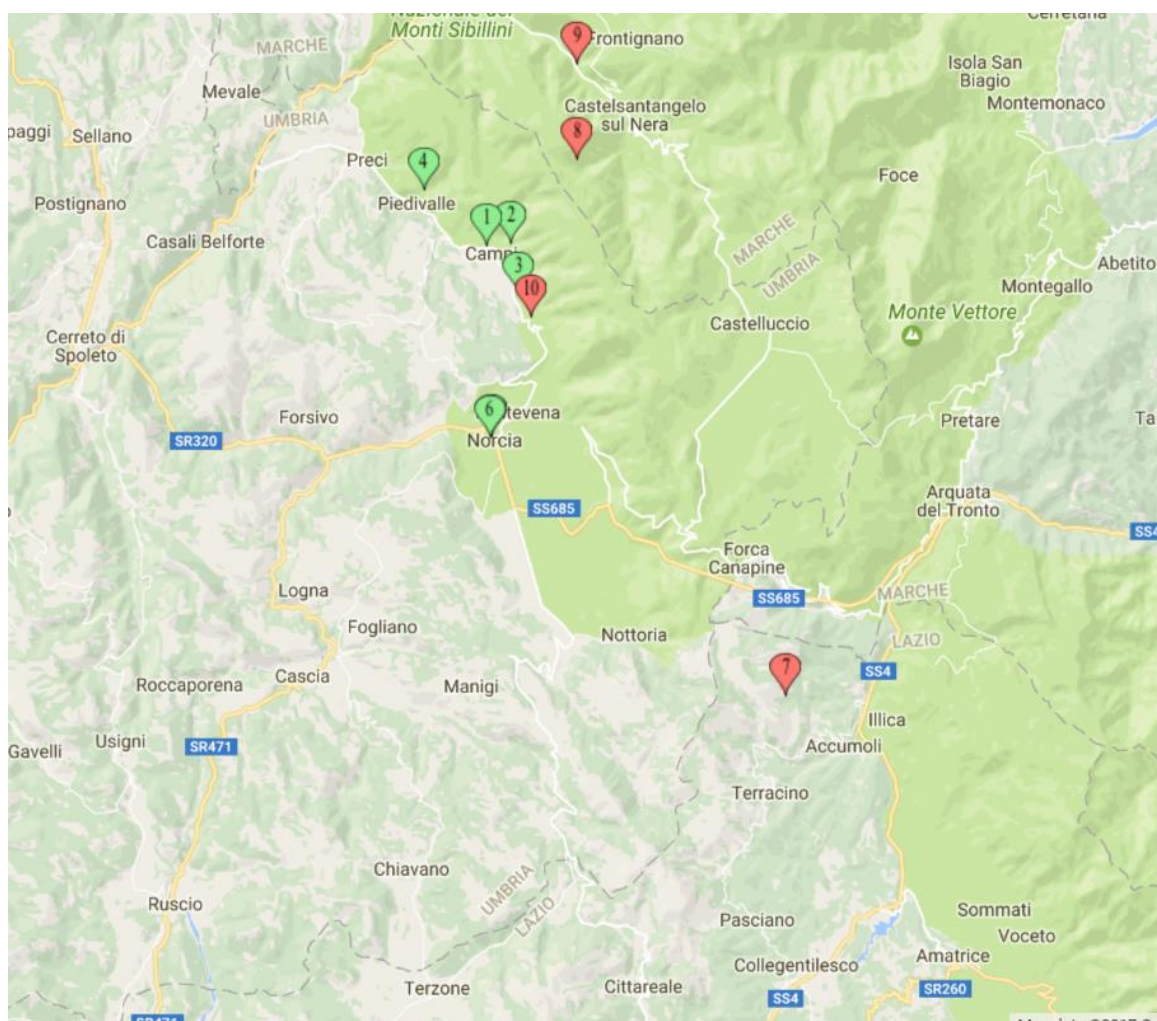
Figure 6-1 Map of the location of the churches and the epicentres of the strong motions of the period 24th August to 30th October 2016

6.2 Field Observations

6.2.1 *S. Andrea Church in Campi Alto, description and observed damage*

The Church of Sant'Andrea is located close to the XIV century entrance door to the upper part of Campi village, approximately 6km north on Norcia. It was built in the XIV century under the Sant'Eutizio Abbey dependencies. The church level is raised about 5.00m above the ground level along the hill slope, and it is fronted by a roofed porch added in the XVI century which is supported

by five arches on its longer side, built up askew of the church alignment on a retaining wall (Figure 6-2). The porch was severely damaged by the 1997 Umbria and Marche earthquakes and reconstructed with timber joists and steel ring beams in the years following the event.

The interior has a floor of stone slabs with tombs and it is divided into two naves and three spans of pillars supporting the cross vaulted ceiling (Figure 6-3). The left nave is part of the original building; the right is a Renaissance addition. The apse (now the sacristy), is separated from the left nave by a false wooden wall, built in 1596. The roof structure above the vault is of modern construction (likely following the 1979 earthquake) and made of precast concrete beams and reinforced concrete ring beams, supporting hollow clay plank elements (known as "pignatte" in Italy) with a thin concrete slab and clay tiles (Figure 6-3).

At the back of the church, there is a bell tower which is part of the overall building complex. The tower shows numerous ties likely to be made of iron. There are two portal entrances under the porch: on the left the entrance which was part of the original building and on the right a new one built during the Renaissance extension. The wooden doors are dated 1570.

Figure 6-2 Church of S. Andrea in Campi Alto. Front elevation and new porch roof structure.

Figure 6-3 Views of church interior and the modern roof structure.

At the time of the EEFIT visit, the church was closed to the public following the recommendation of the post-earthquake assessment. The external porch showed no sign of damage, not even slight, indicating a good seismic response against the 24th of August seismic loads. Internally, widespread cracking was observed in all structural elements including floor plates, columns and vaults.

The main potential collapse mechanism identified was the overturning of the front façade wall. This was highlighted by a vertical crack at the building corner indicating detachment of the facade, particularly above the porch roof.

Figure 6-4 Interior view highlighting widespread cracks and detachment of the front façade wall; b) Vertical crack between the façade and the edge spine wall.

The cracked building corner is shown in Figure 6-4b where the loose quoin elements can also be observed. Further indications of the façade overturning mechanism were: (1) large cracking at the cross-vaulting edge at the façade support (Figure 6-4a), and (2) shear damage at the springer of the central spine wall arch with associated pull out of the timber tie.

Following the 26th October shocks, the church suffered severe damage. Figure 6-5a shows that the façade overturning mechanism further developed as highlighted by the wall rotation and width of the crack, which appears much wider than what observed during the EEFIT mission. The porch structure appears to have restrained the façade (possibly preventing the total collapse), however, it suffered severe horizontal displacements in the order of over 100mm. The wrought iron ties likely prevented collapse of the porch structure, but induced shear failure of the columns, possibly triggered by the stiffness of the steel edge beam.

A second visit by EEFIT members in December 2016 collected some photographs at distance providing information on the damage that the church suffered after the 30th October earthquake (see Figure 6-5b). The façade wall and entrance porch had totally collapsed. The gate arch annexed to the porch also suffered total collapse. The bell tower appears still standing although it shows severe cracks. The concrete roof slab has collapsed in several locations. The internal ceiling vaults appears still standing although their level of damage is not known.

Figure 6-5 a) Damage to the front façade and entrance porch after the 26th October shocks (courtesy of Ing. Andrea Giannantoni); b) Collapse of the front façade and entrance porch after the 30th October earthquake.

6.2.2 S. Salvatore Church in Campi

The Church of San Salvatore in the village of Campi dates back to the end of 1400s. The church is a regular isolated gabled roof building, with two naves covered by cross vaulted ceilings. The church original building corresponds roughly to the north nave whereas the south nave was a later addition built in the XV century.

The façade has two rose windows and two portals with pointed arch entrances and a narrow porch supported by a central column and two side walls. The façade masonry shows evidence of the different construction phases as it can be observed in Figure 6-6a. The perimeter wall on the south side is buttressed. At the back of the church, on the south-east corner, there is a bell tower abutting the building. The church interior presents three internal pillars supporting the ceiling vaults. On the northern nave, a choir screen, arched structure, gives access to the extrados of the vaulted ceiling. This structure was propped with a system of timber shoring at the time of the visit (Figure 6-6b). The interior is decorated with frescoes in good state of conservation. Access above the vaults revealed how these had been strengthened (likely in the 1980s) with a concrete capping slab and the walls lined with reinforced concrete jacketing. The primary roof structure is composed by timber joists supporting a concrete slab above timber planks.

Figure 6-6 a) Front view of the S. Salvatore Church in Campi; b) The screen supported by a timber shoring system in the northern nave

The church was closed to the public at the time of the visit following the recommendation of the post-earthquake assessment. The assessment also recommended shoring works but these had not been carried out at the time of visiting. The propping on the *screen* arches dated to before the 24th of August 2016, highlighting that damage was likely present before the earthquake. The *screen* structure was still standing in early October 2016, although with sever cracking (Figure 6-7). The façade showed various cracks, the most notable being a diagonal crack through the north rose window (Figure 6-8a). Further cracks were observed at the interface between the ceiling vaults and the façade, highlighting possible detachment of the wall. These cracks were observed from both below and above the vault surface. One of the central pier pillar had a vertical split. The two parts were likely built at different times and presented no through thickness elements. The overall crack pattern highlights that a transversal mechanism of vibration was activated for this church.

Following the 26th October earthquakes, the church suffered severe collapses. Figure 6-9a shows that the façade wall, ceiling vaults, central piers and roof have all collapsed. The side and back walls, and bell tower were still standing although cracks are visible in these elements. The screen structure is not visible, but it is likely to have partially collapsed. A second visit by EEFIT members in December witnessed the additional inflicted by the 30th October earthquake (Figure 6-9b). The building had collapsed completely with only a portion of the southern and back walls still standing. The bell tower also completely collapsed. Building works were taking place to construct a canopy roof above the entire church footprint. This was possibly for the protection and recovery of the fresco decorations.

Figure 6-7 Sever damage of the screen structure, showing overturning of the balustrade and shear failure of the supporting wall.

Figure 6-8 a) Diagonal crack through the rose window; b) Pillar split through vertical crack, and shear failure of the top part corresponding to the same damage observed in figure 6.7for the screen wall.

Figure 6-9 a) Church collapse after the 26th October earthquakes (image from http://www.umbria24.it); b) Complete collapse after the 30th October earthquake

6.2.3 *Madonna Bianca Church in Forca d'Ancarano*

The Church of Madonna Bianca is located in Ancarano village, some 3km north-east of Norcia. Its initial construction dates back to 1361. The structure was completed in 1508 but was altered in several instances later. The building was severely damaged after the 1979 earthquake and partially reconstructed.

The church front façade and bell gable are built with white stone masonry. An arched portico, sheltering the main entrance to the west and the southern elevation, fronts the main façade (Figure 6-10). The bell gable shows numerous metal ties. The interior is divided into two naves and it has a timber roof supported by circular columns (Figure 6-11). The presbytery at the back is enclosed by arches and covered by two masonry vaults.

The portico roof was accessed and revealed a steel structure (likely from the 1980s works), with steel trusses supporting a lightweight metal deck roof (Figure 6-12). The presence of horizontal steel braces was also observed above the church entrance indicating possible seismic considerations in the structural design.

Figure 6-10 Madonna Bianca Church front elevation.

Figure 6-11 a)Church south elevation and b) interior view of the nave with tie rods n the arched spine wall .

Figure 6-12 Portico steel structure: a) horizontal bracing and b) roof trusses.

The church was closed to the public at the time of visiting following the recommendation of the post-earthquake assessment. The assessment also recommended shoring works to the portico but these had not been carried out at the time of the visit. The level of damage was not particularly significant if compared with the other church buildings inspected. The only damage of significance were some transversal cracks in the southern most arch and vault of the porch (Figure 6-13), indicating a local detachment of the porch from the main façade. Distributed small width cracks were also observed in the church side walls, without a clear pattern. The bell gable showed no sign of damage at the time of visit.
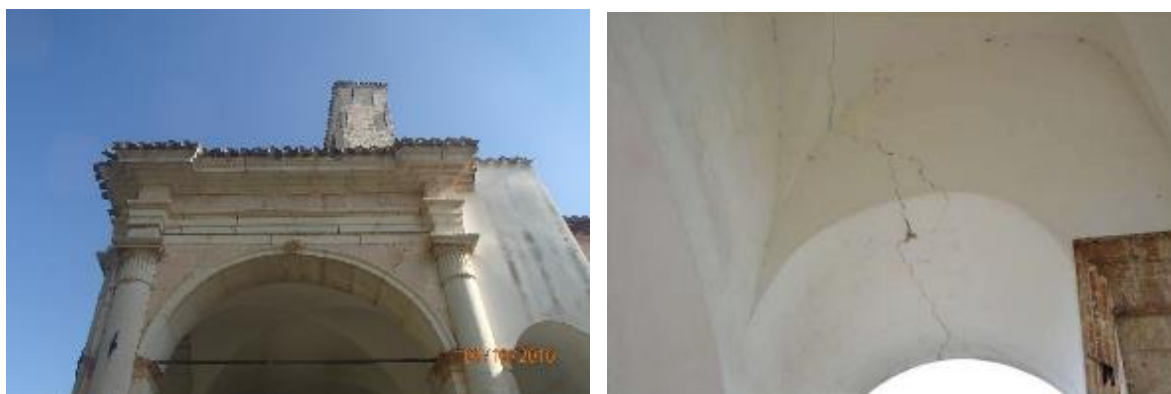
Figure 6-13 a) Loose stones and b) transversal cracks, in the porch southern arches.

Limited information is available on the damage suffered due to the 26th October earthquakes. Figure 6-14a shows some damage to the bell gable, specifically shear cracks to one of the piers. The follow up EEFIT visit in December 2016 found the fire brigade carrying out temporary shoring works for the bell gable. The southern pier had suffered further damaged and had been removed by the fire brigade. In fact, the large piece of gable missing was laying on the church front yard and did not appeared to have collapsed onto the roof (see Figure 6-14b).

The side walls of the presbytery have suffered partial collapse of the outer masonry leaf. This highlights possible three leaf masonry type. Such wall collapse is visible in Figure 6-15 along with a long horizontal crack on the northern wall elevation. This horizontal crack was likely caused by the thrust exerted by the roof timber rafters which was further magnified by the seismic accelerations.

The Madonna Bianca church is located approximately 1km distance from the 30th October M$_w$ 6.5 earthquake epicentre. The damage observed after this event is surprisingly moderate indicating that the 1980s repair works have been quite effective.

Figure 6-14 a)Front elevation after the 26th October shocks(image from http://www.umbria24.it); b) Front elevation in December 2016. Note damage to the bell piece laying on the front yard.

Figure 6-15 North elevation in December 2016.

6.2.4   *Sant'Eutizio Abbey*

The Abbey of Sant'Eutizio is located in Piedivalle, an isolated area 9 km north of Norcia overlooking the Castoriana Valley. The Abbey is one of Italy's oldest monasteries which was probably founded in the late V century A.D. by the Syrian monk Eutizio.The Church of the Abbey is set adjacent to a steep rock wall as seen in Figure 6-16. The façade wall to the west presents an arched portal entrance and a rose window. The interior consists of a single nave covered by a timber trussed double pitch roof (Figure 6-17a). The walls are made of regular stonework with a miscellaneous fabric suggesting that construction occurred over at least three different stages.

The eastern end of the nave is concluded with a polygonal apse with pointed arches built in the XIV century. Under the presbytery, there is a crypt divided into three naves with cross vaults bearing on two stone columns, which probably belonged to the ancient oratory. Adjacent to the church façade, above the rock cliff, is positioned the masonry bell tower (Figure 6-17b).

Figure 6-16 Sant'Eutizio Abbey. Note the church building at the centre of the site.

Figure 6-17 a) View of the nave interior; b) Relative position of bell tower and the façade on the right.

The church was closed to the public at the time of the visit following the recommendation of the post-earthquake assessment. The assessment also recommended shoring works to the façade and bell tower, but these works had not been carried out at the time of the visit.

The team observed widespread cracks on the church building with the following being the most notable damage. The chancel arch presented evidence of the formations of three pins (see detail of the cracks in in the photographs in Figure 6-18) with the likely trigger being the overturning of the southern side wall. This was highlighted by the pull out of the steel tie on the south side as well as by further detachment cracks in the chancel vault. The rotations of the pins, as suggested by the direction of openings of the cracks, is also compatible with a two-bar mechanism moving towards the southern wall (Figure 6-19).

Figure 6-18 View of chancel arch and cracks highlighting hinges formation. Note pull out of the steel tie.
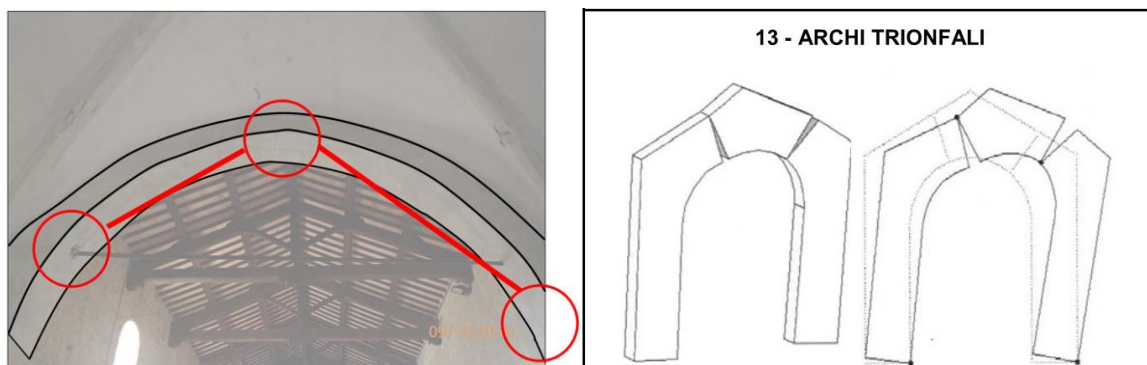
Figure 6-19 a) Schematic mechanism at the chancel arch. b) Mechanism as tabulated in [1].

Figure 6-20 a) Cracks on the façade wall by the rose window. b) Cracks on the bell tower.

Notable damage was observed on the façade wall both on the external and internal surfaces. Severe cracks originated under the roof timber purlins and propagated to the rose window (Figure 6-20a). Further cracks were observed in the annexed sacristy building. The bell tower also showed some cracks between the piers (Figure 6-20b).

The EEFIT members have not had the opportunity to carry out a follow up visit in December 2016 as the road leading to the Abbey was closed because of landslides. Some information on the damage suffered after the October earthquakes are reported, based on photographs published in the press. It is known that a portion of the top façade collapsed due to the 26th October shocks (Figure 6-21a). This collapse is compatible with the top façade mechanism observed during the EEFIT visit as described above. Greater damage due to the 30th October earthquake can be observed in Figure 6-21b and Figure 6-22. The cliff on the church north side partially detached and collapsed. The collapse involved part of the cemetery buildings above as well as the entire bell tower. It appears that debris have fallen onto the church demolishing part of the roof, façade and northern wall. The wall by the apse, which extended above the roof, has also partially collapsed.

Figure 6-21 Partial façade collapse a) after the 26th October; and b) after the 30th October earthquakes (images from http://www.umbria24.it).
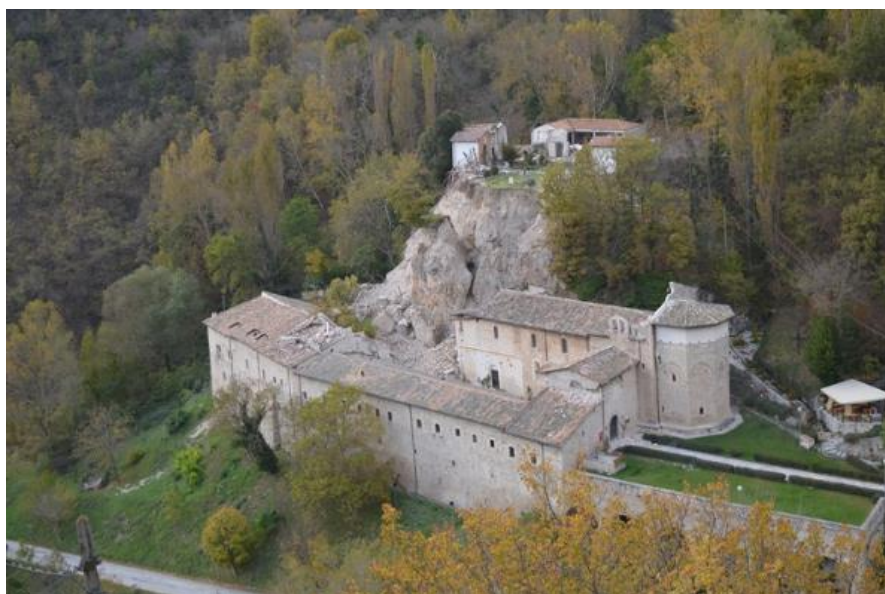
Figure 6-22 Abbey site after 30th October earthquake with bell tower collapse and cliff failure visible (image from http://www.umbria24.it).

6.2.5 *S. Benedetto Cathedral in Norcia*

The S. Benedetto Cathedral and annexed monastery houses the Order of Benedictine Monks of Nursia. The church is located, according to tradition, above the V Century ruins of the house of St Benedetto and his twin sister St Scolastica. The site has been the location of monastic communities since the X Century AD, (see Figure 6-23).

The church building dates back to the thirteen-century and it has been modified and reconstructed several times in history. It is located in Norcia's main square (Piazza S. Benedetto) adjacent to the town hall. The Basilica has a Latin cross plan, with a single nave. The gable roof is supported by timber trusses. The façade, the side portal and the lower bell tower date from the late XIV Century. In 1570, a portico (Portico delle Misure) was added on the south elevation to shelter a local market. The apse and the internal dome were reconstructed in the 18th Century. Only the XIV Century triumphal arch,

restored in the 1950s, remains from the original Gothic nave to date. The church was damaged by both the 1979 and 1997 earthquakes that struck Norcia. Strengthening works were implemented between 1999 and 2000, when it re-opened to the public as part of the Jubilee year celebrations. The scope and extent of such works is not known.

Figure 6-23 a) S. Benedetto Cathedral from the main square; b) Interior view of the church nave (courtesy of Ing. Andrea Giannantoni).

Figure 6-24 Cracks and initial pull-out of purlins a) on the front façade and b) above the chancel arch

The church was closed to the public at the time of the visit following the recommendation of the post-earthquake assessment. The assessment did not recommend any shoring works. There were scaffolding installed at the time of visit which the team understood were required by internal redecoration works (Figure 6-23b). The church structure presented widespread cracks and numerous debris on the floor. Numerous cracks were observed at the roof walls connections, particularly the purlins had partially pulled out from the front façade and above the chancel arch (Figure 6-24).

The side walls also showed numerous large cracks. The crack patterns appeared either sub vertical or in direction that followed discontinuities within the masonry fabric e.g. niches and side altars (Figure 6-25).

Figure 6-25 Large cracks on the side walls.

One of the piers supporting the chancel arch detached from the adjacent south transept wall as can be observed in Figure 6-26 highlighting sub-vertical cracks suggesting pounding among the two structures.

As a result of the 30th October earthquake, the church sustained very severe damage. Large portions of the building collapsed: roof, side walls, southern transept, portico and bell tower. The adjacent monastery buildings appear not to have collapsed.

Figure 6-26 Detachment of the chancel arch pier from the south transept wall.

The front façade is still standing with moderate damage, showing only a vertical crack that runs from the portal through the rose window and gable (Figure 6-27 and Figure 6-28).

Several press articles reported that the bell tower collapsed onto the Cathedral building during the earthquake causing widespread collapse of the main nave and transept. Although this is unverified, the substantial collapses to the building southern side by the bell tower are compatible with such assumption (Figure 6-27). The fire brigades installed a steel shoring structure to stabilise the now freestanding façade.

Figure 6-27 Collapse of the S. Benedetto Cathedral following the 30th October earthquake (image from http://www.umbria24.it).

Figure 6-28 Cathedral front façade still standing after 30th October earthquake (note the vertical crack), and with the shoring structure installed in December (images from http://www.umbria24.it).

6.2.6   *S. Maria Argentea Cathedral in Norcia*

The Cathedral of St Maria Argentea stands on the south-west corner of Norcia's main square. The current location of the church dates back to 1556-1570 when the adjacent fortress (Castellina) was also built. Throughout its history, the church building suffered several collapses because of earthquake events. The Gothic bell tower collapsed in the XVIII century. The church was then rebuilt in neo-classical style with one central nave and two side aisles. Only the baptistery remains of the

original Renaissance building. The exterior of the Cathedral is characterized by a gabled façade with masonry made of stone blocks. The façade has a neoclassical portal with a pediment and a circular rose window above (Figure 6-29). The east side elevation is characterised by a very thick (up to approx. 2m) buttressed wall with a Gothic arched portal. The interior of the Church is composed of one central nave, two side aisles and two domed chapels either side of the chancel (Figure 6-30a). The two side aisles have cross vaulted ceilings with metal ties whereas the main nave has a flat ceiling of assumed concrete construction. The team was told by a local engineer that the central nave ceiling structure includes in-plane steel cross-bracing.

The church was closed to the public at the time of visit following the recommendation of the post-earthquake assessment. The assessment did not recommend any shoring works. The roof structure is of recent construction (likely 1980s) and made of reinforced concrete trusses and concrete ring beams supporting a concrete slab above hollow clay planks (Figure 6-30).

Figure 6-29 St Maria Argentea Cathedral front view.

Figure 6-30 a) Interior view of the St Maria Argentea Cathedral from the front entrance (image from Google Street View). b) Building roof structure (courtesy of Ing. Andrea Giannantoni).

The widespread cracks observed in the building interior conformed to a repeating pattern in which: (1) the central pillars (either side of the nave) had horizontal cracks at their base on both sides; (2) the side walls had horizontal cracks facing the pillars; (3) the vaulted aisle ceilings had longitudinal (i.e. along the church length) crack at their crown. Examples of such cracks can be observed in Figure 6-31.

Figure 6-31 a) East aisle cracks at the pillar base (top left), b) at the vault crown (right) and c) at the side wall base (bottom left).

The cracks observed were compatible with a portal frame type mechanism for the overall building on the transverse (east-west) direction (Figure 6-32). The church geometry suggests a possible global three bay frame arrangement in which the two side frame bays were composed by the external walls and central pillars interconnected by the vaulted ceilings (and metal ties); and the central frame bay was composed by the pillars connected by the central nave ceiling slab. No cracks were observed at the central nave ceiling which is likely related to the more modern and less vulnerable to lateral movement, concrete construction.
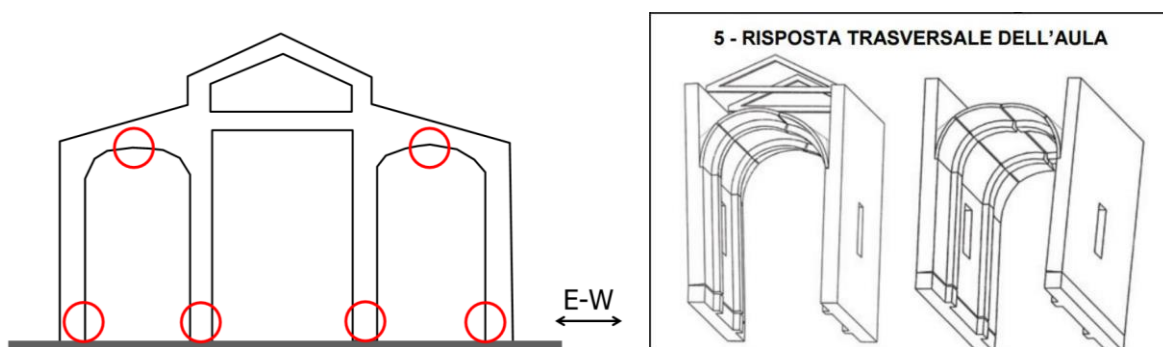
Figure 6-32 a) Schematic transverse mechanism. b) Mechanism as tabulated in MiBAC (2006)

Other significant damage was observed from the outside of the building. The front façade gable showed horizontal cracks just above where the roof connects (Figure 6-32a). This cracking was compatible with an overturning mechanism for the upper portion of the façade (Figure 6-32b).

Following the 30th October earthquake, the St Maria Argentea Cathedral suffered severe damage and partial collapse. Photographs published in the press show that the church roof has completely collapsed, most likely because of the high mass of the concrete construction (Figure 6-33*)*.
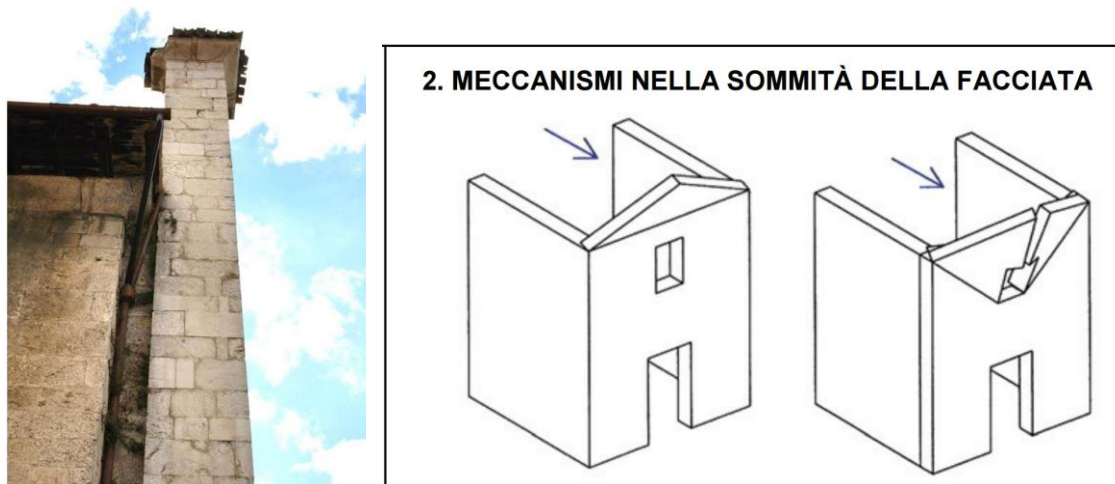
Figure 6-33 a) Horizontal cracks at the façade gable. b) Mechanism as tabulated in MiBAC (2006).

The façade gable has also collapsed on the square in front. The possibility of such mechanism was identified during the mission. The portion of the façade still-standing has lost part of the outer masonry leaf highlighting a layered stonework fabric (Figure 6-33*)*. The bell tower is still standing although it appears severely damaged by the bell chamber.

Figure 6-34 St Maria Argentea Cathedral front view after October the 30th earthquake (images from http://www.umbria24.it).

6.3 Conclusions

A number of churches that had been affected by the 24th August earthquake have been visited during the mission (Figure 6-35). All the church buildings suffered some damage and were closed to the public at the time of the visit. Some of the church damage observed matched the collapse mechanisms tabulated in the Protezione Civile's Scheda per il rilievo del danno ai beni culturali – Chiese. The report captures the key observations and photograph taken during the mission. The churches investigated suffered progressive damage, in some cases leading to partial or total collapse, as results of the October the 26th and the 30th seismic events (Figure 6-36). The report highlights the known cases in which such collapses resulted from the evolution of the mechanisms observed during the initial mission.
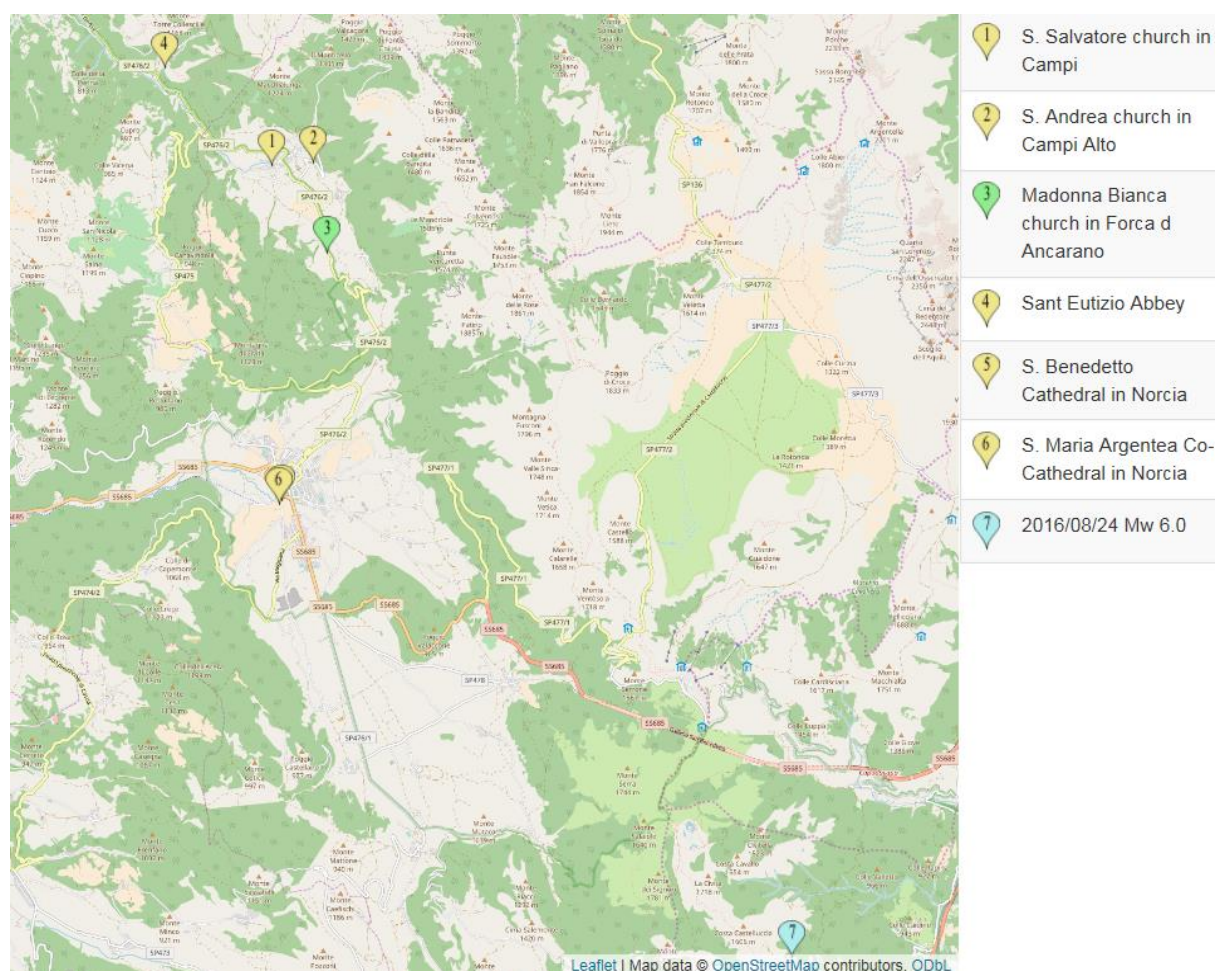
Figure 6-35 Map of the location of the churches and the 24th August epicentre. (Green, yellow and red pins indicate slight, moderate and severe damage/collapse, respectively).
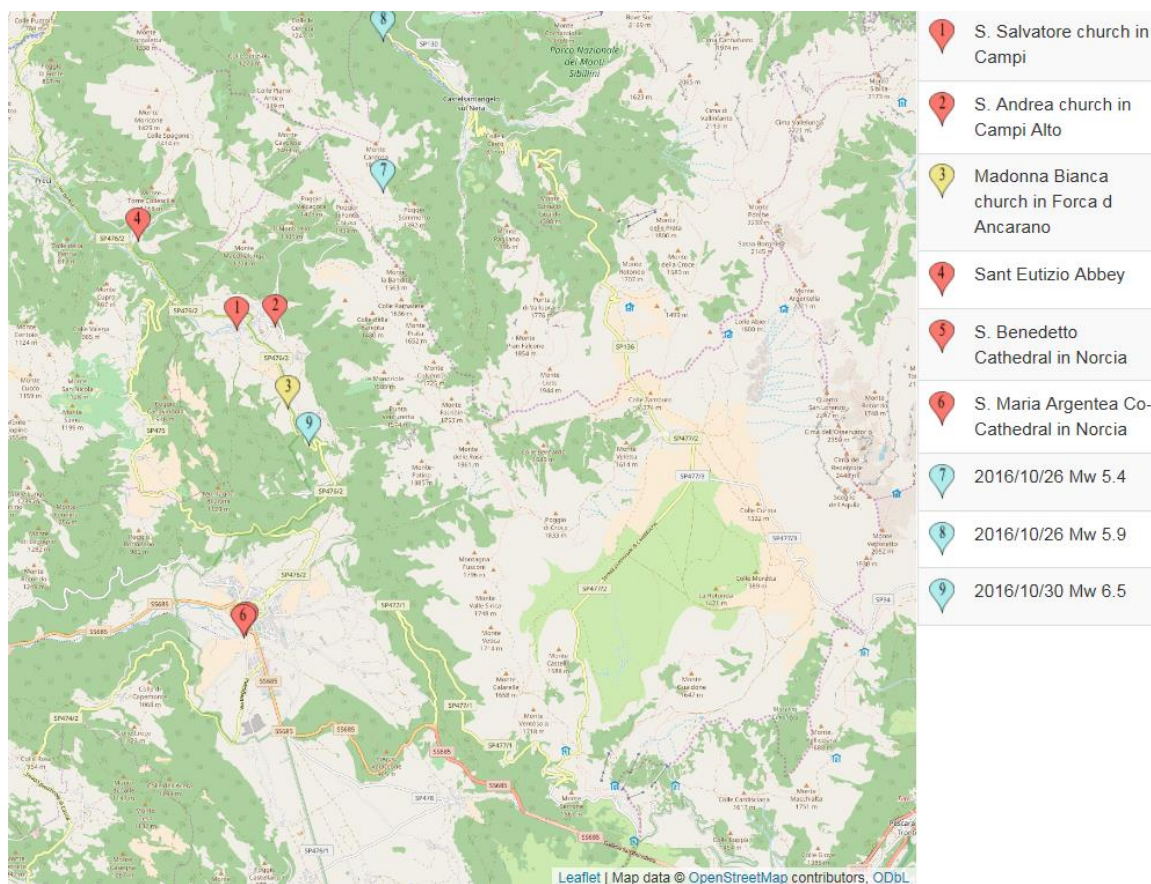
Figure 6-36 Map of the location of the churches and the 26th and the 30th August epicentres. (Green, yellow and red pins indicate slight, moderate and severe damage/collapse, respectively).

References

da Porto F., Silva B., Costa C., Modena C., (2012) Macro-Scale Analysis of Damage to Churches after Earthquake in Abruzzo (Italy) on April 6, 2009, Journal of Earthquake Engineering, 16:6, 739-758, DOI: 10.1080/13632469.2012.685207

Istituto Nazionale di Geofisica e Vulcanologia INGV, (2016) http://cnt.rm.ingv.it/

Lagomarsino S. and Podesta` S., (2004), Seismic Vulnerability of Ancient Churches: I. Damage Assessment and Emergency Planning. Earthquake Spectra: May 2004, Vol. 20, No. 2, pp. 377-394.

MiBAC (2006), Modello A-DC PCM-DPC. Scheda per il rilievo del danno ai beni culturali. Chiese. Available at http://www.beniculturali.it/mibac/multimedia/MiBAC/documents/1338454237471_allegato4.pdf (in Italian)

7 PERFORMANCE OF REINFORCED CONCRETE STRUCTURES AND SCHOOLS

7.1 Seismic Regulations for Reinforced Concrete Structures and Schools

In Chapter 5 the level of seismic hazard of each town and the corresponding expected PGA were introduced. These apply to reinforced concrete (RC) structures as well. To gain an understanding of the standard to which the observed RC structures might have been designed, it is worth considering that 50% of the buildings in the municipalities of Amatrice, Accumoli, and Arquata del Tronto were constructed before 1945 and another 30%, approximately, before 1980. There are, therefore, a very limited number of structures built in the more recent decades (Del Gaudio, Ricci, & Verderame, 2017). This means that the majority of RC structures were designed according to the 1975 code. According to the zonation of the time the maximum base shear coefficient for which these buildings would have been designed would be $(F_h /W) = 0.07g$.

Although design was based on assumption of elastic behaviour, the base shear coefficient would take into account a strength reduction factor evaluated upon dissipative capacity of the structure. After the L'Aquila earthquake, with the DM14/01/2008 the NTC08 was approved, introducing capacity based design, explicitly considering q factors and ductility for the detailing of the structural elements assumed to resist the seismic action.

The limited amount of RC buildings means statistical analysis of the data collected by this mission is difficult. Since L'Aquila is very close to the epicentral area of this earthquake, some comparison with data and conclusions from the 2009 earthquake can be attempted to check to which extent the 2016 event validates some of the empirical and analytical tools developed using the 2009 L'Aquila earthquake data (Liel & Lynch, 2012; De Luca et al., 2015).

The performance of RC buildings in these towns is of importance, as often they host infrastructure of critical relevance to the community, such as schools and hospitals, although masonry structures are also used for these functions. It is important to emphasize, however, that the real problem is not the construction material of these buildings, but that most of them were built with obsolete design provisions and they do not comply with the current seismic classification of the area.

7.2 RC Residential Structures

The team collected rapid survey damage data on 42 RC buildings. The majority were in Amatrice and Arquata del Tronto with just three in the municipalities of Accumoli and Norcia.

Data on these buildings emphasized that most of the structures were classified as non-ductile RC buildings with masonry infill (C3 according to the PAIGER classification in the rapid survey form used). The number of storeys reflected the ISTAT data, even if a limited number of buildings with more than three storeys was included.

The general performance of RC buildings was reasonably satisfactory. Heavy damage to the non-structural infill was frequently observed but structural damage to the RC structure was rarer. The typology of this observed structural damage was shear failure in columns, emphasizing the lack of capacity design between beams and columns typical of C3 building and confirming a trend already observed in L'Aquila (Ricci et al., 2011) and, to a lesser extent, in the Emilia 2012 earthquake (Manfredi et al. 2014). It has been proved that obsolete seismic design practices (from 1970s up to 1990s in Italy) can be more critical for the occurrence of shear failures with respect to gravity load design. Seismic obsolete design criteria used to result in RC sections with higher longitudinal reinforcement with respect to gravity-only design. At the same time, no significant increase in the transversal reinforcement was put in place. This condition led to a more likely shear failure in the element given

the higher flexural strength capacity of the section making easier the onset of a preemptive brittle shear failure in the element, see also De Luca and Verderame (2013).

In Figure 7-1, a map of the surveyed buildings and their EMS-98 (Grunthal, 1998) damage classification is shown.

(a)   (b)
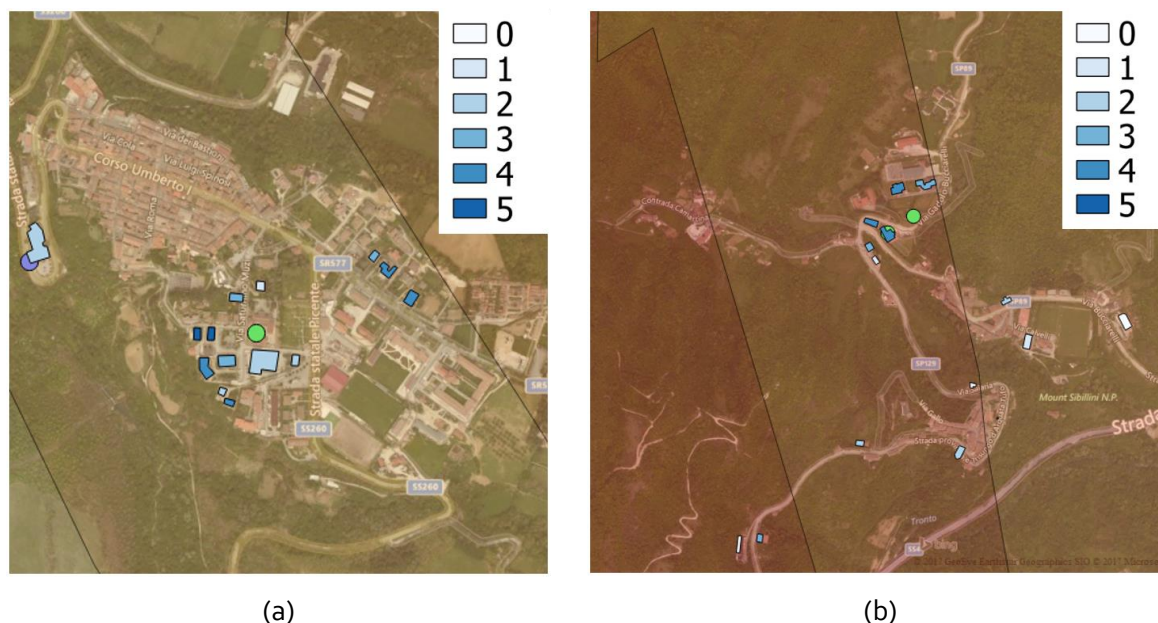
Figure 7-1 Damage map of the RC buildings surveyed during the mission in the municipalities of (a) Amatrice and (b) Arquata del Tronto. Grades are DG0 to DG5 according to EMS '98 classification

There was evidence of improvements implemented in the area probably, as a result of the 1997 Umbria earthquake. Examples included chicken wire or other types of fibre reinforcement in the external plaster, a relatively cheap intervention. More significant, structural improvements had also been made to some schools as shown in the next subsection. In Figure 7-2 an example of damage to an RC structure in Amatrice is illustrated. This 5-storey building was probably constructed in the late 1970s or early 1980s. It showed some of the poorest performance of RC buildings with highly evident non-structural failures; partial collapse of the masonry infill panels, and shear failure of some columns. This building was classified in damage state DG4 according to the rapid survey form filled during the mission (se Appendix 10.1). Another building, Figure 7-3, very close to that in Figure 7-2, performed better. It had more storeys (six) but it was probably built later, say the late 1980s but certainly more recently than the example illustrated in Figure 7-2.   The onset of damage and the medium cracks observed in the infill panels (see Figure 7-3) meant this building was classified as DG2. In this case, it is worth noting the presence of reinforcement in the plaster, Figure 7-3b.

(a)   (b)   (c)

Figure 7-2 Amatrice, latitude 42;37;33.25 – longitude 13;17;27.58, 5-storey RC building, DG4

(a)   (b)   (c)

Figure 7-3 Amatrice, latitude 42;37;33.74 – longitude 13;17;27.46, 6-storey RC building, DG2.

(a)   (b)   (c)

Figure 7-4 (a) New building in Amatrice (lat. 42;37;39.597; long 13;17; 39.911), three storeys DS0; (b) and (c) three storey RC building DS4 (lat. 42;37;39.083; long 13; 17; 39.171).

A final example was of a very recently constructed building Figure 7-4. At the time of the survey it was still unoccupied and is assumed to be designed according to the most recent code. There was no observed damage and the relative dimensions of columns with respect to the beams emphasize the capacity design principle used for its design. An interesting comparison can be made to an older RC building on the same street where the infill masonry panels were damaged (Figure 7-4b) and shear failures documented (Figure 7-4c).

7.3 Performance of Schools Buildings

The structural integrity of schools is, understandably, a high priority for pupils, staff and communities. Indeed access to an education is noted as a human right (Smyth et al., 2004) and school buildings provide, amongst other functions, potential emergency shelters (UNESCO, 2017).

During the 2002 Molise earthquake, 27 school children died under the Francesco Jovine elementary school (Augenti et al., 2004). In its aftermath a more consistent investement was made in Italy on school safety. This event was also the trigger for the new seismic classification in Italy and for the enforcement of the capacitybased design for all new structures (OPCM 3274, 2003).

Many research studies at national and European level have been made since the Molise event to deliver a conprehensive seismic assessment of school buildings for the whole country, showing that

the number of schools with a significant PGA capacity deficit was substantial (e.g., Grant et al., 2007), see Figure 7-5. In the subsequent years, funds have been given to different municipalities aimed at the retrofitting of schools (DPC, 2017). The damage observed during the mission indicates that the work done to date is definitely not sufficient and lot more needs to be done to robustly enhance school safety.

Information on schools in Italy is compiled into a national database owned by the Italian Ministry of Education (http://cercalatuascuola.istruzione.it/cercalatuascuola/). Figure 7-5b shows the example of the section related to construction characteristics of buildings publicly available for schools in Italy.

The EEFIT team visited schools in the municipalities of Norcia, Acccumoli, Amatrice and Arquata del Tronto. Figure 7-6a and Figure 7-6b shows the shake map data downloaded form the USGS website for the event from PGA and macroseismic intensity, respectively. Different intensity was observed during the 26 August event. It is clear that the different municipalities were subjected to different intensity, with the highest peak of PGA in the area of Arquata del Tronto and a limited localized peak in the village of Amatrice, where the shake map include a limited area at very high PGA.

(a)   (b)
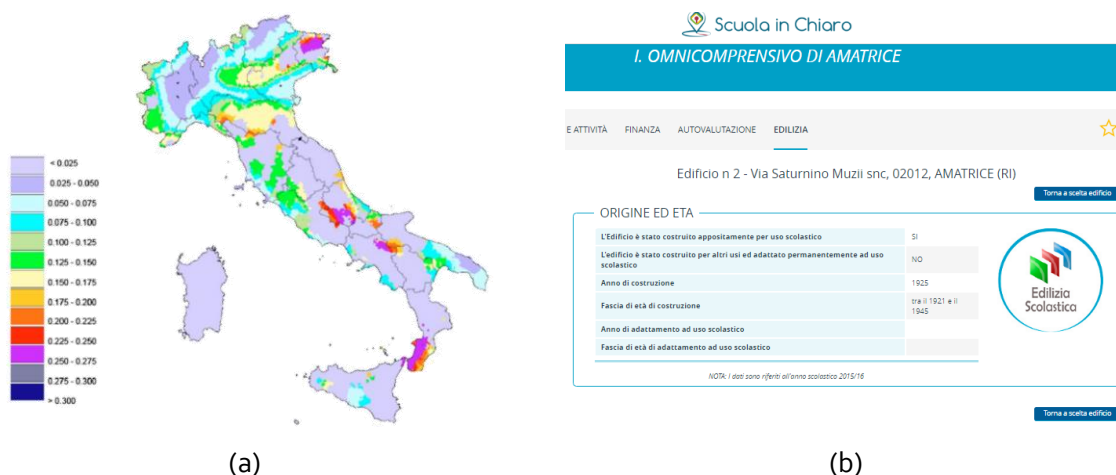
Figure 7-5 a) PGA deficit for school designed between 1984-2003 (from Grant et al., 2007). (b) Example of the database entries related to the page "Edilizia" of the database scuolainchiaro owned by the Italian Ministry of Education and publicly available at

(a)   (b)
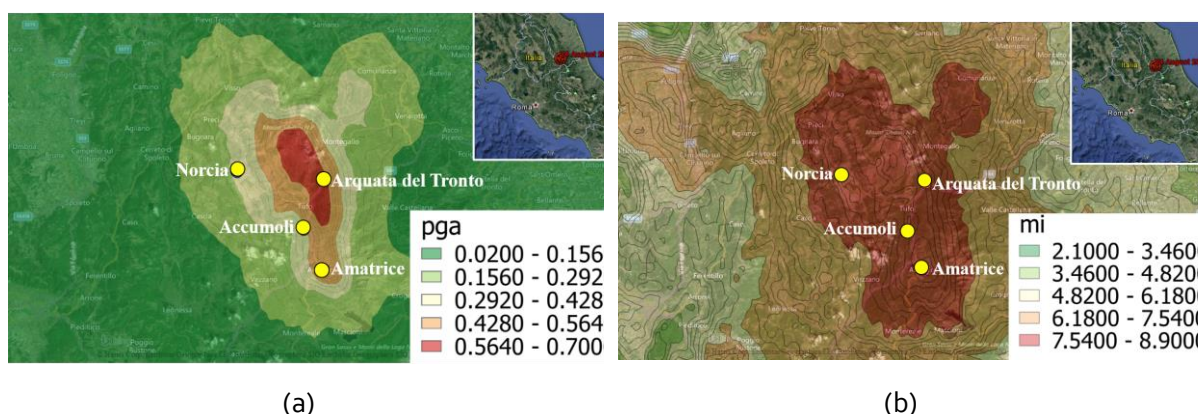
Figure 7-6 USGS shake map for (a) PGA and (b) macroseismic intensity of the epicentral area (USGS, 2017)

The team visited three schools in Norcia, one school in Accumuli, one school in Amatrice and two schools in Arquata del Tronto. The aim of each site visit was to observe the seismic performance of these buildings and, in particular, to observe the performance of any retrofitting schemes. In each case, it was only possible to view the school buildings from the outside and this limited the observations. The construction of the schools varied and included masonry and RC. Two of them were

masonry buidings, the other RC structures. Earthquake damage ranged from minor local (DG1) to very heavy (DG4) damage.

7.3.1 *Norcia, Istituto Tecnico Commerciale*

The Istituto Tecnico Commerciale consists of a single, three-storey block with a pitched roof and basement. On plan (Figure 7-7), the building is regular albeit with a minor step in the vicinity of the main entrance. The ground appears to have been excavated to construct the school with the basement generally subterranean on the north side but at the ground level to the south.

The construction is RC with brick masonry infill (Figure 7-8). The roof and floors are assumed to be reinforced concrete slabs. The building has been retrofitted with steel bracing.

The school was not significantly damaged during the 24th August earthquake and was operational at the time of the EEFIT mission (i.e., mid-October). Some very minor cracks were observed in the west gable elevation (Figure 7-9a). There was also some indication of damage to the columns, probably from previous events (e.g., Central Italy 1997) and subsequently repaired (Figure 7-9b). Based on the information available, it is not possible to determine whether the damage observed resulted from this seismic event, but repairs appear to have been undertaken possibly before the August earthquake (Figure 7-9 and Figure 7-11).

Figure 7-7 Aerial view of the Istituto Tecnico commerciale (lat. 42.791702, long. 13.095641), form Bing map, Norcia.

Figure 7-8 Istituto Tecnico commerciale (lat. 42.791702, long. 13.095641), form Google Street map.

The school had been retrofitted (probably after the 1997 Umbria earthquake) with tubular steel bracing. This was seen in a number of bays along the length of the building (Figure 7-10) and at least the basement and first storey levels (Figure 7-11). It was not possible to see if any bracing intervention

was made at the top floor, but presumably, for regularity reasons, the bracing system was placed at all storeys.

A further modification appears to have been made to the roof. The aerial photograph from Bing (Figure 7-7) indicates uniform material, presumably heavy tiles. The team observed a non-uniform, apparently lightweight material (Figure 7-12). This is assumed to be a waterproofing membrane, which replicates the appearance of tiles but removes objects with the potential to fall.

(a)   (b)
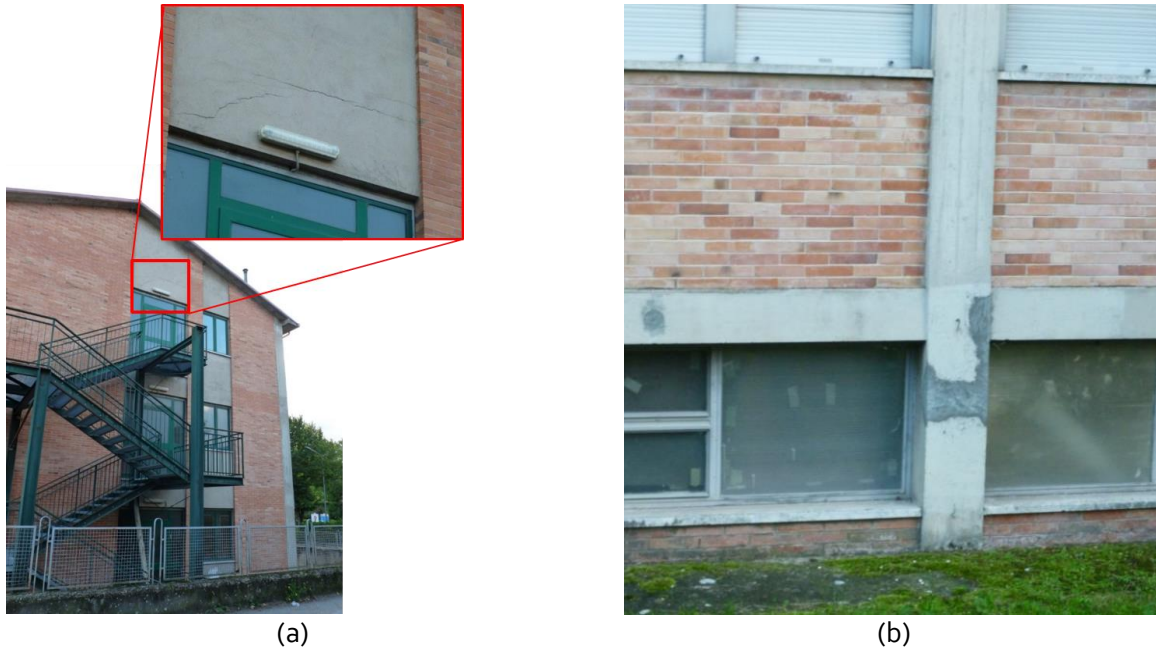
Figure 7-9 Istituto Tecnico commerciale (lat. 42.791702, long. 13.095641), (a) minor cracking in the gable end; (b) possible repaired damage to the column. (DG1)

(a)   (b)
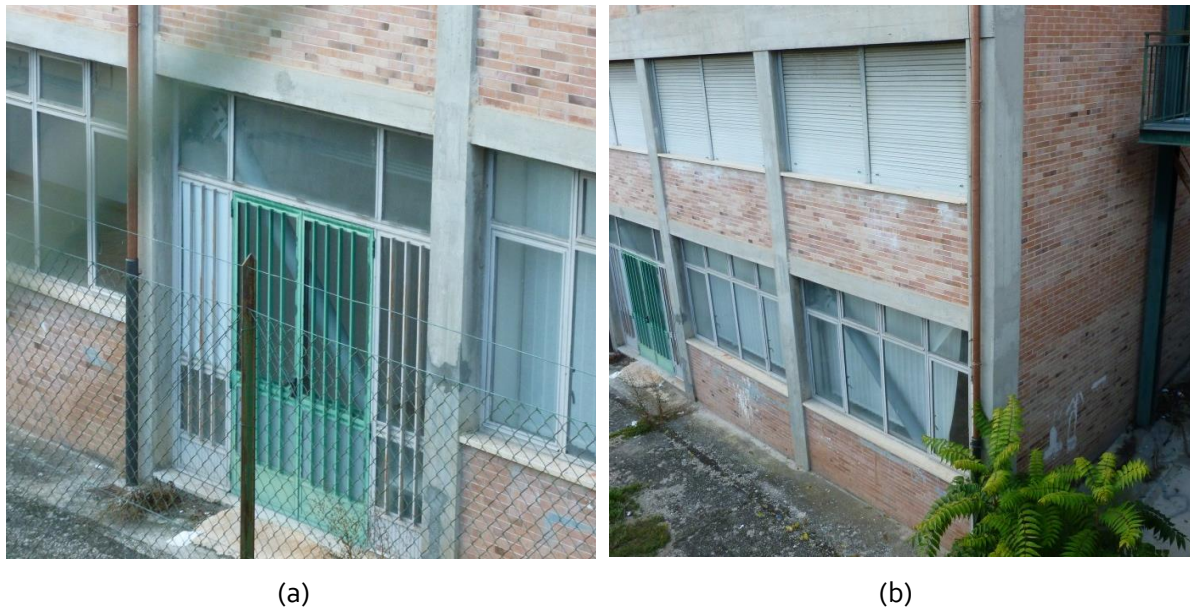
Figure 7-10 Istituto Tecnico commerciale (lat. 42.791702, long. 13.095641), (a), (b) North elevation illustrating tubular steel bracing in bays along the length of the building and possible, repaired damage to the columns.

Even if other nearby RC framed structures also performed well; it is judged, however, that the retrofitting put in place in the building, and the additional steel bracing system contributed to the

continued operation of this school. The team assigned EMS-98 DG1 to this structure. It is noted, however, that further damage to the gable occurred in the subsequent earthquake on the 30th October (Figure 7.13). The way the gable damaged still suggest the presence of a kind of reinforcement in the plaster or in the finishing such as fibres.

(a)   (b)

Figure 7-11 Istituto Tecnico commerciale (lat. 42.791702, long. 13.095641), (a) North elevation - tubular steel bracing in the basement and first storey levels (at least) and (b) detail.

Figure 7-12 Istituto Tecnico commerciale (lat. 42.791702, long. 13.095641), roof appears to have been retrofitted to a thin, light weight material.

7.3.2   *Norcia, Istituto Comprensivo Materna Elementare e Media*
The Istituto Comprensivo Materna Elementare e Media i.e., elementary school campus (42.791217, 13.095542) comprises two buildings. The 'C'-shaped building is two storeys and it forms a central courtyard with the single storey building (Figure 7-14). In plan, there are minor steps in the 'C' building (Figure 7-15). The rectangular building appears to have been extended and has vertical irregularity (Figure 7-16). Both buildings are masonry with pitched roofs. The piers and spandrels are generally regular. The buildings are founded at the ground level with no apparent basement (Figure 7-17). There may be a services pit (Figure 7-17a).

Figure 7-13 Norcia Istituto Comprensivo (lat 42.791217, long 13.095542), aerial view of the school in Norcia from Bing

Figure 7-14 Norcia Istituto Comprensivo (lat 42.791217, long 13.095542), elementary school looking northwest (from Google Earth, Street View).

Figure 7-15 Norcia Istituto Comprensivo (lat 42.791217, long 13.095542), elementary school looking southwest (from Google Earth, Street View).

Figure 7-16 Norcia Istituto Comprensivo (lat 42.791217, long 13.095542), central courtyard looking South.

The team observed in plane damage to the masonry panels (Figure 7-17), which did not appear to be significant. The school was, however, closed. It is, therefore, assumed that there is extensive internal damage. The school had been retrofitted with regular, bi-directional ties at the first-floor level. Information on the time of this intervention is not available. It was not possible to determine whether there is a roof ring beam. The roof does, however, appear to have been modified in a similar manner to the Istituto Commerciale. The aerial photograph from Bing (Figure 7-13) again shows a uniform material. The team observed a non-uniform, apparently lightweight material (Figure 7-18). Such intervention can be also the result of regular maintenance actions taken in recent years and not related to seismic interventions.

(a)

(b)

(c)

Figure 7-17 Norcia Istituto Comprensivo (lat 42.791217, long 13.095542), (a), (b) 'C' building, example of external damage and possible service pit, (c) zoom on large vertical crack, DG2

Figure 7-18 Norcia Istituto Comprensivo (lat 42.791217, long 13.095542), (a), (b) 'C' building, example of external damage and possible service pit, (c) zoom on large crak. Roof appears to have been retrofitted to a tin, light weight material.

The EEFIT team assigned EMS-98 DG2 on the basis of the external damage, even if the expectation is that official surveys classified the school in higher DG. It is likely that they managed to get into the building and to observe more extensive damage leading to the non-use condition found in October during the mission.

7.3.3 *Norcia, Nursery*

This nursery (42.789383, 13.098063) is adjacent to Norcia Hospital. It is quite a complex building; trapazoidal on plan with a pitched roof at different angles and levels (see Figure 7-19).

The construction is a one-storey reinforced concrete frame with masonry infill (Figure 7-20). The roof and floors are assumed to be reinforced concrete slabs. It is irregular on plan and elevation and it has an irregular mass distribution. The ground appears to have been excavated to construct the nursery. There is no apparent basement. The nursery was operational at the time of the visit and could only be viewed from a discrete distance. There did not appear to be any damage.

(a)

(b)

Figure 7-19 Norcia Nursery (lat 42.789383, long 13.098063), (a) location with respect to Norcia old city, (b) aerial view, zoomed location from Bing map.

Figure 7-20 Norcia Nursery (lat 42.789383, long 13.098063), lateral view (from Google Earth Street View).

7.3.4 *Accumoli – Scuola dell'Infanzia*

(a)

(b)

Figure 7-21 Accumoli Scuola dell'Infanzia (lat. 42.693956, long. 13.246677), (a) location of the nursery (yellow point) with respect to the central square of the village (red dot), source Bing map. (b) view of school's location form the road

Figure 7 22 Accumoli Scuola dell'Infanzia (lat. 42.693956, long. 13.246677), front view of the school.

The school is located on the side of Accumoli village (lat. 42.693956, long. 13.246677), see Figure 7-21. It is a two-storey building. From the inspection it appears to be a RC frame structure with clay brick masonry infills. However, given the lack of access and limited level of damage to the masonry infills, it was not straightforward to determine the structural typology. The school is built on a slope; but is

relatively regular (**Error! Reference source not found.Error! Reference source not found.**). The in spection showed evidence of damage to the roof (Figure 7-22a and Figure 7-22b) and limited damage to infills (Figure 7-23b). The school was not in use at the time of the inspection (Figure 7-23), and significant cracks in the internal infills were observed (Figure 7-23b). The school was classified as DG2 according to EMS98 on the basis of roof damage and cracks observed. The classification from the survey was of a level of damage between DG1 and DG2, but the evidence of the school not in use, made the building to be classified in DG2, given also the fact it was located on a slope.

(a)	(b)

Figure 7-22 Accumoli Scuola dell'Infanzia (lat. 42.693956, long. 13.246677), (a) East and (b) North views of the school.

(a)	(b)

Figure 7-23 Accumoli Scuola dell'Infanzia (lat. 42.693956, long. 13.246677), (a) main entrance of the school with indication of prevented use. (b) cracks in masonry infill walls.

7.3.5   *Amatrice – School Capranica*

The School Capranica in Amatrice collapsed (DG5 according to EMS98) and was widely reported on the media. The building was made of an older masonry building to which a RC building was added

later, probably in the 1970s (see Figure 7-25 and Figure 7-26. The school was subjected to retrofitting in 2012, consisting of confinement of columns with frp wrapping. This appear to have involved only the RC structure. At the time of the EEFIT mission the masonry part of the school, which collapsed during the August event, was being demolished. Debris was removed and it was easy to observe from the outside the intervention made in recent years to the RC frame (see Figure 7-26). Evidence of fibre reinforced material (FRP) applied in stripes to the columns of all storeys to increase shear capacity was evident (Figure 7-26a), and application of reinforced plaster was clear form the way crack occurred in the finishing of the RC part of the building (Figure 7-26b).

Figure 7-24 Amatrice School Capranica (lat. 42°37'38.10"N, long. 13°17'27.49"E), aerial view (Bing map)

| (a) | (b) |

Figure 7-25 Amatrice School Capranica (lat. 42°37'38.10"N, long. 13°17'27.49"E), (a) West and (b) North view of the undamaged building (Google Street view)

| (a) | (b) |

Figure 7-26 Amatrice School Capranica (lat. 42°37'38.10"N, long. 13°17'27.49"E), (a) evidence of the retrofitting intervention with FRP on columns of the RC part of the building; (b) evidence of cracked plaster from which the presence of fibres of reinforcement as prevented failure and produced a more widespread cracking.

Figure 7-27 Amatrice School Capranica (lat. 42°37'38.10"N, long. 13°17'27.49"E), Photo of the collapsed school taken in the aftermath of the event from newspaper archives online (http://www.huffingtonpost.it/2016/08/28/scuola-amatrice-crollata-_n_11746166.htmlview)

The collapse of this school had a very high profile in the media. Newspapers and televisions reported the pictures of the collapse of the "retrofitted school" in Amatrice. Figure 7-27 shows a photo collected from newspaper archive reporting the collapse of the masonry building. However, the interventions documented in Figure 7-26 appear to have worked reasonably well, even if it is evident that the retrofitting did not target the more vulnerable masonry building.

7.3.6   *Arquata del Tronto – Scuola Media Ruffini*

The Scuola Media Ruffini in the "Borgo" area of Arquata del Tronto (Figure 7-28) is most likely a two-storey masonry structure, reasonably recent (probably constructed between 1980 and 1990 or subjected to recent interventions) with quoins in the corners (Figure 7-29). The school was heavy damaged after the earthquakes (Figure 7-30). During the survey, it was classified as DG3 and it was clearly unusable. Damage was widespread in all the piers of the structure, see Figure 7-31, with evident cracks in the roof and the quoins (Figure 7-31b).

Figure 7-28 Arquata del Tronto – Scuola Media Ruffini (lat. 42°46'34.82"N, long. 13°17'38.90"E), aerial view (Bing map).

Figure 7-29 Arquata del Tronto – Scuola Media Ruffini (lat. 42°46'34.82"N, long. 13°17'38.90"E), undamaged view (Goole Street map).

(a)

(b)

(c)

Figure 7-30 Arquata del Tronto – Scuola Media Ruffini (lat. 42°46'34.82"N, long. 13°17'38.90"E), (a), (b) damage of the main entrance and (c) in the front façade of the building.

(a)

(b)

(c)

Figure 7-31 Arquata del Tronto – Scuola Media Ruffini (lat. 42°46'34.82"N, long. 13°17'38.90"E), (a) full view of damage in the main entrance, (b) damage to the quoin, (c) heavy damage and cracking to walls.

7.3.7 *Arquata del Tronto – Scuola Materna Gallo Flavi*

The Scuola Materna Gallo Flavi is very close to the Scuola Media Ruffini (Figure 7-32), it is located right after the corner of via Gadolo Bucciarelli in the Borgo area of Arquata del Tronto (Figure 7-32b). The school is a 2-storey RC building, irregular in plan with masonry infills (Figure 7-33). The school has been probably constructed in mid-1980.

The evidence of shear failures in columns is a typical characteristics of obsolete RC seismic design and similar failures were observed in the damage surveys made after the 2009 L'Aquila earthquake in Italy as shown in damage reports (Ricci et al., 2011) and empirical approaches for the potential evaluation of shear failure occurrence in RC columns (e.g., De Luca and Verderame, 2013).

(a)   (b)

Figure 7-32 Arquata del Tronto – Scuola Materna Gallo Flavi (lat. 42°46'38.82"N, long. 13°17'44.58"E), (a) relative position in map of Scuola Materna Gallo Flavi with respect to Scuola Media Ruffini (Google map); (b) aerial view of Scuola Materna Gallo Flavi (Bin

(a)   (b)

Figure 7-33 Arquata del Tronto – Scuola Materna Gallo Flavi (lat. 42°46'38.82"N, long. 13°17'44.58"E), (a) undamaged view of the building (Bing map), (b) school name tag.

(a)   (b)

Figure 7-34 Arquata del Tronto – Scuola Materna Gallo Flavi (lat. 42°46'38.82"N, long. 13°17'44.58"E), (a) localization of corner crushing of the masonry infill,) zoom of corner crushing

(a)

(b)

(c)

Figure 7-35 Arquata del Tronto – Scuola Materna Gallo Flavi (lat. 42°46'38.82"N, long. 13°17'44.58"E) , (a) secondary entrance of the building, (b) onset of shear failure in column, (c) general overview of the damage in the building.

(a)

(b)

Figure 7-36 Arquata del Tronto – Scuola Materna Gallo Flavi (lat. 42°46'38.82"N, long. 13°17'44.58"E) (b) side view of the main entrance of the building, (b) corner crushing in the infills.

7.4 Preliminary comparison with 2009 L'Aquila observational fragilities

A preliminary comparison of the damage evaluation carried out for three of the schools surveyed during the mission (see Table 7-1) is provided with respect to empirical fragility curves derived on the basis of damage data collected after the 2009 L'Aquila earthquake (Figure 7-37). In particular, the Istituto Commerciale of Norcia, the Scuola dell'Infanzia in Accumoli and the Scuola Materna Gallo Flavi, classified respectively as DG1, DG2 and DG3 are compared assuming Peak Ground Acceleration (PGA) as intensity measure and assuming the value of the USGS shake map of the 24th of August earthquake. A fair agreement between the most likely predicted damage is find in both the cases of fragility calibrated for regular structures (Figure 7-37a and Figure 7-37b) and non-regular structures (Figure 7-37c and Figure 7-37d). The school in Accumoli shows some mismatch with De Luca et al. fragilities functions (calibrated on regular buildings only) and such difference might be the result of the additional vulnerability caused by the fact the building is built up on a slope.

Table 7-1 Schools, Location, PGA and Damage classification

School	Istituto Commerciale	Scuola dell'Infanzia	Scuola Materna Gallo Flavi
Location	Norcia	Accumoli	Arquata del Tronto
PGA [g]*	0.32	0.40	0.64
EMS98 damage**	DG1	DG2	DG3

* As evaluated from the shake map of USGS
**As evaluated from the surveys made during the mission

(a)   (b)

(c)   (d)
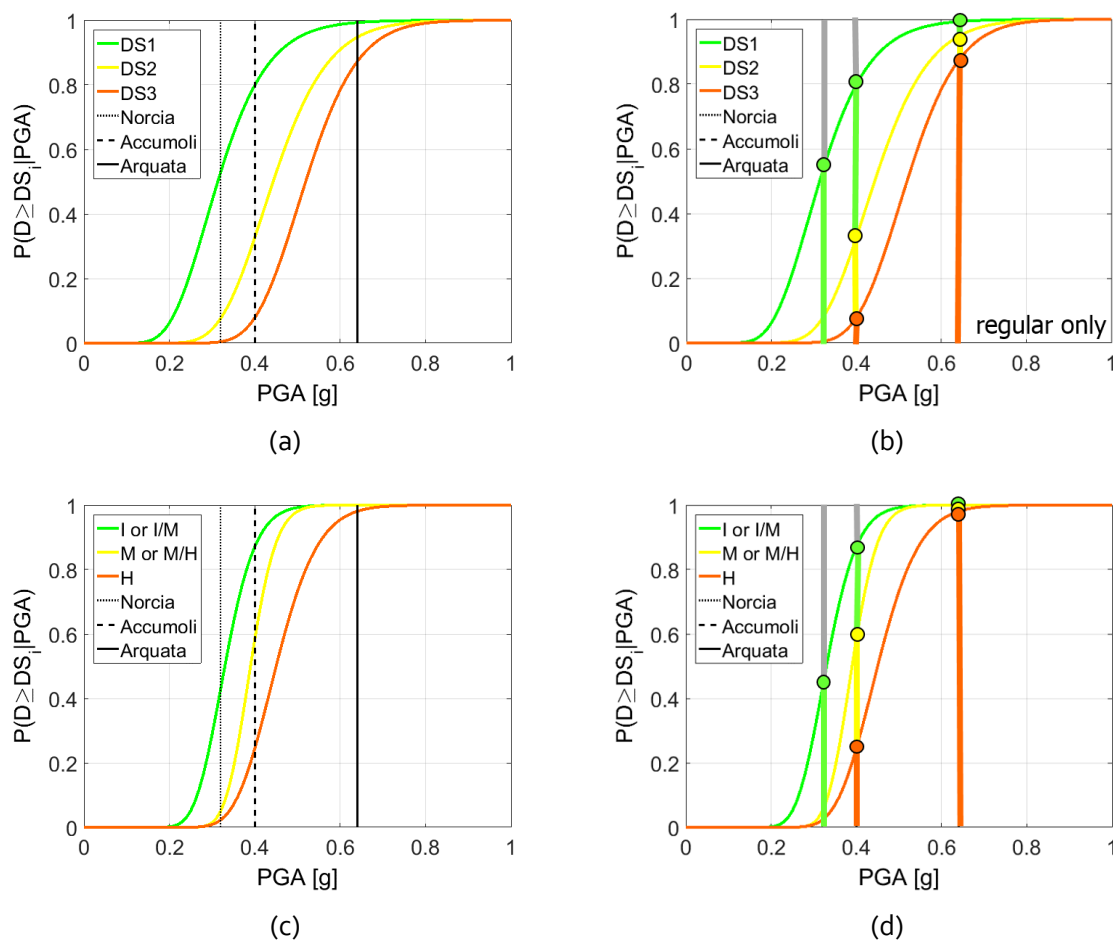
Figure 7-37 Observational fragility curves calibrated on RC survey data from L'Aquila earthquake (a) De Luca et al. (2015), (c) Liel and Lynch (2012) and evaluation of damage probability at the PGA of Norcia (0.32g), Accumoli (0.40g) and Arquata del Tronto (0.64g)

7.5   PERFORMANCE HOSPITALS BUILDINGS

7.5.1   *Norcia Hospital*

The team carried out a visual inspection of the Norcia Hospital. Norcia Hospital is classified as a "territorial" hospital, providing traditional, day hospital and day surgery services to the population from the surrounding area.
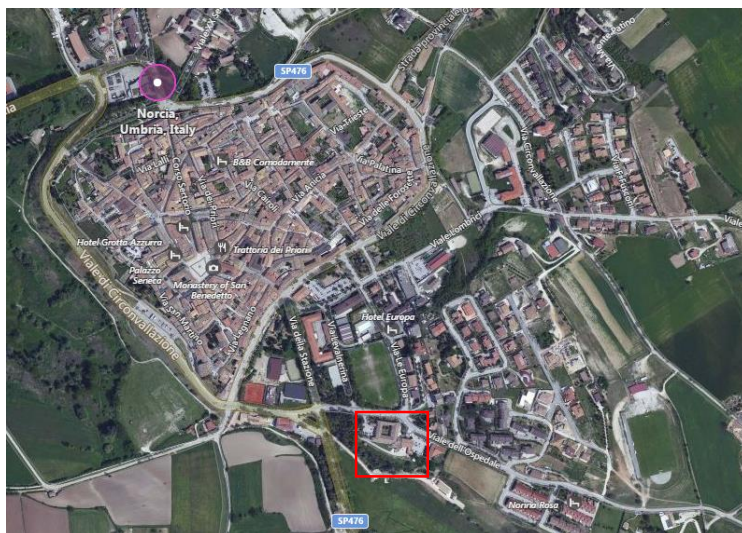
Figure 7-38 Norcia hospital (lat. 42°47'22.83"N, long. 13° 5'50.28"E). Location of Norcia hospital (Bing map).

Figure 7-39 Norcia hospital (lat. 42°47'22.83"N, long. 13° 5'50.28"E). Aerial view of Norcia hospital (Bing map).

The Hospital is composed of two blocks. The main building, with an internal courtyard, is the older of the two blocks, with the largest footprint area. A second wing, of more recent construction, is dedicated to the emergency services. Figure 7-38 and Figure 7-39 below provides the localization with respect to Norcia historical centre and the aerial view of the hospital structure.

The structure did not suffer significant damage during the 24th August earthquake and it was fully operational, at the time of the visit. Therefore, an external survey only has been undertaken, showing only minor damage. The main block only has been surveyed (Figure 7-40), this being the only one having reported minor damages. The building is a 2-storey masonry structure with timber roof. The

internal floorplates have not been inspected and therefore the construction typology is unknown. The associated PAGER classification is UFB5, a vertical irregularity is not expected and neither is a plan irregularity, despite the fact that the actual distribution of the internal walls is not known. Figure 7-41 shows the east elevation of the building. It below shows that the extent of cracking on the external facades is minimal, in this case a flexural crack over the arched windows.

Figure 7-40 Norcia hospital (lat. 42°47'22.83"N, long. 13° 5'50.28"E). East Elevation.

Figure 7-41 Norcia hospital (lat. 42°47'22.83"N, long. 13° 5'50.28"E). Cracking above window.

Some cracking between the 1st and 2nd storey windows was observed by the team. An example of the cracking is provided in Figure 7-42, where a shear crack has been observed in the masonry spandrel. Figure 7-43 shows that the building was provided with some antiseismic protection, consisting in the

use of rods to provide out-of-plane stability to the masonry walls. The building was assigned an EMS-98 DG1 by the team. During the mainshock of 26th October, the week after the end of the EEFIT mission, the hospital has reported more severe damage and has been temporarily closed.

(a)   (b)

Figure 7-42 Norcia hospital (lat. 42°47'22.83"N, long. 13° 5'50.28"E). (a) Onset of shear cracking in piers, (b) zoom of cracks.

Figure 7-43 Norcia hospital (lat. 42°47'22.83"N, long. 13° 5'50.28"E). Steel ties.

7.5.2 *Amatrice Hospital*

The hospital in Amatrice was inspected by the team and due to the level of damage it was not in use. Located half way up the hillside on the outskirts of the main town centre of Amatrice (see Figure 7-44a), the building is composed of several blocks which can be broadly split into two components, the older southern blocks and the newer northern blocks (see Figure 7-44b). The hospital complex is of mixed construction, with the southern blocks constructed of masonry, and the northern block being RC with masonry infill. The slope gradient is significant from the east to the west with the SS260 road winding around the perimeter. When the team inspected the hospital the three-storey masonry part of the building had performed the worst with visible masonry in-plane failures throughout (Figure 7-45).

(a)   (b)
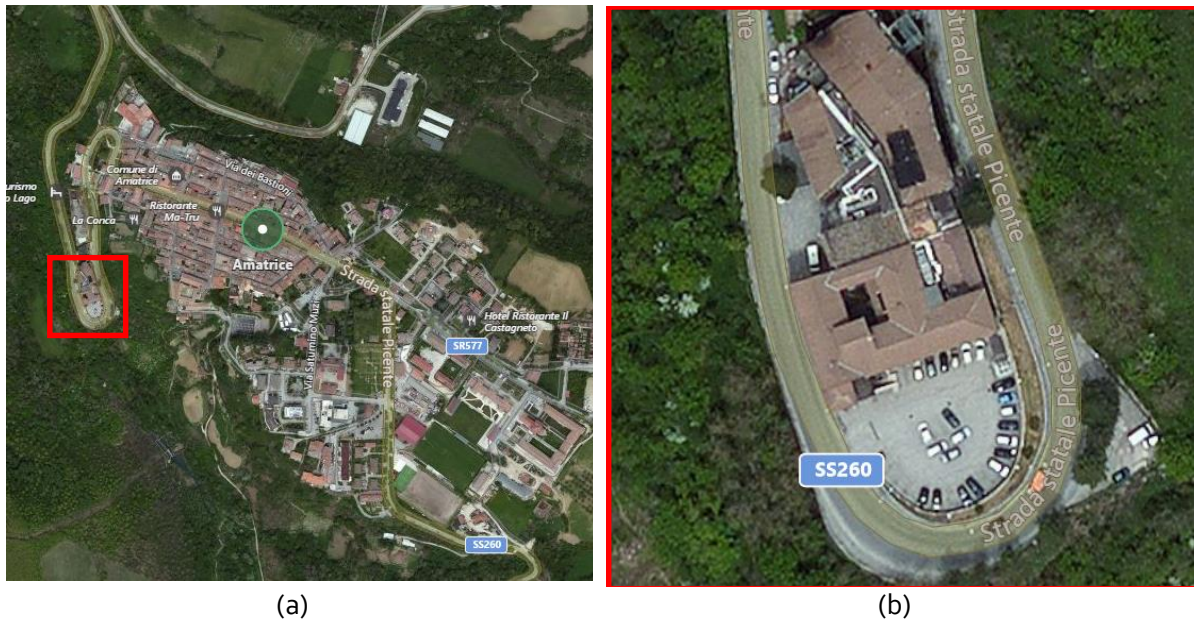
Figure 7-44 Amatrice hospital (lat. 42°37'40.85"N, long. 13°17'10.37"E). (a) localization within the town, (b) aerial view of Grifoni hospital in Amatrice (zoomed map); source Bing map

Figure 7-45 Amatrice hospital (lat. 42°37'40.85"N, long. 13°17'10.37"E). Three-storey masonry part of the hospital.

Damage to the mixed 5-6 story RC northern blocks was generally limited to in-plane cracking and failure of the infill wall panels and non-structural damage spalling of the render (Figure 7-46). Overall

the RC part was classified as DG2 on the EMS-98 scale, while the masonry part was classified as DG3. Such evaluation matches with other survey made in the aftermath of the August event from other teams (see Celano et al. 2016).

(a)   (b)

Figure 7-46 Amatrice hospital (lat. 42°37'40.85"N, long. 13°17'10.37"E). RC part of the building, damage to masonry infills, no structural damage was detected form the survey made from the outside of the building.

Notwithstanding the absence of significant structural damage in the RC part of the structure, the level of damage observed in the Amatrice hospital can be considered unacceptable for a critical structure for which the operational limit state should be the critical design criterium. Damage to the hospital had a high profile in the media and impact on public opinion. In the aftermath of the event patients in the wards had to be evacuated (e.g., Today, 2016). The hospital was reported to have an insurance against seismic events and a the end of November newspapers were announcing the availability of funds to rebuild the structure with the insurance payout (Agi.it, 2016).

7.6   PERFORMANCE OF OTHER CRITICAL STRUCTURES

Among critical structures excluding schools and hospitals, police stations and electricity transformers were surveyed. The first are critical for the important functions they have in the aftermath of a seismic event, while the electricity transformers are related to the safety and functionality of lifelines such as the electricity network in the area.

The team visited three police buildings in the towns of Norcia and Amatrice. Police buildings are critical structures which are necessary for the immediate emergency response to an earthquake event. The police buildings considered are masonry structures. Each structure was either 2- or 3-storeys. Earthquake damage ranged from minor local damage (EMS-98 DG1) to significant in-plane masonry damage (EMS-98 DG3). Each police station was examined by visual inspection from the outside of the structure.

7.6.1 Norcia – Caserma Carabinieri

The team examined the "Tenenza Carabinieri Station" in Norcia (lat. 42°47'41.37"N; long. 13° 5'31.19"E), referred to as the Norcia Caserma. It is a two-storey masonry wall building. The Norcia Caserma has significant plan irregularity. The location of the police station is shown in Figure 7-47 with the plan irregularity clearly visible. The rear of the structure follows the historic city wall. It appears that at least one extension was added to the building. The building experienced pounding damage during the earthquake. Pounding damage between two portions of the building was visible, as well as pounding damage between the building and the city wall. The pre-earthquake condition (from Google Street View) and the post-earthquake damage is shown in Figure 7-48 and Figure 7-49. Some cracking between the 1st and 2nd storey windows was observed by the team. An example of the cracking is provided in Figure 7-50. The building was classified as EMS98 DG1 by the team. The Norcia Caserma was in at least partial use during the EEFIT visit.

Figure 7-47 Norcia Caserma (lat. 42°47'41.37"N; long. 13° 5'31.19"E), aerial view emphasizing irregularity in plan (source Bing map).

(a)   (b)

Figure 7-48 Norcia Caserma (lat. 42°47'41.37"N; long. 13° 5'31.19"E). Joint of building with city wall, (a) pre- (Google Street View) and (b) post- earthquake condition.

(a)   (b)

Figure 7-49 Norcia Caserma (lat. 42°47'41.37"N; long. 13° 5'31.19"E). Location of building irregularity, (a) pre- (Google Street View) and (b) post- earthquake condition.

Figure 7-50 Norcia Caserma (lat. 42°47'41.37"N; long. 13° 5'31.19"E). Cracking between windows

7.6.2   *Norcia National Civil Protection Local Centre (Centro Operativo Comunale)*

During the mission the Local Operative Centre set up by national Civil Protection in the municipality of Norcia was surveyed. The structure did not show any significant damage and, in fact, it was selected as location for the Centro Operativo Comuniale (**Figure 7-51**). The only nonstructural damage observed was the incipient detachement of a precast panel in its top corner (see Figure 7-52).

(a)

(b)

(c)

Figure 7-51 Norcia COC (lat. 42°47'43.89"N; long. 13° 5'29.26"E). (a) and (b) National Civil Protection centre in Norcia (a), (b) during the survey, (c) pre-earthquake photo dating back to August 2011 (Google Street View).

Figure 7-52 Norcia COC (lat. 42°47'43.89"N; long. 13° 5'29.26"E). nonstructural damage to precast panel.

7.6.3   *Amatrice -Caserma Carabinieri*

The team investigated police station located in Amatrice (Comando Stazione Carabinieri Amatrice), referred to as the Amatrice Caserma Carabinieri. The location of the Amatrice Caserma is indicated in Figure 7-53. It is a 3-storey, masonry wall structure with a rectangular plan. It was retrofitted in 2012 with 5 ties in the longer dimension and 8 ties in the shorter dimension. The ties are irregularly spaced in elevation. The condition of the building as of July 2011 is shown in Figure 7-54; this picture was taken previous to the 2012 retrofit. It should be noted that the details of the 2012 retrofit are

unknown. In addition to the bi-directional ties, several vertical lines of grey patchwork are visible under the majority of the ties, they are probably reinforced cement injections with function of corner quoins to allow the development of the so called box behaviour. The ties and patchwork can be seen in Figure 7-55.
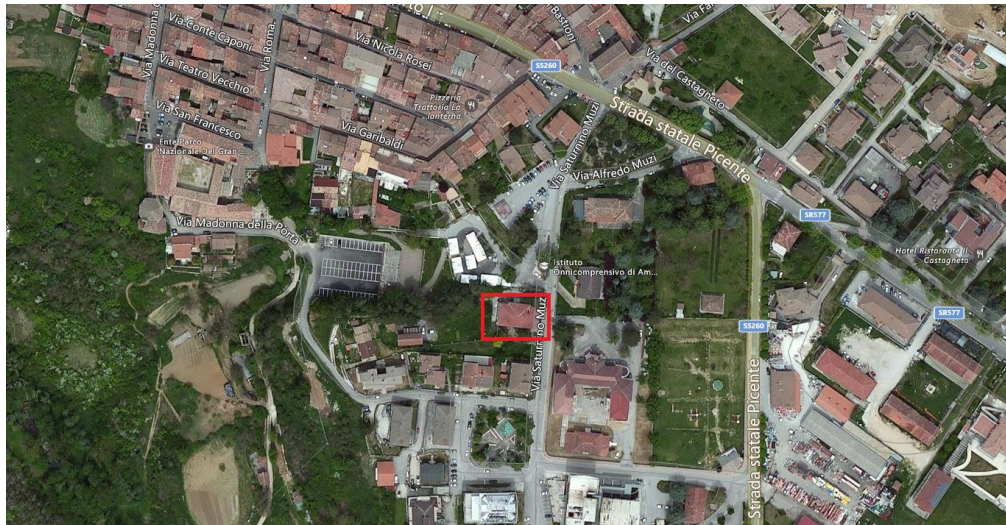
Figure 7-53 Amatrice Caserma Carabinieri (lat. 42°37'37.72"N; long. 13°17'27.14"E) aerial view (Bing map).

The Amatrice Caserma was not occupied at the time of the EEFIT mission (October 2016). Significant in-plane masonry damage was observed, as well as non-structural damage to the windows. The majority of damage was observed on the east face of the structure. An EMS-98 DG3 was assigned to the building. The post-earthquake condition is shown in Figure 7-55.

Figure 7-54 Amatrice Caserma Carabinieri (lat. 42°37'37.72"N; long. 13°17'27.14"E) pre-event condition dating back to July 2011 (Google Street view).

(a)   (b)

Figure 7-55 Amatrice Caserma Carabinieri (lat. 42°37'37.72"N; long. 13°17'27.14"E) damage (a) in South and East facades, (b) North façade.

7.6.4 *Amatrice – Corpo Forestale*

The Amatrice Corpo Forestale is a 2-storey masonry wall structure. It has a rectangular plan (see Figure 7-56). The pre-earthquake condition of the building (Google Maps) is shown in Figure 7-57. The team observed cracking on all exterior walls (Figure 7-58). An EMS-98 DG2 was assigned by the team.

Figure 7-56 Amatrice Corpo Forestale (lat. 42°37'34.33"N long. 13°17'31.24"E) aerial view (Bing Map).

Figure 7-57 Amatrice Corpo Forestale (lat. 42°37'34.33"N long. 13°17'31.24"E) pre-earthquake condition (Google Street View), West façade.

| (a) | (b) |

Figure 7-58 Amatrice Corpo Forestale (lat. 42°37'34.33"N long. 13°17'31.24"E) damage observed, widespread cracking to (a) East and (b) North facades.

7.7   PERFORMANCE OF INFRASTRUCTURE SYSTEMS

7.7.1   *Electricity Transformers*

During the mission a number of electricity transformer buildings were inspected in some of the towns visited (i.e., Accumoli, Arquata del Tronto and Amatrice). These provide an indication of the resilience of the electricity network in the aftermath of an event. During the mission it was not possible to collect infomration on the operativity of the electricity network after the earthquake, but other reports provide general info on some problems to lifelines in general; EERI, (2016) reported that: "Power outages have affected nearly 6,000 end-users as well as services, especially in the Lazio

region". Two electricity transformer buildings were surveyed in the city of Accumoli (Figure 7-59), both were constructed in RC and showed a very limited amount of damage with some limited cracking to the first one (buried cables type, see Figure 7-59a), and evidence of concrete spalling at the base of the column for the second (aerial cables types, see Figure 7-59c). The damage level of the two transformers was classified as DG1 according to EMS98. Both transformer building seemed to be operational at the time of the inspection.

| (a) | (b) | (c) |

Figure 7-59 Accumoli (a) Electricity Transformer with buried cables (lat. 42°39'24.966''N; long. 13°16'14.808''E), (b) with visible aerial cables (lat. 42°41'40.9826''N; long. 13°14'43.1531''E (c) concrete spalling zoom of damage at base column of transformer in (b)

| (a) | (b) | (c) |

Figure 7-60 Arquata del Tronto – Electricity Transformer (lat. 42°46'21.912''N; long.13°17'50.022''E), very heavy damage in masonry with deep cracks in piers and spandrels.

Figure 7-61 Arquata del Tronto – Electricity Transformer (lat. 42°46'21.912''N; long.13°17'50.022''E), zoom of damage at the roof level.

A masonry electricity transformer building was surveyed in the city of Arquata del Tronto (Figure 7-60and Figure 7-61). The level of damage was very heavy cracking throughout the spandrel and piers. This transformer was classified in DG3 according to EMS98. Notwithstanding the very heavy damage the cable system seemed to be still functional, even if the visual survey did not provide any evidence on the functionality of it (considering also that the all area around was evacuated at the time of the inspection).

A masonry electricity transformer building was surveyed also in Amatrice (Figure 7-62). The level of damage was heavy also in this case with deep cracks in the masonry walls. The damage was classified as DG3 also for this transformer. No information was available on the functionality of the transformer at the time of the survey. An electricity transformer building was survived along the SS4 Salaria road between Grisciano and Pescara del Tronto (Figure 7-63). The transformer was in RC with irregularity in elevation between the first and the second level. Some cracking at the level of the door entrance was visible, but the level of damage was considered to be minor leading to a DG1 classification. The transformer building appeared to be functional at the time of the survey.

(a)   (b)

Figure 7-62 Amatrice – Electricity Transformer (lat. ,42°37'4.19''N; long 13°17'33.79''E), buried cables.

(a)	(b)

Figure 7-63 SS4 between Grisciano and Pescara del Tronto – Electricity Transformer (lat. 42°44'25.440''N; long, 13°15'55.212''E).

References

Agi.it (2016). http://www.agi.it/regioni/lazio/2016/11/28/news/terremoto_assicurazione_salda_1_mln_per_danni_ospedale_amatrice-1280873/ (last accessed February, 2017).

Augenti, N., Cosenza, E., Dolce, M., Manfredi, G., Masi, A., & Samela, L. (2004). Performance of school buildings during the 2002 Molise, Italy, earthquake. *Earthquake Spectra*, *20*(S1), S257-S270.

Celano F., Cimmino M., Coppola O., Magliulo G., Salzano P. (2016). Report dei danni registrati a seguito del terremoto del Centro Italia del 24 Agosto 2016 (Release 1). Available at http://www.reluis.it (in Italian).

De Luca, F., & Verderame, G. M. (2013). A practice-oriented approach for the assessment of brittle failures in existing reinforced concrete elements. *Engineering Structures*, *48*, 373-388.

De Luca, F., Verderame, G. M., & Manfredi, G. (2015). Analytical versus observational fragilities: the case of Pettino (L'Aquila) damage data database. Bulletin of Earthquake Engineering, 13(4), 1161-1181.

Del Gaudio C., Ricci P., Verderame G.M. (2017). First remarks about the expected damage scenario following the 24th August 2016 earthquake in Central Italy. Proceedings of the 16th World Conference on Earthquake Engineering, Santiago (Chile), 9-13 January.

DPC Dipartimento Protezione Civile Presidenza Consiglio dei Ministri (2017), last accessed February, 2017) http://www.protezionecivile.gov.it/jcms/en/sicurezza_scuole.wp?request_locale=en (last accessed February, 2017).

EERI, (2016) http://www.eqclearinghouse.org/2016-08-24-italy/2016/09/14/summary-of-impacts-to-lifelines-and-utilities-from-the-august-24-2016-amatrice-italy-earthquake/ (last accessed February, 2017).

Grant, D. N., Bommer, J. J., Pinho, R., Calvi, G. M., Goretti, A., & Meroni, F. (2007). A prioritization scheme for seismic intervention in school buildings in Italy. *Earthquake Spectra*, *23*(2), 291-314.

Grünthal G, Musson RMW, Schwarz J, Stucchi M (1998) European Macroseismic Scale 1998. Luxembourg, Cahiers du Centre Européen de Géodynamique et de Séismologie 15

Huffington Post (2017), http://www.huffingtonpost.it/2016/10/31/scuola-norcia-terremoto_n_12733382.html [last accessed February 2017]

ISTAT, 2011. 15° Censimento della popolazione e delle abitazioni 2011. Istituto Nazionale di Statistica. http://www.istat.it/it/censimento-popolazione/censimento-popolazione-2011.

Liel, A. B., & Lynch, K. P. (2012). Vulnerability of reinforced-concrete-frame buildings and their occupants in the 2009 L'Aquila, Italy, earthquake. *Natural hazards review*, *13*(1), 11-23.

Manfredi, G., Prota, A., Verderame, G. M., De Luca, F., & Ricci, P. (2014). 2012 Emilia earthquake, Italy: reinforced concrete buildings response. *Bulletin of earthquake engineering*, *12*(5), 2275-2298.

Masi, A., Santarsiero, G., Gallipoli, M. R., Mucciarelli, M., Manfredi, V., Dusi, A., & Stabile, T. A. (2014). Performance of the health facilities during the 2012 Emilia (Italy) earthquake and analysis of the Mirandola hospital case study. *Bulletin of earthquake engineering*, *12*(5), 2419-2443.

Ministerial Decree (DM) n. 40 del 3/3/1975 (1975) Approvazione delle norme tecniche per le costruzioni in zone sismiche. G.U. n. 93 dell'8/4/1975 (in Italian).

Ministerial Decree (DM) del 14/1/2008 (2008) Approvazione delle nuove norme tecniche per le costruzioni. G.U. n. 29 del 4/2/2008 (in Italian).

Ordinance of the Prime Minister (OPCM) n. 3274 del 20/3/2003 (2003) Primi elementi in materia di criteri generali per la classificazione sismica del territorio nazionale e di normative tecniche per le costruzioni in zona sismica. G.U. n. 105 dell'8/5/2003 (in Italian).

Ricci, P., De Luca, F., & Verderame, G. M. (2011). 6th April 2009 L'Aquila earthquake, Italy: reinforced concrete building performance. Bulletin of Earthquake Engineering, 9(1), 285-305.

Smyth, A. W., Deodatis, G., Franco, G., He, Y., & Gurvich, T. (2004). Evaluating earthquake retrofitting measures for schools: a cost-benefit analysis. *School Safety and Security: Keeping Schools Safe in Earthquakes*, 208-216.

Today (2016), http://www.today.it/citta/terremoto-amatrice-crollato-ospedale-24-agosto-2016.html (last accessed February, 2017).

UNESCO (2017), http://www.unesco.org/new/en/right2education (last accessed February, 2017).

USGS (2017) https://earthquake.usgs.gov/earthquakes/eventpage/us10006g7d#executive (last accessed February, 2017).

8 PERFORMANCE OF BRIDGES

8.1 Background to the Italian Seismic code for bridges

The Building Code in force in Italy at the time of the Central Italy earthquake was the "Decreto Ministeriale 14 Gennaio 2008" NTC2008. This has now been superseded by the recently issued NTC2018, "Decreto Ministeriale 17 gennaio 2018, Aggiornamento delle Norme tecniche per le costruzioni".

The 2008 Building Code, valid from April 2009, represented an important development for building codes in Italy for two main reasons. Firstly, it implements the Eurocodes design standards. Secondly it introduces a new Italian seismic mapping system, which assumes the entire national territory as exposed to seismic action, through the uniform hazard spectrum, with varying level of peak ground acceleration (refer to chapter 5).

The bridge sections of the NCT2018 standard focuses on concrete and steel bridges, acknowledging that masonry structures are rarely adopted for new bridges. The seismic design criteria for bridges, contained in section 7.9 of the code, requires the deck and the foundations to remain elastic, while dissipation of energy (e.g. structural damage) is allowed to occur in piers or anti-seismic devices only.

The lack of information on the original design of the bridges inspected during the EEFIT mission, does not allow to confirm whether these structures have been designed to resist seismic actions or not. However, it is reasonable to assume that some of them were not.

8.2 Road infrastructure damaged by the 24th August event

Bridges represent a critical element of the transport infrastructure within a region and their functionality can be vital for the rescue operations in the aftermath of an earthquake or other exceptional events. When only one or few access roads are available to reach a given urban settlement, the bridges' category (i.e. importance) becomes higher, as their failure would isolate the population.

The 24th August seismic event hit a large number of small mountain villages. The most affected areas feature few access roads, mainly classified as secondary roads with narrow carriageway accommodating two-way traffic. Figure 8-1shows the locations of all bridges surveyed in relation to the 24th August seismic event epicentre. According to the ESM database the value of PGA recorded by the closest AMT station in Amatrice was 0.867 (g).

The road network into the town of Amatrice was particularly hit by the earthquake and the EEFIT team carried out a detailed survey of the bridges constituting the critical access to the hill top town. As shown in Figure 8-2, there are four access roads to Amatrice: one from the North direction, two from South and one from East. The North access road was closed after the 24th August earthquake because of the damage on the so called "Ponte a Tre Occhi" bridge. Traffic on the East access road was limited by the damage to the so called "Ponte delle Rose" bridge. These two bridges are discussed in detail in sections 8.3.1 and 8.4.1, respectively.
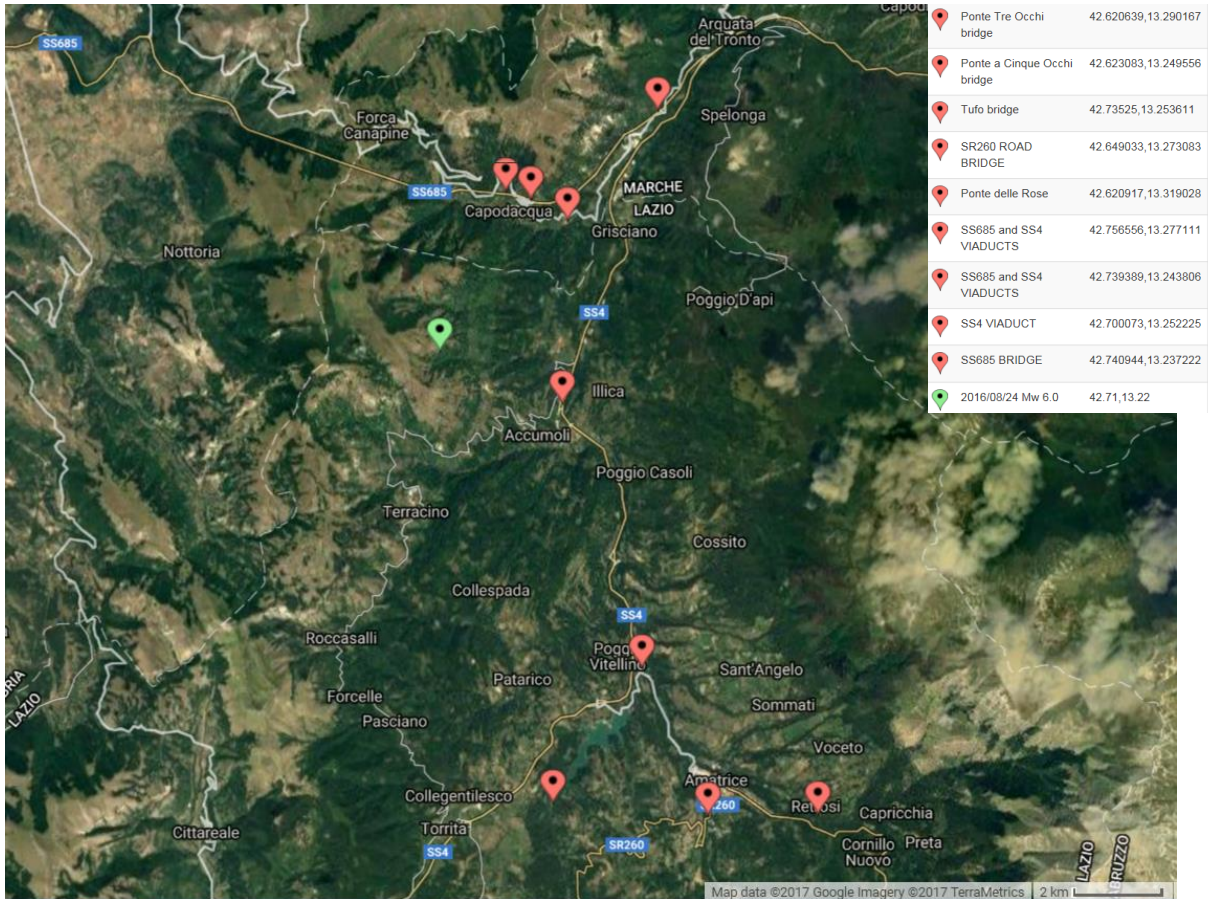
Figure 8-1 *Location of all bridges surveyed (background image from maps.google.co.uk)*

Figure 8-2 Amatrice plan view, showing the access roads and the bridges inspected (background map from maps.google.co.uk).

Remedial actions were undertaken in the short period after the seismic event in order to guarantee service of these roads, allowing the emergency services to reach Amatrice.

Figure 8-3 Temporary bridge bypassing Ponte a Tre Occhi; b) Temporary bridge near Ponte delle Rose.

Thanks to the collaboration between Italian Civil Protection and the Army, two temporary bridges were built. Figure 8-3 shows a temporary bridge which is part of a road by-passing the closed "Ponte a Tre Occhi". Built very rapidly and opened to traffic only 10 days after the earthquake struck, this bridge is crossing a small river with a limited water flow. This allowed an upstream diversion of the river in order to realise a concrete sublayer slab on the riverbed, and the placement of ten 3x3m precast concrete culverts. A cast in situ deck slab was overlaid to distribute the vehicles loads over the vertical webs of the precast elements. The restored river flow passes through the precast elements. At the time of the visit, ground Investigation were underway as part of the construction of a new permanent bridge that will eventually replace the temporary bridge and possibly the damaged pre-existing bridge if deemed not repairable.

A second bypass bridge (shown in Figure 8-3b) was built to increase the traffic capacity of the East access road as an alternative to the "Ponte delle Rose" bridge. It was opened at the beginning of October 2016 according to press reports. Despite the damage sustained (refer to section 8.4.1), the Ponte delle Rose was not closed, but created a bottleneck to the traffic due to its limited width. The army built a 12m span Bailey bridge to address the issue. The bridge is a typical military construction type that can be deployed quickly. Its modular construction allows to cover relatively small spans by assembling preformed steel frames connected into truss beams. Two truss beams are connected by transverse steel beams forming the deck and also form the bridge parapets.

8.3   Masonry Bridges on access roads to Amatrice

8.3.1   *"Ponte a tre occhi"*

The "Ponte a Tre Occhi" bridge (which can be translated from Italian as "three eyes bridge") is a 70m long structure located along the SR260 road approximately 1 kilometre South of Amatrice (42°37'14.3"N - 13°17'24.6"E). According to the ESM database the bridge would have experienced a value of PGA equal to 0.867 (g) (Luzi et al., 2016).

The bridge spans above the Rio Castellano river along the southern access into town. In the aftermath of the 24th August earthquake, the bridge failure made the national headlines as it was closed to traffic cutting off one of the key access routes for the emergency services. Its strategic importance triggered the requirement, delivered by the Italian Army, to construct a new by-pass road as discussed in section 8.2.

The bridge is a masonry arch structure with the three main barrel vaults made of solid brick circular arches spanning approximately 20m each. The barrel vaults are approximately 5m wide and are supported on cut-stone masonry piers with cutwater edges. The pier toes on the riverbed are capped with reinforced concrete walls, most probably a later addition. The two abutments are of stone masonry construction of varying quality and support the bridge approaches at a height up to approximately 10m above the riverbanks. The abutment infill, exposed by the damage, is made up of loose soil and rubble stones.

Figure 8-4 "Ponte a Tre Occhi" bridge southern view. Concrete buttresses on the eastern abutment

The deck is approximately 10m wide and composed of a reinforced concrete slab bearing directly onto the abutment and arch infills. The deck in its current form is of later addition, likely in the 1980s. It was probably reconstructed to widen the bridge as the slab cantilevers some 2 to 2.5m either side of the masonry arches. The abutments were probably modified as part of these work as they match the deck width in its current dimension; the top concrete slab is connected to the abutment walls and fill with vertical rebars (exposed by the damage), aiming to increase movement compatibility at the interface of the different materials.
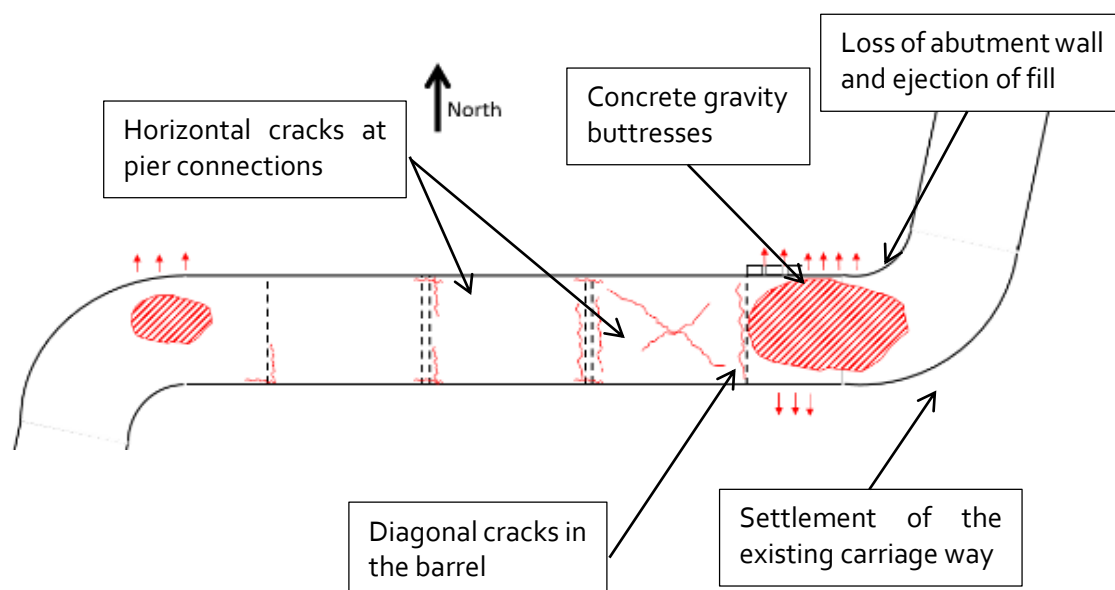
Figure 8-5 Layout of the bridge and summary of observed damage

The galvanised steel barriers are connected directly onto the deck slab edge. The barriers appeared undamaged by the earthquake and still aligned with the carriageway. The bridge is on a straight alignment with only the two abutments being part of tight 90 degree turns to approach the bridge.

The bridge presents some structural elements not part of the initial structure which were part of later strengthening works. Three unreinforced concrete gravity buttresses are placed against the northern wall of the East abutment (see Figure 8-4). Several tie rods crossing the full bridge width is also visible on the abutments and at the arch spandrels. The general condition of the bridge is very good with little decay observed in all elements. The masonry appears in good state with evidence of relative recent re-pointing works.

The most significant damage observed for the bridge are vertical settlements of the carriageway by the two abutments. The sag is particularly severe above the eastern abutment where the maximum displacement reaches over 200mm (Figure 8-6). This damage likely led to the decision of closing the bridge.
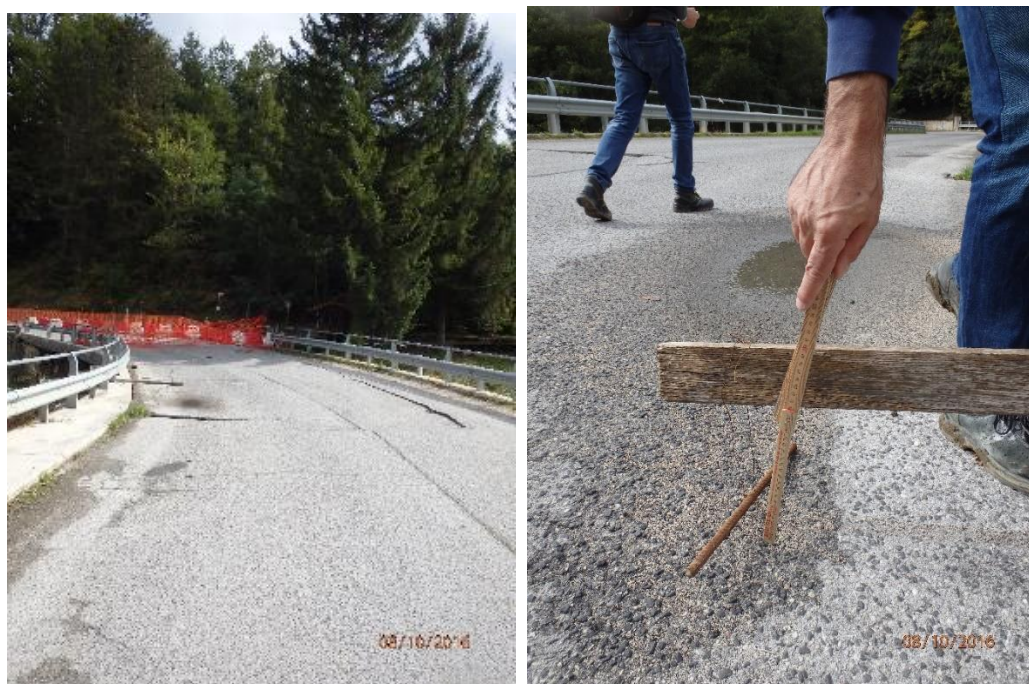
Figure 8-6 Vertical sag of the carriageway at the eastern abutment

The settlements are caused by failure of the retaining walls with substantial loss of infill beneath the deck at both abutments. The level of damage at the eastern abutment is particularly extensive and was observed on both the southern and northern walls as shown in Figure 8-7.

The southern wall retains approximately up to 5m of loose infill and partially collapsed (see Figure 8-7). The retaining wall demonstrated to be of insufficient thickness, being constructed with one leaf of irregular stones only. The failure exposed the bridge deck concrete slab and steel connectors, which were not effective in anchoring the loose material and wall below (see Figure 8-8).

Figure 8-7 Failure of the East abutment southern wall; b) detail of the exposed deck slab connectors

The northern wall shown in Figure 8-7 and Figure 8-8 is the part of the structure that suffered most damage. The wall retains up to approximately 10m of fill and has three concrete buttresses, which have been added at some point during the lifetime of the bridge (Figure 8-7). These are probably the result of previous issues with the stability of the abutment, possibly determined by the uneven overall soil loading on the abutment walls. This uneven ground pressure was then likely further exacerbated by the seismic accelerations.

The gravity buttresses shown in Figure 8-8 have been ineffective as shoring measure, showing signs of both global overturning failure as well as shear failure at the cold joints between different pours. The abutment masonry retaining walls are, as in the southern wall, made of a single leaf of irregular stones which has collapsed in multiple points leading to the loss of infill. The wall has also collapsed by the tie rod anchorages leaving them exposed and further indicating inadequate quality of the anchorage detailing (refer to Figure 8-9).

Figure 8-8 Gravity buttresses failure

Figure 8-9 Failure of the East abutment northern wall; b) detail of tie rod anchorages exposed

Failure was also observed at the West abutment northern wall, where the retaining masonry wall partially collapsed leading to the loss of infill material and settlement of the carriageway above. The extent of damage is limited if compared with the East abutment.

The barrel arches show a cracking pattern that can be attributed to the 24th August earthquake. The eastern arch presents X-shaped cracks typical of cyclical seismic movements (see Figure 8-10). The cracks start at the arch springer by the East abutment and develop to beyond the crown. The SE-to-NW crack appears more developed than the NE-to-SW one and it is likely associated with the movements suffered by the abutments which also triggered the buttresses failure.

Figure 8-10 Photographs of the eastern arch X-shaped cracks.

Recurring horizontal cracks were observed at all pier heads both by the arch springers and at the cutwater caps as shown in Figure 8-11. The cracks are the likely results of the seismic base shear forces transferred from the bridge onto the piers. No evidence of horizontal displacements was observed in all but one pier i.e. the one by the East abutment. This has the edge cutwaters dislodged further confirming the movements highlighted by the diagonal cracks observed at the adjacent arch soffit.

Figure 8-11 Horizontal cracks at pier heads

Based on the damage observed, it is possible to speculate that the East abutment failure during the earthquake led to the loss of a positive lateral restraint at the eastern side span. This side span might have behaved as a cantilever on the horizontal plane which led to the lateral cyclical movements compatible with the cracks observed in the arch soffit.

8.3.2 *Ponte a Cinque Occhi*

The "Ponte a Cinque Occhi" bridge (which can be translated from Italian as "five eyes bridge") is a 60m long structure located along the Strada Romanella road leading into Amatrice (42°37'23.1"N - 13°14'58.4"E). The bridge spans above the tail of the Scandarello Lake, a man-made basin whose dam is located approximately 2.5 km downstream, on a straight alignment. According to the ESM database the bridge would have experienced a value of PGA equal to 0.867 (g) (Luzi et al., 2016). The bridge was likely constructed at the beginning of the 20th century (the dam itself dates 1924). Its primary structure is composed of five stone masonry barrel arches spanning approximately 12m each (see Figure 8-12), providing a deck width of approximately 5m. The deck level is achieved with low quality infill material above the barrel vaults comprising a mix of loose soil and stone masonry courses. The bridge piers are (likely) of masonry construction and founded on shallow pads.

Figure 8-12 "Ponte a Cinque Occhi" bridge North West view

The bridge was refurbished and strengthened, with varying success, most likely in the 1980s. The interventions observed comprised: (1) encasing the abutments with reinforced concrete walls hiding the pre-existing structure (Figure 8-12). (2) Rendering the arches soffit with a thin (~50mm) unreinforced concrete lining (Figure 8-13). (3) Concrete lining walls were possibly also applied onto the piers, although this is uncertain (Figure 8-14). (4) Creation of masking walls made of clay hollow bricks at the spandrels (Figure 8-15). (5) Unreinforced concrete deck-edge upstands and metal parapet railings.

The only emergency measure implemented as part of the post-earthquake response was the restriction of the maximum allowed vehicle load to 3.5 tonnes. It is understood that further measures (including load testing) were recommended but have not been implemented at the time of visit as priority was given to maintaining the bridge fully operational.

Figure 8-13 Images showing the RC abutment walls and arches concrete lining

The bridge appeared in a moderate-to-severe state of decay which is the likely result of lack-of maintenance in the years leading to the seismic event. The decay was further exacerbated by the inappropriate deck drainage system implemented as part of the strengthening works. As a result, not all the damage can be attributed in its entirety to the 24th August earthquake.

One pier foundation was exposed and presented slight signs of scour, though this cannot be directly linked to the seismic actions. The EEFIT team were told that the reservoir level was drawn down following the seismic events uncovering the scour phenomena. No deformation was observed at road level suggesting that no foundation settlements occurred. The piers presented a widespread vertical cracking patterns as shown in Figure 8-14. Some of these cracks can be reasonably attributed to an increase of vertical load onto the piers during the bridge dynamic response or possibly to increased horizontal pressure of slumped loose saturated fill. The abutment reinforced concrete walls showed no sign of damage nor cracking highlighting that the strengthening works have been reasonably successful (Figure 8-12). This is confirmed by the lack-of settlement observed along the carriageway at the interface between the abutments and the arched spans.

The main arch showed widespread damage (Figure 8-14 and Figure 8-15) with substantial reduction of the cross section at the pier springers, up to the formation of a hinge. The hinges are identified through substantial horizontal cracking, and localised ejection of both concrete liner and masonry voussoirs. The hinges may have formed as a result of relative longitudinal (i.e. along the bridge length) displacements between the arches-deck-abutments rigid system and the taller piers.

Little secondary masonry cracks were observed on the arches as these are probably hidden below the concrete liners. Only one-barrel vault shows longitudinal cracks running along its length highlighting the lack-of transverse connections. The spandrel masking walls have completely failed, and they were observed still lying on the ground. This was likely due to general decay (note the substantial vegetation overgrowth) and lack of any positive connection combined with the horizontal accelerations imposed by the earthquake.

Figure 8-14 Images highlighting foundation scour (left) and vertical cracks in the bridge piers.

Figure 8-15 Hinges by the pier springers

Figure 8-16 Localised ejection of material at the arch soffit (left), bridge arch longitudinal cracking (right)

The spandrel failure shown in Figure 8-16 highlighted some loss of fill at the arches extrados. This is of particular concern in localised zones adjacent to the carriageway kerb in which the deck edge is practically unsupported. It is understood that restriction to a single lane traffic system was requested to prevent vehicle tyre imposing concentrated loads onto the critical deck edges, however, this was not implemented at the time of the visit.

Figure 8-17 Spandrel masking walls failure

The bridge deck surface, edges and balustrades show no damage that could be attributed to the earthquake, though they were found in poor state. The main issue noted was the lack of an appropriate drainage system which was evident both in the running surface as well as in damp patches observed in the barrel soffits.

8.3.3   *SR260 Road Bridge*

The bridge is located along the SR260 road at approximately 2.5km distance from Amatrice, on the North approach road into town (42°38'56.52"N - 13°16'23.1"E). The bridge is a single span masonry arch, carrying two road lanes and spanning approximately 10m over a river. According to the ESM database the road bridge experienced a value of PGA equal to 0.867 (g) (Luzi et al., 2016).

The bridge is mostly made of cut stone masonry, see Figure 8-18. The only exceptions are the deck, which is a reinforced concrete slab likely part of later widening works, and the northern spandrel wall, which is also of concrete construction. The bridge and SR260 road were fully operational at the time of the visit. However, the SR260 road was subject to an extensive rock-fall just 100m south of the bridge that led to its closure in the aftermath of the 24th of August earthquake. The road was re-opened through the slewed diversion shown Figure 8-18. The bridge was likely repaired and strengthened after the seismic event; the road diversion included a new construction vehicle access to the bridge. At the time of the visit, the river embankments and bridge abutments earthworks (including gabion walls) appeared of fresh construction. The abutment masonry appeared recently repointed (Figure 8-19) and the bridge arch northern edge included new steel tie rods (Figure 8-20).

Figure 8-18 SR260 Road Bridge North view

Figure 8-19 SR260 diversion (left), newly made earthworks and gabions at the West abutment (right)

The only damage observed during the visit was the detachment of the side arches at either edge of the barrel vault. These are highlighted by the presence of meridian cracks running along the back of the facing stones as shown in Figure 8-21. The cracks point to a lack of transverse masonry connection within the masonry barrel vault, which led to the side displacements under the horizontal seismic accelerations. Such damage was (partially) repaired in the recent works and the northern arch was tied back with a series of steel capping plates anchored inside the masonry with threaded steel rods (Figure 8-21). There is no evidence of the rod passing through the body of the bridge and anchoring on the South elevation

The North side also presents a concrete spandrel wall that differ from the southern one, retaining the original stone wall. Possibly the bridge North side suffered the higher level of damage and was therefore subject to the more extensive repair works.

Figure 8-20 Meridian cracks by the side arches, South on the left and North on the right

Figure 8-21 Tie rods and concrete spandrel at the bridge North side

8.3.4 *Masonry Bridge in Tufo*

This bridge is located along the SP129 road by the village of Tufo (42°44'06.9"N - 13°15'13.0"E). The bridge crosses over a steep gorge with a small stream, accommodating a sharp 180° bend in the road. According to the ESM database the bridge would have experienced a value of PGA equal to 0.867 (g) (Luzi et al., 2016). The structure is composed of three circular arches each spanning approximately 10m (Figure 8-22). The entire structure, including piers, arches, spandrels, abutments and parapets,

is made of cut stone masonry. The bridge width is approximately 10m. The barrel vault soffits are lined in unreinforced concrete. These are likely not part of the original construction and they are the only evidence of structural modification at a visual inspection. The bridge appeared in fair condition with no severe sign of decay but just some vegetation overgrowth and damp patches.

Figure 8-22 Tufo bridge East view

Figure 8-23 Collapse (left) and damage (right) of the masonry parapets.
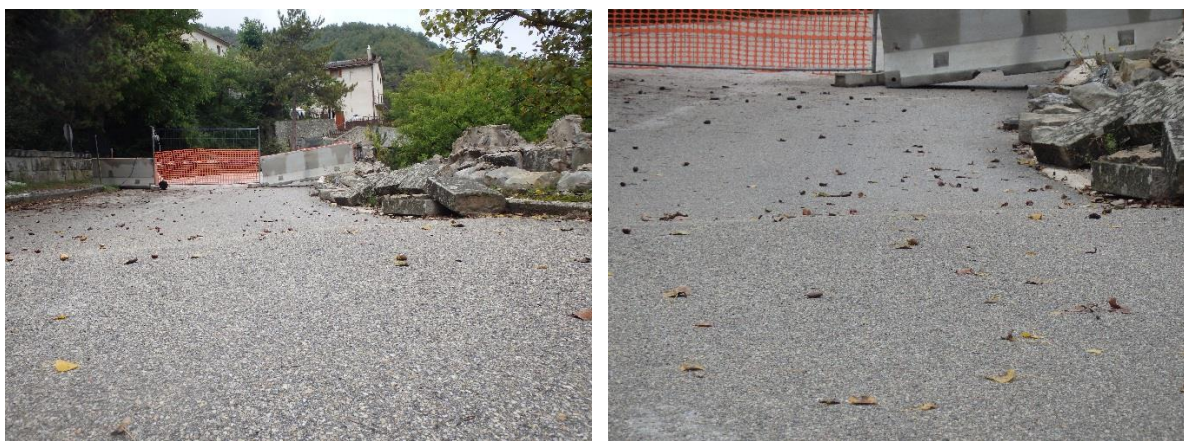
Figure 8-24 Vertical sag by the North abutment

The bridge showed widespread damage caused by the August the 24th earthquake and it was closed to traffic at the time of the visit. There was severe damage of the masonry parapets, which partially collapsed in various points as shown in Figure 8-23. The carriageway shows a vertical sag (approx. 100mm) in correspondence of the North abutment (Figure 8-23). This can be related directly to the damage observed in the first span below where the abutment wall is partially collapsed from the arch springer to the foundation level (Figure 8-24). This led to loss of structural wall and to the infill behind being exposed. The same barrel presents a detachment of the edge arch at the spandrel connection in the area just above the collapse (Figure 8-24). The detachment is related to a diagonal crack that

extends halfway into the barrel vault. This zone is likely to have suffered from a combination of sideway pressure imposed by the abutment infill and loss of support from the abutment wall collapse.

Figure 8-25 North abutment failure (left); detachment of the edge arch at the spandrel connection (right)

All the arches presented widespread cracking, the most notable being recurring horizontal cracks at the southern haunches (Figure 8-25). These indicate the possible formation of hinges caused by the seismic acceleration. One of the piers shown in Figure 8-25 presented vertical cracks indicating the possibility of increased axial loads during the earthquake.

Figure 8-26 Horizontal cracks at the haunch (left), pier vertical cracks (right)

8.3.5 *Conclusions on Masonry Bridge Typology*

Masonry arched bridges are the typology that suffered most damage during the earthquake. The road network in the surrounding of Amatrice was severely affected by their damage and urgent temporary works have been necessary to facilitate the emergency services.

The bridges are located on secondary roads (e.g. strada provinciale SP or strada regionale SR) and usually carry low volume of traffic. Still their damage impacts on the immediate earthquake response as Amatrice has only four access road into town. This suggests that the seismic importance factor of a structure should be "high" even for structures part of local road networks, if they represent a critical and vital element of the road infrastructure for a community.

The two bridges closed to traffic suffered damage to the earth-retaining abutments suggesting that this particular structural element needs careful consideration in bridge seismic design. Masonry barrel arches showed that they can perform their structural function even if they suffered damage, e.g. cracking, thanks to their inherent structural redundancy. The failure of the Tufo bridge masonry parapets highlights that these elements also need careful consideration in seismic design even if they are not part of the primary structure.

8.4   CONCRETE BRIDGES

8.4.1   *Ponte delle Rose*

This bridge is shown in Figure 8-27 a symmetric concrete bridge of 3 spans, approximately 22m each, for a total length of 66m. According to the ESM database the bridge experienced a value of PGA equal to 0.867 (g) (Luzi et al., 2016).

The deck has a variable depth, constant in the mid-span and near the abutments, increasing on both sides over the two central piers, implying continuity of moment over the piers. The cross section presents three rectangular main girders connected at the top by a concrete slab and transversally by rectangular secondary cross girders spaced approximately 5m. A typical joint (in Italian called "Sedia Gerber" joint) is visible at mid-span of the central span (Figure 8-28). The presence of a joint on the top slab as well enables to identify the static scheme adopted: the deck is divided in two independent structures, each constituted by one and half span cantilevering from the pier towards the centre. This means that differential movements are likely to occur during a seismic event.

The age of the bridge is unknown, but the structure is likely to have more than 60 years. The articulation of the bridge at the abutments and the connections over the central piers are unknown, but the lack of any device capable of transferring horizontal forces is a reasonable assumption considering the age of the construction. Both piers and abutments appear to be constituted by brickwork. Their dimensions suggest that masonry was adopted as load bearing material rather than just as an external cladding layer.

Figure 8-27 General views of Ponte delle Rose (42°37'15.3"N 13°19'08.5"E)

According to information gathered on site form the military troop guarding the bridge, following the seismic event of the 24th of August, the bridge was not closed but a restriction was imposed to a maximum weight of 3.5 tonnes to passing vehicles. Even though the damage on the primary elements of the bridge were not significant, some significant damage to its parapet required this restriction.

Figure 8-28 Damage on the parapet and details of the parapet

As shown in Figure 8-29, the parapet is made of steel tubes embedded in a small concrete wall. The edge of one tube is directly in contact with the edge of the following one, so that transfer of forces in compression is possible even without considering friction to concrete.

Figure 8-29 "Sedia Gerber" type joint at the middle span

The earthquake heavily damaged the parapet's small columns; some of them have been completely detached from the deck and were only supported by the steel tubes. The damage suggests a faulty detail connection for the parapet members. In fact, the damage concentrated mainly where movement of the deck was not restrained. At mid-span, the joint in the deck was not matched by a joint in the parapet, and on the abutments the last parapet column appears to be rigidly connected to the abutment and not to the deck.

8.4.2   *Viaducts along SS685 roads*

Two viaducts have been observed along the SS685 road. The Strada Statale 685, is a national level road and one of the major connections between the Appennines and the Tirreno sea, branching out of the SS4, just south-west of Arquata del Tronto and ending in Civitavecchia, through its connection to the SS675. It was built in the Seventies to facilitate mobility in the Val Nerina, connecting it to the Tronto valley and to the SS4. According to the ESM database the bridge would have experienced a value of PGA equal to 0.867 (g) (Luzi et al., 2016). A typical schematic arrangement of the viaducts built on the SS685 in the area inspected during the mission is reported in Figure 8-30 and Figure 8-31 below.
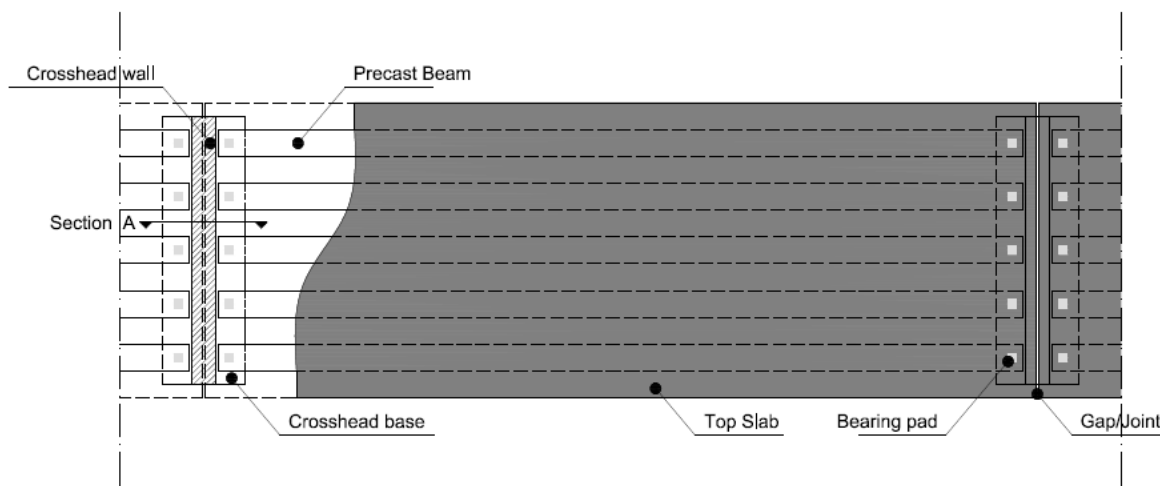
Figure 8-30 Plan arrangement of the typical simply supported concrete viaduct
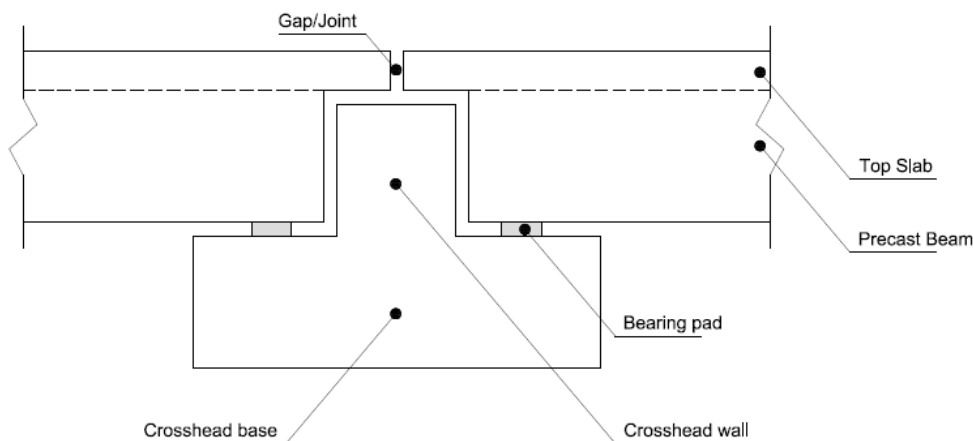
Figure 8-31 Nodal zone detail of the thypical simply supported concrete viaduct

Bearings pads, pre-installed on the crosshead base, support the precast beams both during the construction phase and the permanent configuration. The cast in situ top slab provides the continuity among the beams, so that the deck becomes monolithic and behaves as a rigid diaphragm in its plane. Other transversal connections between the precast beams (cross beams and end diaphragm) have not been shown in the schematic arrangement for reason of clarity.

The bearing pads material has not been identified, but it is likely to be rubber with a steel plate inside to increase its vertical stiffness. The pads distribute the load coming from the beam onto the structure below, and accommodate the small deck rotations due to the loads deflections. These elements are

not explicitly designed to carry horizontal loads, or to provide horizontal stiffness like the modern rubber isolators. They allow small displacements like the thermal one (in this case a few millimetres for the typical span length of around 30m), without generating significant forces at the interface because of the flexibility of the rubber material. At the same time, this conceptual design relies on the friction between the rubber pads and the concrete to transfer all the horizontal loads due to wind or traffic actions (braking, traction, centrifugal forces in curves). This means that the deck is horizontally unrestrained and differential movements between superstructure and substructure are to be expected under the action of horizontal loads.

Longitudinal displacements are allowed by the gap between the end face of the precast beams and the crosshead wall, or the gap between two adjacent top slabs. Typical dimensions of the gap is in the order of centimetres, i.e. enough to avoid contact due to thermal expansion, or pounding due to longitudinal forces like braking and traction. Transverse displacements can be limited by shear keys at the end of the pier crosshead, or sometimes not even limited manifesting the lack of any seismic restraint.

The simply supported pre-stressed concrete beams can lead to very dangerous phenomena of loss of support where displacements are not properly controlled under seismic loading. That is why this type of decks usually sits on piers crossheads of large dimensions. These must be able to accommodate the predicted displacements and, at the same time, have enough room for bearing replacement and maintenance operations.

Figure 8-32 shows the first viaduct of this type inspected during the mission. This is a large multi span viaduct with span length of approx. 22m, characterized by single column piers of different height. The deck spans are separated by a vertical diaphragm above the pier heads, so two movement joints are formed at every pier. No shear keys have been identified so transversal displacement are unrestrained. The lack of proper drainage between the deck spans produces rundown and leakage at the pier crosshead, which shows signs of deterioration of the concrete cover and advanced state of corrosion of the exposed reinforcement.

Figure 8-32 General view of the first viaduct investigated (42°45'23.6"N 13°16'37.6"E)

For the seismic behaviour of this viaduct type, each pier can be idealised as a single degree of freedom system supporting the mass of a single span (half-span on both sides) when the friction forces between bearing pads and concrete are not exceeded. Therefore, each pier has its own fundamental period which depends on its height. Once friction is exceeded, major flexibility and energy dissipation can be expected, which could be even beneficial for the structure if pounding does not occur. It can

be generally assumed that the fundamental periods of the piers (apart from the shortest) are of the order of 1 sec, so the expected accelerations should not be the highest on the spectrum. The uncontrolled seismic displacements can cause issues. As shown in Figure 8-33 below, structural damage was identified on one pier crosshead wall, where a visible crack has been probably caused by the pounding effect during the seismic event.

Figure 8-33 Damage observed on the first viaduct investigated (42°45'23.6"N 13°16'37.6"E)

The second concrete viaduct inspected is also multi-span, with a typical span length of approx. 22m, with piers of varying height (Figure 8-34). In this case the slabs of adjacent spans extend over the pier's crosshead wall, resulting in only one movement joint (Figure 8-34). Shear keys are visible on both sides of the pier crosshead to limit transversal displacement. It has been possible to inspect the piers' crossheads, with the support of Vigili del Fuoco, checking the presence and the condition of the bearing pads. These are shown in Figure 8-35.

Figure 8-34 General view of the second viaduct investigated (42°44'21.8"N 13°14'37.7"E)

No structural damage after the earthquake was identified. The general good state of the bearing pads suggests they may have been recently replaced. On the other hand, poor detailing of the expansion joint creates a poor water drainage system which causes leakage and deterioration of the pier crossheads. It was not possible to identify the presence of a specific device adopted as expansion joint. In the gap between the concrete slabs only a curved sheet probably of plastic material collecting water is visible. Furthermore, in Italy it is quite common to find the expansion joints filled with the upper tarmac layer, which should accommodate the small predicted displacements of the deck. This asphalt fill material can break under larger displacements imposed by major seismic event, creating

discontinuities on the road surface which require small repair. This appears to be the case for this viaduct. In fact, Figure 8-36 shows strips of fresh tarmac by the joints where some early interventions after the earthquake were carried out.

Figure 8-35 Bearing pads of the second viaduct investigated

Figure 8-36 Expansion joint and repair works on the surface of the second viaduct investigated

8.4.3 *SS4 Viaduct*

The Strada Statale SS4 is a national level road which connects Rome with the Adriatic Sea near Porto D'Ascoli. Its alignment dates back to an historic Consular Roman road, however is alignments and

carriageway have been extensively modernised through time, and, for the most part, is today a double carriage way with two lanes in each direction. The inspection a viaduct along the SS4 (shown in Figure 8-36) was difficult because of its location, so only some details have been observed. According to the ESM database the bridge experienced a value of PGA equal to 0.867 (g) (Luzi et al., 2016).Apart from the drainage deficiency, causing advanced deterioration, the presence of a shear key at the abutment restraining transversal displacement can be observed. This element probably failed during the seismic event. In fact, a visible crack can be observed in Figure 8-37, and this suggests the lack of seismic provisions in the original design.

Figure 8-37 General view of the SS4 viaduct (42.700073 N, 13.252225 E)

Figure 8-38 Damage observed at the viaduct abutment

8.4.4 *SS685 Bridge*

The longest-span bridge in the area of investigation is shown in Figure 8-39. It has not been possible to reach the base of pylons and one of the abutments. According to the ESM database the bridge would have experienced a value of PGA equal to 0.867 (g) (Luzi et al., 2016).

The only abutment investigated, accommodating an expansion joint, has been found in good conditions. The deck structure is integral with the piers and the bridge is therefore characterized by a different dynamic behaviour from the simply supported deck viaducts presented before. Due to its dimensions, it is likely that the fundamental periods of the structure are large enough to maintain a low level of accelerations, even if big displacements must be expected.

Figure 8-39 General view of the fifth viaduct investigated (42°44'27.4"N 13°14'14.0"E)

8.5 Conclusions on the concrete viaduct typology

Damage on concrete viaduct structures was found to be limited, and mainly related to pounding effects. It should be noted that such damage did not directly affect the operability of the structure, and repair works could be performed easily. It can be generally said that concrete viaducts of the type observed, even if not explicitly designed to resist seismic actions, did not show very high seismic vulnerability because of their intrinsic characteristics. Such consideration can drastically change when the seismic demand in terms of displacement is bigger, and loss of support phenomena can be expected. Fortunately, the displacement demands related to the 24th of August seismic events appear not to have been particularly high.

References

Petrangeli M.P. "Evoluzione della progettazione dei ponti e degli interventi sull'esistente". Relazione ad invito alle Giornate A.I.C.A.P. 2011, Padova 19-21 Maggio 2011.

Pinto P.E., Mancini G. "Seismic Assessment and Retrofit of Existing Bridges". Relazione ad invito alle Giornate A.I.C.A.P. 2011, Padova 19-21 Maggio 2011.

Calvi M., Priestley N., "Seismic Design and Retrofitting of Reinforced Concrete Bridges", Proceedings of the International Workshop held in Bormio on April 2-5, 1991, edited by LitoLine Arti Grafiche, 1991.

Luzi, L., Pacor, F., Puglia, R., Lanzano, G., Felicetta, C., D'Amico, M., … Chioccarelli, E. (2017). The Central Italy Seismic Sequence between August and December 2016: Analysis of Strong-Motion Observations. *Seismological Research Letters*, *88*(5), 1219–1231.

Luzi, L., Puglia, R., Russo, E., & ORFEUS, W. (2016). *Engineering Strong Motion Database*.

9   SOCIAL ASPECTS

9.1   Introduction

This section considers the situation in the disaster area from the point of view of the basic needs of the affected population. Furthermore, it deals with the transition from the initial emergency to the longer-term reconstruction. Details are given of how things stood at the time of our fieldwork, 6-7 weeks after the 24th August 2016 earthquake. Observations are made on the situation in each of the affected settlements, where local public administrators and residents were interviewed. The results of a questionnaire survey of emergency responders regarding practical challenges, information sharing and modalities of communication are also reported

9.2   The Transition from Emergency to Recovery

The fieldwork was conducted during the phase of early recovery and transition from emergency responses to a more settled long-term set of solutions to community problems (Ingram et al. 2006). One fundamental question to answer is to what extent did this phase harbour an effective and efficient transition from the short-term to the long-term? In the research literature, attention is usually focussed on emergency response or the recovery and reconstruction processes (Lizarralde et al. 2010). The transition between these phases is often neglected but it is important, as it represents a critical juncture between two very different sets of strategies for managing the crisis caused by the disaster (Alexander 2007).

In the aftermath of the 2009 L'Aquila earthquake, 50 km south of the area affected by the August 2016 tremors, some 97,000 civil protection volunteers left their imprint upon a city of 72,800 inhabitants (Alexander 2013, p. 61). In 2016, about 7,500 volunteers were at work in a disaster area with a registered population of 5,100 inhabitants, of whom probably fewer than 4,000 were physically resident in the affected area (Blasetti et al. 2018). Hence, there was a massive presence of rescue personnel and vehicles, dominated, as usual, by the Italian Fire Brigades which are the lead agency in earthquake emergencies.

A primary problem that remained vitally important at the time of our visit 6-7 weeks after the 26th August earthquake was accessibility and traffic circulation. As seen in Chapter 7, Amatrice is served by three main access roads, SR (regional road) 260 north, 260 south and 577. All three were initially impassable to road traffic as a result of landslides, accumulations of rubble, damage to carriageways and bridges. In October 2016, the bridges remained closed and one route was open by virtue of a temporary track through a wooded area and a Bailey bridge across a small valley. At 169 sq. km, Amatrice is a relatively large municipality and it contains 69 villages, hamlets or small groups of houses, in Italian called *frazioni*. Some of these houses had collapsed across roads and the rubble had been cleared only enough to allow the passage of vehicles. The other towns in the area had fewer problems of access.

In October 2016, the functions of town councils were being restored. Amatrice had its headquarters in a one-storey earthquake-proof prefabricated building that had been constructed as a strategic response to the risks revealed by the 2009 L'Aquila earthquake. Accumoli had transferred its municipal functions to a factory on the main road, the SS4 Via Salaria, 1-2 km from the town which was largely evacuated. Arquata del Tronto ran most of its municipal functions from prefabricated and container buildings installed in a car park in an easily accessible place on the periphery of the urban area. At the time of the EEFIT visit, medium- and long-term plans were being formulated. Meetings

were underway to establish where to locate long-term temporary housing and to discuss how to revitalise the local economy. Economically, the local area depends on agriculture (largely stock rearing), some processing of agricultural products, a limited number of service activities and tourism, including agri-tourism. Activities linked to agriculture had been badly affected by damage to structures, including animal stalls. Tourism had been devastated by the loss of major attractions and the general state of damage and disarray, and service activities were gradually being re-established in temporary accommodation. Saleable stock was being salvaged from damaged shops and plans were being made to create an area of temporary shops in prefabs. Basic services such as health care functions were still accommodated in tents, pending relocation to modular containers.

At the time of the EEFIT team fieldwork, the tent camps (Figure 9-1) that had been erected at Amatrice and Arquata del Tronto were gradually being emptied as their inhabitants were transferred to hotels or elsewhere. This had already happened at Accumoli, while for Pescara del Tronto the inhabitants were amalgamated with those of nearby Pescara. Those residents who had an alternative to being lodged at the expense of the Regional Governments in hotels could request a *contribuzione di autonoma sistemazione*, a monetary support to help them find their own lodging. Many of the hotels were distant from the affected area in major towns such as Rieti, Ascoli Piceno and Teramo, as locally there was relatively little hotel accommodation and any such structures tended to be damaged.

Figure 9-1 Tent camp at Arquata del Tronto, 8 October 2016.

9.3   Phases of the emergency from impact to reconstruction

When the earthquake occurred, the response by the Italian Fire Brigades was immediate. Fire stations in a radius of 50-100 km sent battalions immediately and then set to work to prepare relief convoys,

which are organised at the regional level (the earthquake occurred at the borders of Abruzzo, Marche and Lazio regions). Fire Service activity consisted of three phases. The first of these involved urban search and rescue (USAR), in which survivors and the bodies of victims were extracted from the rubble. Within 24 hours of the earthquake, this also involved sensing hazardous materials, such as asbestos dust, and painting warning signs on affected buildings Figure 9-2). Secondly, buildings were secured by buttressing and limited movement of rubble. In a few cases the Fire Services demolished buildings that were in precarious condition and occupied key positions. One of these was the school complex in Amatrice, which was demolished during the period of our visit. The third phase was to retrieve valuables from damaged buildings, having at the outset established a cordoned area, or 'red zone' of interdicted access. People's personal effects were salvaged. Firemen complained that some people expected them to risk their lives to recover mementos rather than indispensable items such as vital documents. In fact, spontaneous collapse or damage during aftershocks made the task of retrieving items risky. In other cases, firemen emptied shops of saleable goods (and perishable items that could attract vermin or lead to a contamination hazard), or they secured shops against the weather by attaching tarpaulins (Figure 9-3). To a certain degree, the three phases overlapped.

Figure 9-2 Fire Service notation of hazardous materials in a damaged building

The overall coordination of the emergency was effected from a command centre (DICOMAC - *direzione di comando e controllo*) located in Rieti 65 Km from the affected area and run by the national Department of Civil Protection. Local operational command (*Comando operativo*) was established in Amatrice and Arquata del Tronto, in coordination with the DICOMAC. The phases of emergency shelter and accommodation were planned as follows. First, the people who had lost their homes were accommodated in tent camps for about six weeks. These included canteens and links to services, including temporary schools and clinics. People either then found their own accommodation,

possibly with government subsidies, or were accommodated in hotels, mostly outside the affected area. Within seven months (i.e. by April 2017) it was planned to erect prefab villages close to the devastated settlements. In the end, given delays of various kinds, the villages were more or less complete by late summer 2017.

Figure 9-3 Firemen securing a commercial premises in Amatrice centre.

The role of national Department of Civil Protection (DPC) was expected to finish when there was a clear definition of plans to accommodate people. At that point, the management would be handed over to the regional government, which would also initiate reconstruction.

At the time of the EEFIT team visit it was estimated that reconstruction would begin within two years and be completed in seven to ten years. More time might be needed for the restoration of churches and major historical monuments, which are managed by the Italian Ministry of Cultural Heritage (MIBAC). It is not clear how the 26th and 30th October earthquakes might have set back these estimates by creating more, and more complex, damage. For information on cumulative damage to churches, see Chapter 6 of this report.

One salient aspect of local culture is a very strong attachment to place (Alexander 1989). Some 40,000 inhabitants of Rome have strong links with Amatrice and usually return there in the summer months. As a result of this, and lack of local economic opportunities, in Amatrice at the time of the earthquake there were four second homes to every occupied house. Usually in Italy, when government indemnifies property owners for earthquake damage, a strong distinction is made between first and second homes. The mayor of Amatrice anticipated that this would not be the case there, as the Government had accepted that the restoration of the urban fabric depended on an even-

handed approach to adjacent buildings. This was confirmed when, on 19th July 2018, Parliament approved a decree-law for post-earthquake reconstruction in central Italy

Although little can be written with confidence about the probable long-term future of the four affected settlements, there is some likelihood that Pescara del Tronto will be abandoned, as it is built on highly unstable ground. The others will no doubt be reconstructed, albeit at a slow pace.

Although Amatrice is a small town within a rural-agricultural area and L'Aquila is a university centre and regional capital city, the two have in common the fact that they have rather marginal economies and are somewhat isolated from the mainstream of national life in Italy. However, the situation in Amatrice is less complex and less overwhelming. Strong local leadership may save the day and ensure that the pitfalls of L'Aquila are not encountered in the aftermath of the 2016 tremors.

9.4 Health sector response to the earthquake

As the August 2016 earthquake damaged a well-defined and geographically limited area, hospitals in nearby major towns were unaffected and remained able to treat the 390 seriously injured survivors. Ambulances were not damaged and, despite the extensive damage to roads and bridges, accessibility was rapidly restored to the affected towns. Moreover, telephone communication was not interrupted. During the early emergency, good weather meant that rescue helicopters could fly and thus evacuate the seriously injured.

After two days local health services were restored, including a pharmacy and a clinic with general practitioners and specialists. However, emergency cases needed to be sent to nearby hospitals. People with disabilities who needed specific assistance were moved to specialised health structures outside the area. Cases recorded and shared using standardised guidelines and a form (SVEI - *Scheda speditiva per la valutazione delle esigenze immediate delle persone fragili e con disabilità* - Form for the rapid assessment of the immediate needs of vulnerable people and people with disabilities; Ciciliano 2014). It was anticipated that local health structures would be fully restored within two years, but this prediction may have had to be revised after the October earthquakes. At the time of the publication of this report (in 2018) the hospital in Amatrice has not been fully rebuilt and conflicts persist over the location of the new hospital. On the good side, the German Government has recently confirmed the allocation of funds to rebuild it.[5]

9.5 The role of relief workers

The earthquake emergency was managed according to procedures that are nationally standardised on the basis of long experience with disasters caused by natural hazards. The brigades of the Italian National Fire Service Corps have primary responsibility for urban search and rescue, buttressing buildings, moving rubble and accompanying residents into the 'red zone' to retrieve belongings. Like other organisations that participated in the emergency response, they concentrated on specific practical tasks and were not briefed on the wider picture and general plans.

Incorporated civil protection volunteer services (such as Misericordie and ANPAS) set up and manage the tent camps. Army personnel, Carabinieri and Forestry Corps guards are used to manage road blocks and monitor the developing situation. The Italian Red Cross Society coordinates relief efforts and takes part in USAR activities. The national Civil Protection Department (DPC) assigns specific

---

[5] For details of the plans and controversies, see
http://www.ricostruzionelazio.it/ricostruzionelazio/accordo-nuovo-ospedale-amatrice/
and https://www.ilmessaggero.it/rieti/rieti_amatrice_grifoni_ospedale-3822160.html.

tasks to the Red Cross. The DPC operates from the DICOMAC (see previous section). Its seismological group undertakes technical and geological surveys. Other duties include damage assessment, monitoring of public facilities and coordination of the activities of other organisations. Local areas in Italy are incorporated into municipalities, of which nationally there are 8,104 distributed among 80 provinces and 20 regions. Town councils reside in the municipal operations centre (COC - *centro operativo comunale*). The mayor is the primary civil protection authority and carries final ultimate responsibility for local public safety. In the transitional phase, town councils initiate negotiations with the national government about medium- and long-term recovery plans, including where to establish transitional settlements (SAE - *soluzioni abitative provvisorie*) and how to revitalise the local economy.

9.6   The situation in the individual towns in early October 2016

At Amatrice, six weeks after the earthquake about 50 people were still living in tent camps but were destined to be moved into hotels in the very near future. The local elementary school was investigated by the Italian authorities because it had been retrofitted against earthquakes in 2010 and yet partially collapsed in 2016. On 7th October it was demolished by Fire Service engineers. The site will be cleared and used for a prefabricated temporary school. In the meantime, lessons were held in tents. These were also used for a pharmacy and health clinics.

Almost all buildings in the historical centre of Amatrice collapsed partially or totally, and hence in its entirety it was interdicted and designated as a 'red zone' (see Chapter 5). The City Council had already defined the areas designated for residential and commercial prefabs. Other areas were to be designed for hotels and school facilities. Besides the move from tents to hotels discussed above, some survivors were also accommodated in the apartments of the C.A.S.E. project in L'Aquila (i.e. post-2009 transitional accommodation – Alexander, 2013) and in houses offered by people who live elsewhere (through the *Amatrice Solidale* solidarity initiative). Containers were not used, but people were due to be resettled in wooden prefabs. Given that the earthquake occurred in late summer, care had to be taken to ensure that people were properly housed and protected against the weather by the time the harsh mountain winter occurred, in which temperatures would quickly fall to freezing point. Despite this, the winter of 2016 was characterised by extreme temperatures and many settlements remained isolated for several weeks, which resulted in further economic damage to animal livestock.

The City Council envisaged three phases. First, in two years, the temporary settlements were intended be up and running. Secondly, between two and four years the main reconstruction would start. The reconstruction of the city centre was expected to take place between years seven and ten. In addition, Amatrice hospital would be rebuilt in two years. At the time of the publication of this report (in 2018) this seems not to be the case.

Seven weeks after the earthquake, at Arquata del Tronto, on 8-9 October, people were moved from tents to temporary accommodation in a local hotel or with relatives. Residents whom we interviewed complained that it was a struggle to encourage and maintain social cohesion, which had not been strong before the earthquake. At Pescara del Tronto, one third of the population died in the earthquake and damage was both profound and universal. One resident continued to live on the edge of the red zone, where damage had been less pronounced, and refused to move out of it. Survivors were grouped together with those of nearby Arquata, as this is the municipality of reference.

At Accumoli seven weeks after the earthquake the local tent camp had been dismantled and about 600 residents had been accommodated in hotels at San Benedetto del Tronto, 82 km away on the Adriatic Sea coast. Children had been registered in the schools at San Benedetto.

From these brief notes on conditions in the main affected towns, one can see that they each had a rather different fate. Diverse conditions required different solutions, and these were applied. Although all four settlements are close to each other in the Tronto valley, Arquata and Pescara are in Marche Region, while Amatrice and Accumoli are in Lazio Region. Hence they are under different jurisdictions, which may account for some differences in strategy, but they are also very different settlements. Amatrice was the dominant town and the largest pole of attraction for tourism and cultural activities, as well as being the home of sanatoriums and nursing homes. The largest of these had been built by the Italian Fund for the Mezzogiorno in the immediate post-war period. Although damaged, it was rapidly repaired. Other such structures did not escape as lightly. The other affected towns were essentially agricultural settlements.

9.7   Communication with the Public

In Italy communication between the emergency services takes place via well-established channels and there is no reason to suppose it was anything but fully functional in the aftermath of the August 2016 earthquake. Communication between the authorities and the public is another matter, and something that responds to an entirely different culture. It was at best unsystematic. The largest share of communication was carried out face-to-face, by word of mouth, with minor reliance on radio (Radio Amica). There were few printed materials and we noted a rather variable attitude towards new media.

The town councils of Amatrice and Arquata made good use of their websites, while Amatrice also used Facebook and Twitter. It is noteworthy that, despite the small size of the municipality, the town council of Arquata del Tronto also started a Facebook page in October 2016 to provide updates about early and medium-term recovery to its citizens (the last post on this page is dated April 2017). This is in line with what happened in other post-disaster contexts (e.g. Christchurch and Emilia-Romagna earthquakes) where disasters brought about innovations in the way official communications were carried out (Sutton, 2012; Russo et al., 2016).

We sensed that the degree to which these means of communication were employed probably depended strongly on the skills and good will of individual council officers, rather than on a coherent plan. In addition, there is the question of who in the community uses Internet resources to find information. No data on this was collected, but it appeared that young and middle-aged people were quite able to access sites such as Facebook. Civil protection volunteer workers gave information informally, but this was not specifically part of their duties. Local people whom we interviewed complained about the lack of systematic communication, especially as some of them had become aware of critical information by chance rather than by design. However, in a closed mountain community, people may be reluctant to express their needs, or so it was according to a person in Arquata del Tronto, who was endeavouring to collect data about the needs of residents.

Despite the very traditional, and undeniably inefficient means of government-to-citizen communication in the disaster area, there were some positive signs. For example, on Facebook a group of young people from Arquata had created a community-based knowledge source entitled *Chiedi alla Polvere* ("Ask the Dust" - https://www.facebook.com/centroItaliaterremoto/?fref=ts). It collects and publicises official information. The authors of the site asked to collaborate formally with authorities, but the offer was declined. This is a pity as Ask the Dust had 6,100 adherents by late 2016 and nearly 10,000 by mid-2018. Its inventors eventually turned it into an association. Another site (http://terremotocentroitalia.info/) collected requests of assistance and goods and passes them on to relief workers. It also acts as an information source for people affected by the earthquake. It carries a Telegram app (which is similar to WhatsApp) which enables subscribers to receive updates. Table 9.1 summarises the use of new media for local communication in the aftermath of the August 2016 earthquake.

Table 9-1 Communication initiatives after the 2016 earthquakes in central Italy

Site	Web address	Description	Social media	Geographical coverage
Terremoto Centro Italia	http://terremotocentroitalia.info/	A volunteer-run web platform to gather and distribute information about needs and initiatives after the earthquake.	Facebook https://www.facebook.com/groups/1758670357733881/ Twitter @terremotocentro Telegram https://telegram.me/terremotocentroitalia	The whole affected area.
Comunicacity	http://comunicacity.net/amatrice/ http://comunicacity.net/accumoli/ http://comunicacity.net/arquatadeltronto/	Web platform for communications between government agencies and citizens or private companies. Currently in use by the municipalities of Amatrice, Accumoli and Arquata del Tronto.		Amatrice, Accumoli, Arquata del Tronto
Chiedi alla polvere / Ask the Dust	https://www.facebook.com/centroItaliaterremoto/	Volunteer-run Facebook group (to become a formal association) that collects and disseminates information about the earthquake. Run by young people living in the affected area.	Facebook https://www.facebook.com/centroItaliaterremoto/?hc_ref=SEARCH&fref=nf	Arquata del Tronto and the rest of the affected area.
Amatrice 2.0	http://www.amatrice2puntoo.it/	Volunteer-run association that aims to keep alive the sense of community in Amatrice and foster social and economic revitalisation. Run by young people living in Amatrice.	Facebook https://www.facebook.com/pg/Amatrice-20-1627862690838290/about/?ref=page_internal	Amatrice
Amatrice, una famiglia alla volta per ritornare a vivere	https://it-it.facebook.com/Amatriceaiutotrasparente/	Facebook group aimed at providing concrete aid to the affected population by putting in contact people in need with those who can provide resources	Facebook https://www.facebook.com/pg/Amatriceaiutotrasparente/about/?ref=page_internal	Amatrice

9.8   A Survey of Relief Workers

The EEFIT team conducted a questionnaire survey of relief workers in Amatrice and Arquata del Tronto. Some 56 valid responses were received. Of the respondents, 72 % were male and 28 % female, and 46 % were civil protection or medical volunteers. One quarter of the respondents were sent to the area immediately after the earthquake, while 37.5 % arrived more than a month after the tremors. The survey probed information flows and communication processes, referred to the sharing of information, awareness of the developing situation and problems experienced during the relief

work. The overall aim was to gain insight into the perspectives of the relief workers, including their version of the common operating picture (see Appendix 10.3).

The questionnaire survey asked people to report their concerns in the immediate aftermath of the earthquake as well as later at the time of the field mission. In the initial emergency the major problem encountered (44.7%) was the accessibility of the working area, given the damage to roads and bridges. Coordination and technical issues, each accounted for 23.1% of answers, and communication with the public accounted for 10.3%. As time wore on, many of the problems were ironed out and the proportion of respondents reporting no problems rose from 16.1 to 19.6%. Technical and coordination issues remained constant, logistical problems diminished to 14.2%, and long-term strategy development rose to 36.4%. Thus relief workers accommodated themselves to many of the challenges they faced, but many of them were unable to see the way forward beyond the start of the transitional phase. Only 12% claimed to have full awareness of the reconstruction strategy, while 22% were unaware and 64% were aware only of the role of their own organisation in progressing to the long-term.

During the early response, 64.9% of respondents had furnished information to the population on personal safety and 51.4% on temporary shelter arrangements. By October, the latter had dropped to 21% and the most common type of information given to survivors was on sources of psychosocial support (32%). In the early emergency, 80.5% of communication with the population was of the face-to-face kind, followed by 24.4% by telephone. That position was maintained over time, although television slightly increased its importance as a source of information from specific organisations. Slightly more than half of the respondents stated that their organisations had no specific plans to help people with disabilities in emergency situations. Two thirds stated that there were no such plans or procedures for the transitional phase.

The questionnaire survey revealed that emergency response workers were strongly focussed on their primary assignments and were given little chance to absorb the bigger picture or appreciate the long-term challenges of providing assistance to a population displaced by earthquake. The heavy reliance on face-to-face communication with the population may to some degree have inhibited access to vital knowledge, but it may also have helped foster social cohesion, as this depends substantially on human relationships. There is little indication in the responses to the questionnaire that relief operatives were particularly involved in the process of making a transition to longer-term recovery. The contrast between the town councils' clear perception of the long-term strategy and the relief operatives' relative lack of perception of the same gives a clear indication that the strategy was not widely shared. One might argue from this that the common operating picture became less clear over time, even though ample scope existed for it to be shared. In the light of increasing worldwide commitment to assisting people with disabilities in the aftermath of disasters (Alexander and Sagramola, 2014), it is disappointing that this aspect was evidently not dealt with well by the respondents' organisations.

9.9   Conclusion

Despite the limited size of the affected area and small number of affected settlements, we noted considerable diversity in the situation encountered at each town. Common elements included a strong desire to map out a clear strategy to guide the recovery over the coming months and years. The overwhelming reliance on face-to-face communication had its inefficiencies, but it may have helped social cohesion, which local protagonists were struggling to maintain. Small, close-knit mountain communities were having to cope with seismic devastation on a scale that had not been witnessed in Italy for more than 35 years. The practical problems were legion.

The August 2016 earthquakes elicited a strong response from the Italian Government and the national emergency management community. There was no shortage of emergency resources and there prevailed a fairly liberal attitude to the recovery demands. Emergency procedures had been consolidated and honed in previous disasters and they functioned well in this one. On the other hand, there was little sense of a shared common operating picture. Indeed, it was not adequately shared with the civil protection operatives or the local population.

The picture that emerged of the social situation in the four towns was one of great strain caused by exceptional loss and damage. The local area is characterised by mass 'emigration' to other parts of Italy and beyond. Indeed, it is estimated that Amatrice hosts about 5,000 second homes often belonging to people residing elsewhere in the Lazio region (mostly in Rome).[6] No doubt this diaspora will rally around its home town. However, considerable isolation and dislocation are being experienced by the survivors. If the social fabric is not unravelling, it is certainly under strain. One saving grace is strong, articulate local leadership, and another is the work of young people to provide on-line points of contact. Hence, the problems faced by the affected towns are probably not unsolvable (with the possible exception of Pescara del Tronto), but they are an exceptionally hard test of mettle for small mountain communities with relatively few resources.

References

Alexander, D.E. 2007. "From Rubble to Monument" revisited: modernised perspectives on recovery from disaster. In D. Alexander, C.H. Davidson, A. Fox, C. Johnson and G. Lizzarralde (eds) *Post-Disaster Reconstruction: Meeting Stakeholder Needs*. Firenze University Press, Florence: xiii-xxii.

Alexander, D.E. 2010. The L'Aquila earthquake of 6 April 2009 and Italian Government policy on disaster response. *Journal of Natural Resources Policy Research* 2(4): 325-342.

Alexander, D.E. 2013. An evaluation of the medium-term recovery process after the 6 April 2009 earthquake in L'Aquila, central Italy. *Environmental Hazards* 12(1): 60-73.

Alexander, D. and S. Sagramola 2014. *Major Hazards and People with Disabilities: Their Involvement in Disaster Preparedness and Response. | Risques Majeurs et Personnes Handicapées: Leur participation à la préparation et à la réaction aux catastrophes.* Council of Europe, Strasbourg, 65 pp.

Blasetti, A.G., E. Petrucci, V. Cofini, B. Pizzi, P. Scimia, T. Pozone, S. Necozione, P. Fusco and F. Marinangeli 2018. First rescue under the rubble: the medical aid in the first hours after the earthquake in Amatrice (Italy) on August 24, 2016. *Prehospital and Disaster Medicine* 33(1): 109-113.

Ciciliano, F. 2014. L'assistenza alla popolazione vulnerabile nelle grandi emergenze. Italian Department of Civil Protection, Foligno, 13 March 2014.
http://www.vigilfuoco.it/aspx/download_file.aspx?id=16775

Ingram, J.C., G. Franco, C. Rumbaitis-del Rio and B. Khazai 2006. Post-disaster recovery dilemmas: challenges in balancing short-term and long-term needs for vulnerability reduction. *Environmental Science and Policy* 9(7-8): 607-613.

Lizarralde, G., C. Johnson and C. Davidson (eds) 2010. *Rebuilding after Disasters: From Emergency to Sustainability.* Spon Press, Abingdon, UK, 283 pp.

Russo, M., Silvestri, P. Bonifati, G., Gualandri,E., Pagliacci, F., Pattaro,A.F., Pedrazzoli, A., Pergetti, S., Ranuzzini, M., Reverberi, M., Solinas, G. Vezzani, P. 2016. Innovation and development after

---

[6] See https://www.comune.amatrice.rieti.it/amatrice-solidale/

the earthquake in Emilia. CAPPaper n. 137 April 2016, Center for the Analysis of Public Policies, University of Modena and Reggio Emilia, Modena, 35 pp..

Sutton, J. 2012. When online Is off: public communications following the February 2011 Christchurch, NZ, earthquake. In: L. Rothkrantz, J. Ristvej and Z. Franco (eds). Proceedings of the 9th International ISCRAM Conference, Vancouver, Canada: 1-6

10 APPENDICES

10.1 Rapid Visual Survey Form – Italy Mission 2016

Date:_____2016   AM   PM   **Inspector:** ____   **Building number:**_

Address	
GPS coordinates:	
Usage:	(Multi)residential Commercial Industrial Education Healthcare Other:
Other features:	

Structural Information

Has building been demolished?	
Tag colour	*Green Yellow Red*
Primary structural system	*RC Masonry Steel Timber Earth Other:*
Roof material	*Timber RC slab Other:*
Floor material	*Timber RC slab Other:*
Lateral load resisting system	*Frame Walls Bracing Combined*
No. of storeys (basement?)	***Basement?** Y N Storeys:*
Age	
Masonry infill	*Y N **Type:** Brick Concrete block Other:*
PAGER classification	
Vertical irregularity	*Yes No N/A Unknown*
Plan irregularity	*Yes No N/A Unknown*
Short column	*Yes No N/A Unknown **Induced?** Y N*
Strong beam-weak column	*Yes No N/A Unknown*
Irregular mass distribution	*Yes No N/A Unknown*
Soft storey	*Yes No N/A Unknown*
Pier irregularity	*Yes No N/A Unknown*
Spandrel irregularity	*Yes No N/A Unknown*
Through thickness type	*Solid Three Leaf Cavity Unknown*
Chimney	*Yes No N/A Unknown*
Ring beam	*RC masonry N/A Unknown*

Ties	Yes No N/A Unknown Regular? Y/N Bi-directional? Y/N
Quoin	Yes No N/A Unknown
Foundation type	
Built on slope	Yes No Unknown
Notes:	

Damage observed

EMS-98 damage grade	No damage DG1 DG2 DG3 DG4 DG5	
Primary and secondary damage types observed: *No visible damage* *No structural damage* *Masonry in-plane damage/failure* *Masonry OOP damage/failure* *Masonry corner damage* *Masonry partial collapse*	*RC column damage/failure* *RC beam damage/failure* *RC soft storey at ground* *RC soft storey upper levels* *RC soft storey more than 1 storey* *RC connection damage/failure* *RC pancake collapse* *RC masonry infill damage/failure* *RC failure of 1 or more bays*	*Frame distortion* *Roof damage* *Pounding* *Floor collapse* *Total collapse* *Geotechnical (ground movement/slop failure*
Non-structural damage:		

Notes:

10.2 PAGER TYPOLOGIES

W	Wood
W1	Wood stud-wall frame with plywood/gypsum board sheathing. No masonry infill.
W2	Wood frame, heavy members (with area > 5000 sq. ft.), industrial.
W3	Light post & beam wood frame. Floors and roofs do not act as diaphragms. No bracing, poor seismic load resistance path, poor connectio
W4	Wooden panel or log construction. Walls are made of timber logs sawn horizontally in a square or circular cross section.
W5	Walls with bamboo/light timber log/reed mesh and post (Wattle and Daub/Bahareque).
W6	Unbraced heavy post and beam wood frame with mud or other infill material.
W7	Braced wood frame with load-bearing infill wall system of brick masonry, adobe, or wooden planks or wattle & daub infill.
M	Mud walls
M1	Mud walls without horizontal wood elements
M2	Mud walls with horizontal wood elements
A	Adobe blocks (unbaked sundried mud block) walls
A1	Adobe block, mud mortar, wood roof and floors
A2	Adobe block, mud mortar, bamboo, straw, and thatch roof
A3	Adobe block, straw, and thatch roof cement- sand mortar
A4	Adobe block, mud mortar, reinforced concrete bond beam, cane and mud roof
A5	Adobe block, mud mortar, with bamboo or rope reinforcement
RE	Rammed Earth/Pneumatically impacted stabilized earth
RS	Rubble stone (field stone) masonry
RS1	Local field stones dry stacked (no mortar) with timber floors, earth, or metal roof.
RS2	Local field stones with mud mortar.
RS3	Local field stones with lime mortar.
RS4	Local field stones with cement mortar, vaulted brick roof and floors
RS5	Local field stones with cement mortar and reinforced concrete bond beam.
DS	Rectangular cut-stone masonry block
DS1	Rectangular cut stone masonry block with mud mortar, timber roof and floors
DS2	Rectangular cut stone masonry block with lime mortar
DS3	Rectangular cut stone masonry block with cement mortar
DS4	Rectangular cut stone masonry block with reinforced concrete floors and roof
MS	Massive stone masonry in lime or cement mortar
UCB	Unreinforced concrete block masonry with lime or cement mortar
UFB	Unreinforced fired brick masonry
UFB1	Unreinforced brick masonry in mud mortar without timber posts
UFB2	Unreinforced brick masonry in mud mortar with timber posts
UFB3	Unreinforced brick masonry in lime mortar
UFB4	Unreinforced fired brick masonry, cement mortar. Timber flooring, timber or steel beams and columns, tie courses.
UFB5	Unreinforced fired brick masonry, cement mortar, but with reinforced concrete floor and
RM	Reinforced masonry
RM1	Reinforced masonry bearing walls with wood or metal deck diaphragms
RM2	Reinforced masonry bearing walls with concrete diaphragms
RM3	Confined masonry
C	Reinforced concrete
C1	Ductile reinforced concrete moment frame with or without infill
C2	Reinforced concrete shear walls
C3	Nonductile reinforced concrete frame with masonry infill walls

10.3 Appendix – Questionnaire for members of response organisations

Sex   M   F   Age ....   Organisation ....

Role............. .Provenance ....   Here since ....

RESPONSE PHASE

1.   **Immediately after the earthquake, how did your work to help the affected population begin?**

2.   **What problems did your organisation encounter in the initial phase of operations?**
       (a) Difficulty in coordinating with other organisations.
       (b) Difficulty in communicating with the population.
       (c) Technical problems (e.g. inadequate equipment).
       (d) Difficulty in reaching the site of your operations in the affected area.
       (e) Other.

3.   **Avete piani di soccorso specifici per persone vulnerabili (es. anziani e disabili)?**
       (a) Yes.
       (b) No.
       If yes, give details ....

4.   **During the first week after the earthquake, what type of information did you give to the affected population?**
       (a) Personal safety.
       (b) Safety of buildings and infrastructure (including accessibility).
       (c) Temporary shelter.
       (d) Work activities.
       (e) Economic help.
       (f) Other ....

5.   **Through what channels did you provide information to the population during the first week after the earthquake?**
       (a) Speaking directly to individual people
       (b) Telephone (calls and SMS)
       (c) Radio
       (d) Television
       (e) Social networks (Facebook, Twitter etc.)
       (f) Written or printed material (e.g. newspapers or pamphlets)
       (g) Other ....

PRESENT PHASE

6.   **What problems are you currently facing?**

(a) Difficulty in coordinating with other agencies.
(b) Difficulty in communicating with the affected population.
(c) Technical problems (e.g., inadequate equipment)
(d) Difficulty in developing strategies for the medium and long terms
(e) Difficulty in reaching the affected areas.
(f) Logistical problems.
(g) Other ………………

7   **What kind of information are you providing to the affected population?**

(a) On social and psychological support.
(b) On the safety and accessibility of buildings and infrastructure.
(c) On the availability of temporary shelter.
(d) On work opportunities.
(e) On monetary assistance.
(f) On long-term recovery and reconstruction strategies.
(g) Other ………………

8.   **Through what channels are you providing information to the affected population?**
(a) Speaking directly to individual people
(b) Telephone (calls and SMS)
(c) Radio
(d) Television
(e) Social networks (Facebook, Twitter etc.)
(f) Written or printed material (e.g. newspapers or pamphlets)
(g) Other ………………

9.   **Does your organisation have medium- and long-term plans to help vulnerable people (e.g. the elderly and handicapped)?**
(a) Yes.
(b) No.
If yes, give details ………………

LONG-TERM PROSPECTS

10.   **What strategies are being planned for long-term recovery and reconstruction?**

11.   **What do you know about the long-term recovery and reconstruction strategies?**
(a) I am fully aware of the long-term strategies.
(b) I am only aware of my agency's role in the recovery process, not of the overall strategy.
(c) I have been given no information about long-term recovery and reconstruction.
(d) I am not interested in learning about the long-term recovery and reconstruction situation.
(e) Other ………………

EEFIT
Earthquake Engineering Field Investigation Team

EEFIT is a UK based group of earthquake engineers, architects and scientists who seek to collaborate with colleagues in earthquake prone countries in the task of improving the seismic resistance of both traditional and engineered structures. It was formed in 1982 as a joint venture between universities and industry, it has the support of the Institution of Structural Engineers and of the Institution of Civil Engineers through its associated society SECED (the British national section of the International Association for Earthquake Engineering).

EEFIT exists to facilitate the formation of investigation teams which are able to undertake, at short notice, field studies following major damaging earthquakes. The main objectives are to collect data and make observations leading to improvements in design methods and techniques for strengthening and retrofit, and where appropriate to initiate longer term studies. EEFIT also provides an opportunity for field training for engineers who are involved with earthquake-resistant design in practice and research.

EEFIT is an unincorporated association with a constitution and an elected management committee that is responsible for running it activities. EEFIT is financed solely by membership subscriptions from its individual members and corporate members. Its secretariat is generously provided by the Institution of Structural Engineers and this long-standing relationship means that EEFIT is now considered part of the Institution.

This report can be downloaded from www.eefit.org.uk